NUMERICAL AND EXPERIMENTAL INVESTIGATION OF BURIED LARGE-DIAMETER

STEEL PIPES WITH CONTROLLED LOW-STRENGTH MATERIAL

by

MARGARITA TAKOU

Presented to the Faculty of the Graduate School of

The University of Texas at Arlington in Partial Fulfillment

of the Requirements

for the Degree of

DOCTOR OF PHILOSOPHY

THE UNIVERSITY OF TEXAS AT ARLINGTON

August 2016

Acknowledgements

Abstract

NUMERICAL AND EXPERIMENTAL INVESTIGATION OF BURIED LARGE-DIAMETER

STEEL PIPES WITH CONTROLLED LOW-STRENTH MATERIAL

Margarita Takou, PhD

The University of Texas at Arlington, 2016

Supervising Professor: Ali Abolmaali

The main goal of this research was to gain an in-depth understanding of the behavior of buried large-diameter pipes with controlled low-strength material (CLSM). Design equations were developed based on extensive parametric studies that aimed for an optimized design for designers in industry. Both experimental and numerical methods were espoused in the investigating procedure. The pipe-soil structure characteristics of the experimental analysis were: (a) steel pipe diameter of 108 in., (b) steel pipe thickness of 0.47 in., (c) mortar liner applied at the inner surface of the pipe with thickness of 0.5 +1/6 in., (d) CLSM applied around the pipe at a depth of 70% of the pipe's diameter, (e) selected compacted soil applied at a depth of pipe's diameter, and (f) compacted native soil with overall depth of 6ft. applied until the ground level. The staged construction method was applied, which means that the application of each part was done in a specific order. The stages of the construction were: (a) pipe placement, (b) CLSM applied at a depth of 30% of pipe's diameter (OD), (c) CLSM applied at a depth of 70% OD, (d) compacted select fill layer applied 1 ft. above the pipe's crown, and (e) consecutive compacted soil layers of 12 in. depth until the ground level.

Experimental measurements were conducted at the site to measure the deflection of the pipe during the construction stages. Two methods were applied: MOP-119 and video

laser profiler (VLP) method. The MOP-119 is a method based on the ASCE Committee on Buried Flexible (Steel) Pipe Load Stability Criteria and Design of the Pipeline Division. The laser profiler method is based on a laser ring projected at the inner surface of the pipe. Due to physical obstacles inside the pipe, for this research, the VLP was modified to the photo laser profiler (PLP) method to bypass the issues raised.

A Finite Element Model (FEM) was developed to mimic the experimental conditions of the pipe tested. The geometrical dimensions, boundary conditions, material properties, and construction stages were all applied based on the site conditions. A model-change algorithm was used for an accurate representation of the staged construction method. Geometry, material, and contact nonlinearities were implemented. A Newton-Raphson algorithm was used for the model convergence. Overall, 28 sections were analyzed with the FEA, and the results for the deflection at springline and invert were compared with the experimental data.

The material properties of the CLSM were investigated in the Civil Engineering Laboratory (CELB) at the University of Texas at Arlington. Compression, flexure, and triaxial material tests were conducted based on ASTM D4832, C31, and D 4767, respectively. A material law was developed based on the test results.

Unique design equations were developed for large-diameter steel pipes with CSLM. A total of 3500 models were run, and a regression analysis was conducted. The dependent variables were horizontal and vertical deflection, moment, thrust, and shear of the pipe; while the independent variables were pipe diameter, pipe thickness, CLSM layer height, backfill material used above the CLSM layer, trench width, and trench wall stiffness.

Table of Contents

List of Illustrations

List of Tables

Chapter 1

INTRODUCTION

1.1   About this Research

Pipes have been used for thousands of years by agriculturalists who diverted water from streams and rivers into their fields, and later by people in the cities who transferred water into their homes from springs, as shown in Figure 1-1. Pipes are found in many ancient countries, i.e., Greece, Egypt, and Central America. Based on archeological findings, reed pipes were used in China as early as 2000 B.C. Greeks were the first to use pipes in Europe. Eupalinos built the first water-transfer engineering "miracle" in the 6th century B.C, used for transferring water on Samos Island, as shown in Figure 1-2. The pipeline was actually a tunnel, 1 km (0.62 miles) long with 8 m (26.2 ft.) width/height. The outstanding point of this project was that the excavation of the tunnel started at the same time from both the beginning and end of the line. The coordination of the tunnel excavation was so precise that both excavation brows met in the middle of the pipeline's length. Later, the ruler of Athens, Peisistratos, constructed a 1.7-mile-long (2,800 m) aqueduct for transferring water from mountain Hymettus to the city of Athens. The water was then distributed inside the city through a buried pipeline system.
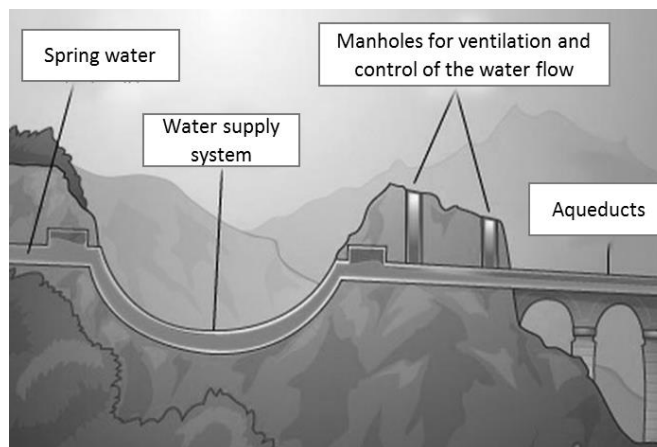
Figure 1-1 Water transfer through the springs
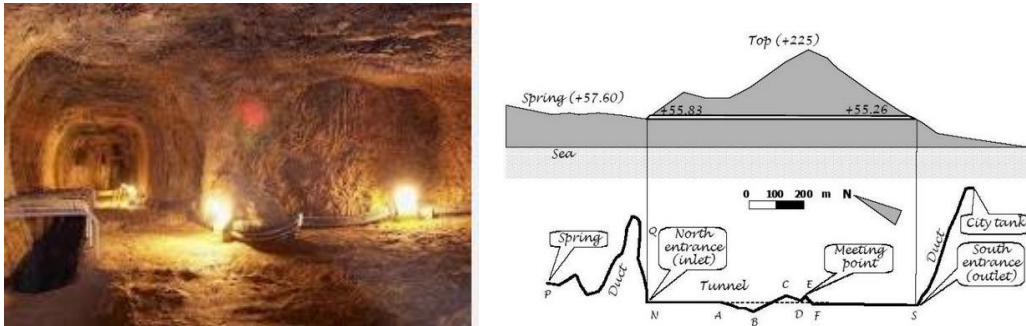
Figure 1-2 Eupalinio Tunnel in Samos

Another unique water transfer method was developed in Persia around the 7th century B.C. These were known as the Qanat tunnels. The tunnels were hand-dug and large enough to hold the person that was doing the digging. Vertical shafts were sunk at intervals of 20-30 km (12-18 miles) to remove the excavated material and to provide ventilation and access for repairs, as shown in Figure 1-3. Romans started building pipeline systems around 100 to 300 A.D. through aqueducts and buried lead pipes, that transferred water to the houses of the elite.
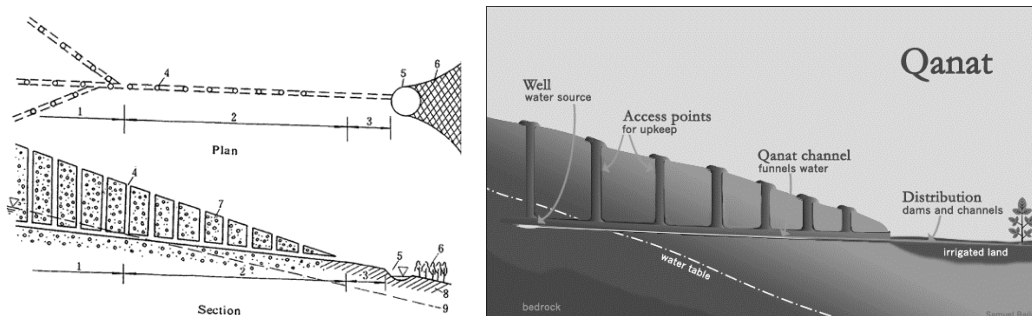
Figure 1-3 Persian Qanat tunnels

In tropical countries, the use of bamboo was popular for the construction of pipes. Based on Cates (1), colonial Americans used wood for similar purposes, and the first waterworks was made in Boston in 1652 by using hollow logs. The development of the first welded steel pipe can be traced back to the early 1800s, when William Murdock invented

a coal-burning lamp system. The first easy production of metal pipes was introduced in 1825 by Comelious Whitehouse, who developed, for the first time in history, long iron pipes by drawing flat strips of hot iron through a bell-shapes die. Then came the Bessemer process, which is the basis for the current pipe-making procedures, based on Watkins (2). The first furnace opened in 1831 in Philadelphia, which is considered the first stage in development of steel pipes based on Cates (1). The second stage was recorded in 1855 in the age of steel, and it was based on the Bessemer process. The open-hearth furnace in 1825 allowed the mass production of steel and, therefore, of steel pipes too. The pipes were formed into tubes with longitudinal, riveted seams with crimped ends so they could be stabbed into the next pipe. The third stage was the Lock-bar pipe in 30-foot lengths. It was first fabricated in New York and had two halves of semicircular pipes that were attached to an H-shaped cross section. The fourth stage was the automatic electric welding, which became popular in the pipe industry during the 1940s. From 1858 to 1970, approximately 29,520,000 feet of steel pipes were installed in the United States. Based on Cates (1), more than 12,320,000 feet installed pipes have reached a 100-year mark.

During the evolution of pipe production, there was also progress in soil-handling and excavation machines. During World War II, the development of equipment increased dramatically, and mule-drawn scrapers and Fresnos were replaced by graders, bulldozers, carry-all-loaders, and gigantic dump trucks. The grade-all was developed for shaping cuts and fills. In 1905, the "tractor-on-a-track" or "caterpillars" first appeared, allowing movement in the mud without spinning.

In late 1930, Spangler, also known as "the father of buried flexible pipe analysis," conducted soil box tests and discovered the effectiveness of soil support at the sides of flexible pipes. Based on Watkins (2), Spangler developed an equation for predicting the ring deflection of buried flexible pipe, with a limitation on the dimensions of a "modulus of

elasticity" of the soil. Watkins and Spangler corrected the dimensions and published the Modified Iowa Formula in 1958. Based on William (3), the Iowa Formula is an elastic model which predicts the horizontal deflection of buried flexible pipe, taking the pipe-soil interaction into consideration. The Iowa Formula is not a model for designing buried steel pipes. The Iowa equation had a specific number for the "modulus of elasticity" representing the compacted soil-structure interaction. In 1977, Howard (4) published a table of modulus of soil reaction (E') for various pipe supports. These values have been developed based on 113 laboratory large-scale tests performed, considering different types of soil placed beside the pipe at different degrees of compaction. This method is an empirical method that defines E', and it only applies to the initial deflections, which are those measured after the installation procedure has been completed. Most of the tests were conducted using small pipes, with a few of them conducted on large-diameter pipes. The trench-width thickness of the compacted soils was not taken into account, based on the assumption that the trench wall material is less compressible than the bedding. When the reverse happened, a highly compacted trench width equal to five times the pipe diameter was recommended. There were new studies after Howard's tests, aiming to calculate a more accurate relationship for the pipe-soil interaction. Krizek et al. (5) introduced the constrained soil modulus, Ms, which is related to the elastic modulus of soil. Hartley and Duncan (6) claimed that E' varies along the depth of the soil. A more recent study from Howard (7) recommends the use of a composite E', which is called "Modulus of Soil Reaction" and represents the stiffness of the embedment soil located around the pipe. Composite E' is actually E', as defined by Howard (4), modified by a "soil support combining factor" which takes into consideration the effect of the combination of the width of the embedment and the stiffness of the in situ trench walls.

Two standard manuals are used as references when designing steel pipes: The M11 (8) standard, published by AWWA, has been used primarily for steel pipe design, and the ASCE's manual introduced the buried flexible steel pipe design, and structural analysis (3). Based on AWWA, 2004, the main failures of steel water pipes are caused by:

- External corrosion such as galvanic, electrolytic, biochemical, stress, and fatigue corrosion

- Internal corrosion, which in some cases affects the quality of water

- Improper handling and storage of pipes

- Excessive deflection or point loads applied at the pipe due to pipe layout

- Defective pipe jointing (Figure 1-4)

- Embedment material which can cause corrosion in the pipe or local buckling

- Contraction and expansion of the pipe due to temperature changes

- Damage of the internal surface of the pipeline due to aggressive water with high mineral content

Figure 1-4 Connection failure on Salt River Project that feeds water from the C.C. Craig Dam and Reservoir to the town of Payson Cronkite News Service, Joshua Armstrong

Table 1-1 Classification of steel pipe failures (9) and (10)

Type of Failure	Mode of Failure	Causes of Failure
Corrosion and Environment	Pitting Holes	Corrosive soils, microbiological influence, stray currents.
	Graphitization	Corrosive soils, hydrogen embrittlement, stray currents, anaerobic bacteria.
	Secondary Effects	Hydrogen embrittlement, chlorides from water, coating damage, dissimilar soils, ground movements
Stress Failure	Transverse Break	Circumferential stress, thermal stresses, transient conditions, mechanical stresses, soil swelling or settlements
	Split Pipe	Ambient temperature differences, transient conditions.
Joint Failure	Brittle Failure	Graphitization, hydrogen embrittlement, coating damage
	Connection Failure	Defects in welding, thermal stresses, fatigue weakening
	Joint Burst	Soil swelling/settlements, differential thermal expansion/contraction.

A recent study by researchers at the Buried Structures Laboratory at Utah State University recorded the failure rates of different pipe materials over a 12-month period. The failure rate for cast iron pipes was 24.4 failures/ 100 miles/ year, for ductile iron pipe was 4.9 failures/ 100 miles/ year, for polyvinyl chloride pipe was 2.6 failures/ 100 miles/ year, for concrete pressure pipe was 5.4 failures/ 100 miles/ year, for steel pipe was 13.5 failures/ 100 miles/ year, and for asbestos cement pipe was 7.1 failures/ 100 miles/ year.

In the US, the water pipe distribution network is over 9,320,600 miles long, and about 13,050 miles of new pipe are added every year. Based on Denise and Barry (11), one of the longest pipeline projects is the Mni Wiconi Rural Water System located in South Dakota, with an overall length of 4,400 miles of 10 and 12-inch diameter pipelines. The pipeline transfers water from the Missouri River to the Pine Ridge Indian Reservation. The California State Water Project (SWP) has an overall length of 700 miles and is a combination of tunnels and pipelines. The SWP collects water from rivers in Northern

California and redistributes it to the southern part of the state. The 500-mile long Central Valley Project (CVP) in California shares some of the facilities with the SWP, mainly containing canals and tunnels, dams and reservoirs, storing the water during the rain periods and later distributing it to the Central Valley area during the dry period. Other smaller projects are those of the Central Arizona Project, Colorado River Aqueduct, Los Angeles Aqueduct, Central Utah Project, and the Hetch Hetchy Aqueduct. One of the biggest projects in Texas is the Integrated Pipeline Project (IPL), which is a 150-mile long pipeline that will provide up to 350 million gallons per day of raw water. Worldwide, the largest water pipeline project, in volume of water transferred and the distance to be traveled, was launched in China. The total length of the steel pipeline is 2,700 miles (4,350 km), about the distance between the coasts of the US.

The methods used to explain the behavior of buried pipes are primarily based on empirical values and focused only on the behavior of pipe and the surrounding soil, through the composite E'. There is a need to calculate the deflection of the pipe based on the actual properties of the materials used and the overall geometry of the analyzed section, taking also into consideration the trench and trench wall. Codes and manuals used for pipe design (12), state that the deflection of the pipe should be monitored during the installation procedure. Even though the codes refer to the need to supervise the deflection of the pipe during installation, there are no actual equations or experimental methods recommended to explain the behavior of the pipe during the staged construction procedure embedded in non-homogenous soil materials.

1.2   Literature Review

1.2.1   Buried Pipe Design and Deflection Measurement

Based on M11 (8), the first step in designing a pipe is to identify the pipe wall thickness, which is affected by many factors such as internal and external pressure, special

physical loading, and coating or lining. External load, including soil compaction, soil at-rest lateral pressure, live load, and internal pressure are among the variables that affect the design of the pipe wall thickness. Hoop stress, which is the circumferential tension stress, is applied at the overall thickness of the pipe, and is the critical stress while internal pressure is applied. Therefore, the thickness of the pipe is defined by Equation (1), known as the Barlow formula. Minimum wall thickness values are defined in M11, considering both pipe diameter and coating or lining.

$$t = \frac{pO.D.}{2s}$$ Equation (1)

Where,

t = minimum pipe wall thickness for the specified internal design pressure, mm

p = internal design pressure, kPa

O.D. = outside diameter of steel pipe (without lining or coating), mm

s = allowable stress design, kPa

The external loads applied at the buried pipes primarily consist of the soil weight and live loads or impact loads. The Marston (13) theory developed in 1929 is used to calculate the soil prism weight and the external loads due to weight. In M11 (8), a simplified method is introduced which calculates the external loads, depending on the trench width and embankment conditions. The backfilling materials used are a very important variable for calculating the loading and the pipe deflection.

The deflection of the pipe is calculated according to the modified Iowa deflection equation (14) shown in Equation (2), which is introduced in manuals for pipe design. This equation predicts the horizontal pipe deflection by using pipe wall and soil stiffness, based on the assumption that the soil is uniaxial and elastic. It should be noted that based on Smith and Watkins (15), Equation (2) was derived to predict the ring deflection of flexible culverts and not as a design equation to determine the wall thickness of pipe materials.

26

Consideration of the pipe deflection during the design is important, since the limits set by the design standards, AWWA (8), are related to the deflection of the pipe. An accurate calculation of pipe deflection is needed for flexible steel pipes since the deflection is a variable that determines whether the pipe meets the established standards.

$$\Delta x = D_l \left(\frac{KWr^3}{EI + 0.061E'r^3} \right)$$
<div align="right">Equation (2)</div>

Where,

Δx = horizontal deflection of pipe, mm (in.)

D_l = deflection lag factor (1.0- 1.5)

K = bedding constant (0.1)

W = load per unit of pipe length, kg/mm (lb/ linear in)

r = radius, mm (in.)

EI = pipe wall stiffness

E = modulus of elasticity, kPa (psi)

I = transverse moment of inertia per unit length of individual pipe wall components

= $t^3/12$, t is in mm (in.)

E' = modulus of soil reaction, kPa (lbf/in^2)

The stiffness of the pipe-soil system is closely associated with the calculation of the modulus of soil elasticity (E'), first investigated by Howard (16). The value of the soil elasticity is not a specific number; dependents on the interaction of factors like pipe diameter, soil type, soil compaction level, etc. Based on M11, there are values provided based on Hartley and Duncan (6), although it is explained that E' is not a material property and cannot be uniquely measured. This is the main reason why determining E' has, historically, been a serious problem for the designers. Krizek et al. (17) introduced the constrained soil modulus M_s, which is the constrained secant modulus of the soil around

the pipe. The value of Ms can be calculated from common consolidation tests, triaxial tests, or plate-bearing tests of the soil material. Ms is also related to the Young's modulus Es through Equation 3. The relationship of the hybrid modulus E' is 0.7 to 1.5 times the value of the constrained soil modulus Ms.

$$Ms = \frac{Es(1-v)}{(1+v)(1-v)}$$

Equation (3)

Buried pipes with diameters of 18 to 30 in. were tested in a large soil container by Howard (16). The load applied was produced by increasing the surcharge load over the pipe. It was observed that the deflected shape of the pipe was either elliptical or rectangular, depending on the pipe-soil stiffness relationship. After the formation of the plastic hinge, it was observed that the pipes whose deflected shape was elliptical were more stable under the increasing load than those deformed in a rectangular shape. A study performed by Hartley J. D. and Duncan J. M. (6), investigated the relationship of E', which in this study is called "modulus of soil reaction." They concluded that the modulus of soil reaction depends not only on soil type and degree of compaction, but also on the cover depth. They conducted a review of published literature on the dependence of E' on backfill depth and examined data available over a range of backfill depths for individual pipe installation. Based on this data, elastic analyses were performed to simulate the field behavior of the buried pipeline, and the E' values were obtained for specified pipe installation and soil conditions. The main tests used in this study were from the East Bay Utilities District (EBMUD) (1964), the United States Bureau of Public Roads and the North Carolina State Highway Commission (1929), and from Martson's tests conducted at the Iowa Engineering Experiment Station (1929). The results from these tests showed that the E' depends on depth, and that values of E' can be used in the Iowa equation and are dependent on depth, as shown in Table 1-2.

Table 1-2 Design values of E' (psi) based on Hartley and Duncan (6)

Type of soil	Depth of cover (ft.)	Standard AASHTO Relative Compaction			
		85%	90%	95%	100%
Fine-grained soils with less than 25% sand content (CL, ML, CL-ML)	0-5	500	700	1000	1500
	5-10	600	1000	1400	2000
	10-15	700	1200	1600	2300
	15-20	800	1300	1800	2600
Coarse-grained soils with fines (SM, SC)	0-5	600	1000	1200	1900
	5-10	900	1400	1800	2700
	10-15	1000	1500	2100	3200
	15-20	1100	1600	2400	3700
Coarse-grained soils with little or no fines (SP, SW, GP, GW)	0-5	700	1000	1600	2500
	5-10	1000	1500	2200	3300
	10-15	1050	1600	2400	3600
	15-20	1100	1700	2500	3800

The values of E and E' were provided from empirical judgments or experimental tests for soil materials that were used as embedment for the pipe installation. Based on Watkins et al. (18), these values do not apply to CLSM backfill systems, which form the basis for the case studies in this research. Therefore, an extended study on pipe systems backfilled with CLSM is recommended.

The deformation of the buried pipe has been studied through the years. Based on Rogers 1988 (19), who studied the relationship of the soil support around the pipe and pipe deformation, not all the flexible pipes are deformed elliptically. Soil system support that offers a poor support to the pipe allows for elliptical deformation, while a good soil support deviates the behavior of the pipe from elliptical. The primary deformation shapes defined from this study are elliptical, heart shaped, inverted heart shaped, and square deformation, as shown in Figure 1-5.
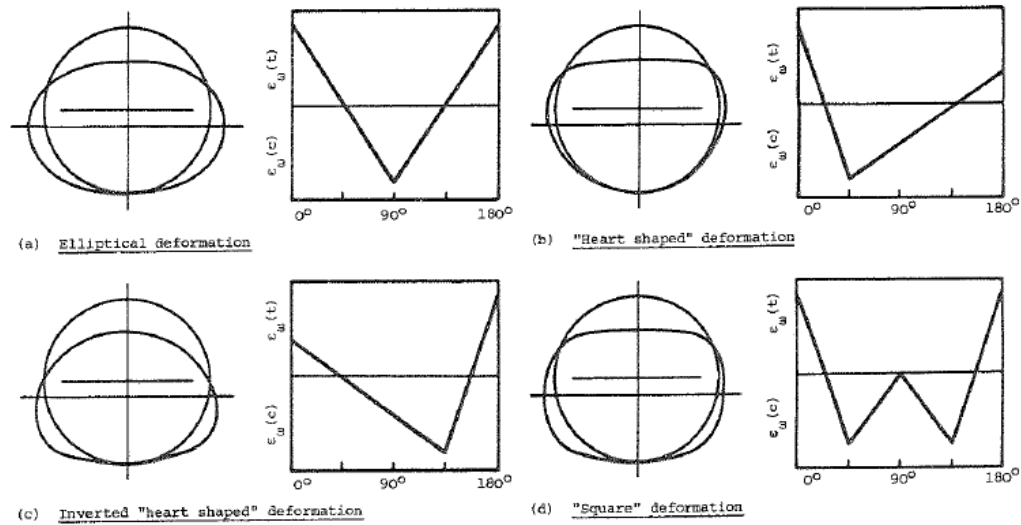
Figure 1-5 Deformation types and strain profile, based on Craig (20)

Another study performed from Kawabata et al. (21) concluded that the behavior of the pipe is directly influenced by the backfilling materials, and that their inhomogeneous strength can cause local deformation of the pipe. They tested full-scale soil-pipe systems which were categorized in five different ways, depending on the backfilling material used and the trench configuration.

An extended experimental work has been performed in this study, to measure the deflection of a buried steel pipe during installation. Three methods were used for this purpose: MOP-119, photo laser profiler, and video laser profiler. MOP-119 is a method introduced by an ASCE committee (ASCE, MOP-119, 2009). The photo and video profiler methods were conducted with a ten-headed laser ring that was projected on the internal side of the pipe. In previous research, extensive on-site measurements were conducted by Abolmaali et al. (2010) for 191 HDPE pipelines, with a total length of approximately 31,000 ft. (9448.8 m). The research showed that video inspection with a laser profiler was an excellent tool for employing quality control and assuring accurate pipeline installation.

Other studies conducted by the Kentucky Transportation Center and Pipeline and Drainage Consultants (2005) for 3,892 ft. (1186.3 m) of HDPE pipeline pointed out the advantages of pipe inspection with video and laser profilers as compared to mandrel testing. A mandrel is a device (formed by metal and wood) used for many years for measuring a pipe's deflection by pulling it from the beginning of the pipeline to the end. Excessive deformation of the pipe prevents the mandrel from being pulled at that point. Pipeline and Drainage Consultants (2005) investigated the deflection of a HDPE pipeline in Ohio with an overall length of 672 ft. (204.8 m). Manual and physical inspections were performed of vertical and horizontal deflections and video profiling, using a laser ring. The advantages of using video-laser inspection, compared with mandrel testing, were specifically highlighted. The main advantage was the capability of the video–laser method to provide significant information about observed defects like cracking, buckling, and tearing. Moreover, they concluded that video-laser profiling measurement was appropriate for the physical inspection of HDPE pipe deflection.

1.2.2   CLSM Mechanical Material Properties

The engineering properties of the materials used during the pipe installation should be considered during the design procedure. For this research, CLSM was the primary material used as backfill, until a height of 70% of the pipe's diameter was attained. Therefore, the investigation of the CLSM properties is a fundamental step for the successful analysis of the pipe-soil structure. CLSM is a flowable, self-compacted material that is used in buried pipe as bedding, and it was first reported by Green in 1999 (22). The mix proportion of CLSM, which mainly consists of native soil, cement, and water, can be varied, depending on the use and type of product. Materials such as fine and coarse aggregate, fly ash, and chemical admixture can be used, depending on the end product desired and the local construction practices. For this study, the CLSM mixture of native

soil, cement, and water was used as bedding for the installation of the buried large-diameter pipe. The main reason for using CLSM was to avoid compaction at the haunch area of the pipe, which reduces the width of the requirement trench. The compaction of the embedment and backfilling materials leads to non-uniform compaction forces which are transferred during the installation procedure of the pipe system. On the other hand, compaction is needed for loose materials to assure a smooth stress transformation from the pipe to the in-situ soil for optimum performance of the pipe-soil system. CLSM is a self-compacted material, which offers the required strength for a smooth transfer of the stresses through the pipe-soil system. Application and material properties of CLSM were investigated by the ACI Committee on Controlled Low Strength Material (229R-99) (23). They used preformed-foam, as part of the mixture proportioning, to produce Low Density CLSM (LD-CLSM), and determined that the typical strength properties varied from 68.9 to 3447.4 kPa (10 to 500 psi). The behavior of CLSM was defined as being somewhere between concrete and soil. Based on ACI, CLSM is produced with materials similar to those used for concrete. Moreover the installation procedure has similarities to the ones used for concrete. The characteristic properties are also affected by the soil properties. In 2004, Green and Schmitz (22) investigated the material properties of soil-based CLSM and reported that it is a material capable of filling large voids that can help decrease the cost of materials, thereby reducing the cost of the construction since compaction is avoided and no land purchase for soil storage is required.

The CLSM mix designs available in the literature range between different cement percentages and categories, soil type, and whether or not admixtures are used. Pons et al. (24) investigated the behavior of the CLSM by analyzing both regular and quick-setting flowable fills. Overall, 4 mix designs were tested: 1) Regular normal setting CLSM, 2)

Master builders quick-set CLSM, 3): Quick-set CLSM, and 4) Quick-set with 2% retarder

CLSM. The mix designs are shown in Table 1-3.

Table 1-3 Mix design Pons et al. (24)

Material	Regular (Mix 1)	Quick-set (Mix 2)	Quick-set (Mix 3)	Quick-set with 2% retarder (Mix 4)
Cement	60lbs. (Type I)	100lbs. (Type I)	100lbs. (Rapid Set)	100lbs. (Rapid Set)
Fly ash Type C	290 lb.	0 lb.	0 lb.	0 lb.
Sand, ASTM C33	2750 lbs.	2925 lbs.	2970 lbs.	2970 lbs.
Water	458 lbs.	585 lbs.	500 lbs.	500 lbs.
Admixture	2 oz. air-entraining agent	80 oz. accelerator (Pozzutec 20) ASTM C494 Type C & E	none	2% citric acid retarder (2 lbs.)
Water/cement ratio	1.31	5.90	5.00	5.00

To test the engineering properties of the flowable mix designs, the penetration resistance, unconfined compressive strength, flow, and the ease of re-excavation were measured. A mortar penetrometer (CT-421A) was used to measure the penetration resistance of the open surface of each mix, while for the flow test, an open 3x6 inches cylinder was used, in accordance with ASTM standards. The unconfined compressive strength tests were performed on cylinders on a 365-day period, past the production day. Six weeks after placement, 6 in. square cubes were removed from each of the mixtures at depths of 1 to 2 ft. below the surface, to determine whether the mixes were diggable. Four experimental trenches were excavated and backfilled with the flowable fill mixtures to determine the in-place bearing strength of the fill. The in-situ soil was classified, in accordance with the Unified Soil Classification System (ASHTOO), as clayey sand to sandy clay with gravel and other construction rubble (asphalt and concrete pavement, etc.). The descriptions of the mix designs are shown in Table 1-4. Flow values ranged from 3 to 5 in.

Requirements for quick-set CLSM (city of Tulsa) for minimum flow value was 4 ½ in. For regular CLSM, the flow value was 9 ½ in. The minimum requirements for CLSM flow is 8 in. The quick-set mixtures were diggable with a hand-held spade. The regular CLSM mixture was hard and not penetrable with the spade.

Table 1-4 Physical property summary of laboratory placements and field trenches Pons et al. (24)

Description	Flow (in)	Unit weight, pcf
Mix 1 - Lab Box	9.5	131.9
Mix 2 - Lab Box	5	127.9
Mix 3 - Lab Box	3	125.2
Mix 4 - Lab Box	5	123.8
Mix 1 - Field Trench	8.5-9.5	134.0
Mix 2 - Field Trench	3 – 4.5	126.9
Mix 2A - Field Trench	3.5	130.6
Mix 4 - Field Trench	4.25	129.3

The average unconfined compressive strength values for the laboratory box for the quick-setting CLSM ranged from 36 to 55 psi at 28 days, from 43 to 65 at 90 days, 40 to 80 psi at 180 days, and 56 to 98 psi at 365 days, as shown inTable 1-5. For Mix 1 (regular CLSM) the unconfined compressive strength was 28 psi at 28 days, 390 psi at 90 days, 510 psi at 180 days, and 615 psi at 365 days. The unconfined compressive strength for the field trench placement for Mixes 2 and 4 ranged from 42 to 67 psi at 28 days, 48 to 76 psi at 90 days, 42 to 77 psi at 180 days, and 56 to 108 psi at 365 days. For Mix 1, the compressive strength was 26 psi at 28 days, and 34 psi at 90 days. Based on Pons et al. (24), the recommendations for a CLSM with good installation properties are: 1) minimum compressive strength of 25 psi at 28 days and a maximum strength of 100 psi at 60 days, and 2) penetration resistance of 400 psi at 14 days.

Table 1-5 Summary of unconfined compressive strength results Pons et al. (24)

Description	6-8 Hrs. Comp. Strength [a]psi	1 Day Comp. Strength psi	7-8 Day Comp. Strength psi	28 Day Comp. Strength psi	90 Day Comp. Strength psi	180 Day Comp. Strength psi	365 Day Comp. Strength psi
Mix 1 - Lab	-	-	4	28	390	510	615
Mix 2 - Lab	-	5	27	55	65	80	98
Mix 3 - Lab	2	12	29	38	43	55	64
Mix 4 - Lab	2	8	13	36	50	40 (b)	56
Mix 1 - Field	-	-	2	26	34 and 970 (c)	54 and 890 (d)	-
Mix 2 - Field	2	8	25	52	57	42	56
Mix 2A - Field		9	41	67	76	67	86
Mix 4 - Field	19	25	34	42	48	77	108

[a] 1 psi= 6.8948 KPa
[b] Sample tested at 119 days
[c] Core re-test at 164 days
[d] Core re-test at 180 days

(a)
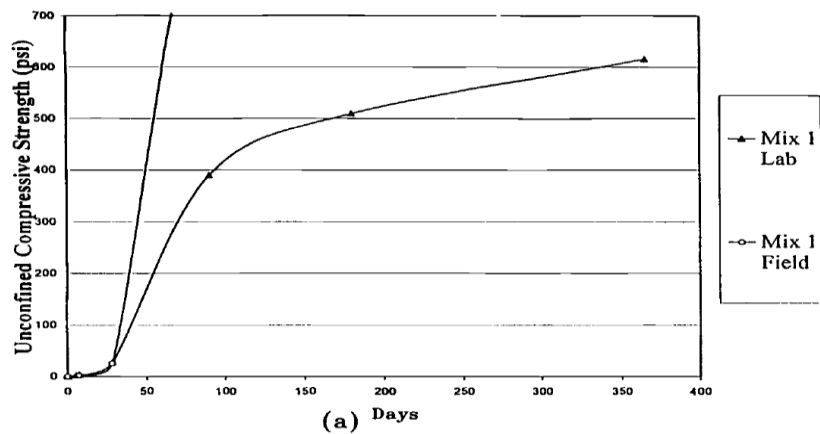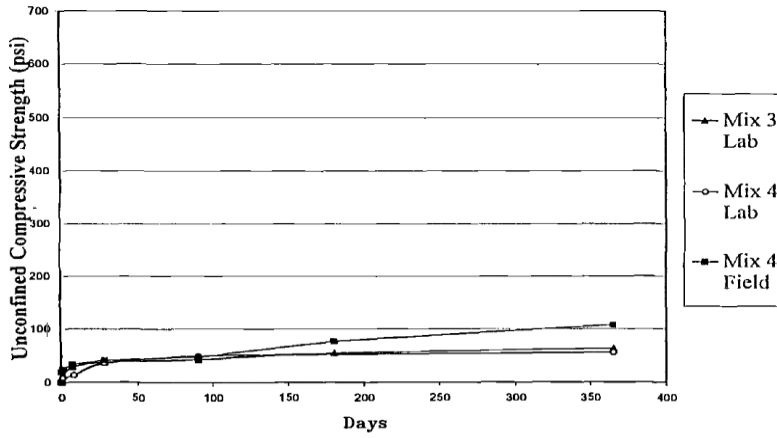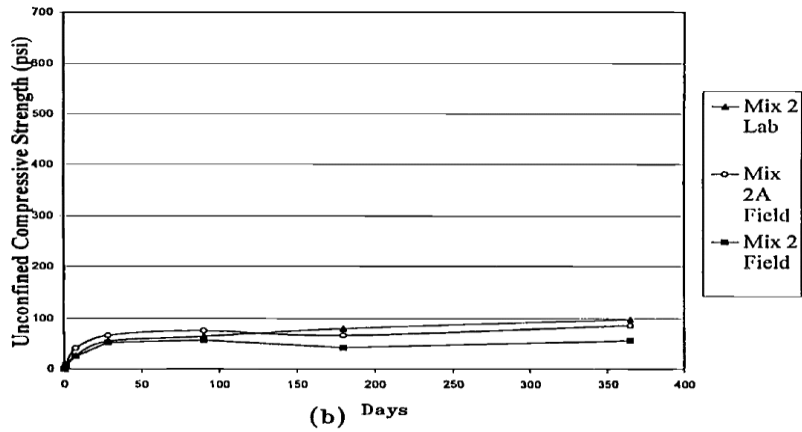
Figure 1-6 Unconfined compressive strength versus time for mixes 1, 2, and 3 for lab and field
Pons et al. (24)

Another study performed by Mullarky et al. (25) investigated the behavior of two different mix proportions in Branchville and Atlanta, which are shown in Table 1-6. The first mix utilized a moist, high-carbon fly ash (about 6-20%), while the the second mix was more typical CLSM formulation, with cement, Class F fly ash and concrete sand used.

Table 1-6 Mix proportions placed at two test sites, Mullarky et al. (25)

	JRL		T	
Materials	East	West	North	South
Cement, lb. /cu yd.	50	48	75	50

36

(kg/m^3)	(29.6)	(28.5)	(44.5)	(29.6)
Fly Ash, lb. /cu yd.	2370	305	100	500
(kg/m^3)	(1406)	(180.9)	(59.3)	(296.6)
Fine Aggregate, lb. /cu yd. (kg/m^3)	-	2375 (1409)	1728 (1025)	2113 (1254)
Water, gal. /cu yd.	59	54	45	55
(liters/m^3)	(292)	(270)	(223)	(272)
Design Air Content	1%	8%	35%	12%

The following tests were conducted for the CLSM mix designs: 1) ASTM PS 28-95 for the flow consistency, 2) ASTME C 143 for the slump of each mix, 3) ASTM PS 28-95 for the unit weight, 4) ASTM C 231 for the air content by the pressure method, 5) ASTM C 1064 for the temperature of fresh concrete, 6) ASTM D 4832 for the preparation of cylinder molds, 7) ASTM PS 31-95 for the ball drop test method to determine the suitability of the CLSM for load application, 8) ASTM C 403 to count the setting time of the mix design based on the test followed for the concrete mixtures. The results from the tests are shown in Table 1-7. It was observed that material NW, which was considered a conventional mix with 40 pounds (18.14 kg) of Portland cement, 305 pounds (1.588 kg) of Class F fly ash, and 2,375 pounds (1077 kg) of concrete sand, had a high strength gain between 28 and 90 days, as shown in Figure 1-7. Material NE, which consisted of 50 lb. (22.7 kg) of Portland cement and 2,370 lb. (1075 kg) of conditioned fly ash per yd^3; and TS, which had a high air content of 12% and a high fly ash content of 500lb/yd^3 (297 kg/m^3), have shown little long-term strength gain, as shown in Figure 1-7. The results show that the air and fly ash content are significant factors in controlling long-term strength gain of CLSM, based on Mullarky et al. (25).

Table 1-7 Test results for CLSM, Mullarky et al. (25)

Trench Code		**NE**	**NW**	**TN**	**TS**
Flow	in	6.25	5.75	8.25	12.5
(ASTM PS 28)	(mm)	(156)	(144)	(204)	(316)
Slump	in	8.75	9	9.5	11.5

(ASTM C 143)	(mm)	(216)	(228)	(240)	(288)
Spread	in	16.13	20.25	NA	NA
	(mm)	(402)	(504)		
Unit Weight	lb. /cu ft.	97.99	128.96	98.8	115.6
	(kg/m^3)	(1570)	(2066)	(1583)	(1852)
Air	%	1.1	0.2	29	6.4
Temperature	^{0}F	84	78	65	66
	(^{0}C)	(29)	(26)	(18)	(16)
Cylinder Strength (6x12 in)(150x300 mm)					
7 Day	Psi	30	23	NA	NA
	(MPa)	(0.21)	(0.16)		
14 Day	Psi	NA	NA	12	19
	(MPa)			(0.08)	(0.13)
28 Day	Psi	50	46	16	20
	(MPa)	(0.34)	(0.32)	(0.11)	(0.14)
90 Day	Psi	59	114	37	22
	(MPa)	(0.41)	(0.79)	(0.26)	(0.15)
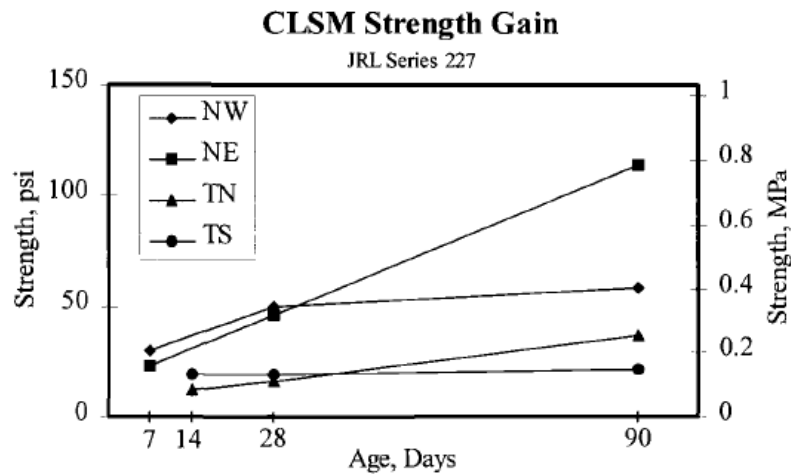
Figure 1-7 Strength gain of CLSM, Mullarky et al. (25)

Based on Nataraja et al. (26), mixture proportions containing industrial by-products, namely fly ash (FA), rice husk ash (RHA), and quarry dust (QD) can be used in CLSM to reduce the cost and to ensure low maximum compressive strength. In this study it was concluded that the flowability, compressive strength, modulus of elasticity, density, and volume change can be satisfactory with a low cement use and a large amount of by-product materials. The w/c ratio and the by-product amount used was defined as linear

based on a satisfactory flowability levels. The compressive strength of the mix was calculated at 28 days, ranging from 51.37 kPa (7.41 psi) to 4233.53 kPa (614.02 psi). Lee et al. (27) investigated the characteristics of alkali-activated, cementless, controlled low-strength material (CLSM) by using industrial by-products through characterization tests. Three different industrial by-products were used. Fly ash and slag were used instead of cement, and bottom ash was used as a fine aggregate for the CLSM production. NaOH solution was used as an activation solution, and the compressive strength, low, and bleeding rate, were calculated equal to 1.0-2.0 MPa (145-290 psi) at 56 days, 200-250 mm (7.87-9.84 in.) and 1.0-1.5%. The main conclusions elicited from this research were: (a) the flowability of the mixture was affected by the amount of bottom ash; the water/binder ratio, the bottom ash/binder ratio, and the compressive strength increased as the amount of slag and NAOH increased. The water/cement ratio (w/c) of the CLSM was one of the main properties tested for checking the appropriateness of the mix design. Based on Howard A.K. (28), who has tested the CLSM in depth, a typical w/c ratio is between 2 and 3.

Literature related to the tensile strength of CLSM was not found. The only research identified, related to tensile strength, was conducted by Weng and Vipulanandan (29) at the University of Houston in Texas. They found that tensile strength was about 8 times lower than compressive strength, but no description of the test configuration or procedure was provided.

The corrosion of steel in cementitious CLSM versus that in soil was researched by Abelleira et al.in 1998, (30). They found that corrosion of the carbon steel was significantly reduced when a CLSM mixture was used rather than good quality sand. Kaneshiro et al. (2004) analyzed and compared the advantages and disadvantages of using controlled low-strength materials for pipeline backfill rather than conventional granular backfill. The

advantages were the ease and safety of using the CLSM, as well as the reduced excavation cost, since compaction was avoided. The main disadvantages were the lack of information available from contractors and laboratories on the applications of CLSM as conventional backfill material, and the lack of literature regarding the material properties of the CLSM.

The production and testing procedure of CLSM are primarily referenced in ASTM standards. In-situ soil was the main component of the CLSM examined in this study. The soil classification was performed based on ASTM D2488 "Standard Practice for Description and Identification of Soils (Visual-Manual Procedure)," ASTM D2487 "Standard Practice for Classification of Soils for Engineering Purposes (Unified Soil Classification System)," and ASTM D6913 "Standard Test Methods for Particle-Size Distribution (Gradation) of Soils Using Sieve Analysis." The mix design was prepared based on ASTM D4832, "Standard Test Method for Preparation and Testing of Controlled Low Strength Material (CLSM) Test Cylinders" and ASTM D5971, "Standard Practice for Sampling Freshly Mixed Controlled Low-Strength Material." The flowability of the mix design was tested according to ASTM D6103-04, "Standard Test Method for Flow Consistency of Controlled Low Strength Material." The density of the mix was tested based on the ASTM D6023, "Standard Test Method for Density (Unit Weight), Yield, Cement Content, and Air Content (Gravimetric) of Controlled Low-Strength Material (CLSM)." The compressive strength of the specimen based on the ASTM D4832, "Standard Test Method for Preparation and Testing of Controlled Low Strength Material (CLSM) Test Cylinders" was used. ASTM C496 "Standard Test Method for Splitting Tensile Strength of Cylindrical Concrete Specimens," was used for the tensile properties since there is no standard for testing the tensile strength of the CLSM. To identify the confined compressive strength of the CLSM, the ASTM D2850 "Standard Test Method for Unconsolidated – Undrained Triaxial

Compression Test on Cohesive Soils" was used, based on the procedure followed for the soils.

1.2.3   Finite Element Modeling

Finite Element Analysis (FEA) capable of simulating the staged construction method was developed in the 1970s. The importance of layer analysis in flexible culverts was researched by Goodman and Brown in 1963, as many investigators mentioned that the slip at the interface of soil and pipe may occur during the load and have an important effect on the behavior of the pipe. This phenomenon can be located with an incremental FEA that accounts for slippage between the soil-pipe structural systems. In 1976, Leonard's et al. (31) developed a FEA method (FINLIN) which predicts the behavior of buried pipe culverts. The fundamentals of finite element analysis are based on the method of variational analysis developed by Raleigh's-Ritz in the early 1900s. Turner et al. (32) developed a matrix approach to structural analysis based upon the finite element idealization. When compared, the two methods had very similar results, with the difference being that the displacement pattern for the Raleigh's-Ritz method was specified in the whole region; while for FEA, it was specified at nodal points of discrete elements. In the work performed by Leonards et al. the soil mesh was simulated with triangular-shaped elements, with a total of six nodes including rotational stiffness, capable of calculating the stresses anywhere within the element through a quadratic displacement function that allowed the linear variation of stresses and strain across the element. To simulate the interaction between the pipe and the surrounding soil, zero-thickness interface elements were used which allowed slip of the elements in contact when shear stress was less than the shear strength of the contact. The material properties used were nonlinear, stress-dependent anisotropic, as developed by Lekhnitskii in 1963. The tangent Young's modulus and tangent Poissons's ratio for any state stress were determined by spline functions,

41

developed by Lade in 1972, fitted to actual test data which are represented in terms of octahedral stresses instead of principal. Lade also introduced the 3-D elastoplastic stress-strain relationship concept in which, during loading, both elastic and plastic strains occur. The elastic part is evaluated using theory of elasticity, and the plastic component is based on the plastic relations. Incremental analysis was performed by the FEA model which was capable of simulating the staged installation method.

Although several studies were conducted on the analysis of buried pipes using soil-pipe interaction theories (Duncan, 1979; Katona, 1976; Leonards et al., 1982; Sharp et al. 1984; Sharp et al., 1985; Zarghamee 1986; Spitzley, 1987; Abdel-Motaleb, 1995; McGrath, 1998; J. Zhang, 2002; Suleiman, 2003; Evans, 2004; Y. Tian, 2008; A. Srivastave, 2013), limited investigations have explored the behavior of flexible pipes during staged construction by using 3-D nonlinear FEM. Allgood and Takahashi (1972) investigated the behavior of buried culverts. A 3-D analysis was performed by taking into account changes in elastic modulus through different values at different depths. No effects of slippage between pipe and soil, non-linear soil properties, staged construction, or compaction of the soil were considered. Based on their comments, the pipes at the site had large differences and behaved very differently. Therefore, it was concluded that the effects not taken into consideration were important.

A study by Katona et al. (33) in 1976 introduced the Culvert Analysis and Design (CANDE), which was a FEA program established to evaluate the behavior of buried structures. CANDE was used to simulate a corrugated metal liner and compacted soil envelope that surrounds the pipe. The main assumptions examined were the large deformation theory and the monolithic structure. Based on this study, recommendations for analytical modeling were made for future studies. To simulate the contact between soil and structure, interface elements were used with frictional sliding, separation, and re-

bonding properties. The soil models available were those introduced by Duncan and Selig, where a hyperbolic formulation was used to define the stress-strain relationship. The total strains were calculated using a stress-dependent stiffness, which was different for both loading and unloading/reloading. The hardening was assumed to be isotropic, depending on the plastic shear and volumetric strains. A non-associated flow rule was adopted when related to frictional hardening, and an associated flow rule was assumed for the cap hardening.

Zhang et al. (34) in 2002 developed a kinematic hardening model for pipeline–soil interaction under various loading conditions, and they conducted experimental tests on the beam centrifuge by using calcareous sand soil. The hardening model they developed required 13 parameters. Tian and Cassidy (35) in 2008 modified the model developed by Zhang et al. and introduced three elasticity models that could be used to simulate pipe–soil interactions numerically. The beam element was used for structural members in the FE model. The developed model was used to model the pipe in ocean environments, using sand material as the bedding. Further study should be conducted to show the efficiency of the developed model by Tian and Cassidy on buried steel pipes in a trench condition, in which there are more loads acting on the buried pipe.

Srivastava et al. (36) in 2013 conducted several laboratory tests on a buried PVC pipe to investigate the response of the soil–pipe system in terms of load settlement. The tests were then compared with a two-dimensional (2D) FE model. The tests were performed on small-diameter PVC pipes (110 mm), and the 2D FE model was used to evaluate the conducted tests. Zarghamee and Tigue (37) in 1986 developed a 2D FE analysis program, FLEXPIPE, and showed that significant flexural stresses are developed in steel pipes at the invert of the pipe after installation. The deflection history of the pipe during installation was not reported in that study. Suleiman et al. (38) in 2002 investigated

the effects of large-deflection behavior on buried plastic pipes. In this study, the small deflection analysis theory was the results of comparing Culvert Analysis and Design (CANDE) software were compared with the large deflection analysis theory, using ANSYS. The authors reported that for deflections above 4%, the difference between the small and the large deformation theory is 10%. McGrath (39) in 1998 conducted a study on pipe–soil interaction during backfilling. Different backfill materials were used at different compaction levels. Several soil box tests and field tests on steel, concrete, and plastic pipes were conducted to compare the results for different backfill materials, trench conditions, trench widths, and bedding materials. A point load was applied on pipe in CANDE, based on the "squeeze method," to model the horizontal effect of compaction on the pipe. This approach has limitations and does not take into account the distributive effects of the compaction force on the pipe. As explained by McGrath, modeling the soil-pipe interaction without considering the effect of compaction is not adequate, and the FEM model which doesn't consider the effect of compaction is incomplete.

Dezfooli (40) in 2013 studied the performance of large-diameter steel pipes embedded and backfilled with compacted soil material, and installed using the staged construction method which was performed by Najafi (41). One of the full-scale, experimental soil box tests conducted is shown in Figure 1-8. The properties of the material used are shown in Table 1-8, Table 1-9 and Table 1-10. The geometrical model properties of the Test 1 are shown in Table 1-11. The pipe in Test 1 was instrumented with 36 strain gauges in three sections, as shown in Figure 1-9. Each section was instrumented with 12 strain gauges. Eight of them were at the inner circumference of the pipe, 1 at the interior wall in the crown in a longitudinal direction, and 3 of them were attached to the springline and crown of the pipe at the exterior side of the pipe. The pipe was also enhanced with 10 load pressure cells to obtain the induced horizontal and vertical pressure, as well as the

44

vertical pressure on the bedding layer and on the pipe crown. Two earth pressure cells were attached to the concrete box close to either end of the pipe to study the effect of installation parallel to the direction of the pipe. Six convergence meters were used to obtain the vertical and horizontal deflection for every test.
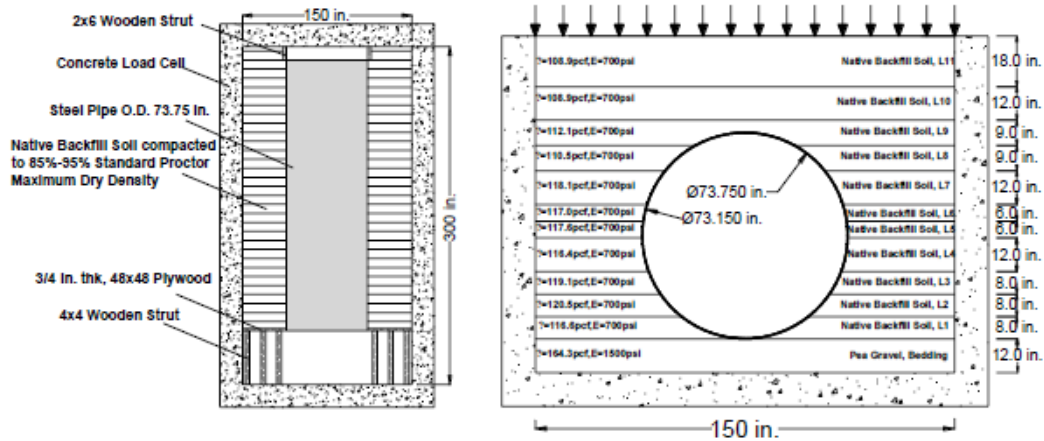
Figure 1-8 Details of soil box Test 1 based on Dezfooli (40) and Najafi (41)

Table 1-8 Steel properties, Dezfooli (40)

Behavior	**Nonlinear Plastic Model**
Density	7.7 kN/m3 (490 pcf)
Yield Stress	248 MPa (36 ksi)
Modulus of Elasticity	200 GPa (29,000 ksi)
Poisson's ratio	0.3

Table 1-9 Pea gravel properties Dezfooli (40)

Density	25. 8 kN/m3 (164.3 pcf)
Modulus of Elasticity	10.3 MPa (1500 psi)
Poisson's ratio	0.4
Angle of friction, φ	45 °

Table 1-10 Native and treated soil properties Dezfooli (40)

	Native Soil	Treated Native Soil
Soil Plasticity	Mohr Coulomb	Mohr Coulomb
Maximum dry density	17 kN/m^3 (108.1 pcf)	15.5 kN/m^3 (98.6 pcf)
Optimum moisture content	16.2 %	19 %
Un-drained cohesion, Cu	100 kPa (14.5 psi)	160 kPa (23.2 psi)

Angle of friction, φ	8.1 o	25.8o
Unconfined compression Strength	156.5 kPa (22.7 psi)	425.5 kPa (61.7 psi)
Poisson's ratio	0.3	0.3
Elastic Modulus Confining pressure=7.5 psi	4 MPa (565.6 psi)	24.5 MPa (3552.4 psi)
Elastic modulus Confining pressure=15 psi	4.35 MPa (630.9 psi)	54 MPa (7826.9 psi)
Elastic modulus Confining pressure=22.5 psi	4.5 MPa (657.03 psi)	53.1 MPa (7701.8 psi)

Table 1-11 Geometrical details of Test 1 Dezfooli (40)

Soil Layer Name	Layer Thickness (in)	Material used	Compaction
Bedding	12	Pea gravel	
Layer 1	7	Native backfill soil	92%
Layer 2	8	Native backfill soil	91.3%
Layer 3	9	Native backfill soil	91.6%
Layer 4	9	Native backfill soil	92.7%
Layer 5	7	Native backfill soil	92.2%
Layer 6	8	Native backfill soil	93.2%
Layer 7	10	Native backfill soil	92.3%
Layer 8	9	Native backfill soil	92.4%
Layer 9	11	Native backfill soil	91.3%
Layer 10	12	Native backfill soil	90.1%
Layer 11	18	Native backfill soil	
Surcharge	84	Pea gravel	
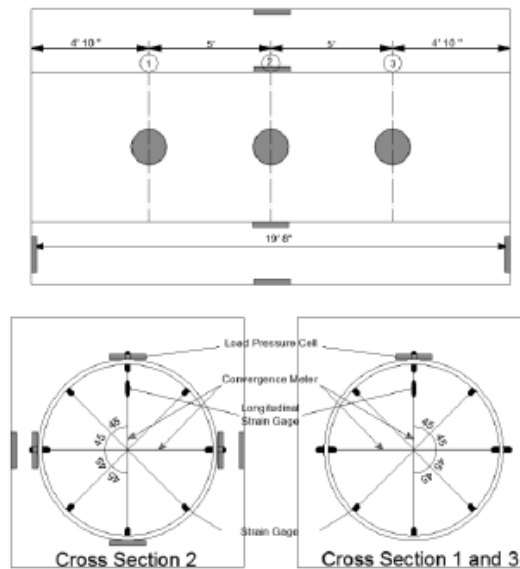
Figure 1-9 Instrumentation for Test 1 based on (40)

A comprehensive, robust, nonlinear, finite element analysis model was developed and verified by four experimental tests, which were conducted at the University of Texas at Arlington by Najafi (41) in 2012. The developed FEM model considered all three nonlinear algorithms, including geometric, material, and contact. The developed FEM model considered the soil compaction, which is an important force in staged construction modeling of the steel pipes. The geometric changes of pipes during construction were also modeled to observe the behavior of the buried steel pipes. Four instrumented large-diameter steel pipes, with diameters of 1.83 m (72 in.), were placed in a 6.1 m (20 ft.) wide rigid trench, with various backfilling configurations. The results of the study indicated that the developed model successfully reflected the experimental tests. The developed FEM model by Dezfooli at al. (42) was further modified by incorporating a flexible trench wall and other unique tools to make it capable of modeling a variety of pipeline designs. Moreover, the modified FEM model was used to verify three field tests which were conducted at the Rolling Hills Booster Pump Station, in Fort Worth, Texas. The comparison of the results showed that the modified FEM model successfully reflected the real field condition.
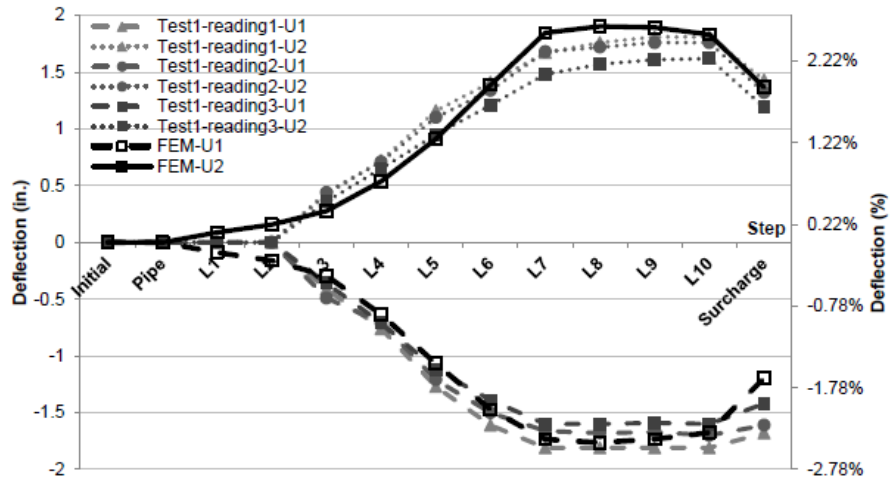
(a)
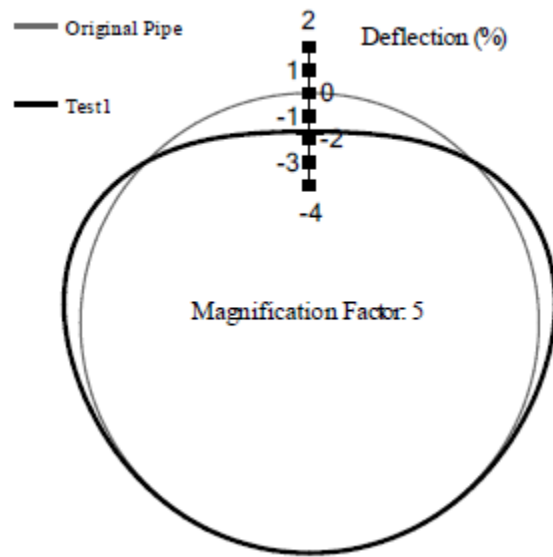
(b)

Figure 1-10 Results for deflection of the pipe (a) Experimental vs. FEM and (b) deflected shape of the pipe at the end of Test 1 based on Dezfooli (40)

48

The finite element tool used in this research was Abaqus, which is a commercial software capable of analyzing three-dimensional models and incorporating the nonlinearities and the staged construction method (43). The nonlinearities used in this work are three: material, geometry, and contact.

1.2.3.1   Material Nonlinearity

The material models with nonlinearities are explained based on the yield criteria, hardening, and flow rules, as follows:

Yield criteria: The behavior of the materials when subjected to uniaxial vs. multiaxial loading condition is different. The materials are either pressure dependent or pressure independent. For pressure-independent materials, yield criteria is defined in terms of second deviatoric stress invariants (J2), and they are independent of the first stress invariant (J1). The yielding criteria representing these materials are Tresca and Von Mises criterion, which are sensitive to deviatoric stress. For pressure-dependent materials, the hydrostatic pressure would affect the yielding. The yielding criteria follows Rankine, Mohr-Coulomb, and Drucker-Prager models.

Stress and strain tensors are composed of two parts: a spherical part associated with a change in volume, and a deviatoric part associated with a change in shape (distortion)

$\varepsilon_{ij} = e_{ij} + 1/3\varepsilon_v * \delta_{ij}$, e_{ij} is the deviatoric strain tensor, volume change or dilatation $\varepsilon_v = \varepsilon_{kk} = \varepsilon_{11} + \varepsilon_{22} + \varepsilon_{33}$

The shape of a failure surface in a three-dimensional stress space can be described by its cross-sectional shapes in the deviatoric planes and its *meridians in the meridian planes*. Cross sections of the failure surface are the intersection curves between the failure surface and a deviatoric plane which is perpendicular to the hydrostatic axis with ξ= const. (ξ,r). Meridians of the failure surface are the intersection curves between the

49

failure surface and a plane (the meridian plane) containing the hydrostatic axis with θ = const. (r,v).

The most well-known yield criteria are:

- Maximum principal stress criterion (William Rankine)

- Maximum principal strain (Adhémar Jean Claude Barré de Saint-Venant)

- Strain energy density criterion (Eugenio Beltrami)

- Maximum shear-stress criterion (Henri Eduard Tresca)

- Distortional energy density criterion (Ludwig von Mises)

- Internal friction criterion (Mohr-Coulomb)

The criteria used more often are: the maximum shear-stress criterion, the distortional energy density criterion, and the internal friction criterion. The first two criteria are mainly used to simulate ductile materials, which matches well with the experimental data, while the third one is mainly used for brittle materials. The yield criteria of the Rankine model is shown in Figure 1-11, while Tresca and Von Mises criteria are shown in Figure 1-12.
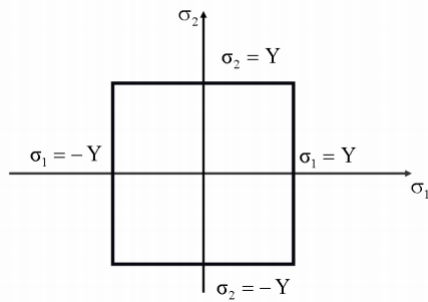
Figure 1-11 Maximum principal stress criterion - Rankine
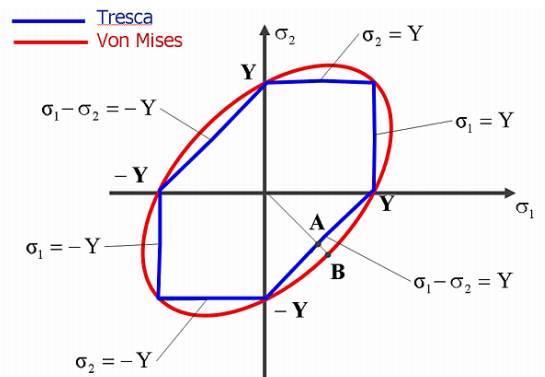
Figure 1-12 Comparison of Tresca and Von Mises criterion yield surface

Hardening: The elastic perfectly-plastic material yields the same in loading, unloading, and reloading cycles. In a material with hardening properties, the yield strength will be different in various load cycles, and will always depend on its previous loading cycles. There are three (3) major hardening theories for materials, including isotropic hardening, kinematic hardening, and mixed hardening based on Chen (44). The isotropic hardening theory assumes that the hardening is the same in all directions and the yield surface will expand symmetrically about its origin. The effect of the isotropic hardening in the stress-strain curve is shown in Figure 1-13.
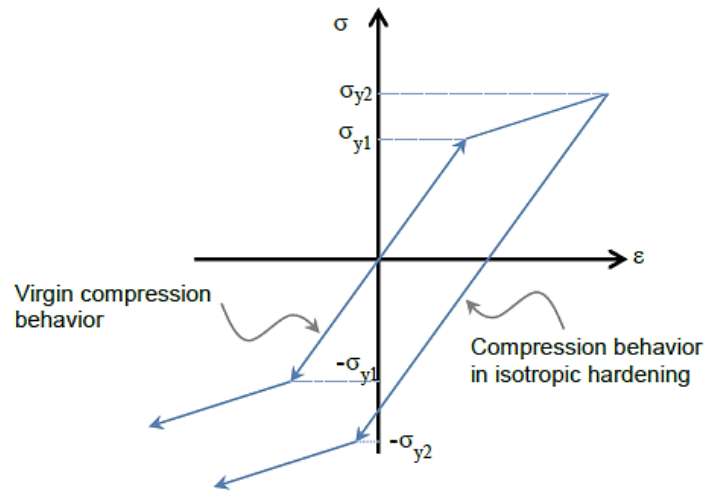
Figure 1-13 Effect of isotropic hardening on stress-strain curve

The kinematic hardening theory assumes that the hardening in one direction will decrease while the hardening in other directions will increase equally. The effect in the stress-strain curve is shown in Figure 1-14.

The mixed formulation model is a combination of both hardening theories.

Flow rule: The direction of the plastic strain increments due to the loading beyond the yield surface is defined by flow rule. For the flow rule, the plastic potential function is adopted to find the direction of plastic strain increments.

Flow rule specifies the ratio of the component of the plastic strain increment tensor, de^p, or the direction of de^p in the strain space, e_{ij}. It should be noted that the plastic strain vector corresponding to a given stress tensor, σ_{ij}, is a vector normal to the potential function. If the potential function, G, is the same as the function for yield criteria, F, then the flow rule is associated; otherwise, the flow rule is non-associated. The associated flow rule is adopted for most cases.
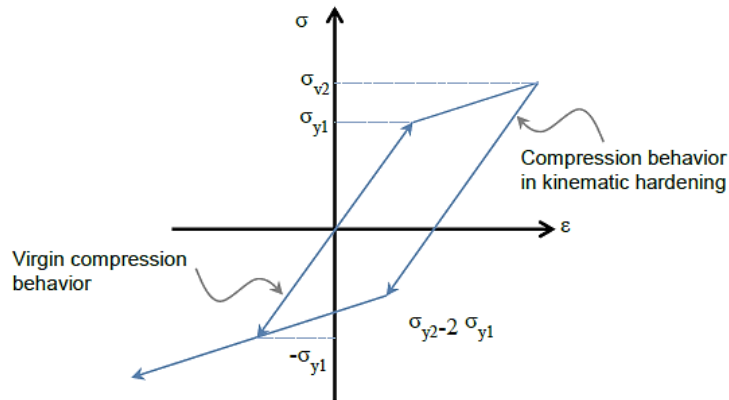
Figure 1-14 Effect of kinematic hardening theory on stress-strain curve

1.2.3.2   Geometric Nonlinearity

A problem can be defined as "small-displacement" or "large-displacement" analysis. In the "small-displacement" or "linear eigenvalue" analysis, the geometric nonlinearities are ignored in the element calculations and the kinematic relationships are linearized, based on the Abaqus Manual (45) and Shen and Lui (46). In this case, only the critical loads of the systems are defined. The behavior of the system after the critical load has been reached, or otherwise mentioned as "post buckling behavior," is not defined. In the "large displacement" analysis, the elements are formulated in the current configuration using current nodal positions. Therefore, the elements distort from their original shape as the deformation increases.

1.2.3.3   Contact Nonlinearity

For defining contacts, two algorithms are available (45); node-to-surface and surface-to-surface. For both algorithms, two surfaces should be defined, including slave and master surfaces. Generally, if a smaller surface contacts a larger surface, it is best to choose the smaller surface as the slave surface. If that distinction cannot be made, the master surface should be chosen as the surface of the stiffer body or as the surface with

53

the coarser mesh if the two surfaces are on structures with comparable stiffness. The stiffness of the structure and not just the material should be considered when choosing the master and slave surfaces. For example, a thin sheet of metal may be less stiff than a larger block of rubber even though the steel has a larger modulus than the rubber material. If the stiffness and mesh density are the same on both surfaces, the preferred choice is not always obvious.

The choice of master and slave roles typically has much less effect on the results with a surface-to-surface contact formulation than with a node-to-surface contact formulation. However, the assignment of master and slave would have a significant effect on performance with surface-to-surface contact if the two surfaces have dissimilar mesh refinement; the solution can become quite expensive if the slave surface is much coarser than the master surface. Also, for each algorithm, the tracking approach should be selected. There are two different tracking approaches available. The first one is finite sliding, which is the most general and allows separation and sliding of finite amplitude and arbitrary rotation of the surfaces. The second approach is small sliding, which assumes that although two bodies may undergo large motions, there will be relatively little sliding of one surface along the other one.

1.2.4   Parametric Study

A comprehensive parametric study was also conducted by identifying the most common geometric and force-related parameters for large-diameter pipe-soil interaction systems. The parametric study models were generated by using a design program (DP), which was developed specifically for this study, to support the main FEM model analysis. The DP allows the designer to feed the developed FEM model with the required design parameters, which will generate the FEM model in a fraction of time compared to conventional manual model development. The results of the parametric study were used

to develop a series of design equations for moment, thrust, shear, and horizontal and vertical deflection of buried steel pipes as a function of independent variables, which were comprehensively identified. The developed equation will be a platform to be used in the steel pipe design manuals.

1.3   Goals and Objectives

The main goal of this study was to understand the behavior of buried large diameter steel pipes with CLSM. For reaching the final goal, four sub-objectives were analyzed and investigated, and their combination led to fulfilment of the initial goal.

The four sub-objectives were:

1. On-site measurements of the pipe's deflection during the installation with the staged construction method. This procedure was applied to the site of a full scale construction project located in Kennedale, Texas.

2. Simulation of the staged construction of the large-diameter steel pipe with the finite element analysis method, and verification of the model through the results from the experimental analysis.

3. Investigation of the CLSM material properties in a controlled laboratory environment through compression, tensile, and triaxial testing. Mix designs for different cement percentages were developed and tested.

4. Conducting a full parametric study with 3400 cases through regression analysis and equation development to predict the maximum values for horizontal and vertical deflection, moment, thrust, and shear.

1.4 Dissertation Contribution

To this date, no study on the behavior of large diameter steel pressure pipes with CLSM has been reported. Design engineers critically need a holistic understanding of this complex soil-CLSM-pipe interaction behavior for different pipe diameters and thickness, different CLSM heights, and trench configurations and widths. The results of this paramount study funded by the Tarrant Regional Water District and the Water Research Foundation will provide the engineering designers with equations and tools that will enable them to perform informed design. This, coupled with its adaptation to the future design specifications for pressure pipes, will globally impact engineers, academicians, and others in the scientific arena. This dissertation is completely in line with two of the University of Texas at Arlington's strategic plans of global environmental impact and data-driven discoveries.

1.5   Structure of Dissertation

This study is divided into six (6) chapters. The three main goals of this research were to investigate and compare the methods available for measuring the deflection of the pipe in the installation site, to produce and test the properties of CLSM in a controlled laboratory environment, and to simulate the staged construction method with FEA. The dissertation structure, therefore, is built based on the composition of the main goals. A literature review is presented in the first chapter, which summarizes previous work conducted relative to this research. The literature review is separated into three different sections, based on the subject of every goal. In the second chapter, the methods used and the results of the experimental measurement of the pipe's deflection at the site are explained. In the third chapter, the finite element algorithms and methodology used to simulate the trench configuration, similar with the one at the site, is introduced. The comparison of the finite element results with the experimental analysis are also shown. In the fourth chapter, the mix design of CLSM produced at the laboratory is analyzed, and the testing of the properties, based on the ASTM standards, is reported. The fifth chapter presents the parametric study conducted, and the equations developed which predict the vertical and horizontal deflection, the maximum moment, thrust, and shear of the buried large diameter steel pipe with CLSM. A discussion on the findings of this work, along with limitations of this study and recommendations for future work, are presented in the last chapter.

In Figure 1-15, the work conducted for this study is also shown in a flow chart view.

```
                        ┌─────────────────────┐
                        │  Design Equations   │
                        └──────────┬──────────┘
        ┌──────────────────┬───────┴────────┬──────────────────┐
┌───────┴────────┐ ┌───────┴────────┐ ┌─────┴──────────┐ ┌─────┴──────────┐
│  Experimental  │ │ ASTM Test for  │ │ Finite Element │ │    Detailed    │
│  Measurements  │ │     CLSM       │ │   Analysis     │ │ parametric study│
└───────┬────────┘ └───────┬────────┘ └─────┬──────────┘ └─────┬──────────┘
```

Experimental Measurements	ASTM Test for CLSM	Finite Element Analysis	Detailed parametric study
MOP-119	Flexure ASTM C78	Intial Model	Pre and Post processor
Photo Profiler	Compression ASTM D4832	Unknown Variables Set	Sensitivity study
Video Profiler	Confined Triaxial	Final Model	Regression Analysis

Figure 1-15 Dissertation work structure flow chart

Chapter 2

EXPERIMENTAL MEASUREMENT OF DEFLECTION FOR LARGE-DIAMETER

STEEL PIPES WITH CONTROLLED LOW-STRENGTH MATERIAL (CLSM)

2.1   Project Information

The techniques used to measure the deflection of large-diameter steel, buried pipes with mortar lining, installed with the staged construction technique are presented in this chapter. The staged construction installation method is generally used for large-diameter pipes, where the backfilling materials are applied and compacted into layers. The application of each layer is considered a different stage and is closely dependent on the properties of the previous layer.

The two-mile long section, analyzed in this study, connects the Kennedale reservoir to the Arlington outlet in the state of Texas. It is part of the Integrated Pipeline Project (IPL), a project undertaken by the Tarrant Regional Water District (TRWD) and the City of Dallas Water Utilities (DWU). It is 150 miles long, and is runs from Lake Palestine to Benbrook Lake, as shown in Figure 2-1. This project will integrate the TRWD's existing pipeline with the Dallas system to provide up to an additional 350 million gallons per day of raw water to North Central Texas. This project will save an estimated $500 million in capital expenses and potentially $1 billion in energy savings over the entire life of the project. The section analyzed in this study was a 2-mile long section, called Line J, which was constructed in a way to facilitate the investigation of the pipe's deflection after each construction stage Since this section was a real project, the coordination of the construction and research teams was an added challenge.

Based on the pipe's designers, the geometrical characteristics of the two-mile section are: (a) the length of the joints ranged from 24 to 50 ft. (7.3 to 15.3m), depending on the topology of the site; (b) the internal diameter was equal to 108 in.; (c) the thickness

60

of the pipe was 0.47 in. (12 mm); and (d) the thickness of the mortar lining was 0.5 ± 1/6 in. (13 ± 4mm). The backfill material consisted of Controlled Low-Strength Material (CLSM) and compacted native soil. The construction stages were: pipe placement, CLSM at a height of 30% of the pipe's diameter, CLSM at 70% of pipe's diameter, and full backfill, as shown in Figure 2-2.
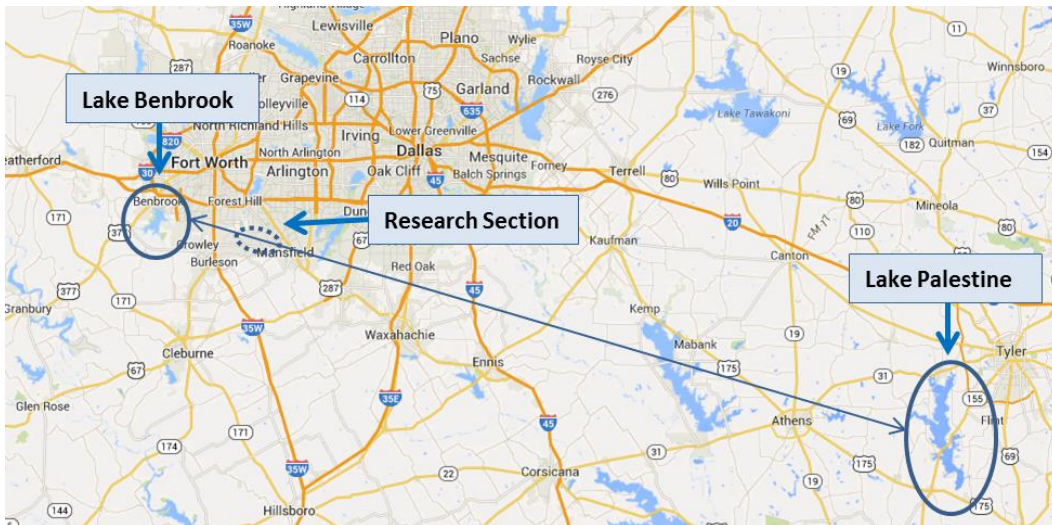
Figure 2-1 Location of lakes connected from the Integrated Pipeline and the section investigated in this research

The trench excavation at the bottom was half circular, reaching the surface with an inclined slope, as shown in Figure 2-2 (a). The trench width varied from 13 to 17.3 ft. (3.9 to 5.3 m), with the wider opening at the joints since extensive construction activities were taking place at the location of the pipeline's joints. For controlling the placement of the pipe, sand bags were placed as supports at three locations along the pipe, as shown in Figure 2-3 (b). The pipe, placed and filled with CLSM at 30% of the pipe diameter, is shown in Figure 2-3 (c). CLSM was used for the pipe bedding up to 70% of the pipe diameter. For the rest of the backfill, the native soil was used, as shown in Figure 2-3 (d). The loading applied to the pipeline was the weight of the backfill materials. There were several sections of the pipeline where live loads were applied from passing cars on the street above. A

sketch of a trench section perpendicular to the length of the pipeline is showed in Figure 2-2. Also shown are the pipe, the trench, the CLSM layer, the backfilling, and the in-situ material. Well-constructed connections were one of the important factors for the successful operation of the pipeline.
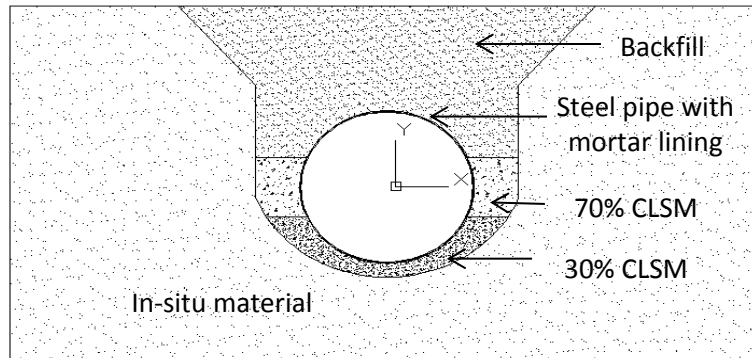
Figure 2-2 Materials used for the backfilling of the pipeline

Three measurement techniques were considered for measuring the pipe deflection: MOP-119 from the American Society of Civil Engineers (ASCE), a photo laser profiler, and a video laser profiler. A 518 ft. section, called the prove-out section, which was part of the two-mile section, was measured using all three methods. The main goal was to compare the results from the three methods and identify the experimental technique which was more accurate for calculating the deflection of the buried large-diameter steel pipes with mortar liner.

(a)

(b)

(c)

(d)

Figure 2-3 Pipe installation (a) trench before pipe placement, (b) placed pipe and details of the support, (c) placed pipe with 30% of the diameter filled with CLSM, and (d) installed pipe backfilled with native soil

The first section measured was a 518 ft. section, called prove-out, which is shown in Figure 2-4, in red. The analytical schedule of the construction activity is shown in Table 2-1. The measurements were conducted on the day that each construction staged activity was completed. Daily reports were prepared after each site visit, with an analytical explanation of the site activities. A team of at least five people were present at the site for each of the experimental measurements. Three methods were used for this section: MOP-119, photo laser, and laser profiler methods.
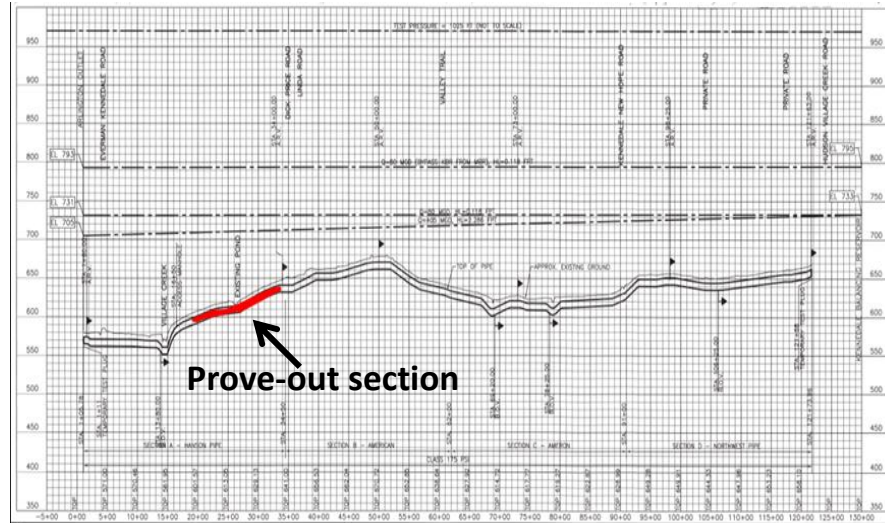
Figure 2-4 Level map of the 2-mile pipeline and location of prove-out section shown in red

Table 2-1 Schedule of site measurements activities

		0'100'	100'-200'	200'-300'	300'-400'	400'-500'
Activity and measurements	**Pipe installation**	Monday, August 19,2013	Monday, August 19,2013	Monday, August 19,2013	Tuesday, August 20,2013	Tuesday, August 20,2013
	30% CLSM	Tuesday, August 20,2013	Wednesday, August 21,2013	Wednesday, August 21,2013	Wednesday, August 21,2013	Thursday, August 22,2013
	70% CLSM	Thursday, August 22,2013	Friday, August 23,2013	Friday, August 23,2013	Friday, August 23,2013	Saturday, August 24,2013
	Full Backfill	Saturday, August 24,2013	Saturday, August 24,2013	Monday, August 26,2013	Tuesday, August 27,2013	Thursday, August 29,2013

2.2   Experimental Techniques Used for Deflection Calculation

The deflection of buried pipe constructed with the staged method was measured.

Experimental measurements were conducted at the prove-out section with three different

methods: MOP-119, a photo laser profiler, and video laser profiler. The most accurate

method was selected for measuring the two-mile section.

The site measurements required safety clothing and measurement equipment. The measurements were conducted inside the pipe, after each construction activity, as mentioned above and shown in Table 2-1. The access of the personnel and measuring equipment was through manholes, as shown in Figure 2-5. The manhole was concrete, circle-shaped, with a diameter of 30 in. One or two connected steel ladders were used for entering or exiting the pipe. Hardhats, steel-toed shoes, and fluorescent jackets were required for all personnel entering the pipe, as shown in Figure 2-6.

(a)

(b)

Figure 2-5 Personnel entrance-exit manhole; (a) from outside the pipe, (b) from inside the pipe
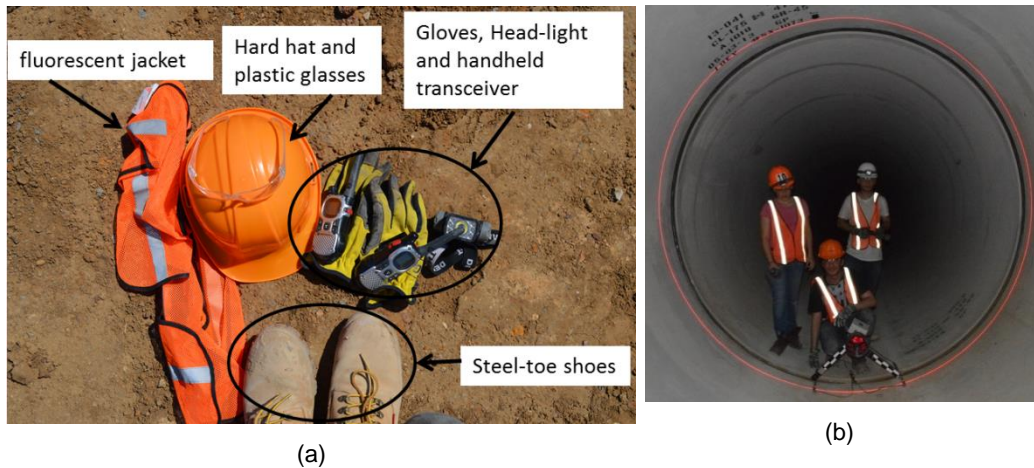
Figure 2-6 (a) Personnel safety clothing required for entering the pipe, (b) personnel inside the pipe

2.2.1   *American Society of Civil Engineers – MOP-119*

The MOP-119 method is based on ASCE's "Manuals and Reports on Engineering Practice" No. 119, and it is used for calculating the deflection of the pipe at every construction stage. Due to the complexity of this method and the need to measure and report each and every point of interest, only a 518 ft. (157.9 m) prove-out section was investigated using this method. The prove-out section had three different length joints, as shown in Table 2-2 and Figure 2-7. Depending on the joint length, 3 or 5 sections were measured for each pipe, as reported in Table 2-2. For each section, two (2) locations were measured using MOP-119, as shown in Figure 2-8 (a). The 90° (springline) and 45° measurements were used for calculation of the maximum deflection of the pipe. The 45° from the crown of a pipe was selected because the maximum stress was expected to occur in that section, which was approximately where the 70% CLSM layer ended. According to the MOP-119, the maximum reading from this method should be used as the radius of the curvature of the pipe. Subsequently, the maximum deflection of the pipe should be obtained by using the graph provided in MOP-119, which is shown in Figure 2-9.

66

Table 2-2 Section measured at the prove-out section

Pipe Number	Length, ft.	Sections per pipe
1066-1072 and 1075-1076	50	4
1073	44	4
1074	24	3
Total	**518**	**43**

The measurements were performed by using a digital caliper attached to a 24 in. (610 mm) rod, as shown in Figure 2-10 schematically, and in Figure 2-11 (a) and Figure 2-11 (b) at the time of measurement inside the pipe. The location of sections of each pipe and the 45° and 90° were measured and marked, so that the same sections could be measured at every stage. The caliper was carefully attached to the marked points. The calculation of the radius of the curvature of the pipe was carried out using the procedure suggested by the MOP-119 (2009). In this method, as shown in Figure 2-8 (a and b) and Figure 2-10, the distance of e was measured by placing a rod with a constant length of L at the two locations of each section. Hence, the radius of curvature of the pipe, r, can be calculated using Equation 4. For estimating the maximum deflection of every measured section, a graph provided from the MOP-119 method, as shown in Figure 2-9 , was used. The maximum estimated deflection for each section was the maximum of the two deflections estimated.

$$r = \frac{4e^2 + L^2}{8e}$$

Equation (4)
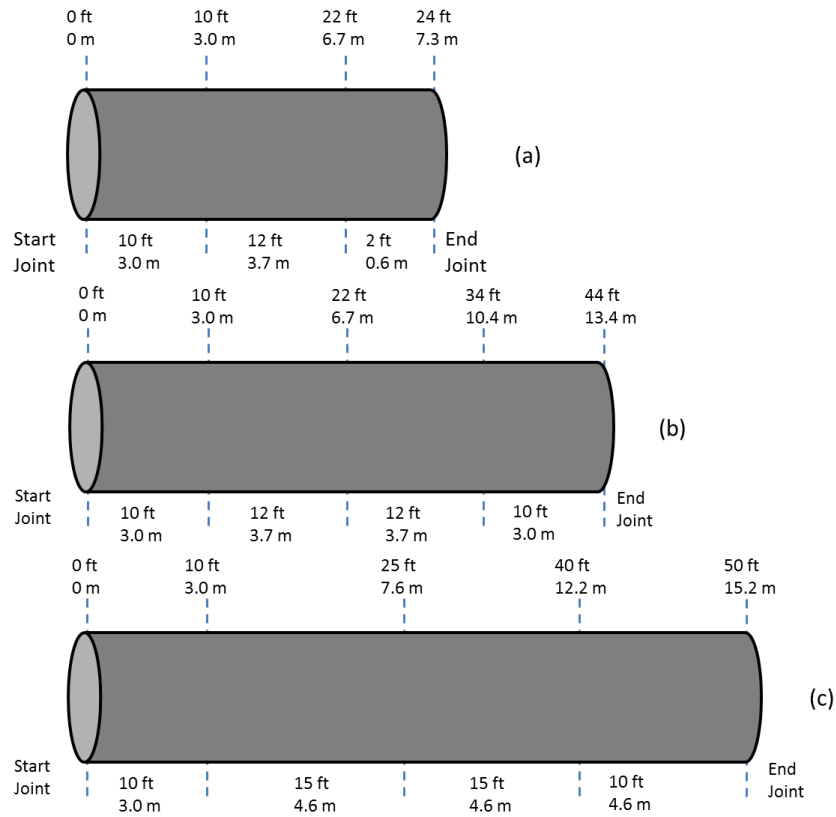
Figure 2-7 Joints analyzed with MOP-119 method (a) 24ft (7.3 m), (b) 44ft (13.4 m) and (c) 50ft (15.2 m) joints length
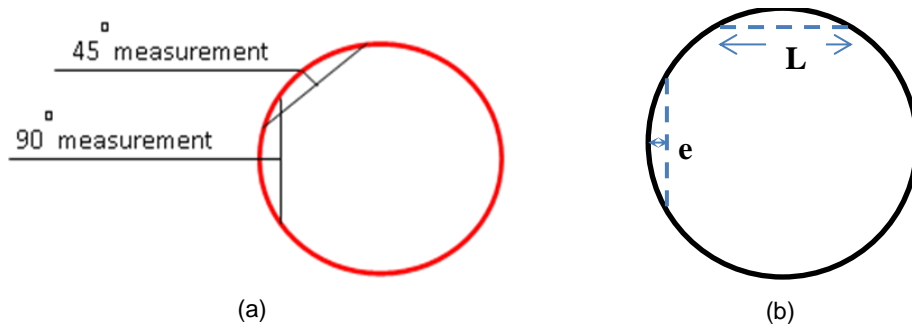
Figure 2-8 (a) Location of the measurement to calculate the radius of curvature by using MOP-119 method; and (b) required measured distance e
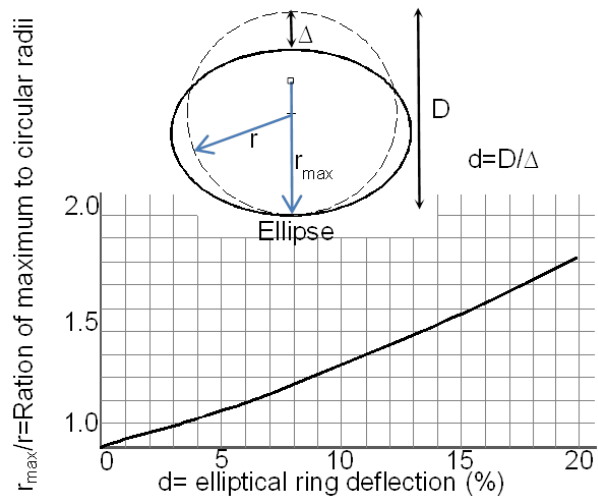
Figure 2-9 Relationship of ratio of radii to elliptical ring deflection (MOP-119)
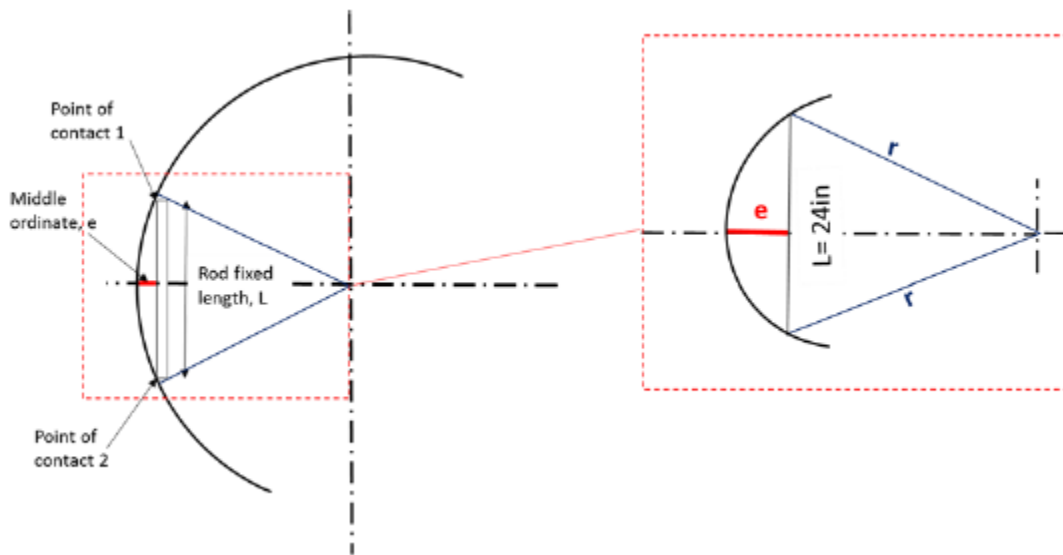
Figure 2-10 Schematic of MOP-119 method
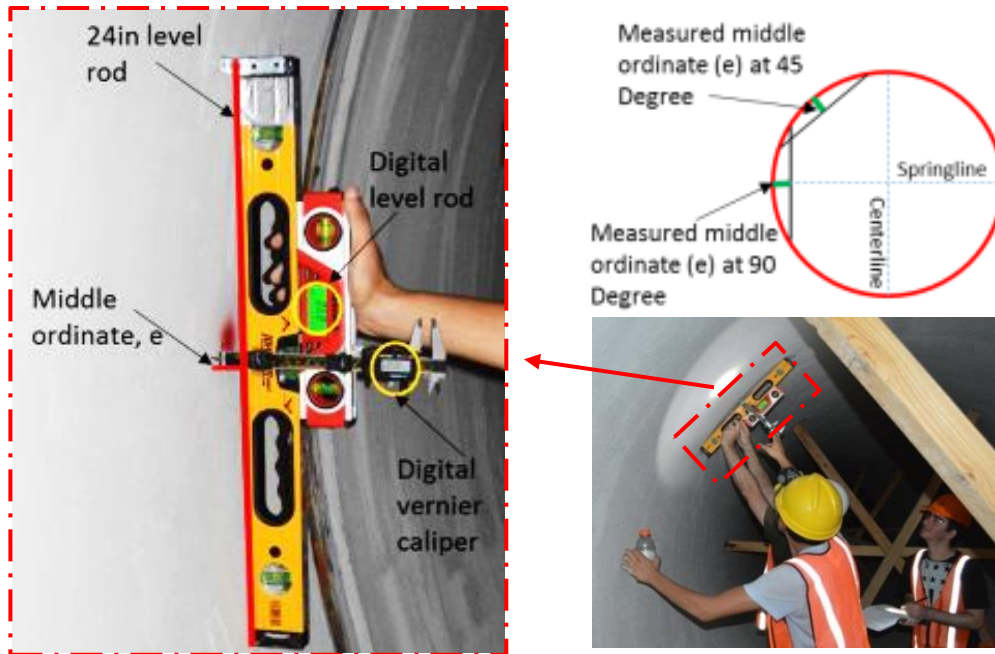
Figure 2-11 MOP-119 deflection measurement equipment; (a) caliper attached to a 24 in. rod and (b) measurement at 45 degree section inside the pipe

2.2.2   Photo Laser Profiler Method

Buried flexible pipes constructed with the staged method are subjected to non-uniform forces because the backfilling materials are applied in stages and they do not have the same mechanical properties. This causes non-uniform deflections on the pipe during construction, which can sometimes lead to failure. To reduce these deflections, wooden stulls are usually installed in the pipe until the end of the construction activities, as shown in Figure 2-12.

The deflection measurement of the pipe with the laser profiler method was conducted by the use of a camera attached to a robot, a ten-head laser ring standing on a skid frame, and a photo camera or a recording center. For the photo profiler method, a ten-head laser ring standing on a skid frame, a scale, and a photo camera were used. as shown

in Figure 2-14. A ring of laser light was projected onto the interior surface of the pipe, perpendicular to the longitudinal axis of the pipe. The sections measured with this method are the ones shown in Figure 2-7. A typical photo, with and without stulls, is shown in Figure 2-13. For calculating the deflection of the pipe, each picture was imported into an image processing computer program, and the vertical and horizontal deflection was calculated as shown in Figure 2-15.

(a)   (b)
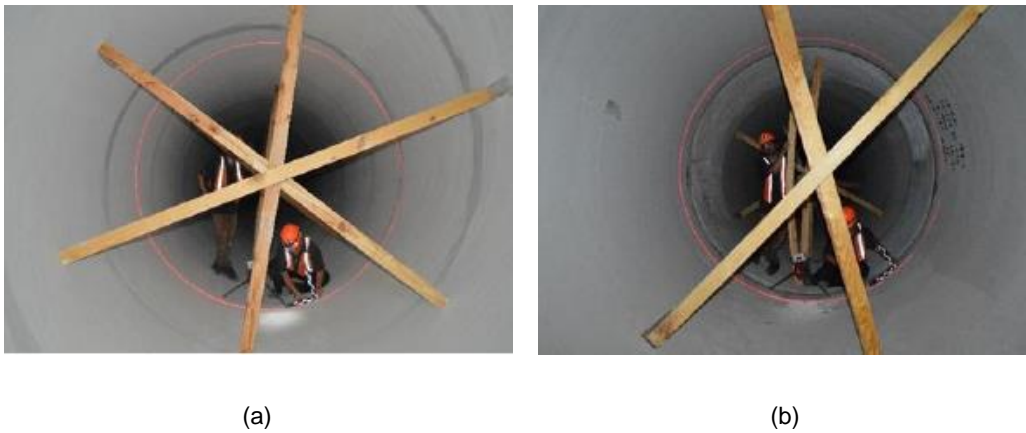
Figure 2-12 Wooden stull configuration; (a) three legs, and (b) crossed

(a)   (b)
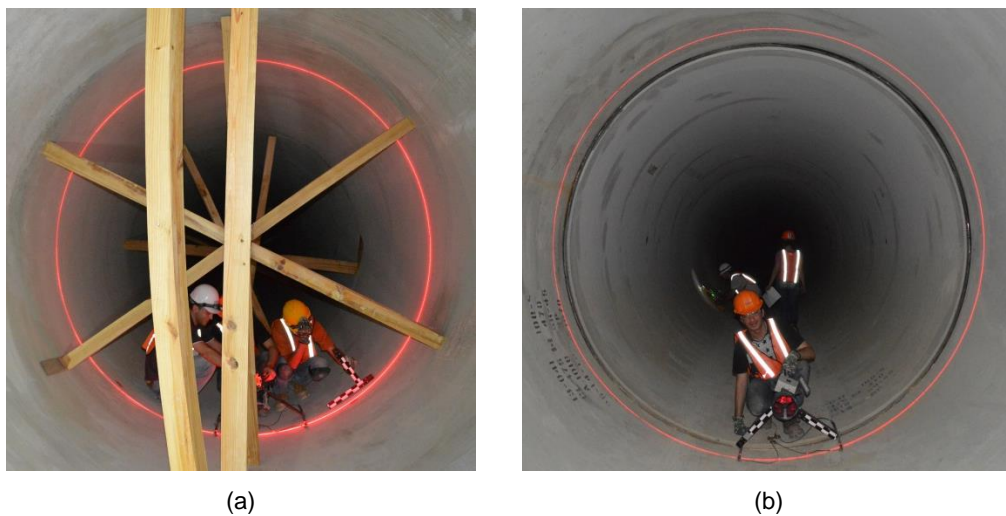
Figure 2-13 Photo profiler method (a) with wooden stulls, (b) without wooden stulls

(a)

(b)

(c)

Figure 2-14 Equipment used for photo laser profiler method: (a) scale, (b) ten-head laser ring standing on a skid frame, and (c) high resolution digital camera
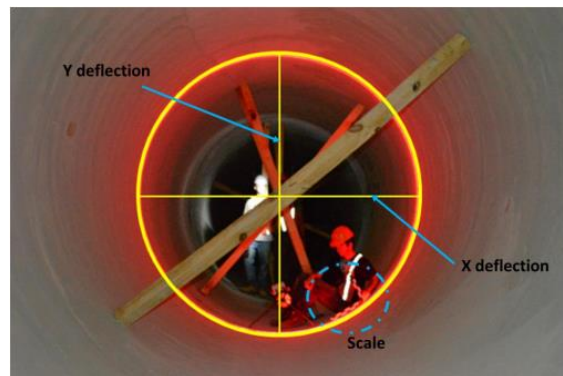
Figure 2-15 Laser photo profiler analysis method; Fitted line on the laser ring for measuring X and Y displacement

2.2.3   Video Laser Profiling Method

This method is devoted to quantitative evaluation of the behavior of the pipelines, which is the calculation of the percentage of deformation of the pipes. The equipment used was a ten-headed laser attached to a skid frame, and a video camera attached to a robot and a control and recording center. In this technique, a ring of laser light was projected onto to the interior surface of the pipe, as with the photo laser profiler method. The laser profiling unit was placed at the end the section to be measured and was pulled back toward the recording center. The path of the robot could be supervised and recorded at the recording center. A sketch of the connection of the equipment and pictures with the equipment are shown in Figure 2-16. The robot and the laser head were connected with a chain so that the distance between them would remain constant. Keeping a constant distance was required so that the scaling of the data processing phase would be set only at the beginning of the analysis. The distance between the recording center and the robot varied from 0-500 ft. An automatic speed controller was used to keep the speed of the robot pace constant. Light was not allowed throughout the whole section measured to maximize the clarity of the ring; although, in some part, light was used for clearing the robot's path.

The acquired results were processed using software provided with the laser profiling unit. The measured data was transformed to actual data with the use of the scale, shown in Figure 2-14 (a). During the post-processing stage, the change of the pipe's diameter, in vertical and horizontal directions, or the deformation of the pipeline was calculated as a percentage variance from the initial internal diameter. The maximum and minimum deflection of the pipe was also calculated.

CONTROL AND RECORDING CENTER   **ROBOT AND CAMERA**   **LASER**
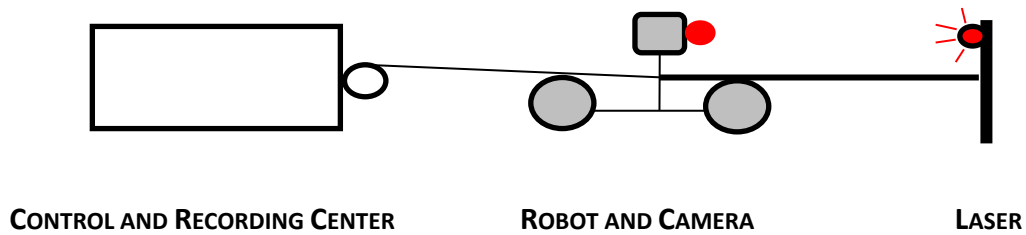
Figure 2-16 Video laser profiler equipment and connection for measurement

2.3   Experimental Measurements Techniques Results and Discussion

Three methods were used for this section: MOP-119, photo laser, and laser profiler. The MOP-119 method and the photo profiler method were conducted where stulls were present inside the pipe. On the removal of the stulls, which was at the last stage of activities, the laser video profiler method was used to measure the deflections of the pipe. The main outcome of the experimental deflection measurement of the prove-out section was the selection of the most accurate and suitable method for the deflection measurement of the 2-mile section.

2.3.1   *American Society of Civil Engineers – MOP-119*

For defining the percent of horizontal and vertical deflection of the pipe with the MOP-119 method, the distance e was measured, as shown in Figure 2-8 and Figure 2-11. From Equation 4, the radius of the measured location was calculated by importing the measured distance e and the length of the rod L. The maximum deflection of the pipe was calculated from the provided graph in MOP-119, also shown in Figure 2-11. This procedure

was followed for both measurements at each of the 43 measured sections, as shown in Figure 2-8 (a). The maximum percent deflection, for each section measured for the five construction stages, is presented in Figure 2-17. At the horizontal axis, the length of the prove-out section is presented, while at the vertical axis, the percent deflection of the pipe is presented for each measured section. The dashed line represents the 2% maximum deflection of buried steel pipes with mortar lining allowed by AWWA. In

Table 2-3 the average percent deflection of the pipe is presented for each construction stage.

It can be concluded that, according to MOP-119, the pipe did not follow the required standards since the deflection for almost all the construction stages was higher than the 2% limit.
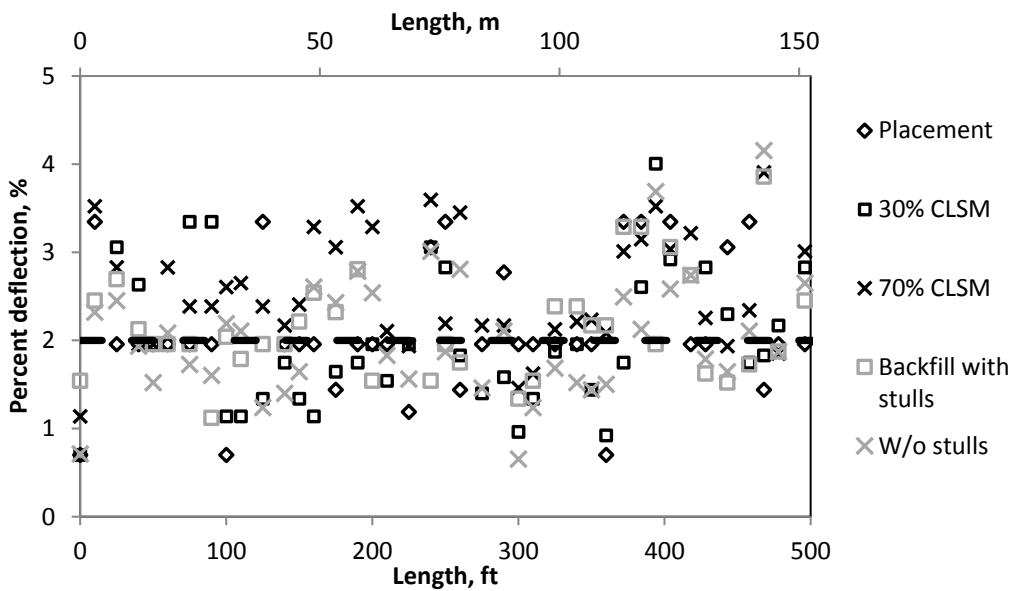
Figure 2-17 MOP-119 percent deflection at every construction stage

Table 2-3 MOP-119 average calculated deflection

MOP-119	
Construction Stage	**Average change (%)**
Placement	2.3
30% CLSM	2.2
70% CLSM	2.6
Backfill (stulls)	2.1
Backfill (w/o stulls)	2.2

2.3.2   Photo Laser Profiler Method

The data processing for this method requires importing each picture into an image-processing computer program. The horizontal and vertical percentage of deflection of the pipe was calculated, and the results are presented in Figure 2-18 and Figure 2-19, respectively. In both figures, the horizontal axis represents the longitudinal length of the prove-out section, and the vertical represents the percent deflection of the pipe. The average values are also shown in Table 2-4. It can be observed that the average horizontal deflection of the pipe at the 70% CLSM stage was smaller than at the placement stage, a change from 0.47% to 0.29%, which can be translated as a squeezing of the pipe at the springline towards the inside direction, due to the application of the CLSM layer. The reverse can be concluded from the results of the vertical deflection, which was greater than the previous construction stage - a change from 0.51% to 0.37%. Also, the horizontal deflection of the pipe at the backfill application was greater than that at the 70% CLSM stage, a change from 0.29% to 0.47%, which means that the pipe was deflected towards the outside direction. The reverse was observed with the deflection at the vertical direction, with average deflection reduced from 0.37% to 0.50%. It was also observed that the

removal of the stulls didn't cause any significant change in the pipe's deflection in either direction, as the average percent deflection changed in a range of 0.05% and 0.02%.
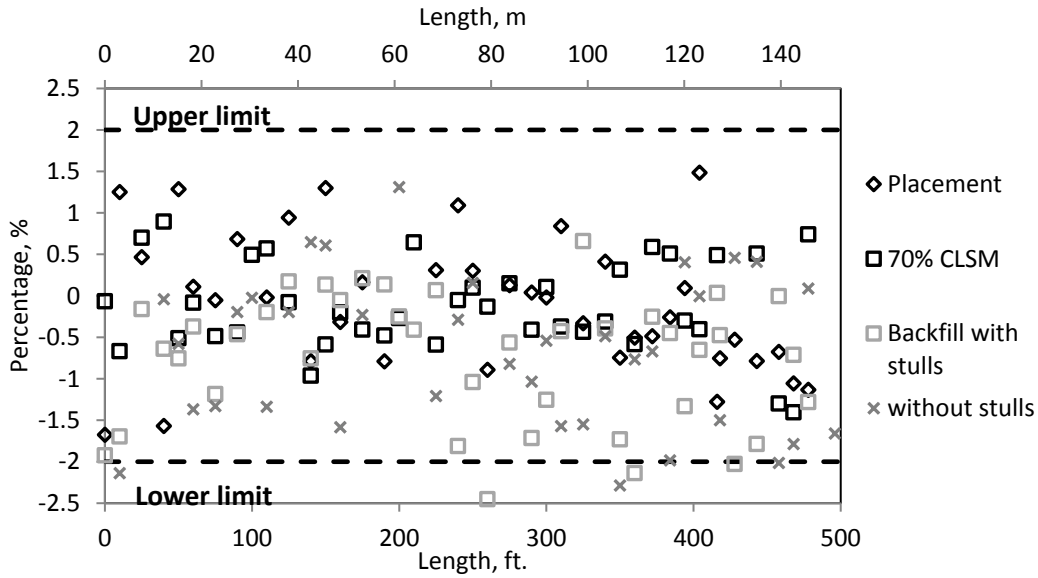
Figure 2-18 Horizontal deflections using the laser photo profiling method at different stages of the pipeline
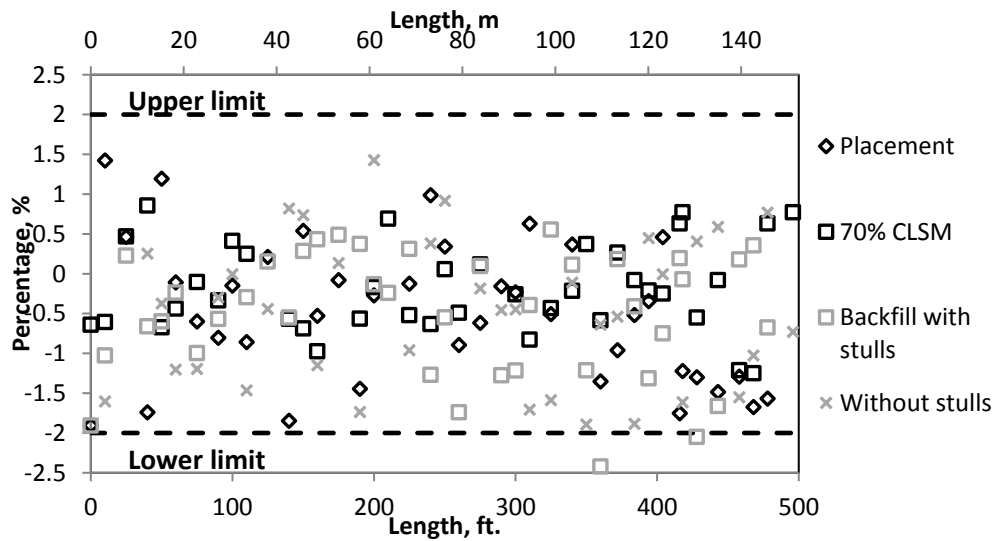
Figure 2-19 Vertical deflections using the laser photo profiling method at different stages of the pipeline

Table 2-4 Average measured deflections with photo laser profiler method

Construction Stage	Horizontal Percent Deflection (%)	Vertical Percent Deflection (%)
Placement	-0.47	-0.51
70% CLSM	-0.29	-0.37
Backfill with stulls	-0.47	-0.51
Backfill w/o stulls	-0.42	-0.48

The horizontal and the vertical deflection of three sections along the prove-out section are shown in Figure 2-20 and Figure 2-21, respectively. Section 1 was located at the first joint, Section 2 was located at the third joint, and Section 3 was located at the seventh joint of the prove-out section. All sections were located 25 ft. from the beginning of each joint. The horizontal axis represents the construction stage, while the vertical represents the percent deflection. The percent deflection of the pipe was calculated with respect to the placement stage.

At the 30% CLSM stage, the vertical deflection of the pipe was increased compared to the previous stage, due to the pressure imposed from the CLSM to the pipe, as shown in Figure 2-21. During the full backfill stage, the vertical deflection of the pipe was decreased due to the weight of the backfilling material that brought the pipe closer to its initial shape. At the last stage, with the removal of stulls, the deflection of the pipe was not critical compared with the placement stage. This indicates that at the stull removal stage, the support provided at the pipe was not important.

In Figure 2-21, the pipe at the 70% CLSM stage has negative horizontal deflection and positive vertical deflection. This was caused by the load applied from the CLSM layer to the side part of the pipe. When the pipe was fully backfilled, load was applied at the top of the pipe due to the weight of the backfilling material. It was observed that the horizontal deformations of the pipe were opposite to the vertical deformations results, which was

expected. It was also observed that, at the last stage, the horizontal stulls were loose and a lot of them fallen and removed, while the vertical stulls were deformed and broken in some sections, as shown in Figure 2-22.
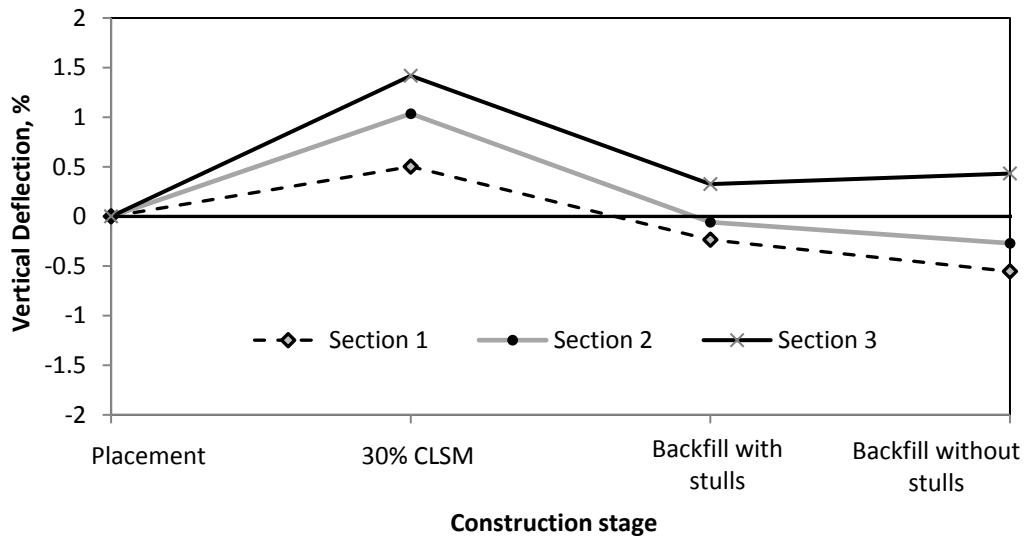
Figure 2-20 Horizontal deflection vs. construction stage for three sections with photo laser profiler method
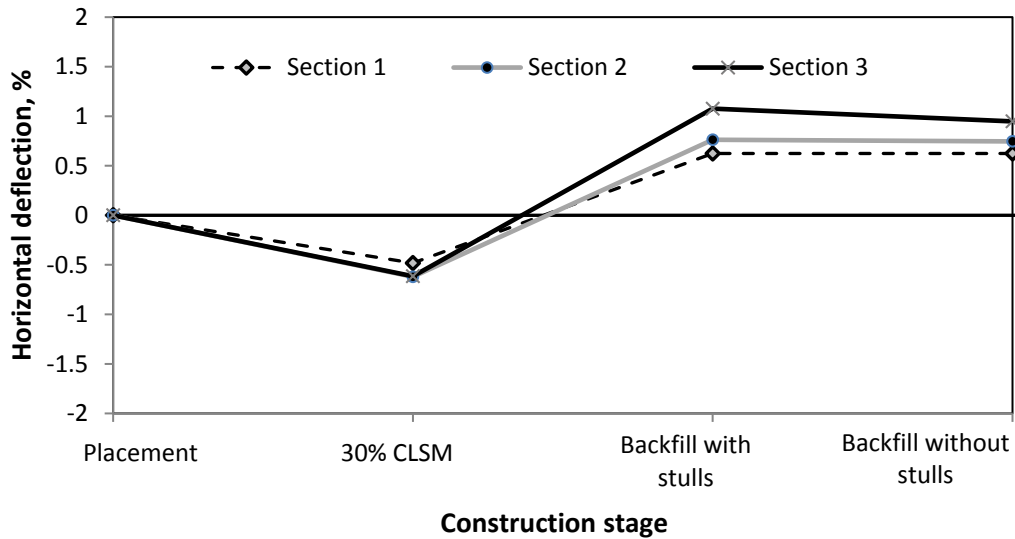
Figure 2-21 Vertical deflection vs. construction stage for three sections with photo laser profiler method

<div align="center">(a)   (b)</div>

Figure 2-22 Deformed stulls at the backfill with stulls construction stage: (a) vertical stulls remained after pipe deflection, (b) deformed vertical stulls remained

2.3.3   *Video Laser Profiling Method*

The video profiler method was applied at the pipe when the stulls were removed and the pipe was cleaned from debris. The laser ring was recorded while the robot was traveling along the longitudinal axis of the pipe. The measurements were separated into 500 ft. increments, the same as the length of the cord that connected the robot with the recording device, as shown in Figure 2-16. The recorded videos were imported to image-processing software for further analysis. A typical view of the profiler used is shown in Figure 2-23. The laser ring and the blue dots on the top of it are the points identifying the laser ring. At the right side of the main screen, the calculation of the horizontal and vertical deflection is shown with a blue line. It can be observed that in Figure 2-23 (a), the blue dots were lying on the red line of the laser, which means that the results were very close to the pipe's deflection. In Figure 2-23 (b), the main blue dots were not lying on the laser red ring. There was also a big fluctuation depicted on the result's screen, on the right side of the main screen. This was caused either by vibrations of the robot or the skid that was transferring the laser head. Since the measurements were conducted at the same time as

site activities, there were unsmoothed joints and debris inside the pipe, which was the main reason for the fluctuations shown in Figure 2-23 (b). The use of the light at some points of the measurements also caused fluctuations in the measurements, but the light was necessary because obstacles were blocking the path of the robot.

(a)   (b)
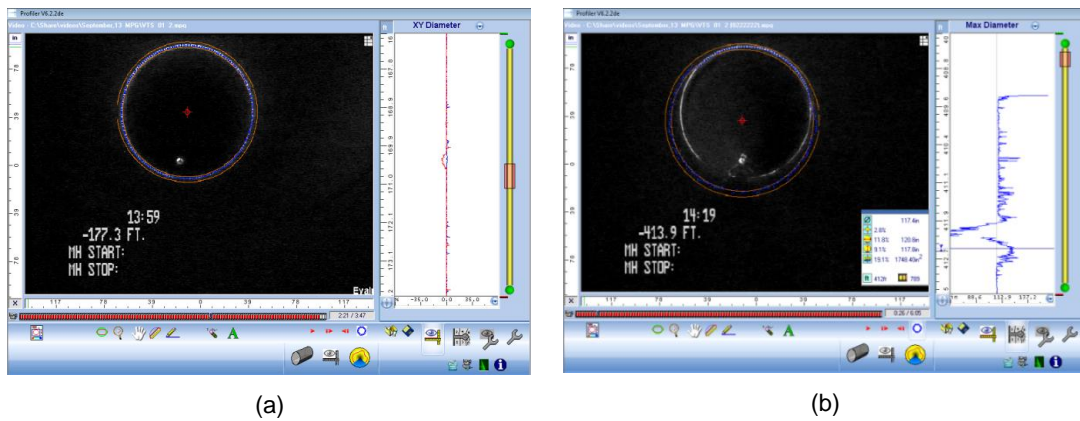
Figure 2-23 Typical view of the image-processing software: (a) accurate post-processing procedure, (b) non-accurate post-processing procedure

The prove-out section was measured with the video laser profiler method, and the percent deflection vs. the length of the measured section is shown in Figure 2-24. It can be observed that the maximum and minimum deflections measured with the video laser profiler method were smaller than the maximum 2% allowed by AWWA. The results obtained were continuous, and the exact location of each measured deflection can be identified. This is very important for on-site pipe monitoring so that the exact location of any potential excessive deflection can be easily identified.

During measurements with the laser profiling method, vibration occurred due to the uneven surface, especially close to the joint area, as shown in Figure 2-23 (b). These vibrations added a systematic error to the results. For calculating the systematic errors due to this phenomenon, measurements were conducted with a laser meter for 1500 ft. (457.2

m) at different sections, with the method shown in Figure 2-25 (b). Results from the measurements, with both the laser profiler and the laser meter, for a section of 500 ft. (152.4 m) long, are shown in Figure 2-26. The percent of difference between the continuous laser profiler method and the laser meter was calculated and shown for thirty sections in Figure 2-27. The difference in percentages ranged from 0-0.5% for both horizontal and vertical measured deflection. This difference indicates that there was a systematic error in the video laser profiler method due to vibrations caused from debris in the path of the measurements. The laser profiling method was conducted at a pipe construction site, where the conditions were not easily controlled since many contractors were working at the same time. Although there was a small systematic error in the results and heavy equipment is needed for the measurements, the video laser profiler method is recommended as an accurate method for site investigation of large-diameter pipelines.
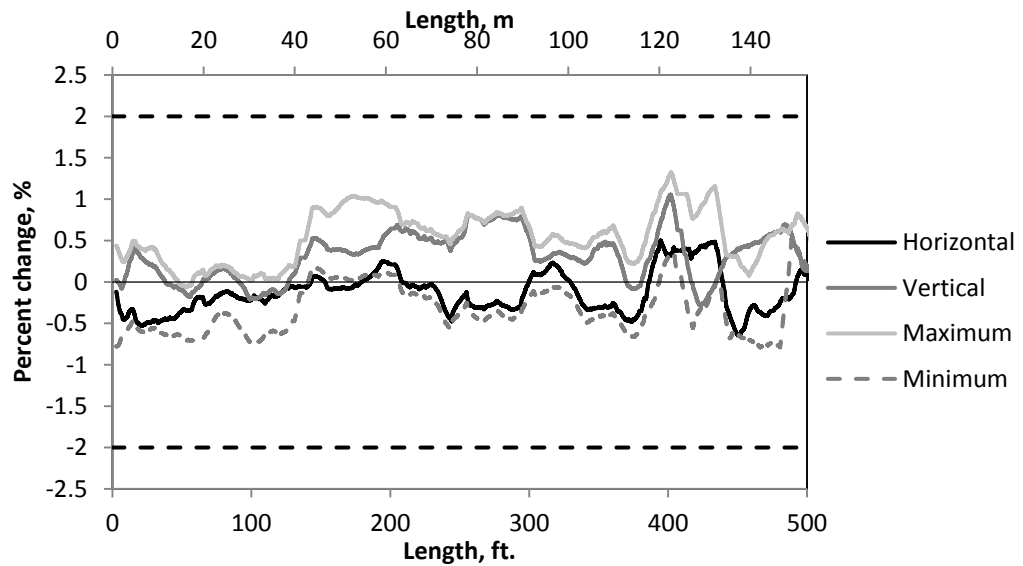
Figure 2-24 Maximum, minimum, horizontal and vertical deflection of different sections of the prove-out part with laser video profiling method

(a)   (b)

Figure 2-25 Video laser verification measurement (a) rod and (b) laser meter measurement for calculating the accuracy of the laser profiling method
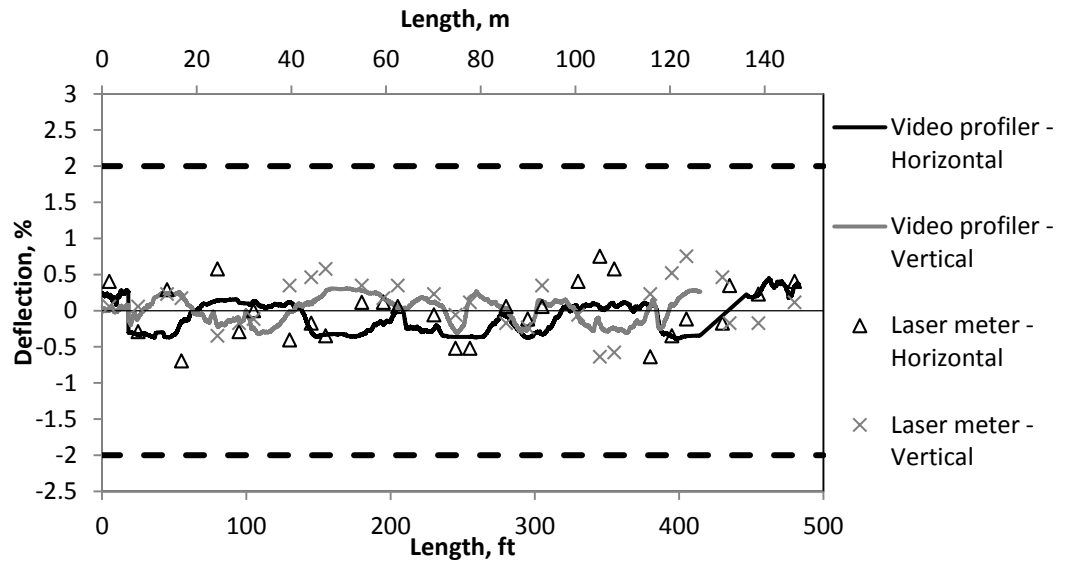
Figure 2-26 Verification of the laser video profiling method with laser meter measurements
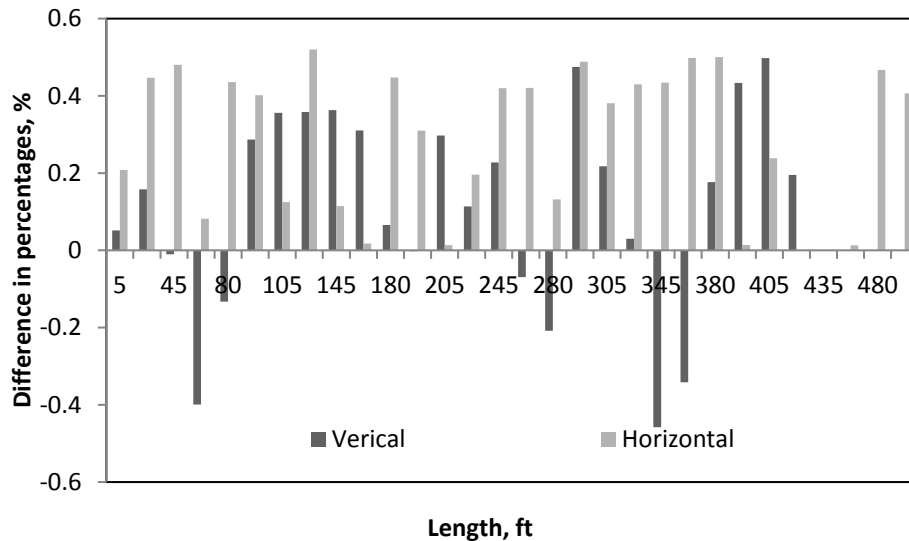
Figure 2-27 Percent difference in laser profiling method and laser meter

The x and y diameter of the 2-mile section measured with the laser video profiler are shown in Appendix 1. The graphs are shown in 500 ft. sections and the number of the pipes are mentioned so that the exact location of the measurements can be identified

2.4   Main Findings

The goal of this section was to investigate the field deflection measurement techniques for large-diameter steel pipes with CLSM. Three methods were used to measure the deflection of the pipe: 1) MOP-119, 2) laser photo profiler method, and 3) continuous laser video profiler method. The three methods were performed and the results were compared for a pipe with a length of 518 ft.. MOP-119 is an easily-applied method, introduced by the ASCE Committee on Buried Flexible (Steel) Pipe Load Stability Criteria and Design of the Pipeline Division, and is used for identifying the maximum deflection of the measured pipe section at every construction stage. The laser video profiler is a method for continuous measurement of the deflection of pipes, and is very useful for identifying the deflections of any point along the section that is measured. The laser photo profiler is a

method substituted for the continuous laser video profiler when physical obstacles are present inside the pipe.

In Figure 2-28, the deflection measured at the final stage with the laser video profiler method was compared with the percent deflection calculated with the MOP-119 method. In the same figure, it is shown that the average percent deflection of the pipe was greater than the 2% limit for the MOP-119 method and smaller for the laser profiling method. In all cases, the MOP-119 method yielded to larger deflections, which is relatively safe, but may result in rejection of otherwise acceptable pipe installations. These differences were attributed to the theoretical assumptions of a pipe buried in a homogeneous, isotropic, elastic material. An empirical graph used to define the maximum deflection, shown in Figure 2-9, is based on empirical values and not realistic values based on the site tested. This method does not account for the support provided by the mortar lining, which increases the stiffness of the pipe and leads to lower deflection. Therefore, it can be said that this method could not reflect the actual condition of the pipeline analyzed. On the other hand, the laser video profiling method was more realistic since it was performed at the site, and the real data was post-processed rather than calculated by using an empirical graph. The laser profiler methods were used to measure the actual deflection of the pipe, based on the actual condition of the pipe-backfill system, which means the measurements were more accurate and realistic.

From the comparison of the results from the three methods, it was concluded that the photo profiler and the video profiler method results were close to the actual condition of the pipe. The photo laser profiler method is recommended when stulls are present inside the pipe, while the video laser profiler is recommended for measurement after the removal of stulls.

Overall, the MOP-119 method was easier to apply at the site and post process. While comparing the accuracy of the results, the laser profiler methods were more accurate than the MOP-119 and gave a complete view of the inner condition of pipe, in contrast to the MOP-119, which provided only the maximum deflection of the pipe.
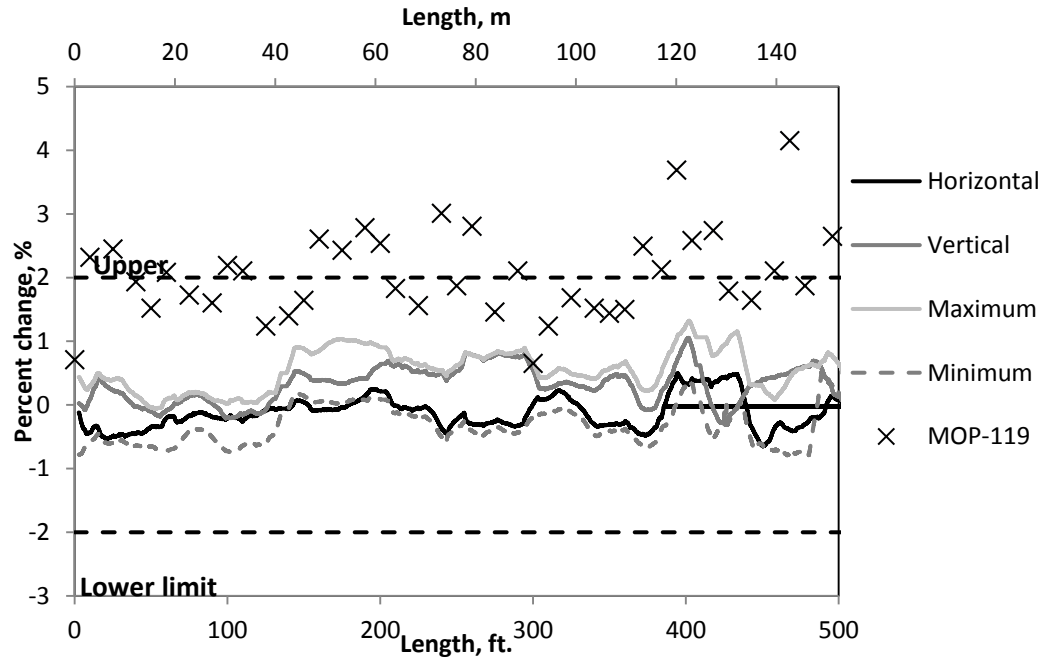
Figure 2-28 Deflection measured with laser profiling method vs. MOP-119

Chapter 3

INITIAL FINITE ELEMENT SIMULATION

The main goal of the finite element analysis was to mimic the construction activities conducted at the site for the pipe installation. The analyses were performed by using Abaqus 6.12, which is a commercial software product that analyzes implicit and explicit engineering problems. The FEM was developed similar to a FEM model developed by Dezfooli (40) at the Center for Structural Engineering Research/Simulation (CSER), as part of a project which was funded by Tarrant Region Water District (TRWD).

The staged construction procedures employed were identical to those applied at the site. The steel pipe with mortar lining was buried in a 14-ft wide trench and backfilled until it reached the ground surface. The geometry of the trench, pipe, and soil layers was measured at the site and simulated accordingly in the FEM model. Controlled Low Strength Material (CLSM) was used as backfill to 70% of the pipe's diameter, while the rest was backfilled with compacted soil materials. The sequence of each applied layer at the site was defined as the activation or de-activation of each layer at the FEM staged construction. The boundary conditions and the loading were applied in such a way as to ensure the simulation of the real site conditions.

The construction stages that were simulated in the FEM model are as follows:

- Placement of the pipe with mortar lining

- Placement of CLSM up to 30 percent of the pipe's outside diameter (O.D.)

- Placement of CLSM up to 70 percent of the pipe's O.D.

- Placement of the select fill up to three inches above the pipe's crown

- Simulation of the compaction force applied by the select fill to the pipe

- Placement of the soil layers in 12 inch depth increments

The CLSM was applied in two stages: at a depth of 30% of the pipe's diameter in the first stage, and up to 70% of the pipe's diameter in the second stage. The construction stages are shown in Figure 3-1. The geometrical details of the sections analyzed with the FEA are shown in Table 3-1.
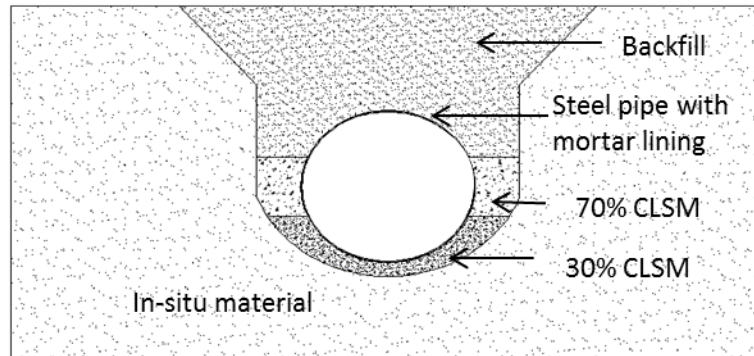
Figure 3-1 Construction stages

The name of each section is defined based on its location along the longitudinal direction of the pipe, as shown in Figure 3-2. There are four locations along the length of each pipe: TW1 is located at the beginning of the pipe, TW Mid at the middle, and TW2 at the end of the pipe. The distance at the springline is referred to as the distance from the installed pipe to the in-situ soil at the same level which is at the mid-height of the pipe, or otherwise called spring line. Therefore, the trench width is defined by adding together the distance "clear north", "clear south" and the pipe diameter. The "distance at crown" defines the elevation of the pipe from the in situ soil at the bottom of the pipe or crown. The geometry of each section was defined based on this data.
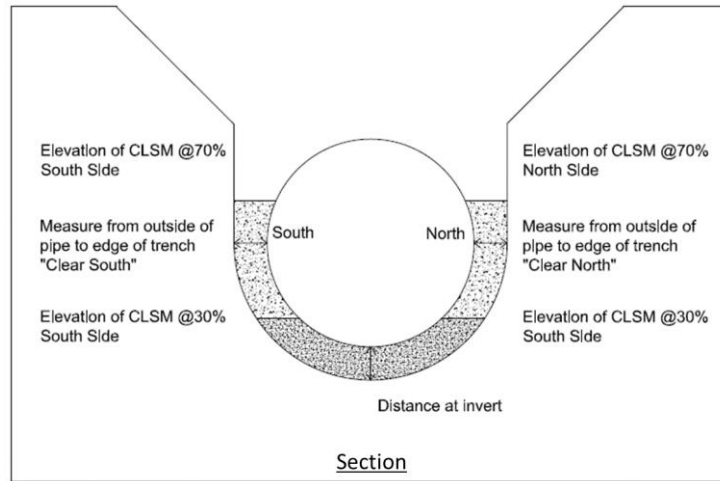
(a)
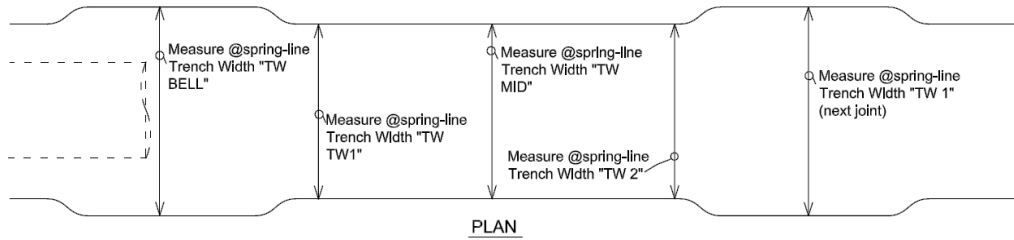
(b)

Figure 3-2 (a) Section and (b) plan view and the related terminology used for defining the dimension of the section

Table 3-1 Trench width measurement and elevation for the 18 joints of the prove-out section that were simulated with FEA

Model	Section	Distance at springline (ft.)		Distance at crown (ft.)
		Clear North	Clear South	
1	TW 1	1.75	2.59	0.67
2	TW Mid	1.34	2.92	1.02
3	TW Mid	2.02	2.01	1.37
4	TW 2	1.84	2.25	0.78
5	TW 1	1.38	2.88	0.79
6	TW Mid	1.30	2.56	1.56
7	TW Mid	1.82	2.08	1.22
8	TW 2	2.50	2.74	1.12
9	TW 1	2.16	1.91	0.86
10	TW 2	1.49	2.41	0.24

11	TW 1	1.93	2.18	0.96
12	TW 2	1.68	2.18	1.63
13	TW 1	1.42	2.59	0.94
14	TW 2	1.68	2.51	0.46
15	TW 1	2.25	2.92	0.96
16	TW 1	2.26	2.60	0.98
17	TW Mid	2.09	2.00	0.44
18	TW Mid	1.99	2.98	0.83

3.1   Model Nonlinear Algorithms

Three nonlinear algorithms were used in this study: material, geometric, and contact nonlinearity. The material nonlinearity is related to the behavior of each material. The behavior of materials is divided into linear and nonlinear behavior. Material behavior is initially linear, and after reaching a specific point, becomes nonlinear. The nonlinear behavior is expressed with a constitutive equation which relates the stress with the strain, and is different for every material. The second nonlinearity, geometric, is related to the nonlinear stress-displacement relationship. The displacement of the model can be explained with small or large rotations, strain, or displacements. The geometric nonlinearities are related to the large deflections of the model and are analyzed with different techniques that are available in the finite element software. The third nonlinearity used in this study is the contact nonlinearity, which explains the behavior of the contact surface between two different materials. Contact nonlinearity is related to the change in the boundary conditions of the two materials in contact. Two types of constraints are applied to the contact nonlinearity: the displacement constraint, where no penetration is allowed; and the force constraint, where the contact between two the surfaces should not remain active under a no-load condition.

3.1.1   Material Modeling

3.1.1.1   Steel Material

An elastic, perfectly plastic bilinear model, as shown in Figure 3-3, was used to simulate the behavior of the steel material. A yielding stress of 42,000 psi and a modulus of elasticity of 29,000 ksi were used for the steel material.
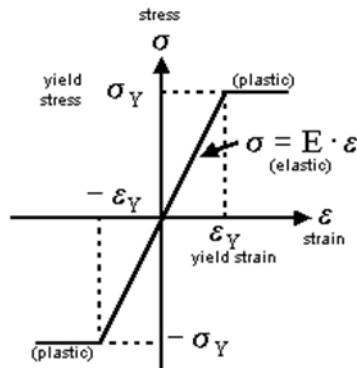
Figure 3-3 Elastic, perfectly plastic steel material law

3.1.1.2   Mortar and CLSM Material

Material models are generally based on the classical theory of plasticity, which includes yield criterion, flow rule, and the hardening rule (47). The major two damage mechanisms in concrete structures are compressive damage and tensile cracking. The latter is an external manifestation of damage in the material.

In the incremental theory of plasticity, elastic-plastic decomposition of the total strain rate, without stiffness degradation, is given by Equation 5, where D is the undamaged elastic stiffness, ε^p is the plastic component of the total strain, and σ is a Cauchy stress.

$$\dot{\varepsilon} = D^{-1}\sigma + \dot{\varepsilon}^p$$ Equation (5)

Damage in tension and compression is defined by two equivalent plastic strains, as shown in Equation 6.

$$\tilde{\varepsilon} = \begin{bmatrix} \tilde{\varepsilon}_t^p \\ \tilde{\varepsilon}_c^p \end{bmatrix} \qquad\qquad \text{Equation (6)}$$

Plastic strain variables increase with tension and compression damage. Based on the continuum damage theory, the stress is governed by effective stress, which can be expressed in terms of undamaged stiffness with Equation 7.

$$\tilde{\sigma} = E_0(\varepsilon - \varepsilon^p) \qquad\qquad \text{Equation (7)}$$

When the isotropic stiffness degradation damage is considered, then Equation 6 will be written as Equation 8, where E_0 is the initial elastic stiffness; the d- degradation variable represents degradation of the elastic stiffness due to the damage of the element.

$$\tilde{\sigma} = (1 - d)E_0(\varepsilon - \varepsilon^p) \qquad\qquad \text{Equation (8)}$$

Tension post-failure behavior is described through a strain-softening mechanism; whereas, compression exhibits initial hardening, followed by softening. A schematic representation of the tension and compression stress-strain responses is shown in Figure 3-4 (a) and (b), respectively.

Although the damaged plasticity model was developed primarily for simulating the behavior of concrete material, it is the model that most accurately simulates the behavior of the mortar liner and the CLSM. Since there is no laboratory test data for these two materials, the compressive and tensile properties for the mortar lining were identified based on literature review. ASTM material tests were conducted, on the CLSM, for both compressive and tensile behavior.
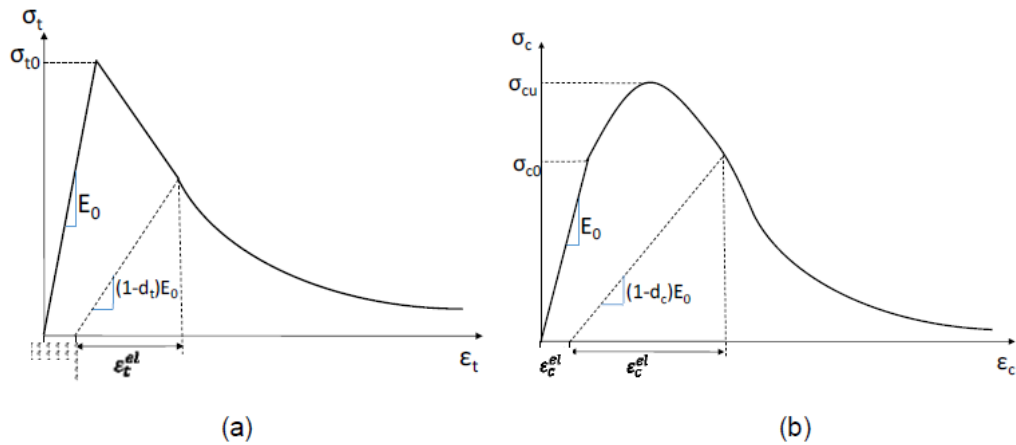
Figure 3-4 (a) Tension and (b) Compression material law used for mortar liner and CLSM

3.1.1.3 Soil Models

There are different soil constitutive models available for different purposes, and the more sophisticated the soil models are, the more information and more parameters are needed for creating the model. Thus, picking the proper soil constitutive model was vital to the study. Some of the available constitutive models for soil are Hooke's law (linear); Mohr-Coulomb, Drucker-Prager, and Duncan-Chang (hyperbolic model); Cam-Clay (modified cam-clay); Plaxis soft soil; and Plaxis hardening soil model, (48)

The Mohr-Coulomb model was used in this study to simulate the soil behavior. Five (5) input parameters, which came from the non-associated flow rule discussed in this chapter, were needed for this model, including Young's elastic modulus (E), Poisson's ratio (v), the angle of friction (φ), cohesion (c), and the dilatancy angle (ψ). The change in volume of the soil in shear is not reversible in shear loading; therefore, the non-associate flow rule parameter, dilatancy angle, was introduced to the Mohr-Coulomb soil model (49). This model assumes that the failure of the material is a function of maximum shear stress, and it depends on the applied normal stress. The Mohr's circles for different states of stress should be drawn as shown in Figure 3-5. The best tangential line to all of the Mohr's circles

93

is the failure line. Moreover, Equation 9 should be used as the equation of failure line. In Equation 9, σ is the normal stress, which is negative in compression and positive in tension; τ is the shear stress c is the cohesion of the material; and φ is the angle of friction.
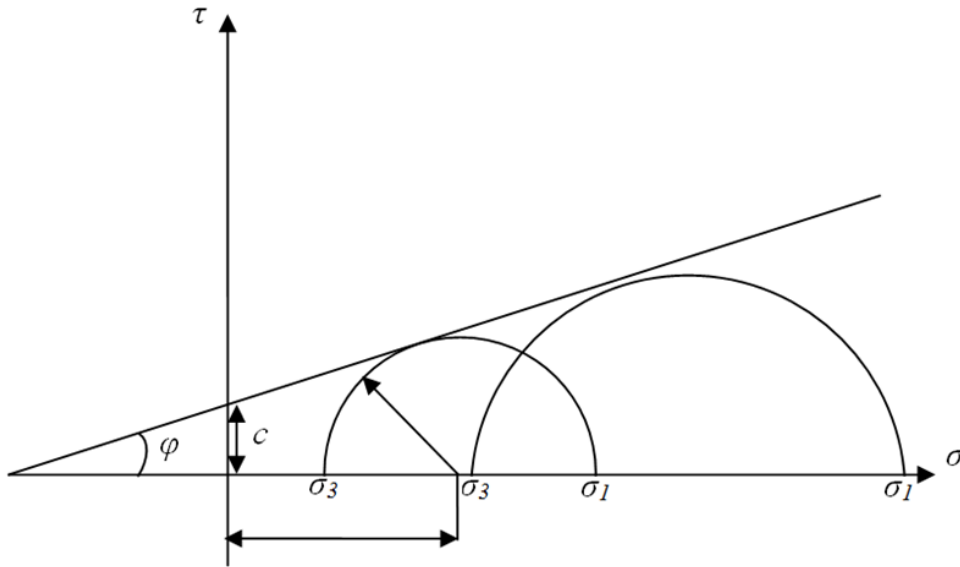
Figure 3-5 Mohr circle for different stress states

$$\tau = c - \sigma \tan \varphi \qquad \text{Equation (9)}$$

3.1.2   Contact Nonlinearity

For defining contacts, two algorithms are available: node-to-surface and surface-to-surface. For both algorithms, the two surfaces should be defined, including slave and master surfaces. Generally, if a smaller surface contacts a larger surface, it is best to choose the smaller surface as the slave surface. If that distinction cannot be made, the master surface should be chosen as the surface of the stiffer body. If the two surfaces are on structures with comparable stiffness, the surface with the coarser mesh should be selected. The stiffness of the structure, and not just the material, should be considered when choosing the master and slave surfaces. For example, a thin sheet of metal may be less stiff than a larger block of rubber, even though the steel has a larger modulus than the

rubber material. If the stiffness and mesh density are the same on both surfaces, the preferred choice is not always obvious. The choice of master and slave roles typically has much less effect on the results with a surface-to-surface contact formulation than with a node-to-surface contact formulation. However, the assignment of master and slave would have a significant effect on performance with surface-to-surface contact if the two surfaces have dissimilar mesh refinement. The solution can become quite expensive if the slave surface is much coarser than the master surface.

The tracking approach should also be selected for each algorithm. There are two different tracking approaches available. The first one is finite sliding, which is the most general and allows separation and sliding of finite amplitude and arbitrary rotation of the surfaces. The second approach is small sliding, which assumes that although two bodies may undergo large motions, there will be relatively little sliding of one surface along the other.

Node-to-surface: For the node-to-surface algorithm, each contact involves a single node on the slave surface and a group of nearby nodes on the master surface, from which values are interpolated to the projection point. In Figure 3-6, the schematic of the node-to-surface contact algorithm is illustrated. At the node-to-surface contact, a nodal area is assigned to each slave node, to convert contact forces to stresses. Therefore, the more refined surface should act as the slave surface, while the stiffer body should be the master.

Surface-to-surface: The surface-to-surface formulation enforces contact conditions, in an average sense, over regions near slave nodes rather than only at individual slave nodes. Figure 3-7 shows the schematic of the surface-to-surface contact algorithm. The averaged regions are approximately centered on slave nodes, so each contact constraint will predominantly consider one slave node but will also consider adjacent slave nodes, as shown in Figure 3-7. Some penetration may be observed at

individual nodes; however, large, undetected penetrations of master nodes into the slave surface do not occur with this discretization.
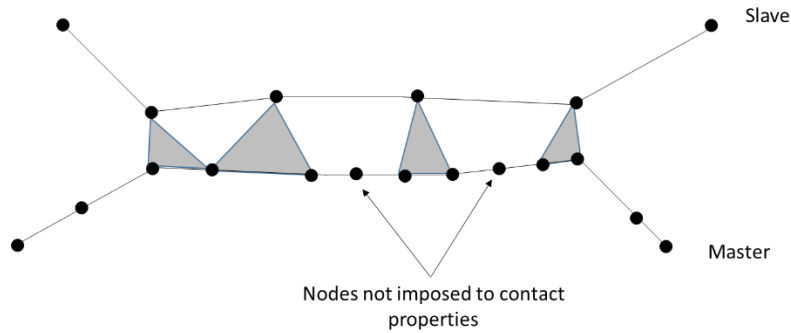
Figure 3-6 Node-to-surface contact
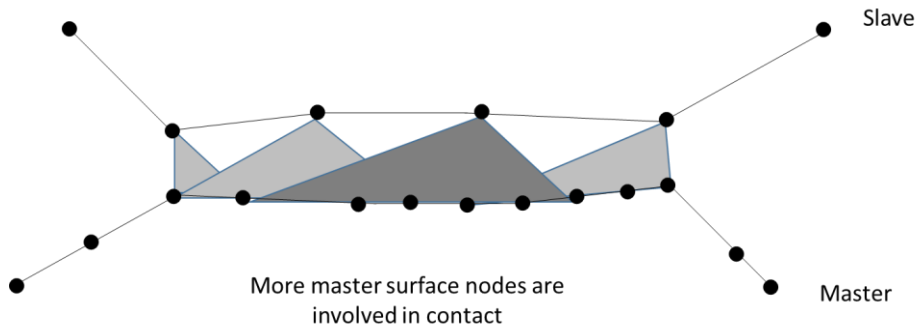
Figure 3-7 Surface-to-surface contact

3.2   Element Types

Solid elements were selected to be the infinitesimal blocks in different components of the model. The elements used were 3-D brick elements, named C3D20R, based on Chen et al. (45) and reduced integration (lower-order integration of the stiffness matrix) that alleviates the intrinsic model stiffness due to finite element approximation. A direct integration static method, using the full Newton solution technique, was selected for the analysis. Eight (8)-node linear brick elements and six (6)-node wedge elements with reduced integration and hourglass control were used for both soil and steel materials.

Hourglass control was also used to improve mesh distortion control due to large deformation and to enhance the nonlinear response. Figure 3-8 illustrates the elements which were employed in this study.
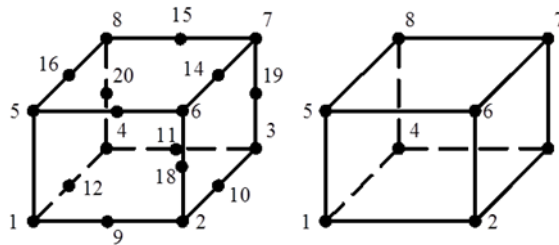
Figure 3-8 3D brick element and 8-noded linear brick

Continuum or soil elements include triangles, tetrahedral, and wedge elements. Figure 3-10 illustrates different types of continuum elements.
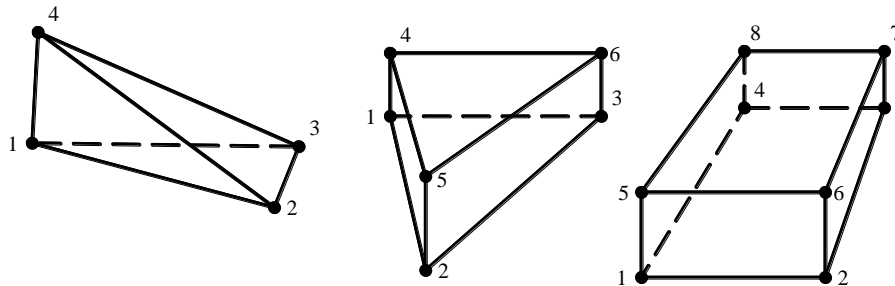
Figure 3-9 Triangles, tetrahedral, and wedge continuum soil elements

3.3   Staged Construction Modeling

The staged construction method was modeled and analyzed with the finite element method. The procedures were identical to those of the installation procedure. The first analysis step was the placement of the pipe on the section in which the pipe and the mortar weight were the only loads acting on the pipe model. Each of the soil layers and the CLSM were added to the system in separate analysis steps. In each step, gravity and compaction loads were applied to the model due to the placing of a new layer. The finite element model

contained several components including the pipe, the mortar liner, CLSM layer, soil layers, and the in-situ soil.

All the parts were introduced and assembled in the initial stage of modeling when the parts were in their undeformed shape. In each step of analysis, the applied loading caused the components to deform.

An algorithm was needed to correct the deformed geometry. For example, when the nth layer was activated, its geometry was corrected to fit and accommodate the pipe's geometrical change due to the applied loads from previous layers, i.e., layers 1 through n-1. This assumption was made in order to simplify the definition of the layers' geometry. In each step of the construction, the geometry of each new layer should be redefined, based on the deformed shape of the pipe and the previous soil layer, caused by the gravity and compaction loads. To overcome this challenge, the deactivation and activation algorithms were employed to capture the geometry of each layer in different stages. The stiffness matrices of the deactivated parts, i.e., layer $n+1^{th}$ and the layers after that, when layers 1 through n were active, were not assembled in the total stiffness matrix of the system, so their effects were eliminated from the model.

These algorithms were introduced to the FEM model so that each deactivated part would be able to map its new geometry after activation, based on the deformation of the pipe caused by the applied loads from the previously applied parts. To resolve this problem in the activation and deactivation algorithms, the deactivated soil elements shared certain nodes with the activated soil and pipe elements. It should be noted that the activated elements could be of either soil or pipe. The activated soil elements considered for the layer n were the compacted soil elements of layer 1 through n-1, while the elements of the soil elements adjacent to the pipe were always activated.

Figure 3-10 illustrates the CLSM and the two layers in contact with the pipe, in the step that only pipe and CLSM were activated in the model. As shown, the elements of the soil layers adjacent to the pipe were always kept activated to capture the updated geometry of the soil layers. The shared nodes, as shown in the figure, were located inside the soil layers, and they were not on the contact surface of the pipe or the soil layer.
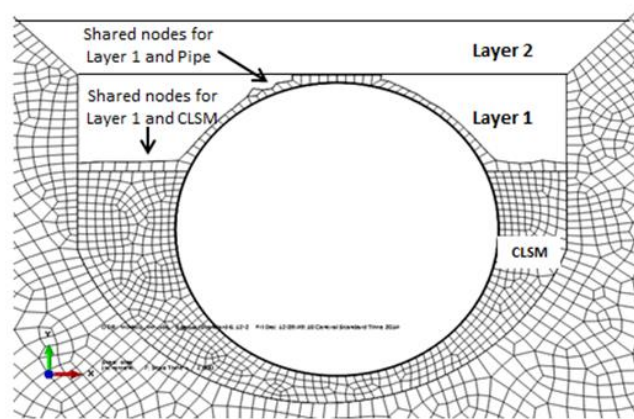
Figure 3-10 Shared nodes for the pipe and layers in contact with pipe

For instance, Layer 1 had four interface neighbors including pipe, CLSM, Layer 2, and the in-situ soil. The shared nodes allowed each part to capture and track the modified geometry according to the deformed shape of its neighboring part. For the aforementioned example, the shared nodes with the pipe deform and track the modified geometry.

3.4   Contact Definition

The interfaces between two different parts of the model were simulated, using the contact algorithm. Two types of contact were defined in this study: the contact between the steel pipe and the soil or mortar liner, and the contact between different soil layers. Figure 3-11 presents the various contact algorithms which were used in the developed model. For a node-to-surface contact, each contact involved a single slave node (Ω_A surface) and a group of nearby master nodes (Ω_B surface) from which values were interpolated to the

99

projection point. In the surface-to-surface contact, discretization enforced contact conditions, in an average sense, over regions near slave nodes ΩA surface), rather than only at individual slave nodes, (50).
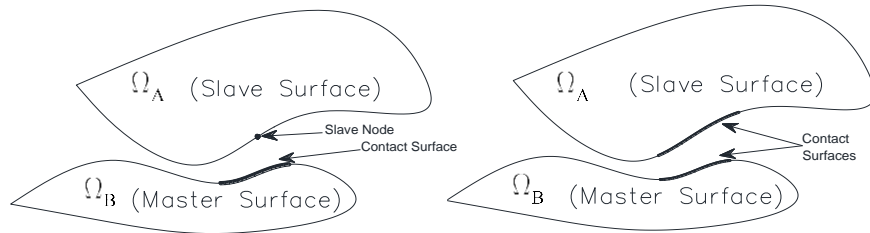
Figure 3-11 Node-to-surface and surface-to-surface contact

The contact properties were defined in two (2) perpendicular directions of tangential and normal. The tangential behavior was defined by a friction coefficient, which was selected, according to Chazli et al. (51), to be equal to 0.3. The normal contact was assumed to be a "hard contact." The hard contact dictates that two contacting parts cannot penetrate each other. The contact between the mortar lining and the steel pipe is shown in Figure 13, and the contact properties are shown in Table 3-2.

A detailed section of the FEM analysis is shown in Figure 3-12 , where a 3-D view is shown in Figure 11 (a) and a section view is shown in Figure 11 (b). The material sections are shown in different colors, CLSM to 0.7 OD, and compacted soil to the ground surface.

Table 3-2 Contact properties

Contact type	Surface to surface
Tangential axis	Friction coefficient 0.3
Normal behavior	"Hard" contact

The loads applied at the pipe were from the self-weight of the parts and from the compaction force applied at the soil layers above the CLSM. Due to the staged construction, each time that a new layer was added, it caused deformation to the parts that

already existed in the model. For this reason, the geometry of the existing parts should be updated before the addition of each part to ensure a more realistic simulation. The compacted loads at the soil layers were added according to the model developed by Dezfooli (42), in which a uniform positive temperature was added to the soil layer in order to simulate the compaction-lateral loading.
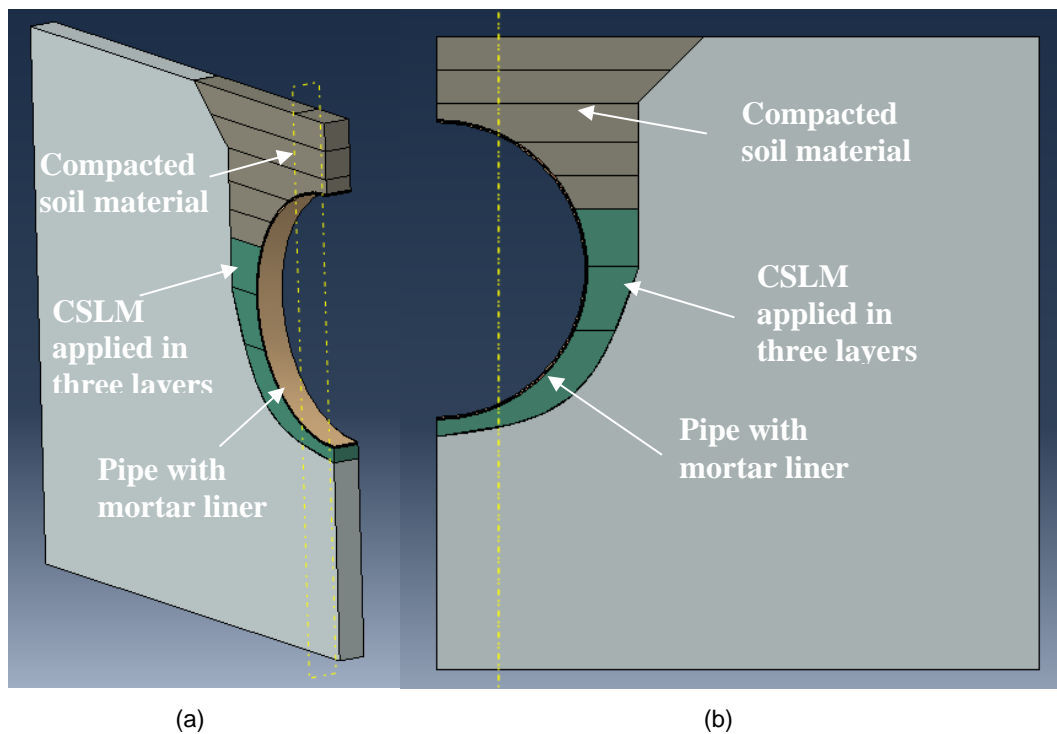
Figure 3-12 Different Views of Schematic Finite Element Representation

3.5   Mortar Liner Contribution

3.5.1   Mortar Liner Material Properties

The behavior of a typical mortar liner and its cracking phenomenon is simulated by concrete damaged plasticity (52). Typical compressive and tensile material constitutive laws are shown in Figure 3-13 and Figure 3-14, respectively.

101
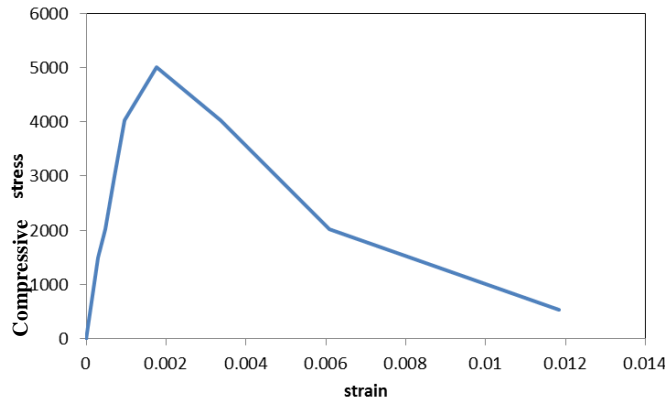
Figure 3-13 Material constitutive law for compressive behavior of mortar liner
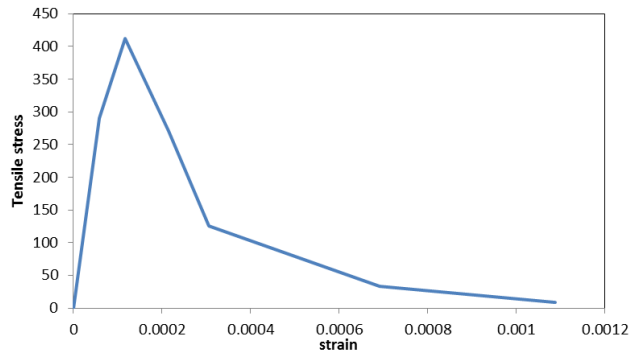
Figure 3-14 Material constitutive law for tensile behavior of mortar liner

The geometry of the mortar liner and the pipe is shown in Figure 3-15. A meshed model for a steel pipe and mortar liner is shown in Figure 3-16. The pipe outer diameter (OD) was 108 in. with a thickness of 0.47 in. The mortar liner, with a thickness of 0.5 in., was placed at the internal part of the steel pipe. The interface (contact) between the mortar liner and steel pipe was modeled by using a special contact algorithm; namely, surface-to-surface contact, as shown in Figure 16. The coefficient of the friction was 0.3 in a tangential direction, and 'hard" contact was used in the normal direction (refer to Figure 6). A uniform meshing scheme was used to model the liner and the pipe in order to achieve a speedy

converged solution during the nonlinear Newton Raphson solution technique. This also ensured a smooth solution during the surface-to-surface interface solution.
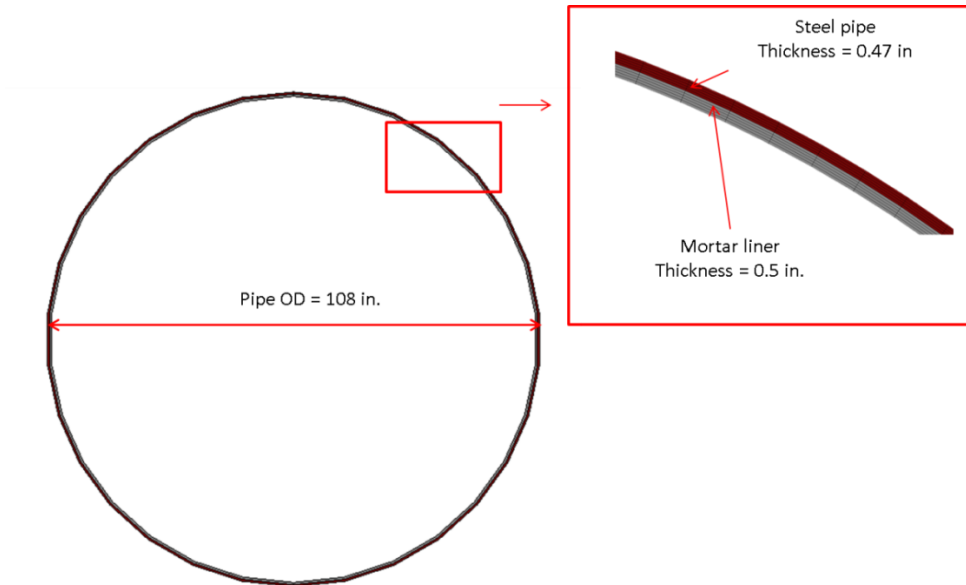
Figure 3-15 Mortar liner and pipe geometry

Steel pipe
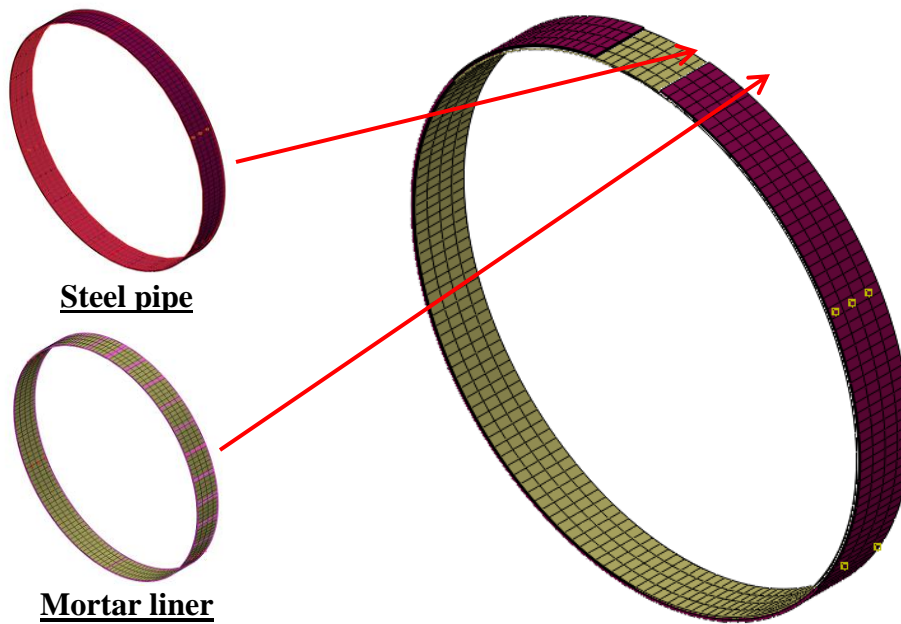
Mortar liner

Steel pipe with mortar liner

Figure 3-16 Pipe and mortar liner connection at FEM

Pipe-Mortar interface
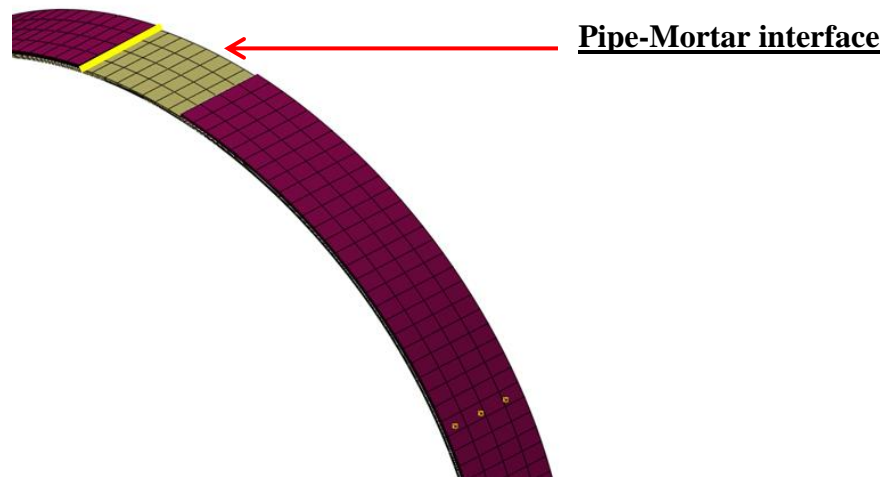
Figure 3-17 Pipe and mortar liner interface

The plastic strain is defined as the strain initiating from the onset of the crack in the damage plasticity algorithm, representing the tensile behavior of concrete during elastic and plastic regimes, as shown schematically in Figure 3-18. The principal plastic strains at the mortar liner, which are indicative of the location of the crack, are shown for different stages for a model with CLSM up to 0.7 of the pipe's diameter (0.7 D), in Figure 3-19. The first column represents the plastic strain in combination with the respective loading stage. The stages shown for this model are: (a) CLSM 0.5 OD, (b) CLSM at 0.6 OD, (c) CLSM at a level of 0.7 OD, (d) 4 layers of compacted soil, and (e) applied surcharge at the top of the last applied soil layer. The second column of Figure 3-19 represents the deflected shape of the mortar liner, along with the plastic strain for the same construction stages.
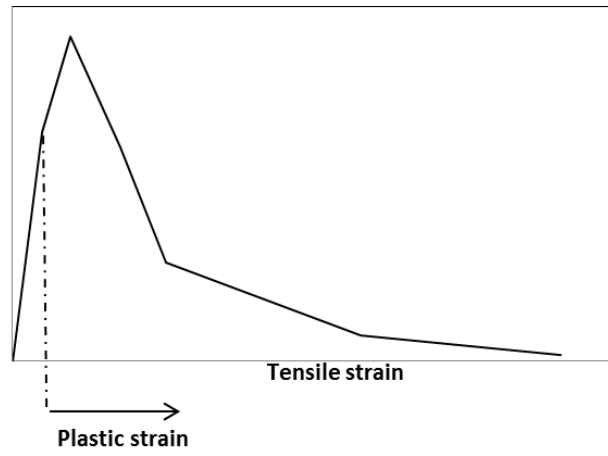
Figure 3-18 Constitutive law for tensile behavior of concrete and plastic strain definition

CLSM 0.5 OD
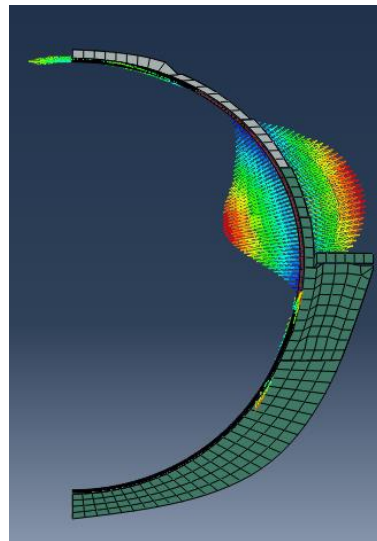
(a) Mortar layer plastic strain for CLSM height at 0.5 OD
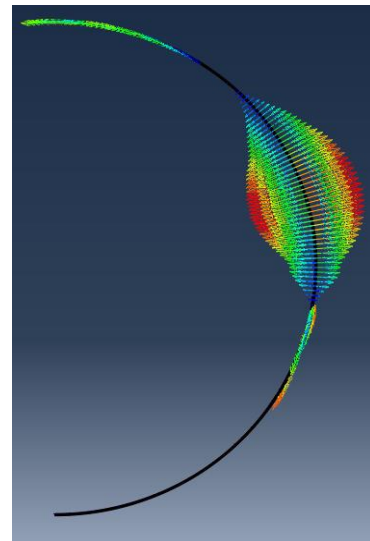
(b) Deformed shape and plastic strains for CLSM at 0.5 OD

CLSM 0.6 OD
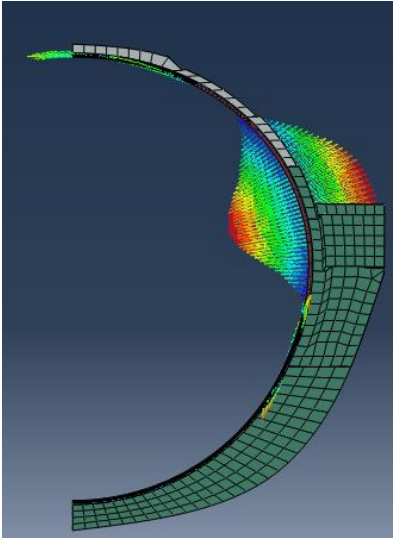
(c) Mortar layer plastic strain for
CLSM height at 0.6 OD
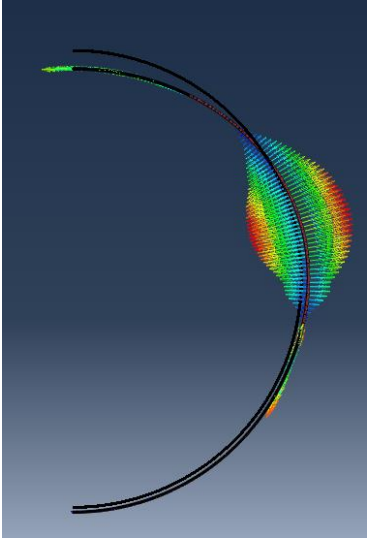
(d) Deformed shape and plastic strains for
CLSM at 0.6 OD

CLSM 0.7
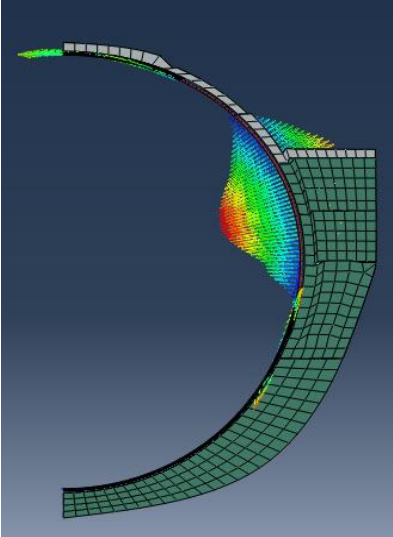
(e) Mortar layer plastic strain for
CLSM height at 0.7 OD
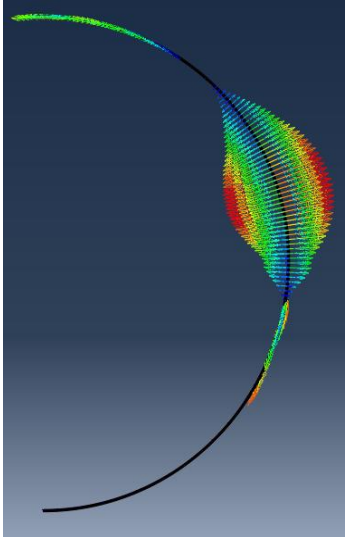
(f) Deformed shape and plastic strains for
CLSM at 0.7 OD

1st Comapcted Soil Layer
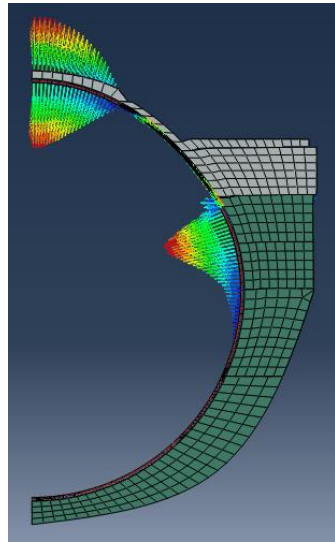
(g)   Mortar layer plastic strain for 1st compacted layer
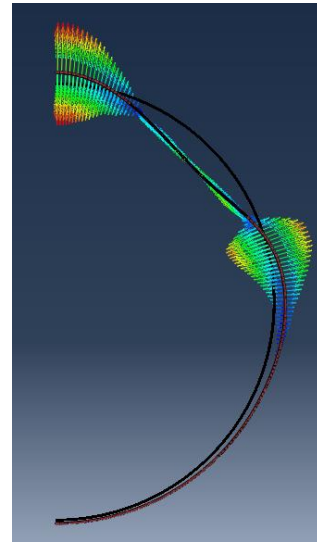
(h)   Deformed shape and plastic strains for 1st compacted layer

2nd Comapcted Soil Layer
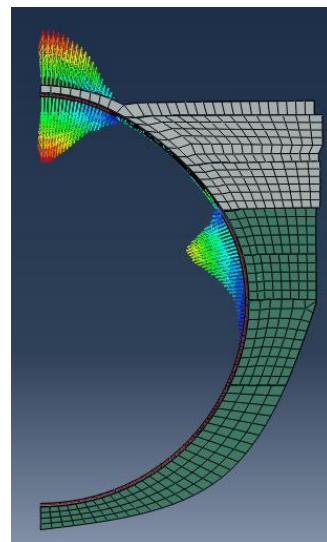
(i)   Mortar layer plastic strain for 2nd compacted layer
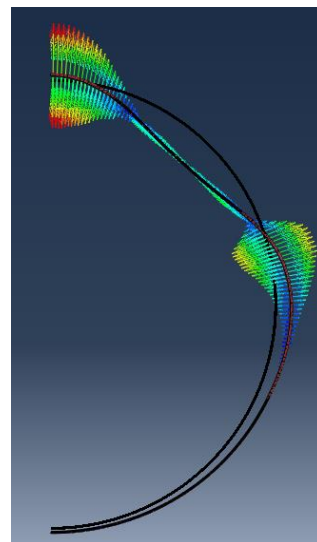
(j)   Deformed shape and plastic strains for 2nd compacted layer

**3rd Compacted
Soil Layer**
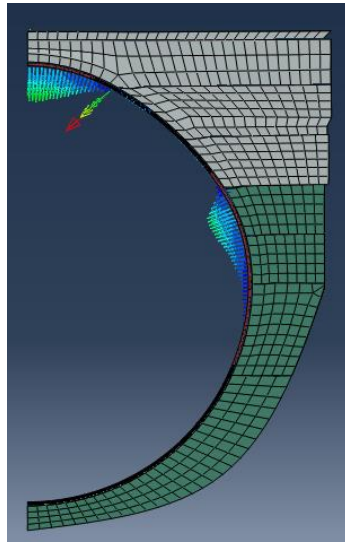
(k) Mortar layer plastic strain for
3rd compacted layer
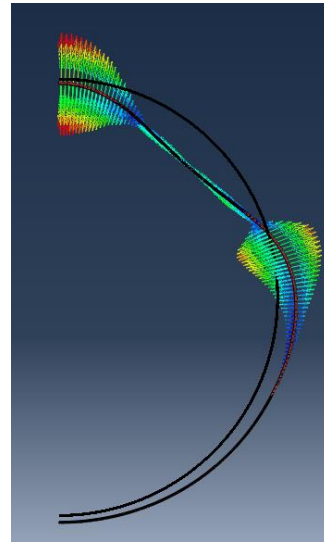
(l) Deformed shape and plastic strains for
3rd compacted layer

**4rth Compacted
Soil Layer**
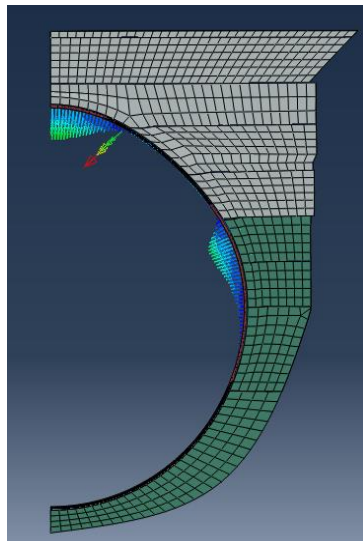
(m) Mortar layer plastic strain for
4th compacted layer
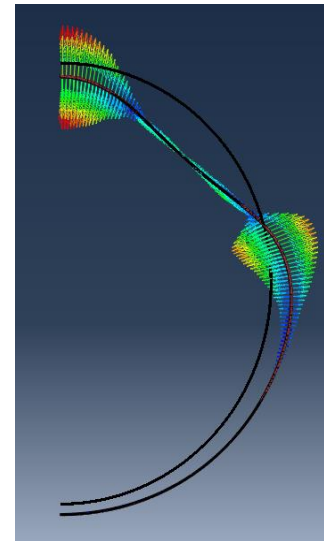
(n) Deformed shape and plastic strains for
4th compacted layer

Surcharge
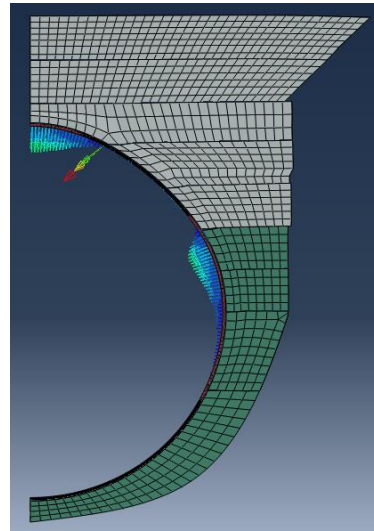
(o) Mortar layer plastic strain for surcharge load
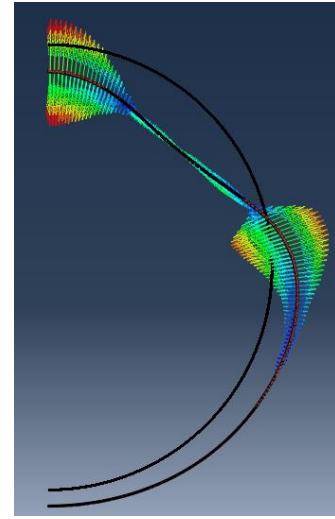
(p) Deformed shape and plastic strains for surcharge load

Figure 3-19 Plastic strain and deflected shape of mortar liner for different construction stages

3.6   Internal Pressure

As shown in Figure 3-20, the internal pressure that was taken into account for this case was 250 psi, and it was applied at the inner surface of the mortar liner. The deflection vs. construction stage plot is shown in Figure 3-21. The vertical deflection of the pipe was calculated as the vertical displacement of the pipe at crown subtracted from the displacement at the invert, while the horizontal was calculated at the springline. At the stage that pressure was applied, the vertical and horizontal deflection happened toward the reverse direction of the previously deflected mode. That means that the internal pressure applied at the pipe relieves the pipe from the previous conditions and it is not a critical condition.

(a)   (b)
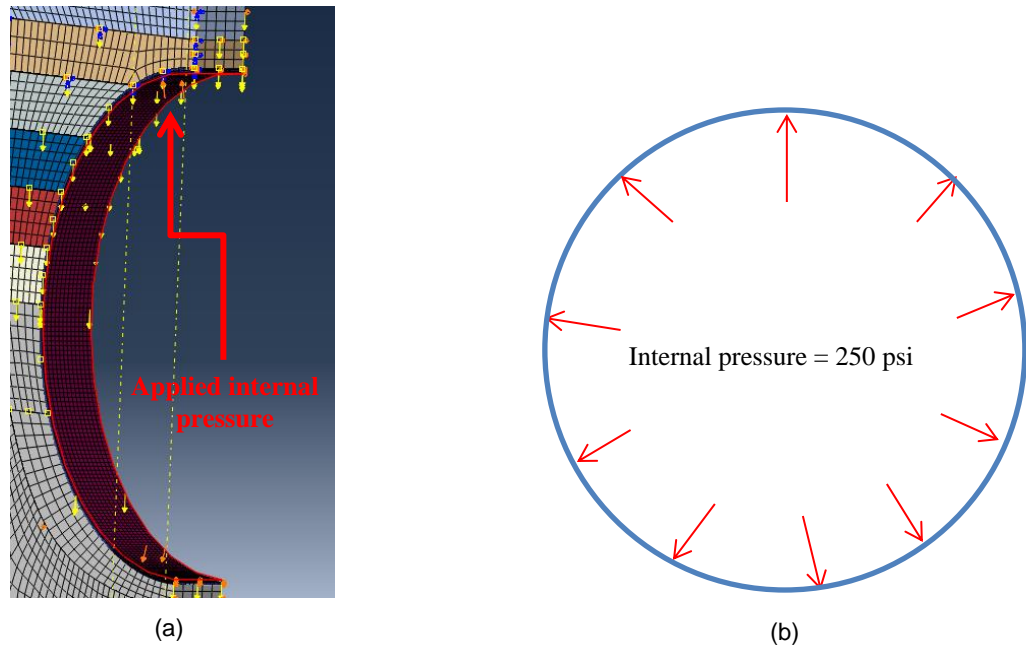
Figure 3-20 Internal pressure applied at the pipe (a) surface that the pressure is applied to and (b)
sketch representing the applied pressure inside the pipe
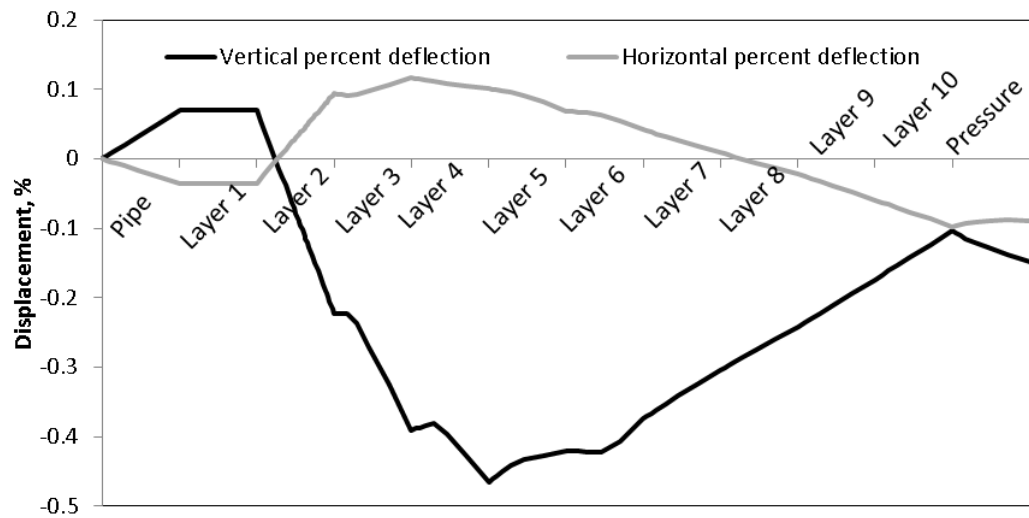
Figure 3-21 Horizontal and vertical deflection of the pipe for different construction stages

3.7 Finite Element Results and Discussion

The horizontal and vertical deflection of three sections calculated with both laser profiler methods and FEA are shown in Figure 3-22 and Figure 3-23, for horizontal and vertical displacement, respectively. The sections analyzed were the same as the sections in Figure 2-20 and Figure 2-21, models 2, 4, and 10 shown in Table 3-1. The deflection was calculated based on the placement phase as the base point, and the stage "backfill with stulls" was included in the FEA analysis. The fluctuation of the deflection of the sections modeled was not high, since the material used and the loading were the same for all the sections, but the dimensions of the trench width were different.

The comparison of the two methods is shown in Figure 3-22 and Figure 3-23, with a 15% vertical error bar in both directions. It can be concluded that the FEA model can simulate the behavior of the buried large-diameter pipes with CLSM within a 15% error limit.
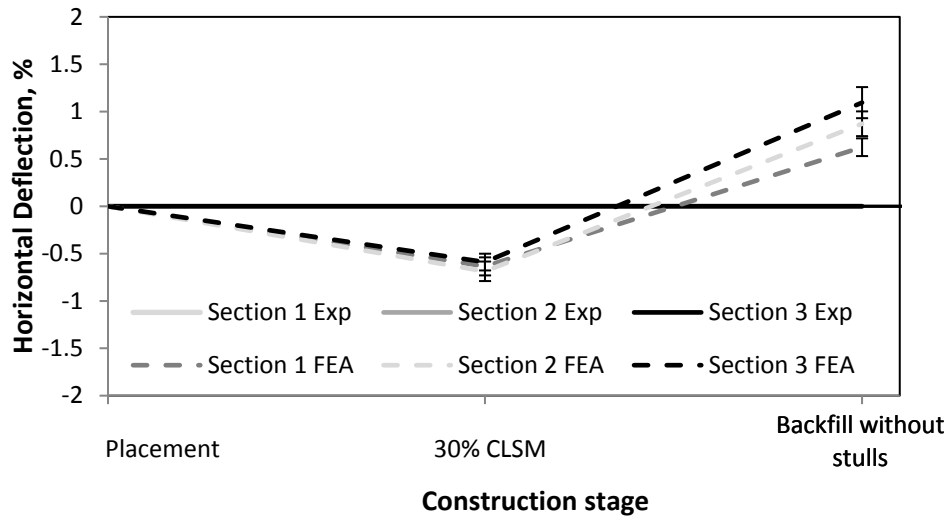
Figure 3-22 Horizontal deflection calculated with FEA vs. experimental with a 15% error band
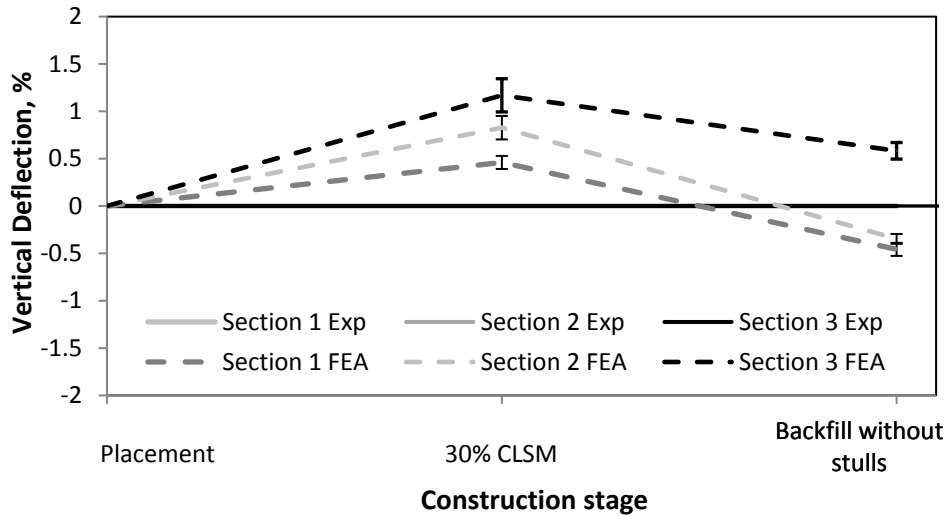
Figure 3-23 Vertical deflection calculated with FEA vs. experimental with 15% error band

3.8   Main Findings

A FEA model was developed for buried, large-diameter pipes with CLSM. The concrete-damaged plasticity (CDP) model, offered in Abaqus software, was used to simulate CLSM and mortar liner, as their behavior is explained mainly through compression and tension models combined with plasticity properties. The steel pipe was simulated as linear, perfectly plastic material, and the soil layers with Mohr-Coulomb. Interaction elements were used to simulate the contact between two adjacent surfaces. The load applied was the self-weight of every part simulated in the model and the compaction load applied to the soil layers. The elements used for the model were C3D8R, 3-D elements with 8 nodes and reduced integration. The model change algorithm was used to simulate the staged construction method. From the analyses conducted, it can be concluded that the FEA can successfully predict the behavior of a buried pipe with CLSM within a 15% error range. The difference between the FEA and experimental measurements can be addressed with a better scaling method on the laser profiler techniques and a more accurate CLSM material testing in a controlled laboratory environment. A better

understanding of the behavior of the CLSM will be a useful tool for understanding the behavior of buried pipes with CSLM.

3.9   Typical Finite Element Model

A typical stage construction simulation is explained in this model.

Step 1: Each section of the model is created as a separate part, which is later assembled based on the coordinates given. Starting from the module **Part,** as shown in Figure 3-24(a), the **Create Part** ( ) section is selected and the window with options to create parts will pop up, as shown in Figure 3-24 (b). For help in understanding the options offered at any time through the modeling procedure, the F1 key will pop up the help options for the module active at that step. First, the 2-D section is created, as shown in Figure 3-25(a), and then the thickness of the part is defined, as shown in Figure 3-25 (b). The coordination system of each member is relative to the final model, and, therefore, is the basis for the geometry of each part. The parts can always be further modified with tools available such as copy, merge, move, etc.
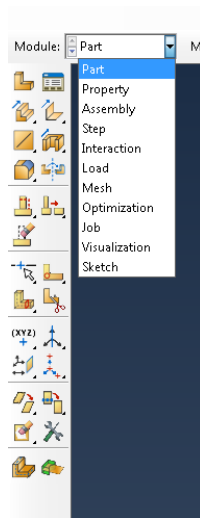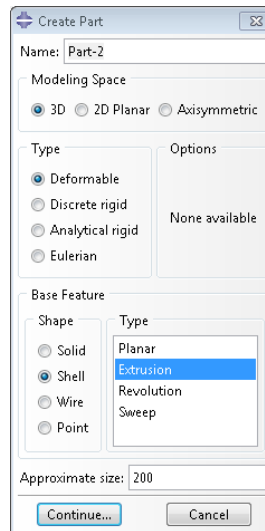
(a)   (b)

Figure 3-24 Part module and create part menu

Step 2: When the geometry of all parts has been created, the next step is to define the material properties and assign each material property to the parts related to it. From the module **Property** shown in Figure 3-26 (a), when selecting the **Create Material** ($\frac{\sigma}{\varepsilon}$) option, the window shown in Figure 3-26 (b) will pop up.
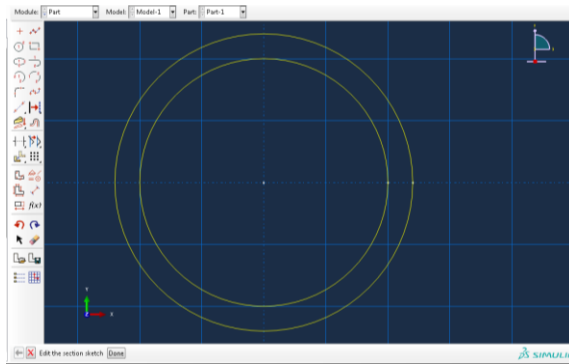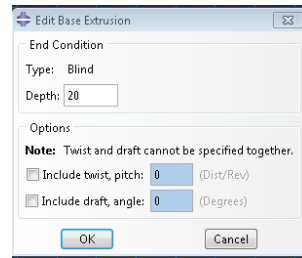
(a)   (b)

Figure 3-25 Section geometry and depth of the part
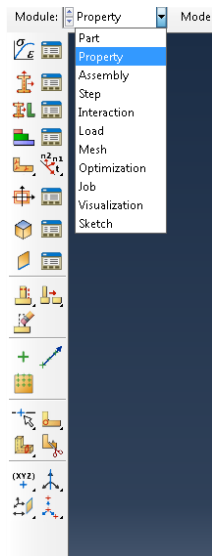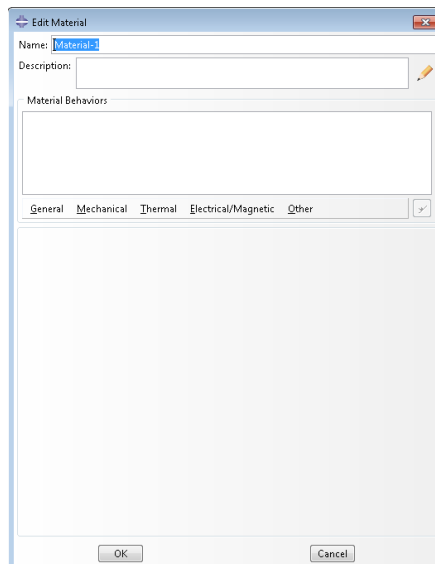
(a)   (b)

Figure 3-26 Property module and create material menu

114

Abaqus has a wide variety of material properties. They are separated into general, mechanical, thermal, electrical/magnetic, and other. Each section has subsections, which can be used to define the material properties used for the model. For this work, the materials used are shown in Figure 3-27 (a), and a detailed list of the properties used for CLSM is shown in Figure 3-27 (b).
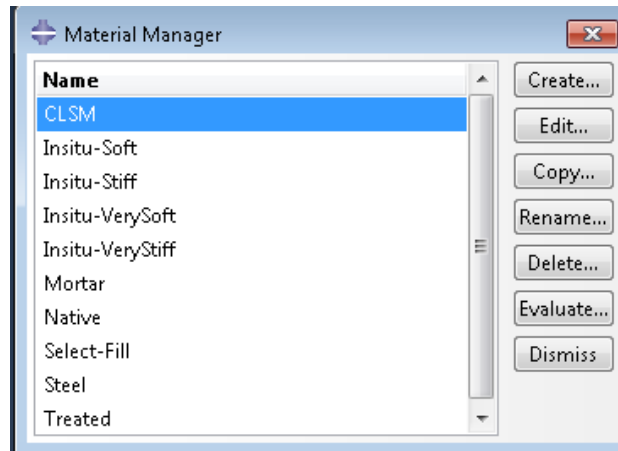
(a)
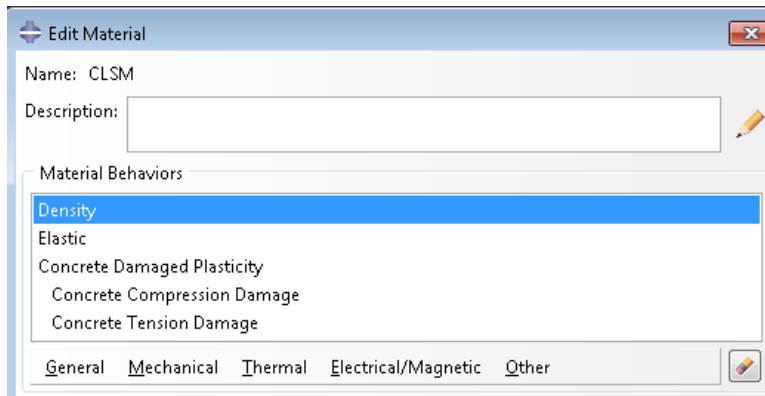
(b)

Figure 3-27 (a) Material used in this model, (b) detailed material properties for CLSM

A detailed explanation of the CLSM material properties will be provided. Initially, from the general menu option, the density is selected, as shown in Figure 3-28 (a). The distribution of the density is selected as uniform, although through the **Create Discrete**

Field option ( ) a filed can be also created for more complicated ways of applying the density, as shown in Figure 3-28 (b). At a later step the self-weight of the material will be applied through the gravitational acceleration g; therefore, the density here is defined as d/g and is shown in Figure 3-29.
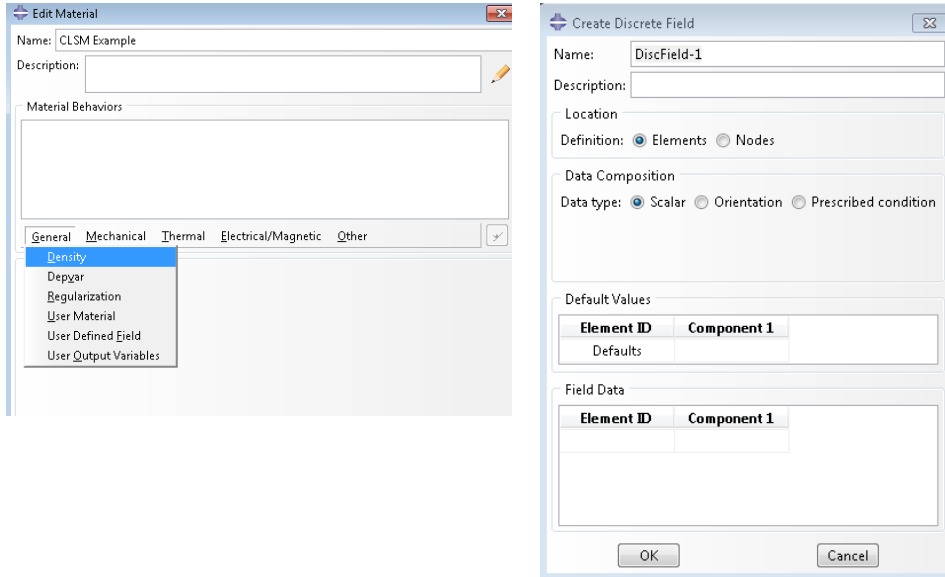
(a)   (b)

Figure 3-28 Definition of general material properties for CLSM
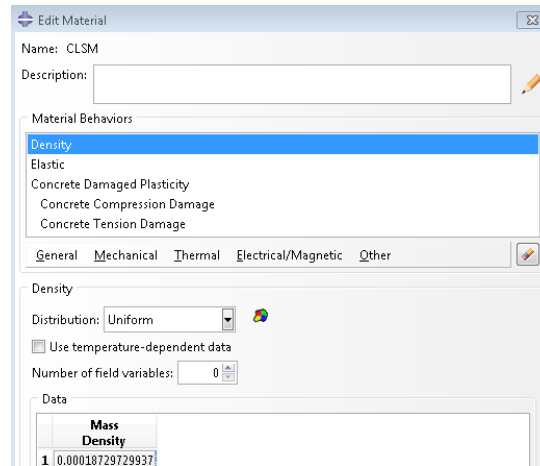
Figure 3-29 Density defined for CLSM

The next variables to be defined are from the **Mechanical** menu. From **Elasticity** →**Elastic.** The isotropic material type is used, with the Young's Modulus and the Poisson's ratio shown in Figure 3-30. In the elastic section, there is a sub-option so that the stress limits for stress-based failure measure can be defined. For the CLSM, this option was not used.
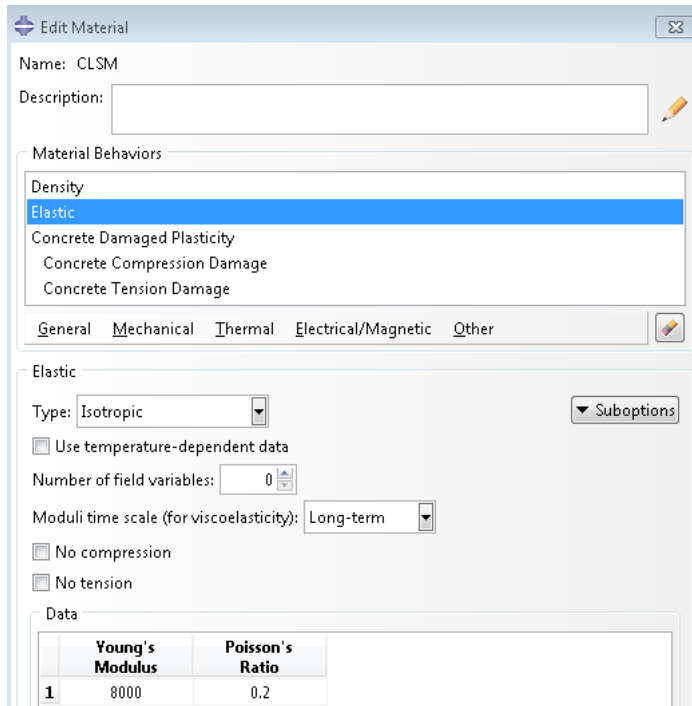
Figure 3-30 CLSM elastic properties definition

The next step for defining the mechanical properties of CLSM was to select the plasticity behavior of the material. The CDP was selected as the material which best describes the behavior of CLSM; therefore, the steps for the CDPM are explained in this section. From **Mechanical → Plasticity → CDMP,** the menu generated is shown in Figure 3-31, where the variables dilation angle, eccentricity, fb_0/fc_0, K, and the viscosity parameter are also shown.
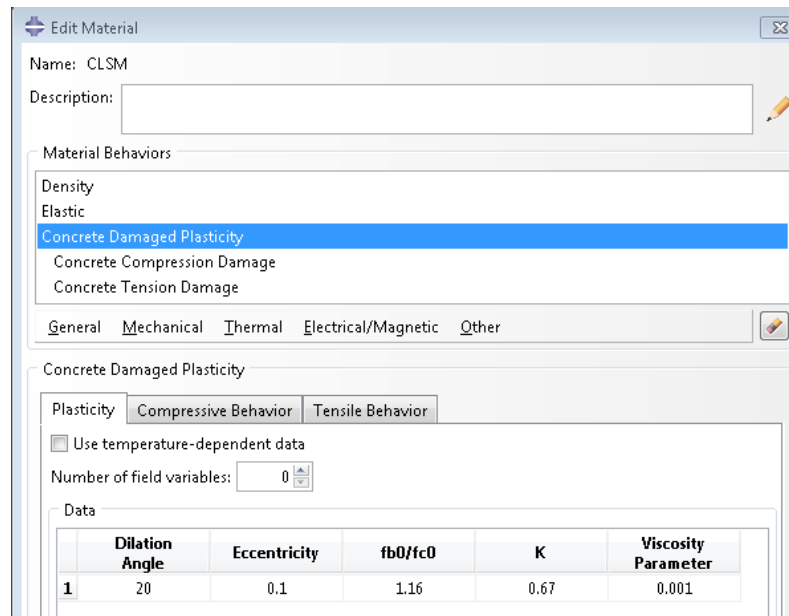
Figure 3-31 Concrete Damaged Plasticity variables

Based on the CDP model, the compression and tensile properties of the material should be defined based on calibration of the data in the laboratory. The compressive behavior was defined based on the compressive test method for CLSM (ASTM D4832) and the tensile form split cylinder test (ASTM C496). The tensile material properties were defined from the inverse analysis based on Abrishambaf et al ((53), and are shown in Figure 3-32. For defining the damage for compression and tension, the sub-option editor should be used. For the tensile properties, the values should be either expressed for displacement or for strain, but should be consistent for tensile behavior and for the tension damage.

The properties of the steel pipe were defined based on the elastic perfectly plastic material for a 36 ksi grade steel. The soil was simulated by using the Mohr-Coulomb yielding criteria, based on the properties of those used at the site. To simulate the compaction of the soil layers, thermal expansion was applied to the material properties,

along with the density, Young's modulus, and the Mohr-Coulomb plasticity option, as
shown in Figure 3-33.
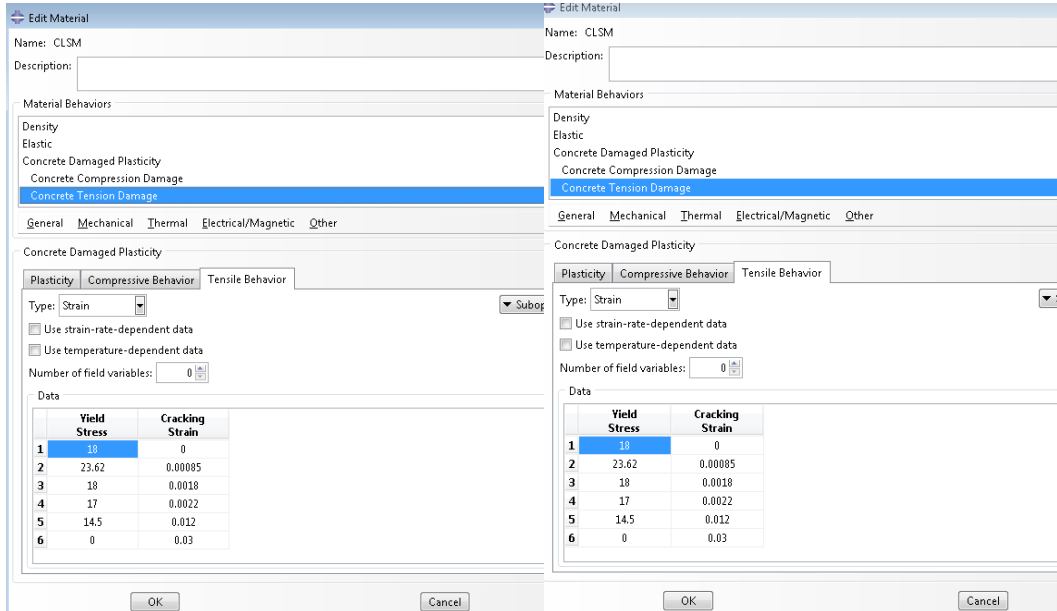
Figure 3-32 Tensile properties of CLSM

To assign material properties at each part at first, sections are created through the

Create Section (⬆), and then the sections created are assigned through the **Assign**

Section tool (⬆) at each part.

Step 3: At this step the parts are assembled to form the final model, as shown in
Figure 3-34.

Name: Select-Fill

Description:

Material Behaviors

Density
Elastic
Expansion
Mohr Coulomb Plasticity

General   Mechanical   Thermal   Electrical/Magnetic   Other

Elastic

Type: Isotropic

☐ Use temperature-dependent data

Number of field variables: 0

Moduli time scale (for viscoelasticity): Long-term

☐ No compression

☐ No tension

Data

	Young's Modulus	Poisson's Ratio
1	7500	0.35

Name: Select-Fill

Description:

Material Behaviors

Density
Elastic
Expansion
Mohr Coulomb Plasticity

General   Mechanical   Thermal   Electrical/Magnetic   Other

Expansion

Type: Orthotropic

☐ Use user subroutine UEXPAN

Reference temperature: 0

☐ Use temperature-dependent data

Number of field variables: 0

Data

	alpha11	alpha22	alpha33
1	5E-005	0	0

Name: Select-Fill

Description:

Material Behaviors

Density
Elastic
Expansion
Mohr Coulomb Plasticity

General   Mechanical   Thermal   Electrical/Magnetic   Other

Mohr Coulomb Plasticity

☐ Specify tension cutoff

| Plasticity | Cohesion | Tension Cutoff |

Deviatoric eccentricity: ⦿ Calculated default
                          ○ Specify:

Meridional eccentricity 0.1

☐ Use temperature-dependent data

Number of field variables: 0

Data

	Friction Angle	Dilation Angle
1	48	20

Name: Select-Fill

Description:

Material Behaviors

Density
Elastic
Expansion
Mohr Coulomb Plasticity

General   Mechanical   Thermal   Electrical/Magnetic   Other

Mohr Coulomb Plasticity

☐ Specify tension cutoff

| Plasticity | Cohesion | Tension Cutoff |

☐ Use temperature-dependent data

Number of field variables: 0

Data

	Cohesion Yield Stress	Abs Plastic Strain
1	12	0

Figure 3-33 Properties for soil material with compaction, using Mohr-Coulomb
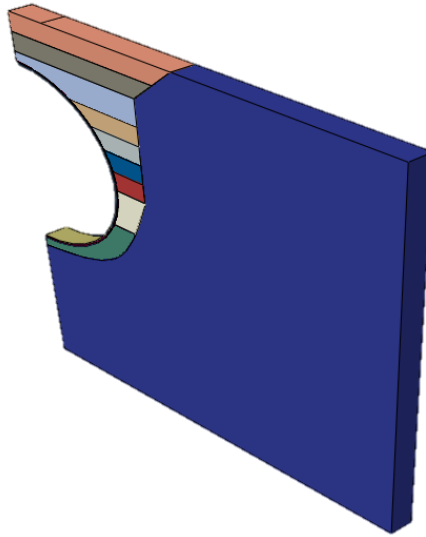
Figure 3-34 Assembled model showing different parts

Step 4: When a staged construction is performed there are several steps, with each step representing the installation of a different layer. At this step the geometric nonlinearities are activated, and the incrementation type is defined as shown in Figure 3-35. An important point at this step is the activation of the F-output ( ) and the H-output ( ), which are actually requests for the program to save specific data that will be useful for the post-processing of the model.

Name	Procedure	Nlgeom	Time
✔ Initial	(Initial)	N/A	N/A
✔ Pipe	Static, General	ON	2
✔ Layer1	Static, General	ON	2
✔ Layer2	Static, General	ON	2
✔ Layer3	Static, General	ON	2
✔ Layer4	Static, General	ON	2
✔ Layer5	Static, General	ON	2
✔ Layer6	Static, General	ON	2
✔ Layer7	Static, General	ON	2
✔ Layer8	Static, General	ON	2

Name: Layer1
Type: Static, General

Basic | Incrementation | Other

Type: ● Automatic ○ Fixed
Maximum number of increments: 1000

| | Initial | Minimum | Maximum |
Increment size: 0.1 | 2E-005 | 2

(a)   (b)

Figure 3-35 (a) Steps definition and (b) incrementation

122

Step 5: Based on the described construction method, every layer or part is installed at different times. In reality, the contact between two materials is defined based on the materials that are coming into contact. The same simulation ideology is followed in the FEA. The parts are assembled in one final model without having any specific property at the point of contact of two different parts. To define the contact between the surfaces and their properties, the **Interaction** menu is used. There are different contact elements offered in Abaqus. For this model, the tie interaction and the surface-to-surface interactions were used.

As explained before in this chapter, there is a need to track the geometric changes of the model that happens at every stage, so that when the next layer is activated, it will have an updated, strain-free, location geometry. This is applied through the model change algorithm which is found in the **Create Interaction** menu. It is created at the first step of the analysis, but it is re-activated at the time of the layer activation. Every part has two layers of activation: the lower one, which is actually the first layer of the meshed elements; and the upper one, which is the mesh elements that remained. The model change interaction is applied at the lower part of each soil layer, which is activated at the same time with the upper part of the previous soil layer, as shown in Figure 3-36.

Interaction Manager

Name	Initial	Pipe	Layer1	Layer2	Layer3	Layer4	Layer5	Layer6	Layer7	Layer8
✔ Layer1-1Upper		Created	Modified	Propagated	Propagated	Propagated	Propagated	Propagated	Propagated	Propagated
✔ Layer1-Layer2			Created	Propagated	Propagated	Propagated	Propagated	Propagated	Propagated	Propagated
✔ Layer2-1Lower		Created	Modified	Propagated	Propagated	Propagated	Propagated	Propagated	Propagated	Propagated
✔ Layer2-1Upper		Created	Propagated	Modified	Propagated	Propagated	Propagated	Propagated	Propagated	Propagated
✔ Layer2-Layer3				Created	Propagated	Propagated	Propagated	Propagated	Propagated	Propagated
✔ Layer3-1Lower		Created	Propagated	Modified	Propagated	Propagated	Propagated	Propagated	Propagated	Propagated
✔ Layer3-1Upper		Created	Propagated	Propagated	Modified	Propagated	Propagated	Propagated	Propagated	Propagated
✔ Layer3-Layer4					Created	Propagated	Propagated	Propagated	Propagated	Propagated
✔ Layer4-1Upper		Created	Propagated	Propagated	Modified	Propagated	Propagated	Propagated	Propagated	Propagated
✔ Layer4-1Upper		Created	Propagated	Propagated	Propagated	Modified	Propagated	Propagated	Propagated	Propagated
✔ Layer4-Layer5						Created	Propagated	Propagated	Propagated	Propagated
✔ Layer5-1Lower		Created	Propagated	Propagated	Propagated	Modified	Propagated	Propagated	Propagated	Propagated
✔ Layer5-1Upper		Created	Propagated	Propagated	Propagated	Propagated	Modified	Propagated	Propagated	Propagated
✔ Layer5-Layer6							Created	Propagated	Propagated	Propagated
✔ Layer6-1Lower		Created	Propagated	Propagated	Propagated	Propagated	Modified	Propagated	Propagated	Propagated
✔ Layer6-1Upper		Created	Propagated	Propagated	Propagated	Propagated	Propagated	Modified	Propagated	Propagated
✔ Layer6-Layer7								Created	Propagated	Propagated
✔ Layer7-1Lower		Created	Propagated	Propagated	Propagated	Propagated	Propagated	Modified	Propagated	Propagated
✔ Layer7-1Upper		Created	Propagated	Propagated	Propagated	Propagated	Propagated	Propagated	Modified	Propagated
✔ Layer7-Layer8									Created	Propagated

Figure 3-36 Model change algorithm

Name	Initial	Pipe	Layer1	Layer2	Layer3	Layer4	Layer5	Layer6	Layer7	Layer8
Layer1-1Upper		Created	Modified	Propagated	Propagated	Propagated	Propagated	Propagated	Propagated	Propagated
Layer1-Layer2			Created	Propagated	Propagated	Propagated	Propagated	Propagated	Propagated	Propagated
Layer2-1Lower		Created	Modified	Propagated	Propagated	Propagated	Propagated	Propagated	Propagated	Propagated
Layer2-1Upper		Created	Propagated	Modified	Propagated	Propagated	Propagated	Propagated	Propagated	Propagated
Layer2-Layer3				Created	Propagated	Propagated	Propagated	Propagated	Propagated	Propagated
Layer3-1Lower		Created	Propagated	Modified	Propagated	Propagated	Propagated	Propagated	Propagated	Propagated
Layer3-1Upper		Created	Propagated	Propagated	Modified	Propagated	Propagated	Propagated	Propagated	Propagated
Layer3-Layer4					Created	Propagated	Propagated	Propagated	Propagated	Propagated
Layer4-1Lower		Created	Propagated	Propagated	Modified	Propagated	Propagated	Propagated	Propagated	Propagated
Layer4-1Upper		Created	Propagated	Propagated	Propagated	Modified	Propagated	Propagated	Propagated	Propagated
Layer4-Layer5						Created	Propagated	Propagated	Propagated	Propagated
Layer5-1Lower		Created	Propagated	Propagated	Propagated	Modified	Propagated	Propagated	Propagated	Propagated
Layer5-1Upper		Created	Propagated	Propagated	Propagated	Propagated	Modified	Propagated	Propagated	Propagated
Layer5-Layer6							Created	Propagated	Propagated	Propagated
Layer6-1Lower		Created	Propagated	Propagated	Propagated	Propagated	Modified	Propagated	Propagated	Propagated
Layer6-1Upper		Created	Propagated	Propagated	Propagated	Propagated	Propagated	Modified	Propagated	Propagated
Layer6-Layer7								Created	Propagated	Propagated
Layer7-1Lower		Created	Propagated	Propagated	Propagated	Propagated	Propagated	Modified	Propagated	Propagated
Layer7-1Upper		Created	Propagated	Propagated	Propagated	Propagated	Propagated	Propagated	Modified	Propagated
Layer7-Layer8									Created	Propagated

Step 6: The boundary conditions and the loads applied to the system is the next step for creating the model. The boundary conditions are applied at the symmetry line of the model, at the lower and right side of the in-situ material part. Also, the model is restrained at the z-direction, which is the longitudinal direction.

The loads applied to the model were the self-weight of the activated layers and the compaction load of the soil layers. As mentioned in the first step, the self-weight load applied here is simulated with gravitational acceleration which, when multiplied with the density given at the material property section, equals the distributed gravity load of each layer. The compaction load applies to the soil layers and is simulated as a thermal load which represents the horizontal stresses induced at each layer due to compaction. This option is offered at the **Create Predefined Field,** and it is activated at the same time that the layer is activated, as shown in Figure 3-37.

Step 7: The last step is the discretization of the model, under the mesh menu. The parts are meshed, based on the elements size. For the pipe and mortar layer, the size used

124

is 1 in, while for the soil layers, 2 in. The element type used for the model is hexahedral 8-noded brick elements, with reduced integration and hourglass control.
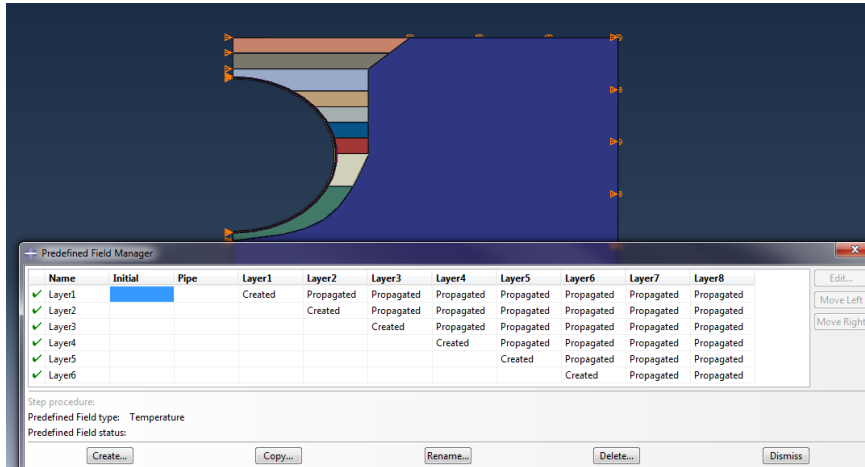
Figure 3-37 Application of the predefined field-thermal loading

Step 8: The last step is to assign the analysis that will be used for this model, as shown in Figure 3-38. When the job is completed, the results of the analysis can be extracted through the 'Visualization' menu.
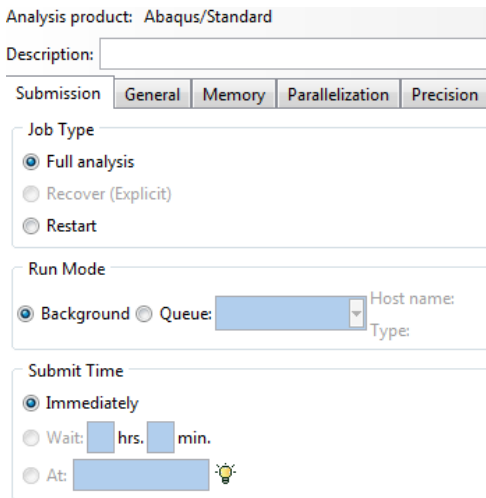
Figure 3-38 Analysis menu

125

Chapter 4

INVESTIGATION OF MATERIAL PROPERTIES FOR CONTROLLED LOW STRENGTH

MATERIAL (CLSM)

Studies have been reported with regard to the compression strength for different CLSM mixes, with or without fly ash, rubber, or in-situ soil. The compression strength is the only engineering property of CLSM that is extensively reported in literature. While simulating the CLSM in the finite element model, the compressive strength is one of the many properties needed. The tensile and plasticity properties need to be investigated and calibrated for gaining an overall knowledge and understanding of the behavior of the CLSM. A comprehensive study is performed in this research that investigates the material properties of different CLSM mix designs, produced and tested under a controlled laboratory environment at the University of Texas at Arlington.

4.1   Mix Design Investigation

The CLSM mix design that was used in this study had three main materials: in-situ soil, water, and cement. In the first step, the soil classification was tested based on Craig R. F. (20), ASTM D2487 "Standard Practice for Classification of Soils for Engineering Purposes (Unified Soil Classification System)", and ASTM D6913 "Standard Test Methods for Particle-Size Distribution (Gradation) of Soils Using Sieve Analysis.. Several initial mix designs were produced, and the final mix was designed based on flowability, cement percentage, and compression strength. The specimens were produced based on ASTM D4832 "Standard Test Method for Preparation and Testing of Controlled Low-Strength Material (CLSM) Test Cylinders" and ASTM D5971 "Standard Practice for Sampling Freshly Mixed Controlled Low-Strength Material." The flowability of the mix was tested based on ASTM D6103-04 "Standard Test Method for Flow Consistency of Controlled Low-Strength Material," and the density was tested based on the ASTM D6023 "Standard Test

Method for Density (Unit Weight), Yield, Cement Content, and Air Content (Gravimetric) of Controlled Low-Strength Material (CLSM)." The unconfined compression test was performed for the final mix design for 1, 3, 7, and 28 days past the production day.

The definition of the soil classification requires determining the percentage by mass of the particles within the different size ranges. There are mainly two types of particle distribution, depending on whether the soil has a high percentage of coarse or fine parts. The calculation of the percentage of coarse or fine materials was defined based on the particle-size distribution graph. The percentage of the amount passed through a series of standard sieves having successively smaller mesh sizes, defines the classification of the soil material. The particle size distribution is plotted in a semi-logarithmic plot, with coordinates of the percentage by mass of the particles smaller than the size given by the abscissa.

The sieves used in descending order were: 3⁄4-in. (19.0-mm), No. 4 (4.75-mm), No. 10 (2.00-mm), No. 40 (425-μm), and No. 200 (75-μm). The results were plotted in a semi-logarithmic plot and are shown in Figure 4-1. The coefficient of the curvature (Cc) and the coefficient of uniformity (Cu) were calculated equal to 13.5 and 1.19 respectively. Based on the results and the ASTM D2487 procedure, the soil that was used was classified as well-graded sand (SW). The particle percentage was: sand 75.6%, gravel 23.2%, and clay 1.22%.

The nomenclature of specimens was based on the percentage of clay-sand-gravel-cement. For example the CLSM mix which is named 1-76-23-1, was the mix which has 1% clay, 76% sand, 23% gravel and 1% cement.

Mechanical analysis plot
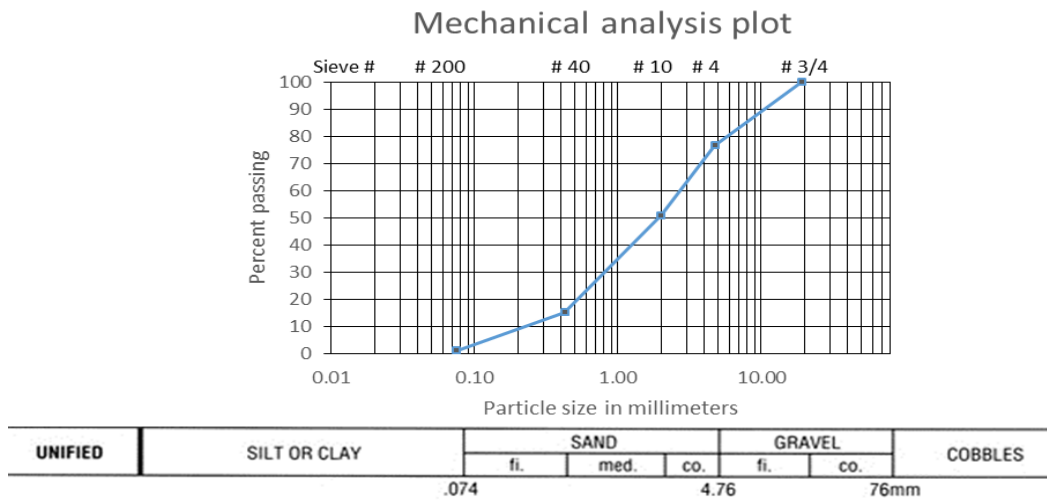
Figure 4-1 Semi-logarithmic mechanical analysis plot for soil classification

A trial mix design, CLSM 76-23-1-6, was prepared in small portions mixed with a kitchen mixer, as shown in Figure 4-2 (a), and the compressive strength was tested on the 3rd day. First, the soil was poured into the mixer bowl and mixed for one minute. Then, the cement was added and mixed for one more minute. The water was then added, and the ingredients were mixed for 3 minutes. Cylindrical specimens with a 4-in. diameter and 8-in. height were used based on the ASTM 4832, and were lubricated before the mixture was poured into them, for ease of demolding. The specimens were covered with a plastic bag and saved in a safe and shaded place for three days. After three days, the specimens were demolded and capped. Three different capping methods were used for capping the specimens: sulfur, gypsum, and quick-dry cement. Due to the low compressive strength of the specimens, the sulfur capping was not appropriate, as shown in Figure 4-3 (a). Applying the gypsum capping was difficult, and it dried very quickly, resulting in the users not having time to level the capping. The fast-drying concrete was the most appropriate capping method, and it was used for the rest of the testing procedure. The specimens were tested

after 3 days with a compressive machine, and the results for the tested specimens showed a compressive strength of 10.35 psi.

New mixes with varying percentages of cement were produced based on the same mix design, as shown in Table 4-1. A concrete mixer, rather than the kitchen mixer, was used for mixing the CLSM, as shown in Figure 4-2 (b).Three specimens were produced from each batch of the CLSM 1-76-23-5, 1-76-23-7, and 1-76-23-8 mixes and were placed in the curing room at 80.5^0 F temperature and 70% humidity. The specimens were demolded and capped on 7th day. Based on the testing standards, the specimens should be tested after 8 hours of demolding. The average compressive strengths of the produced specimens are shown in Table 4-1.

(a)   (b)

Figure 4-2 Material mixing procedure (a) trial mix, (b) final mix

<div align="center">(a)</div>
<div align="center">(b)</div>
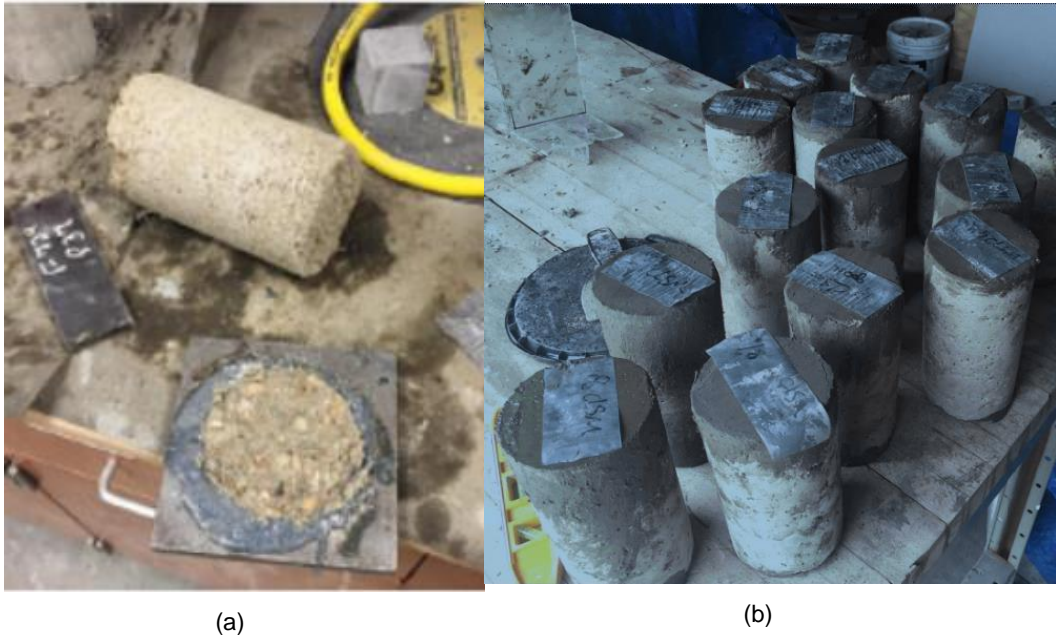
Figure 4-3 (a) Sulfur and (b) fast-drying cement capping

Table 4-1 Initial mix design

Material	CLSM 1-76-23-5	CLSM 1-76-23-7	CLSM 1-76-23-8
Soil (lb.)	8.25	8.25	8.25
Cement (lb.)	0.41	0.58	0.66
Water (lb.)	1.93	2.7	3.08
Avg. compressive strength (psi)	28.8	51.4	213.3

4.2   Investigation of W/C Ratio

The water-cement ratio was investigated by producing the same mix design, but changing the amount of water used. Three different mix designs were produced for the CLSM 1-76-23-5, as shown in Table 4-2. The specimens were stored in a dry and shaded place at the location of production and were transferred to the curing room on the 4th day. The compressive strength of the specimens was tested on 7th day and is shown in Table 4-2.

Table 4-2 Mix design with different w/c percentage

Material	CLSM 1-76-23-5	CLSM 1-76-23-5	CLSM 1-76-23-5
W/C	4.7	3.5	2.4
Soil (lb.)	8.25	8.25	8.25
Cement (lb.)	0.41	0.41	0.41
Water (lb.)	1.93	1.45	0.97
Avg. compressive strength at 7 d (psi)	16.01	16.5	47.7

4.3   Final Mix Design

For the final mix design, the variable that was tested was the flow consistency of the mix, based on the ASTM D6103-04. A cylinder with 3-in. diameter and 6-in. height was used to perform the test based on the standard. CLSM was poured inside the cylinder that was placed on a flat surface. Within 5 seconds of placing the mix, the cylinder was raised 15 cm vertically in a time period of between 2 to 4 seconds. The largest spreading dimension was measured, and a second measurement was taken perpendicular to the first one, as shown in Figure 4-4. For the CLSM, a spread of about 8 in. is considered reasonable based on literature review. Overall, 16 specimens were produced, based on the mix design shown in Table 4-2, with w/c ratio equal to 3.5, and were tested after 1, 3, and 7 days. The specimens remained in a dry, shaded place for the first 3 days and then were placed in the curing room with a 80.5^0 F temperature and 70% humidity. The results of the compressive test are shown in Table 4-3.

Based on further investigation of the behavior of CLSM, 8 different mix designs were produced with cement percentages ranging from 1-8%. For every mix design, 12 specimens were produced, 3 of each to be tested 1, 3, 7, and 28 days after production. The mix designs are shown in Table 4-4. The slump and the density were measured for every batch produced, and the results are presented in Table 4-5.
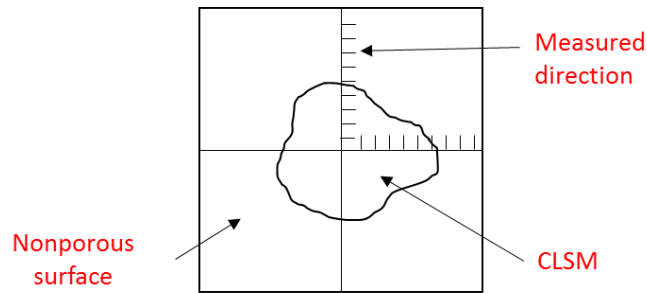
Figure 4-4 Measurement of the spread of the two directions

Table 4-3 Average compressive strength for CLSM 1-76-23-5

CLSM 1-76-23-5	Day 1	Day 2	Day 3
Avg. compressive strength (psi)	12.31	26.1	93.6

Table 4-4 (a) Final mix design

Material	CLSM 1-76-23-1	CLSM 1-76-23-2	CLSM 1-76-23-3	CLSM 1-76-23-4
Soil (lb.)	90.75	90.75	90.75	90.75
Cement (lb.)	0.91	1.82	2.72	3.63
Water (lb.)	18.18	19.00	16.54	17.00

Table 4-4 (b) Continuation of final mix design table

Material	CLSM 1-76-23-5	CLSM 1-76-23-6	CLSM 1-76-23-7	CLSM 1-76-23-8
Soil (lb.)	90.75	90.75	90.75	90.75
Cement (lb.)	4.85	5.45	6.35	7.26
Water (lb.)	13.00	16.50	17.00	16.26

Table 4-5 (a) Slump and density measured for all the mix designs

Tested parameter	CLSM 1-76-23-1	CLSM 1-76-23-2	CLSM 1-76-23-3	CLSM 1-76-23-4
Slump (in)	8.50	8.75	8.00	8.75

| Density (lb./ft3) | 9.88 | 9.55 | N/A | 9.47 |

Table 4-5 (b) Continuation of slump and density table

Tested parameter	CLSM 1-76-23-5	CLSM 1-76-23-6	CLSM 1-76-23-7	CLSM 1-76-23-8
Slump (in)	7.40	8.25	8.44	8.00
Density (lb./ft3)	9.02	9.42	10.26	9.68

4.4   Experimental Testing

The experimental test setup for the different tests performed for this study follow the American Standards Testing Methods (ASTM).

4.4.1   Compressive Test

4.4.1.1   Test Setup

The compressive strength of the specimens was initially tested with hand-jack compression equipment, as shown in Figure 4-5 (a), because of the low compressive strength of the material. As shown in Figure 4-5 (b), the final specimens were tested with a triaxial machine with 1000 lb. capacity, which is mainly used for soil specimens and provides the stress-strain curve. The specimens with a load requirement higher than 1000 lbs. were tested with a compressive machine with higher capacity that is normally used for concrete specimens and provides only the maximum compressive strength of the specimens.

(a)   (b)

Figure 4-5 Testing equipment

The average compressive strength for days 1, 3, 7, and 28 past production are shown in Figure 4-21 for all the mix designs. It is observed from Figure 4-21 that the average compressive strength for the CLSM tested on day 1 lies at a range from 10 psi to 25 psi. The average strength is linearly related to the cement percentage, except for the CLSM 1-76-23-4, which seems to be out of the linear range. The specimen with 6 percent cement had the greatest compressive strength. The specimen with 7 and 8 percent cement were not tested on the first day. The results shown from the 3rd day of testing are in a range of 6 to 54 psi and are linearly related to the cement percentage used in each mix design. The maximum compressive strength was calculated for the mix design 1-76-23-8, and the minimum for the 1-76-23-3. The average compressive strength of the mix designs tested on day 7 followed a linear trend in a range of 4 to 132 psi, as shown in Figure 4-21. The maximum average compressive strength for the mix 1-76-23-8 and the minimum was for mix design 1-76-23-1. Observing the trend of the results for the 7th day, the compressive

strength for 1-76-23-8 was higher than the linearly-dependent values of the rest of the mixes. A slightly elevated average compressive strength was observed for the 28th day, although the overall trend seems linear, which has a resemblance to the results from the 7th day. The mix design 1-76-23-8 had higher compressive strength which cannot be included in the linear trend followed by the rest of mixes. The compressive strength of the mixes was in a range of 7 to 192 psi, with the minimum strength observed for the 1-76-23-1 and the maximum for the 1-76-23-8.
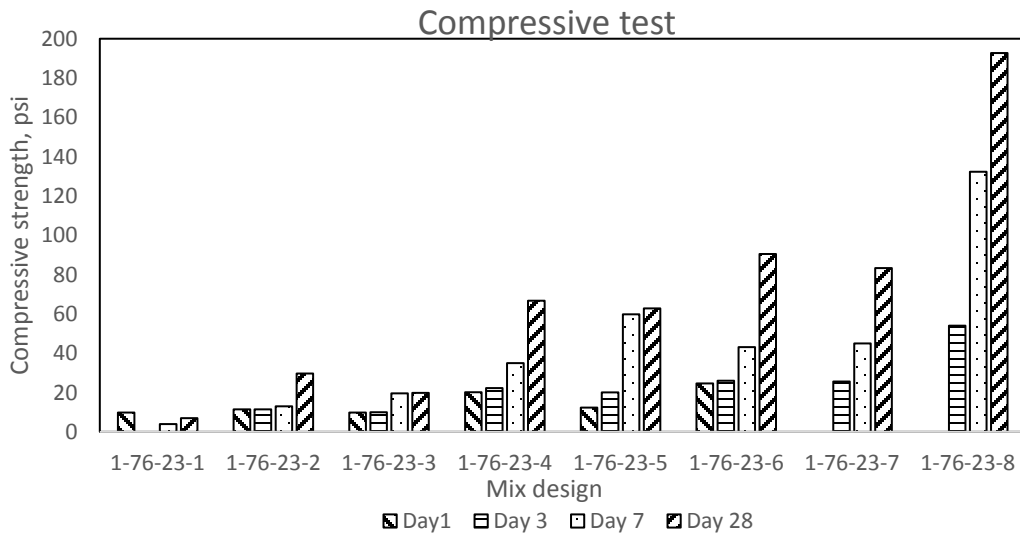
Figure 4-6 Compressive strength vs. testing days for every mix design

4.4.1.2   Compressive Test Results

Compressive strength vs. day of testing

The average compressing strength for different testing days for specimens 1-76-23-1 to 1-76-23-8 are shown in Figure 4-6. It can be observed that for all the mix designs, except that on 1-76-23-1, the compressive strength increases with time. The mix 1-76-23-1 seems to have had an error on the first day, when the pressure was higher than the rest of the days tested. This can be attributed to either errors during production or micro-

cracking during capping. These specimens were very fragile, so it could also have occurred while transferring them to the testing locations. The compressive strength for the 28th day of testing was equal or higher than the 7th day. The compressive strength on the 28th day was almost twice the value of the 7th day for the mixes 1-76-23-1, 1-76-23-2, 1-76-23-4, 1-76-23-6, 1-76-23-7, 1-76-23-8. For the remaining two mixes, the compression strength for the 7th and 28th day was approximately equal. This can be contributed to production errors.

Compressive strength vs. strain

The stress-strain graphs are categorized based on the day of testing after the production. The specimens with required load higher than 1000 lbs. were not tested with this equipment. Therefore, the results that are presented in Figure 4-7 to Figure 4-10 are based on the specimens that were able to be tested with the equipment shown in Figure 4-5 (b). The failure patterns of selected specimens are also shown on the stress-strain graphs. The failure pattern of the specimens were either a distinct shear crack starting at a length of one third of the specimen height, or complete crushing at a height about the middle of the specimen. It should be mentioned that the compressive strength of these mix designs were presented in the previous section.
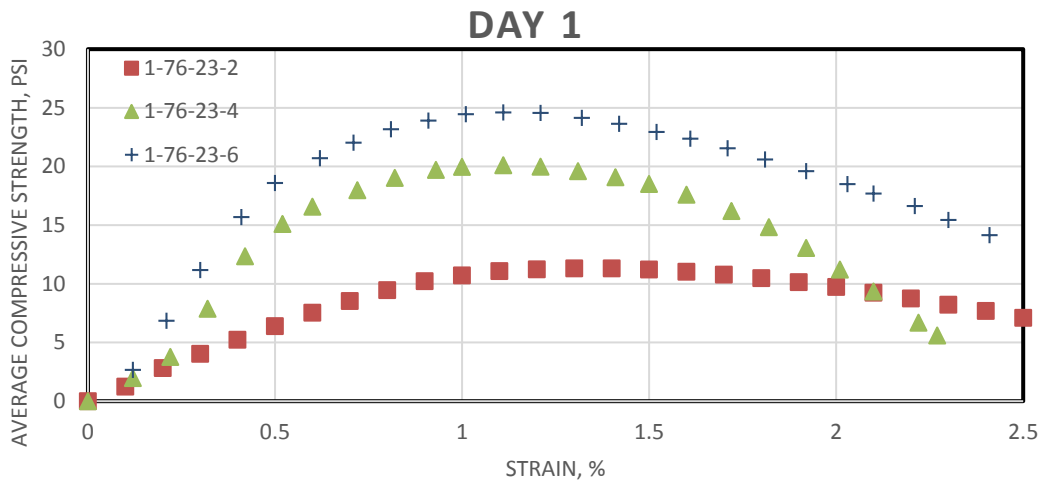
Figure 4-7 Stress vs. strain for first day
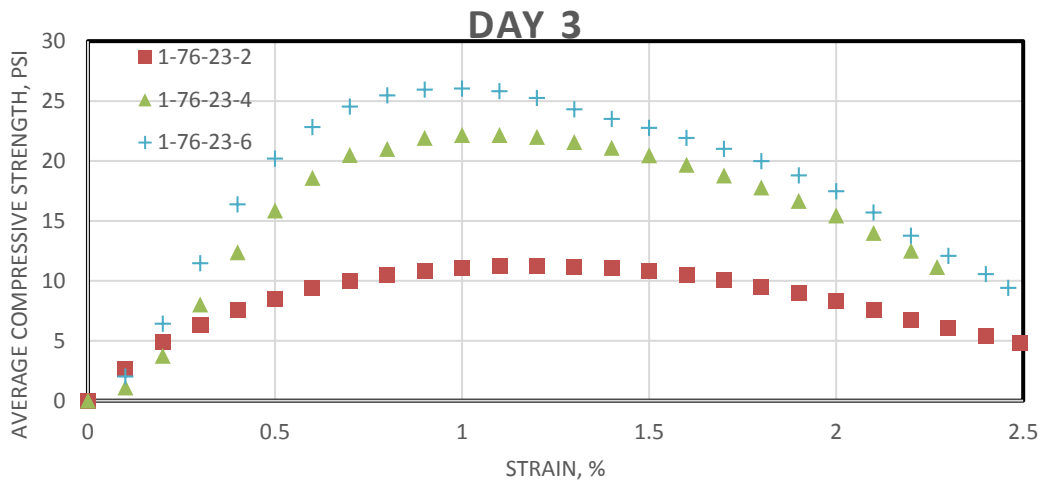
Figure 4-8 Stress vs. strain for third day
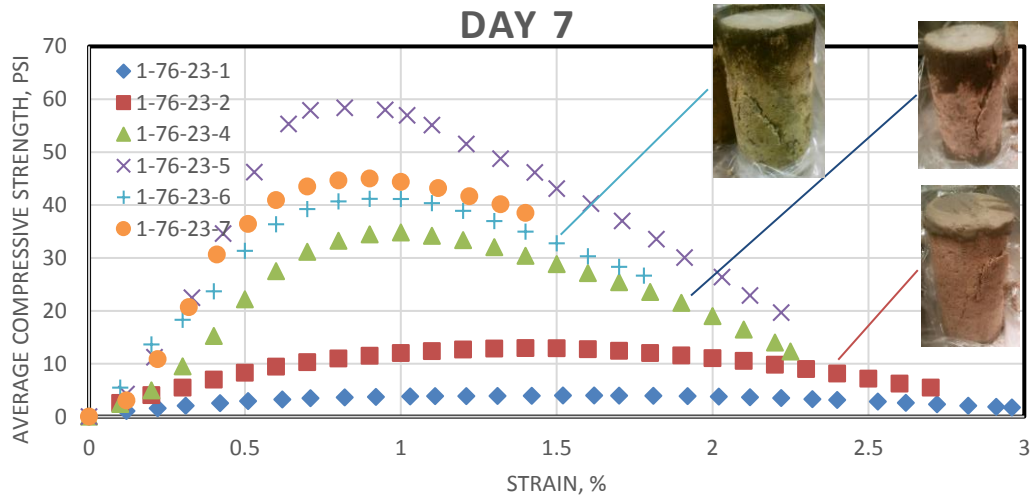
Figure 4-9 Stress vs. strain for seventh day
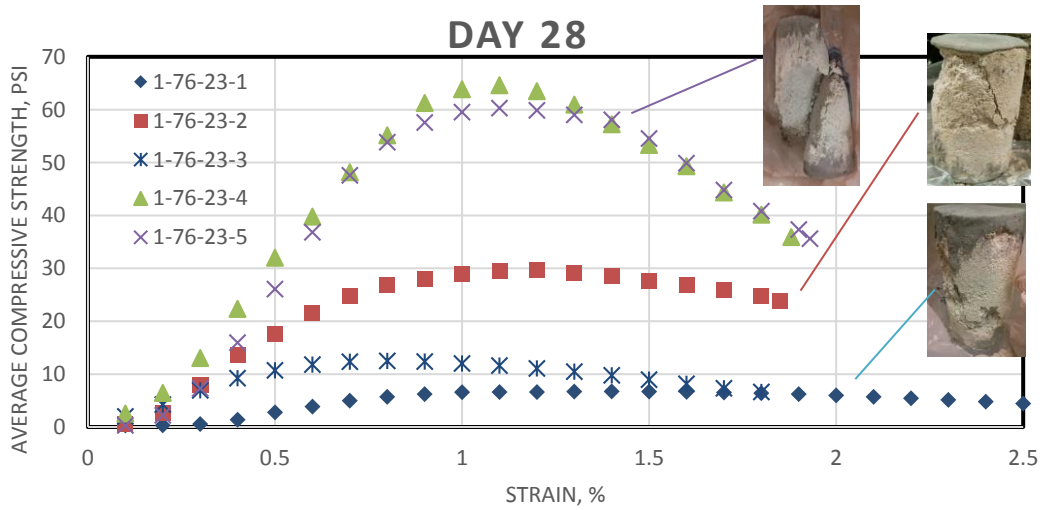
Figure 4-10 Stress vs. strain for twenty-eighth day

4.4.2   Spitting Tensile Cylinder Test

4.4.2.1   Test Setup

The spitting test of the mix design was based on the ASTM standard C496, which is mainly used for concrete, due to the lack of a national standard for investigation of the tensile properties of the CLSM. The test setup is shown in Figure 4-11. A supplementary bearing bar was used om both the top and the bottom of the specimen since the height of the specimens was greater than the one of the bearing plate that was applying the load. Thin plywood was used between the bearing plate and the specimens to assure a smooth distribution of the load applied along the length of the cylinder. Two supplementary bearing bars were used at the top and bottom of the specimens, since they were 1 in. longer than the bearing plates at the top and bottom. Diametral lines were drawn along the ends of the specimens to ensure the load application at the same axial plane, as shown in Figure 4-12. A diametral compressive force was applied along the length of the specimen as displacement. The failure of the specimen was expected to be tensile, expressed with a vertical crack along the circular surface of the cylinder, as shown in Figure 4-12. This happens due to the governing of a state of triaxial compression, which governs at the load application area that allows for higher compression strength than the uniaxial compression strength. Two linear variable differential transformers (LVDT) were used to measure the crack width at the middle of the specimen, as shown in Figure 4-11. The vertical deflection was measured with the LVDT installed on the MTS machine.

\

Line drawn in the middle
section of the specimen

Plywood bearing strips

LVDT

Supplementary bearing plate
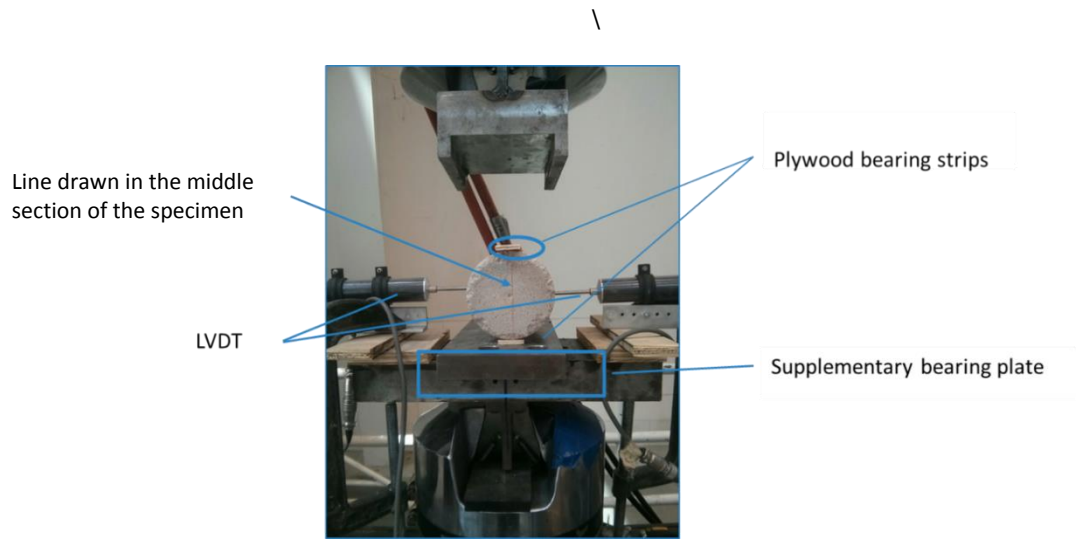
Figure 4-11 Splitting test setup

Figure 4-12 Failure pattern for the splitting tensile test

The maximum and average tensile splitting strength were calculated for each mix design. The average splitting tensile strength vs. the mix design is presented In Figure 4-13. It is observed that, with the exception of mix 1-76-23-8, there is a linear relationship that has higher splitting tensile strength than the rest of the mixes. An example of the load vs. vertical displacement and load vs. horizontal displacement for the mix design 1-76-23-3 is shown in Figure 4-14 and Figure 4-15. A detailed load-displacement curve for every mix design is provided in Appendix C.
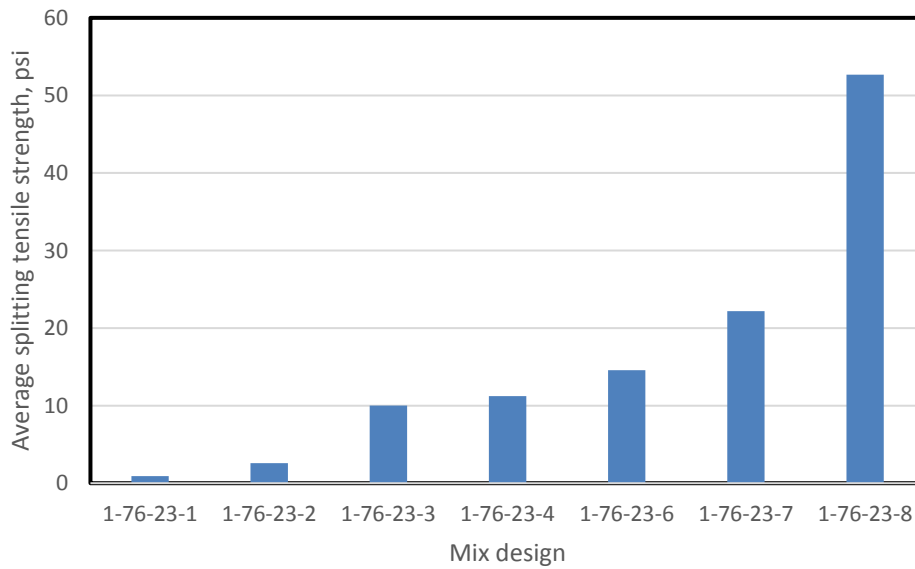
Figure 4-13 Average splitting tensile strength

Figure 4-14 Stress vs. vertical stress for 1-76-23-3 mix design

Figure 4-15 Stress vs. crack width for the 1-76-23-3 mix design

The tensile material properties of the CLSM 1-76-23-6, which were previously tested in the Civil Engineering Laboratory of the University of Texas at Arlington, were also investigated with FEA. Based on Abrishambaf et al. (53), the splitting test is considered an indirect definition of the tensile properties, and inverse analysis is required. Inverse analysis, which is introduced in their study, is actually defining the tensile material properties to be implemented in any FEM model for a direct simulation of the tensile material properties.

The same set up was simulated with FEA, by using ABAQUS 6.14. The model simulated with ABAQUS is shown in Figure 4-16 (a), where the cylindrical specimen and the rigid surfaces used to apply the load and the boundary conditions are shown. The vertical reaction vs. the vertical displacement are calculated at the points that are shown in Figure 4-16 (b). The tensile material properties of the CLSM, calibrated through the "inverse analysis" according to (53), are shown in Figure 4-17. The results from the FEA are compared with the experimental test and are shown in Figure 4-18. It can be observed that the tensile stress and strain of the specimens are identical.

(b)

(a)
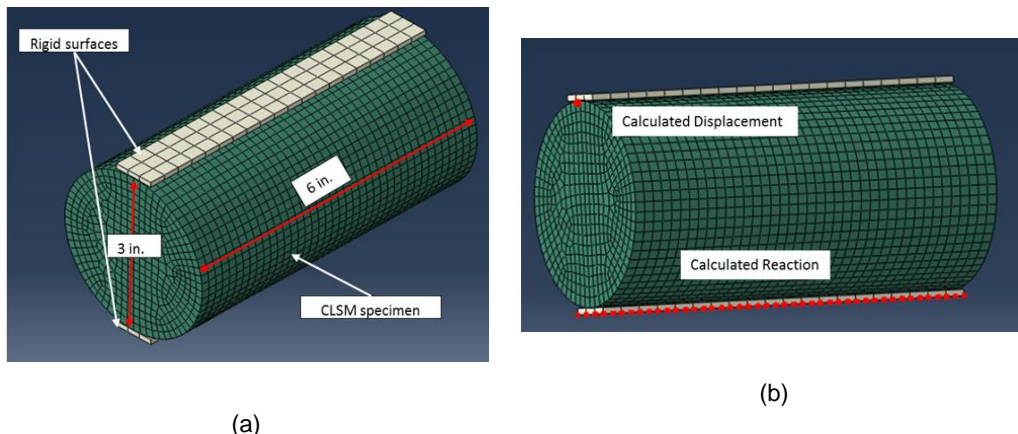
Figure 4-16 (a) Cylindrical specimen representing the spit cylinder test and (b) Points where vertical displacement and reaction are calculated with FEA

The plastic strain calculated with FEA, which simulates the location of the crack opening, is shown in four different phases in Figure 4-19 a-d. Figure 4-19 (a) simulates the beginning of the cracking, while Figure 4-19 (d) simulates the end of the test. In Figure 4-20, the failure mode of the cylindrical specimen is shown at the end of the splitting test. While comparing the experimental failure mode with the plastic strain calculated with FEA, it can be concluded that the FEA successfully simulated the crack opening location.
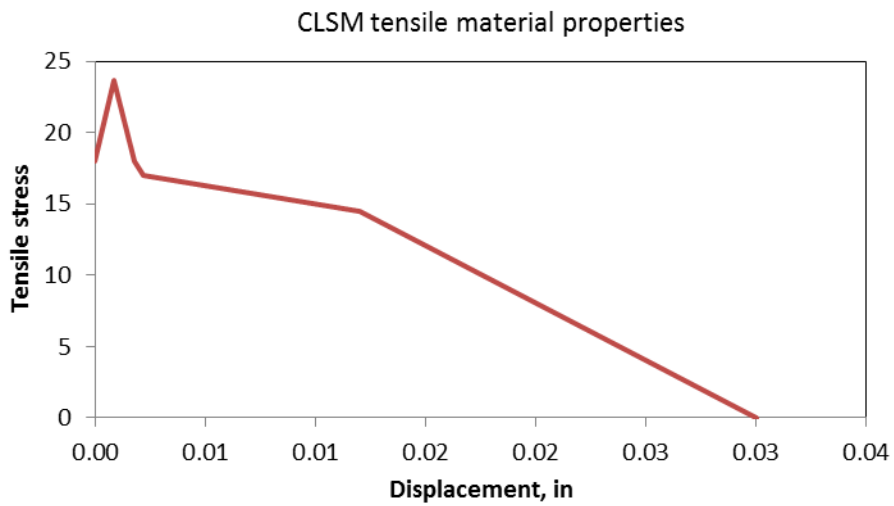
Figure 4-17 Concrete-damaged plasticity - tensile properties for CLSM
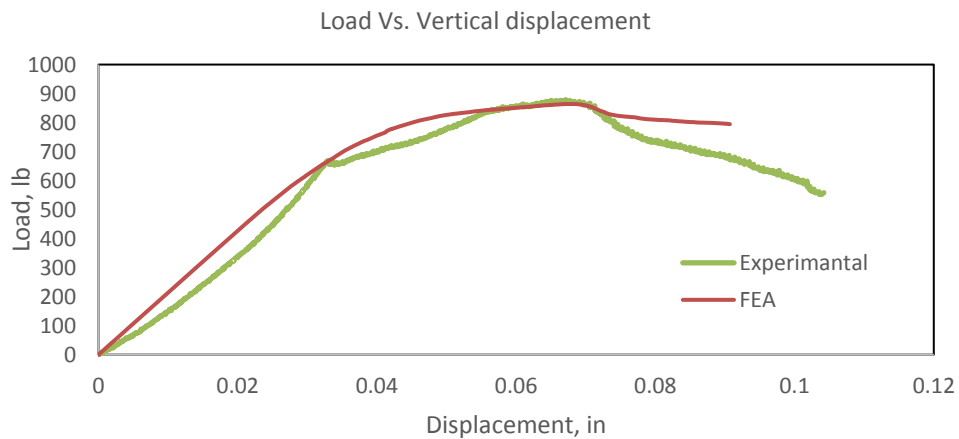
Figure 4-18 Reaction vs. vertical displacement calculated with experimental tests and FEA

144
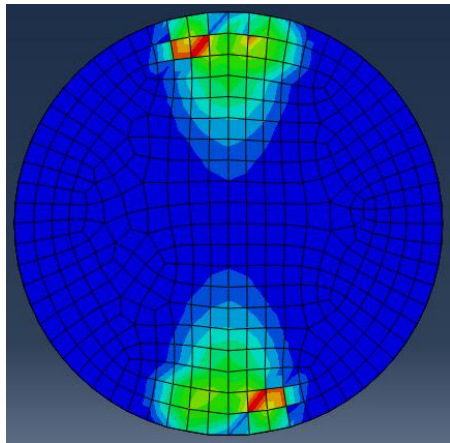
(a)
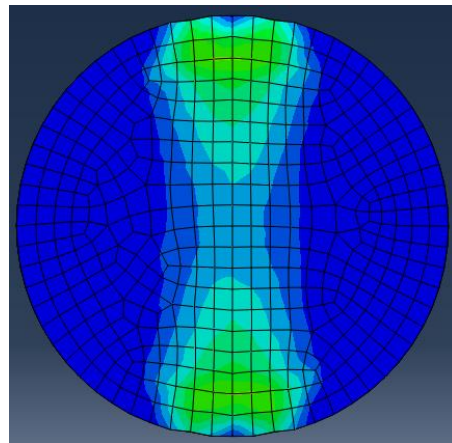
(b)
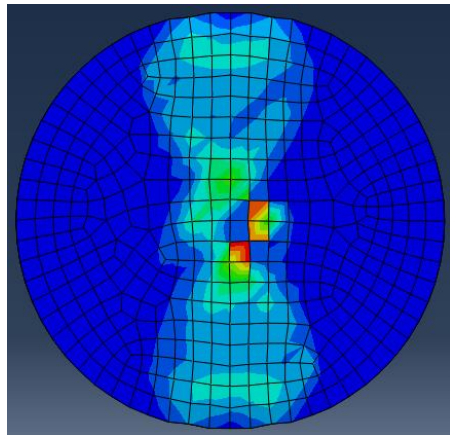
(c)
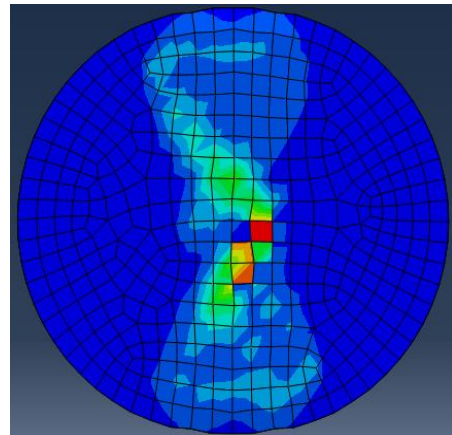
(d)

Figure 4-19 Plastic strain development through the diameter of the cylindrical specimen

Figure 4-20 Failure of the cylindrical specimen at the end of the experimental splitting test

4.4.3   Confined Triaxial Test

4.4.3.1   Test Setup

The confined triaxial test was conducted with the triaxial machine, shown in Figure 4-5 (b) and Figure 4-21. Three different horizontal-confinement pressures were applied to the specimens. Through this method, the Mohr circle was drawn, and the cohesion (c) and the friction angle (φ) were calculated. Based on Schanz et al. (54), the triaxial rate of dilation coincides with the rate of dilation found in plane stress. Based on Bolton (55), the dialtancy angle is related to the friction angle based on Equation 10.

$$\sin \psi = \frac{\sin \varphi - sin\varphi_t}{1 - sin\varphi * sin\varphi_t}$$ Equation (10)

Where,

ψ is the dilatancy angle, φ is the friction angle, and φ_t is the critical state angle

Based on the same study, the friction angle differs when the triaxial strain and plane strains are compared, but the rate of the dilation is strain-independent. For both triaxial and biaxial strain, it was found that there is a constant relationship between the strain peak ratio ($\varepsilon v/\varepsilon_1$)

146

and the relative dilatancy index (I_R), which is equal to 0.3. This supports the idea of a unique angle of dilatancy.

4.4.3.2   Confined Triaxial Test Results

The cohesion and the friction angle were calculated for all the mix designs, as shown in Figure 4-22. Three specimens were tested with the confined method for each mix design, and the deviatoric stress vs. strain are shown in Figure 4-23. The cohesion and the friction angle for all mix designs are shown in Figure 4-24.

Figure 4-21 Confined triaxial test setup
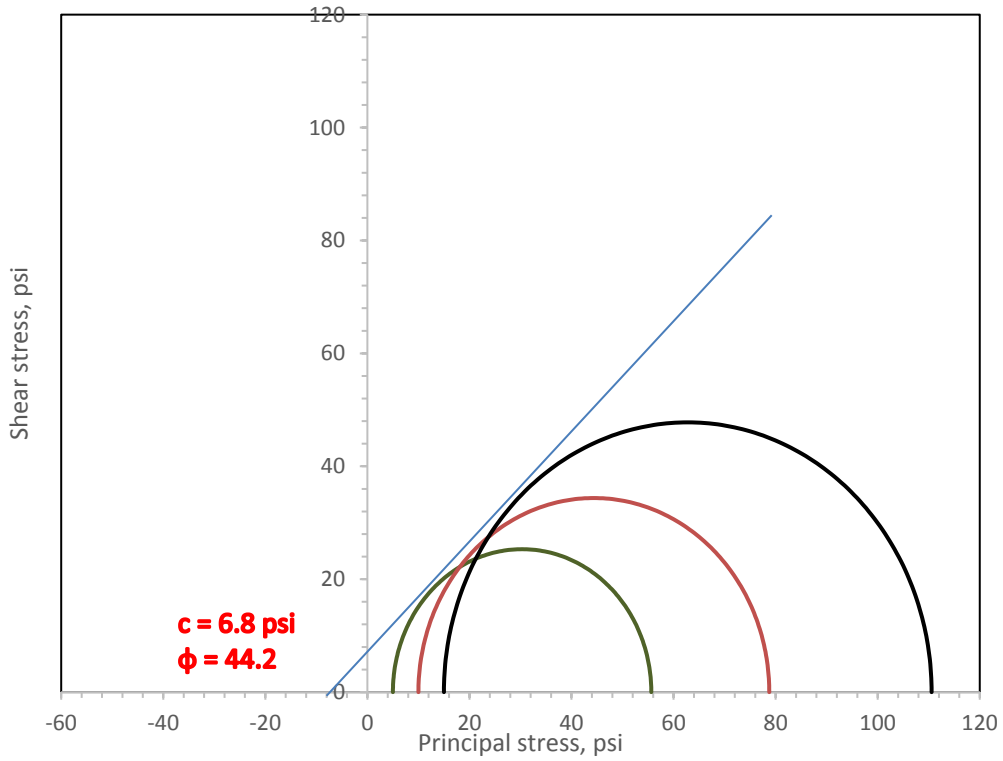
Figure 4-22 Calculation of cohesion and friction angles for the 1-76-23-6 mix design
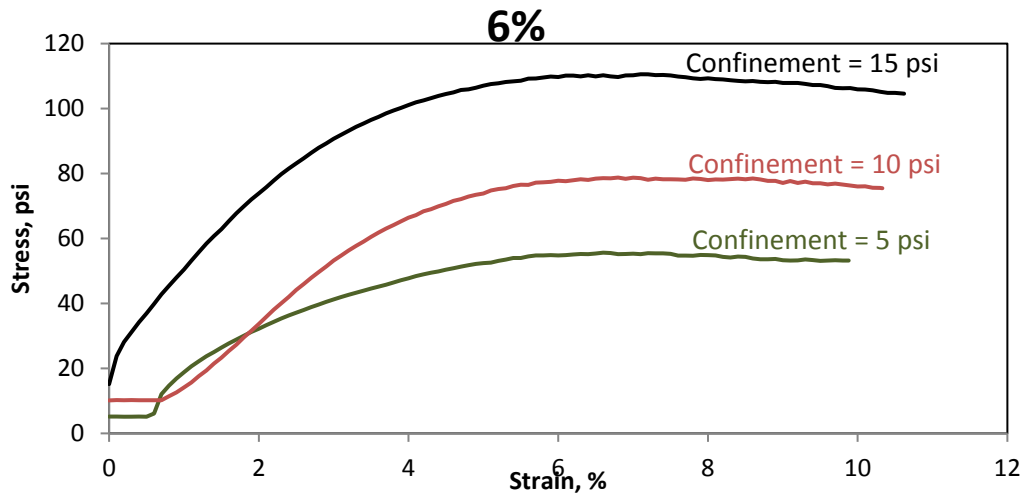
Figure 4-23 Deviatoric stress vs. strain for 5, 10, and 15 confinement stress for the 1-76-23-6 mix design
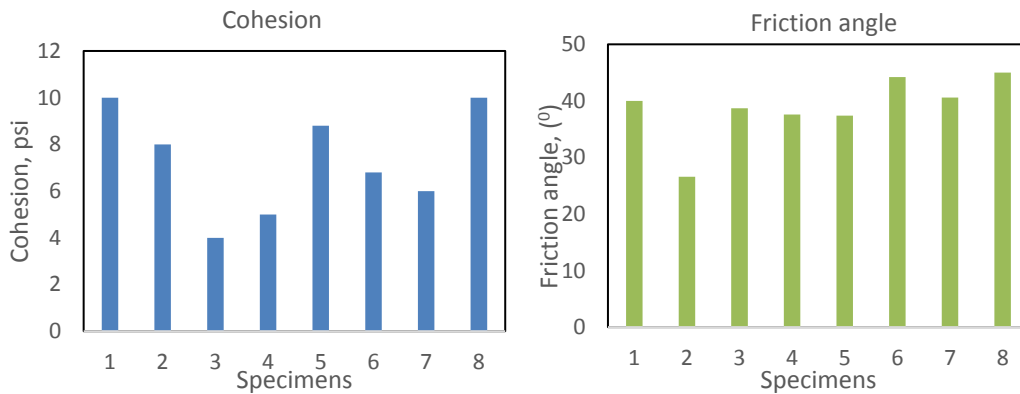
Figure 4-24 Cohesion and friction angle for all the mix designs

In Table 4-6, the mean maximum axial stress or confined compressive strength (σ_{peak}) for each σ_L is given, along other representative results. The σ_L/ fc ratio was calculated with the f_{peak} from the unconfined axial compressive strength tested on the same day as the confined triaxial test. The axial stress and the initial strains at the peak, ε_{peak}, and the initial slope at the axial stress-strain curves (at the beginning of the application of the axial load), E_0^{tan}, are also given in Table 4-6. The initial slope for the confined triaxial test does not represent the modulus of elasticity, except in the case of σ_L= 0.

Table 4-6 Test results

Specimens	σ_L (psi)	Age (days)	σ_L/ fc (%)	$\sigma_{peak,avg}$ (psi)	ε_{peak} (%)	E_0^{tan} (psi)
1-76-23-2	0	3	0.00	11.50	1.30	1,255
	5	3	43.48	38.07	7.50	73,955
	7	3	60.87	32.30	15.20	78,275
	15	3	130.43	50.91	6.90	117,500
1-76-23-3	0	3	0.00	6.20	N/A	N/A
	5	3	80.65	36.65	11.50	85,140
	10	3	161.29	55.89	14.20	97,162
	15	3	241.94	79.69	9.40	138,933
1-76-23-4	0	3	0.00	22.30	1.11	3,778
	5	3	22.42	40.15	7.90	120,254
	10	3	44.84	64.11	8.60	152,511
	15	3	67.26	79.41	8.20	164,633
1-76-23-5	0	3	0.00	20.00	N/A	N/A

5	3	25.00	53.68	6.80	103,700
10	3	50.00	73.87	9.40	158,314
15	3	75.00	90.94	8.60	178,486
	0	3	0.00	26.04	1.11	4,491
1-76-23-6	5	3	19.20	55.64	6.60	122,617
	10	3	38.40	78.75	6.80	185,596
	15	3	57.60	110.56	7.10	259,870
	0	3	0.00	25.61	N/A	N/A
1-76-23-7	5	3	19.52	52.32	7.80	149,106
	10	3	39.05	72.57	8.30	199,511
	15	3	58.57	97.68	8.20	222,222
	0	3	0.00	54.02	N/A	N/A
1-76-23-8	5	3	9.26	72.30	5.90	296,872
	10	3	39.05	87.03	5.80	320,945
	15	3	58.57	132.95	7.00	311,009

4.5   Main findings

The mix design for the CLSM was developed under controlled laboratory conditions, and the material properties were tested based on ASTM standards. The soil was specified as well-graded sand (SW) through the sieve analysis procedure, based on ASTM D2487. The particle percentage was defined as: sand 75.6%, gravel 23.2%, and clay 1.22%. The w/c ratio and the flow consistency of the mix were studied based on literature reviews, Nataraja et al. (26), Lee et al. (27), and Howard et al. (28). The mix design investigation performed in this study for eight cement percentages was for the purpose of defining the differences of the behavior of the CLSM. The material tests conducted, based the ASTM standards, were compression test, split cylinder test, and confined triaxial test.

The compression strength of the specimens was tested for 1, 3, 7, and 28 days past the production day. Overall, 96 cylinders were tested, and the compressive strength for the different tested days were:

- For specimens tested 1 day past the production, the compressive strength ranged from 10 to 24 psi. It should be mentioned that there are no results for the mix designs with 7% and 8% cement.

- For specimens tested 3 days past the production, the compressive strength varied from 10 to 54 psi. It should be mentioned that there are no results for the mix design with 1% cement due to technical problems with the specimens.

- For specimens tested 7 days past the production day, the compressive strength of the specimens varied from 4 to 132 psi.

- For specimens tested 28 days past the production day, the compressive strength varied from 7 to 192 psi.

Based on the results for the compressive strength of the specimens, it was observed that the mix designs with cement percentages from 1 to 3% showed a low strength, the specimens with cement percentage from 4 to 7% showed a higher compressive strength, and the specimens with cement percentage of 8% had a relative higher strength than the other mix designs.

The failure mode of the specimens under the compressive test was also observed for different percentages. The main fracture mode of the specimens was the shear, cone and shear, and columnar failure, as shown in Figure 4-25, and as referred by Neville (56) and the standards (57). When the shear failure happened, which was the most-often observed failure mode, crushing at the top corner occurred at the same time. In other cases, not so often, small columnar cracks were observed along the circumference of the specimens, and small pieces were separated from the main body.

The tensile properties of the CLSM were tested based on the splitting tensile test, or Brazilian test, at 7 days past production. This test avoids the difficult and expensive set-up of the direct tensile test, and it is a good representation of the tensile properties of the material. The failure mode of the specimens occurred, due to tensile stresses, at both round surfaces of the cylinder, as it was expected. The compressive force applied on the

151

two opposite (load and reaction) generatrix of the cylinder causes a uniform tensile stress on the plane containing the axis of the cylinder and the generatrix, leading to Mode 1 cracking, based on Proveti et al. (58), Indriyantho et al. (59), and Lin et al. (60).

(a)
Shear

(b)
Cone and
shear

(c)
Columnar
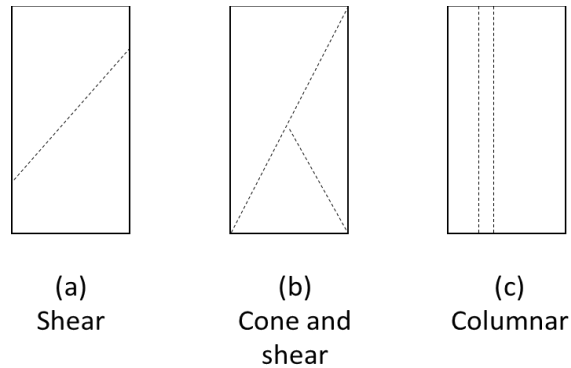
Figure 4-25 Fracture type for the specimens tested

The average tensile strength of the CLSM ranged from 1 psi to 53 psi. For the tensile test, the average strength of the mix design with cement percentages of 1 and 2 are relatively smaller than the stress of the mix with 3 to 7. The mix design with 8% cement percentage has a significant higher stress than the rest of the mix designs.

The average compressive vs. the average tensile strength of the CLSM mixes on the 7th day are shown In Figure 4-26, with the blue dots. A linear relationship is observed between the two strengths, which is shown with a dotted line at the same figure, and it has a slope of 0.4. The equation offered from ACI, which calculates the tensile stress of the concrete to be $7.5*(f_c)^{1/2}$, is not applicable in the case of CLSM, since the compressive strength is small.

To calculate the tensile properties that represent the behavior of the CSLM with 6% cement percentage analyzed with FEA, the inverse analysis was applied. The CLSM with 6% cement percentage was used since it showed a good representation of the

152

average CLSM strengths for both tensile and compressive strengths. Moreover, this percentage is the one used more often in the field. The material properties were defined for the concrete-damaged model available in Abaqus, aiming to match the same load deflection curve from both the experimental and FEA methods.
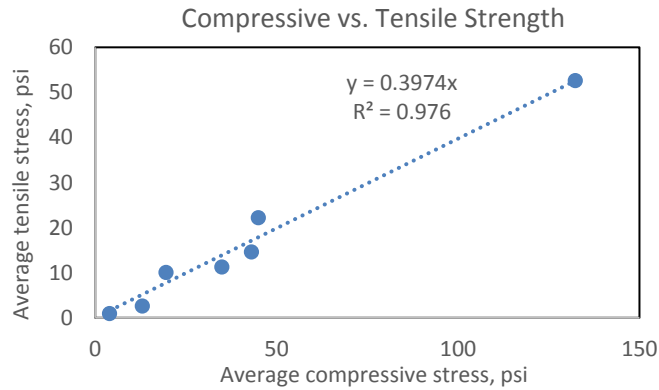
Figure 4-26 Compressive vs. tensile experimental strength of CLSM

The confined triaxial behavior of CLSM was also investigated in this chapter. The cohesion and the friction angle were defined for all the mix designs. No relationship was observed between the calculated values of the cohesion for each mix design. The cohesion ranged from 4 to 10 psi. The highest values were observed for the mix designs with 1, 5, and 8% cement, while the lowest values were observed for the mix designs with 3 and 4% cement.

The friction angle was observed to be constant, around 38-44 degrees for all the mix designs, except for the mix design with 2% cement, which was slightly smaller than the rest of the values, and equal to 27 degrees.

The triaxial compressive stress-strain curve for different confinement stresses is shown in Figure 4-27– 4-29. It can be observed that not only does the compressive strength increase with confinement, but the material becomes more ductile, which was also observed during the testing procedure.
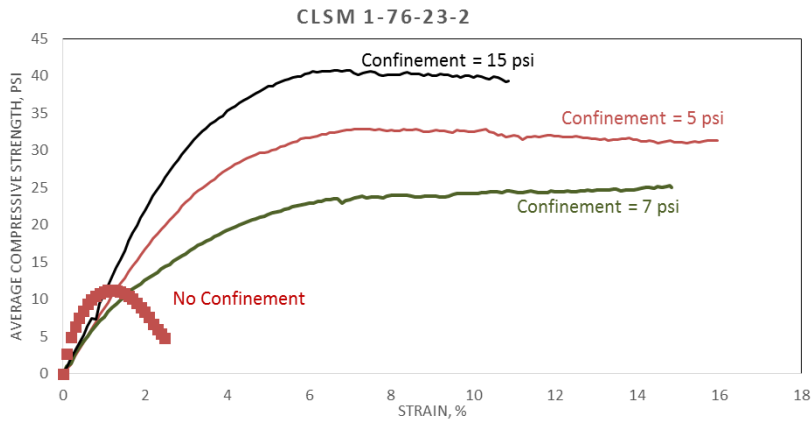
Figure 4-27 Confined and unconfined compressive stress-strain graph for 2%
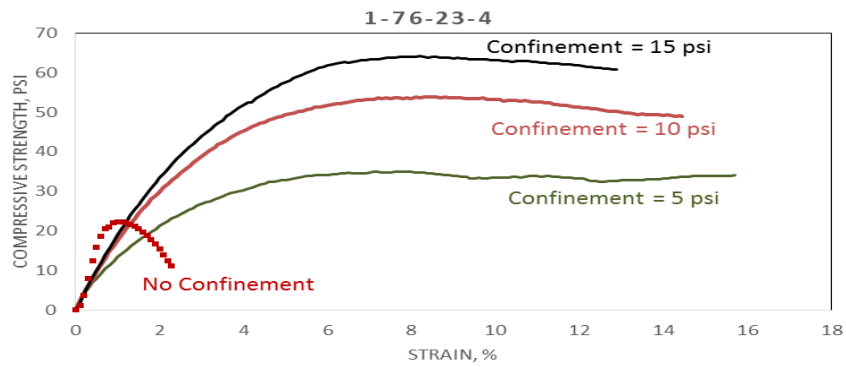
Figure 4-28 Confined and unconfined compressive stress-strain graph for 4%
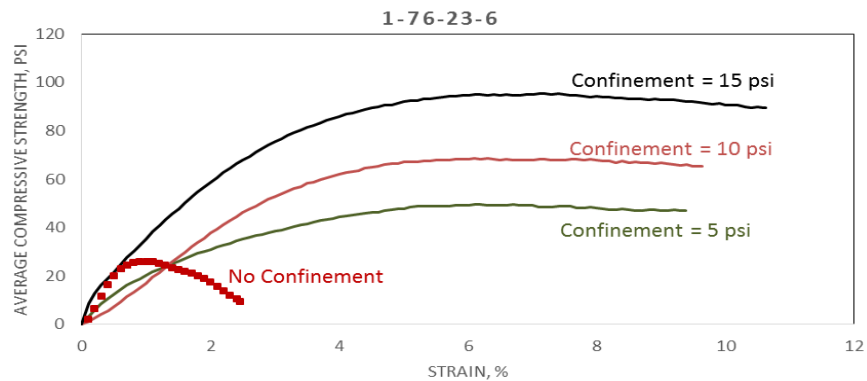
Figure 4-29 Confined and unconfined compressive stress-strain graph for 6%

Chapter 5

PARAMETRIC STUDY AND DESIGN EQUATIONS

5.1   Parametric Study

A detailed parametric study was conducted based on the variables shown in Table 5-1. A total of 3456 model were analyzed with Abaqus software and post-processed to extract results for horizontal and vertical deflection, moment, thrust and shear of the pipe at the last step of the analysis. The results from the analysis software were the input for the regression analysis. The procedure followed is also shown in Figure 5-1.

Table 5-1 Parametric study

Parametric Study of Large-Diameter Steel Pipe with CLSM			
Outer pipe diameter-O.D. (in)	84	96	108	120
Trench Wall Stiffness(ksi)	0.3	0.5	0.7	1.0
O.D./t	220		230	288
CLSM depth	0.3 O.D.	0.5 O.D.	0.7 O.D.	1.0 O.D.
Embedment material	Native Soil		Treated	Select Fill
Trench width	O.D. + < 18'' until 48'' in 6-inch increments>			
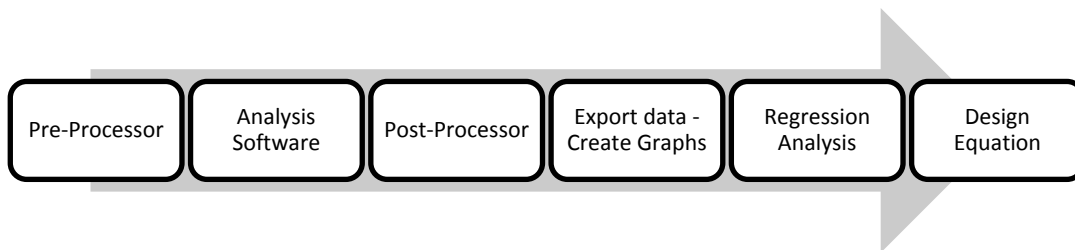
Figure 5-1 Equation design procedure

Pre-processor is a Design Program (DP) that was developed using C# programing language which produces python files scripts. These scripts are imported to the analysis software program and analyzed through the procedure explained in chapter 3. Creating

the script through the DP saves significant amount of time and therefore it is a critical tool for conducting the parametric study. The interface of the DP program, which creates the python scripts, is shown in Figure 5-2. The name of each script defines the case of each model, i.e. "IPL-120-PW200-CLSM3NA-CLSM8-OD+18-SR3.py" is a case of a pipe-soil system where:

1. The first part defines the analysis section that the model belongs

2. The second part expresses the pipe diameter in inches, which for this case is 120 in.

3. The third part refers to the OD/Thickness of the pipe, which for this case is equal to 200 which means that OD/th=200, and therefore the thickness of the pipe is equal to 0.6 in.

4. The fourth part defines a combination of the CLSM height and the soil type used for the embedment layer. The "CLSM3" shows that the CLSM is placed until a level height of 30% of the pipe diameter, which means until a level of 36 in from the pipe invert. The "NA" defines that the native soil material is used after the CLSM.

5. The fifth part defines the modulus of elasticity for the CLSM layer. For this study a CLSM of 8 ksi was used.

6. The sixth part is the one which defines the trench width of the model. In this case the "OD+18" defines that the trench width is equal to the summation of the pipe diameter and the number next to it. For this example the trench width is equal to 120in + 18in.

7. The seventh and last part of the model's name refers to the trench wall stiffness, denoting the elastic modulus of it. SR3 means that the trench wall used for this model had an elastic modulus of 0.3 ksi.
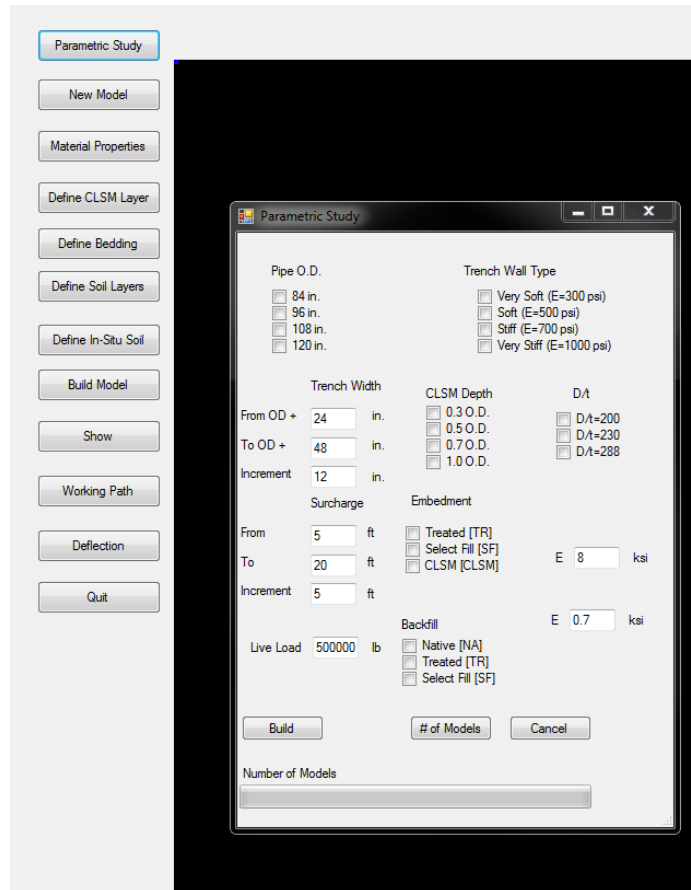
Figure 5-2 Design Program Interface which creates the python scripts

The analysis software analyzes the models and the results are saved and expressed as element or nodal dependent values. The values needed from each model were the deflection, moment, shear and thrust of the pipe-mortar system, as well as the stress state of the soil and CLSM around the pipe during every step of the loading history. For extracting the results a separate python code was developed. The deflection of the pipe was calculated on two paths along its circumference, inner and outer wall. The vertical deflection of the pipe is equal to the vertical deflection at the crown subtracted by the vertical deflection at the invert of the pipe. The net deflection of the pipe is calculated by

this method. The horizontal deflection of the pipe is calculated at the spring-line of the pipe and multiplied by two, due to symmetry.

The moment, thrust and shear at the pipe are calculated through the body forces option, which calculates forces and moments at the pre-defined sections. For this study moments and forces were extracted for every 5°, which is translated into 36 section along the circumference of the half pipe section, as shown in Figure 5-3 and Figure 5-4. A typical graph configuration created with DP is shown in Figure 5-5. For every case the deflected shape of the pipe is shown in a scale factor of ten, at the initial and final stage of the analysis. Also the moment, thrust and shear of the pipe along its circumference are shown for three different loading conditions: 1. end of CLSM layer, 2. when the soil cover reaches the crown of the pipe, and 3. at the end of the analysis. The stresses of the soil for 1 feet distance from the crown and invert, and also at a distance of 2 inches, mid of the trench width and 2 inches from the end of the trench opening from the spring-line of the pipe are also shown in Figure 5-5. Through these graphs one can observe the behavior of the pipe during the loading history.
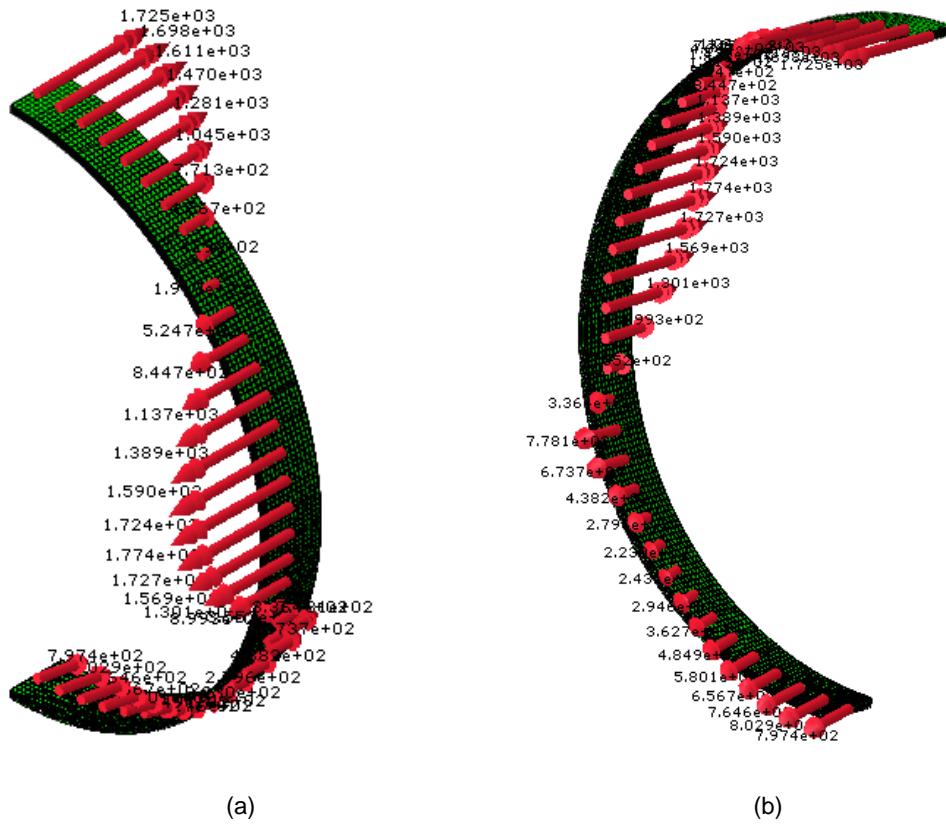
Figure 5-3 Resultant moment along the circumference of the pipe (a) inside wall and (b) outside wall
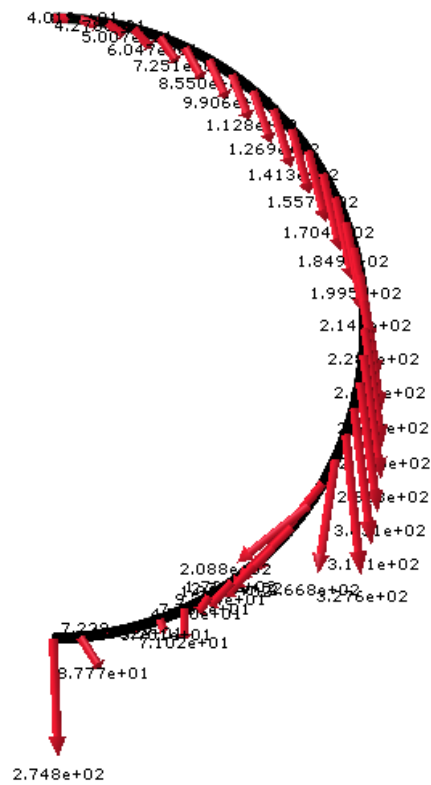
Figure 5-4 Resultant force at the circumference of the steel pipe

Equations are developed from a regression analysis performed aiming to develop equations that predict the horizontal and vertical deflection, moment, shear force and thrust of large diameter pipe with CLSM. The independent variables used for this analysis are:

- Pipe diameter expressed in ft.

- Pipe wall thickness expressed in in.

- Ratio of backfilling material to pipe diameter , alfa

- Modulus of elasticity of the backfilling materials expressed in ksi

- Ratio of embedment material to pipe diameter, beta

- Trench width expressed in ft. and

- Modulus of elasticity of the trench wall expressed in ksi

160
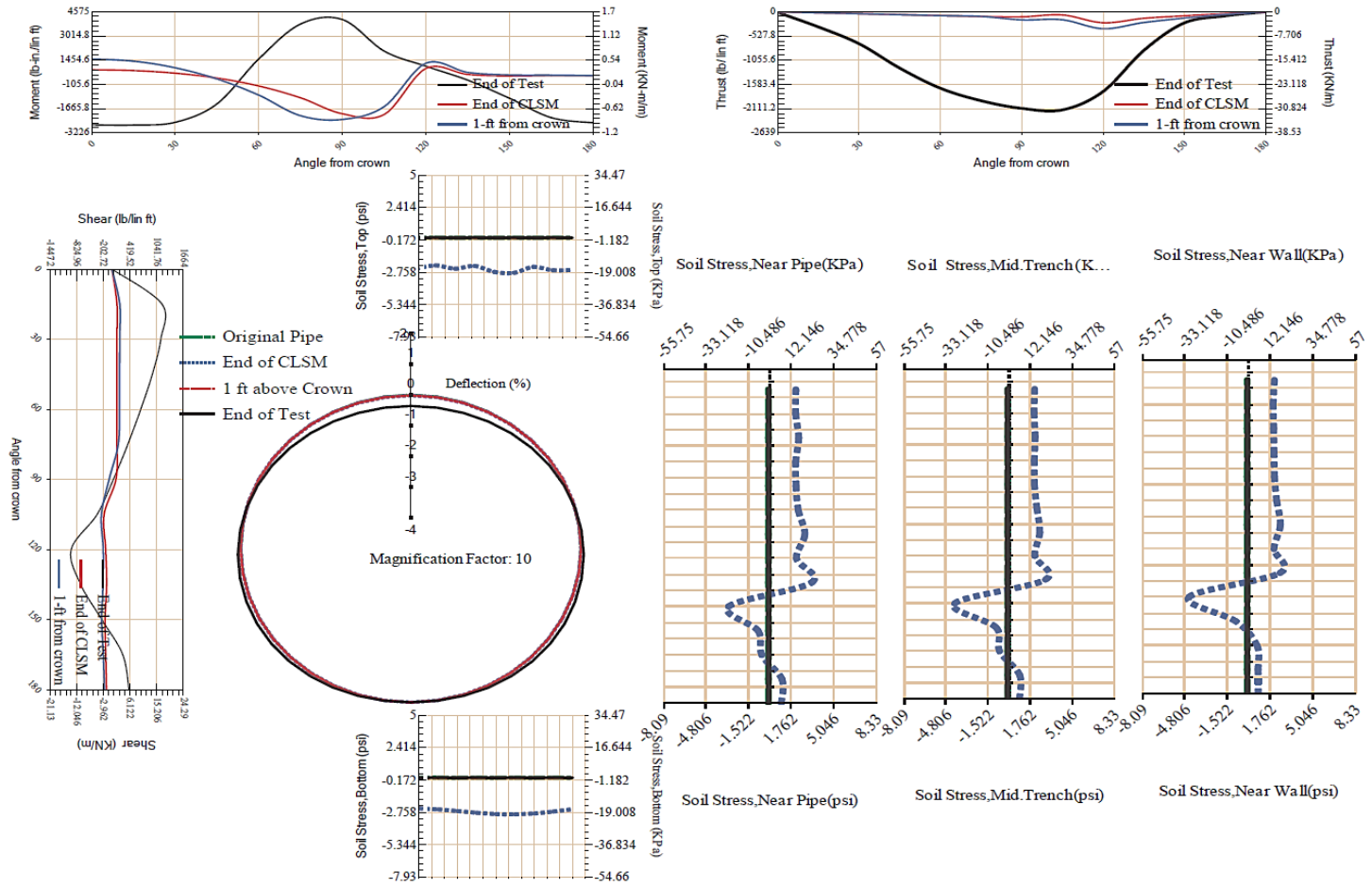
Figure 5-5 Deflected shape, moment, thrust, shear and soil stress of the case IPL-84-PW230-CLSM3NA-CLSM8-OD+24-SR3

161

1   To investigate the condition of the CLSM, cracked or not cracked, at the end of the

2   loading history, a separate code was written in python code. This program extracts the

3   strain value of the elements that belong to the CLSM layer and gives the maximum value.

4   A graph with the maximum strain for the CLSM layer, at the end of the loading history are

5   presented in Figure 5-6. The red line at the same figure shows the cracking strain of the

6   CLSM. All the data above the red line defined the cases that the CLSM is cracked (plastic

7   region), while the data below the red line indicates that the CLSM was not cracked (elastic

8   region). The ratio of the cases that are in elastic region to the overall cases is 39%, while

9   the ones in plastic region is 61%. The cases that are in the plastic region are mainly the

10   cases: (1) CLSM height at 70% of the O.D. and for trench width of O.D.+18'' until 36'', (2)

11   CLSM height at 50% of the O.D. and for trench width of O.D.+18'' until 30'', (3) few cases

12   for CLSM height at 30% O.D. and O.D. 96,108,120.
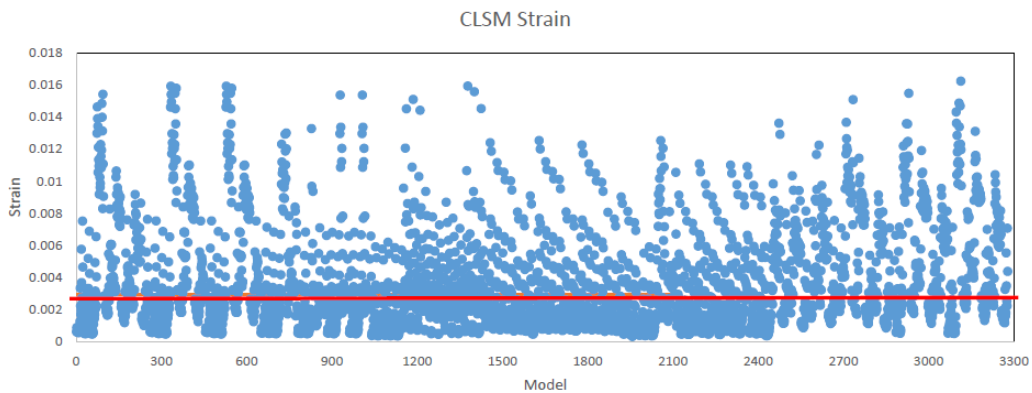
13

14   Figure 5-6 Maximum strain for all the cases

15

16   5.2   Sensitivity Analysis

17   The predictors used for the parametric study were tested in with a sensitivity

18   analysis to check the effect of each independent variable to the response of the dependent

162

1   variable. For example, a steep slope on such analysis indicates that the effect on that

2   independent variable is significant. If the effect of variation of the independent variable had

3   been insignificant, the graph would have a flat slope. The independent variables are shown

4   in Table 5-2 along with the cases analyzed, which are defined by changing one variable at

5   the time and keeping all the rest variables constant. The dependent variables are the

6   horizontal and vertical deflection, moment, thrust and shear.

7   The effect of the independent variables on the horizontal and vertical deflections

8   are shown in Figure 5-7 to Figure 5-11. The deflection of the pipe, expressed in percentage,

9   is shown on the vertical axes of the graphs, while each variable on the horizontal was

10   plotted from is low-to-medium-to-high values. In this way, the effect of each variable could

11   be tested. It was observed that all the variables affected the deflection of the pipe since the

12   graphs shown a trend with the dependent variable. The fitting equation and the R-squared

13   values are also shown in each graph. The variable "pipe thickness and 'trench width had a

14   smaller effect on the deflection variable.

15   The effect of the independent variables on thrust and shear were also studied and

16   are shown in Figure 5-12 until Figure 5-17; while the effect to the moment are shown in

17   Figure 5-18 until Figure 5-23. On each graph, load and moment are shown at the vertical

18   axes; the variable tested is shown in the horizontal axes and varied from is low-to-medium-

19   to-high values. It was observed that the all the variables had an important effect on the

20   dependent variables, therefore they are important for identifying the dependent variables.

Table 5-2 Sensitivity analysis

	variables	OD (in.)				OD/thickness			CLSM (OD %)				Embedment soil			Trench width (OD + in.)						Trench stiffness			
	cases	84	96	108	120	200	230	288	0.3	0.5	0.7	1	NA	TR	SF	18	24	30	36	42	48	Vso	So	St	VSt
1	case OD1	*					*				*			*					*					*	
2	case OD2		*				*				*			*					*					*	
3	case OD3			*			*				*			*					*					*	
4	case OD4				*		*				*			*					*					*	
5	case d/t1		*			*					*			*					*					*	
6	case d/t2		*					*			*			*					*					*	
7	case CLSM1		*				*		*					*					*					*	
8	case CLSM2		*				*			*				*					*					*	
9	case CLSM3		*				*					*		*					*					*	
10	case S1		*				*				*		*						*					*	
11	case S3		*				*				*				*				*					*	
12	case TW1		*				*				*			*		*								*	
13	case TW2		*				*				*			*			*							*	
14	case TW3		*				*				*			*				*						*	
15	case TW4		*				*				*			*						*				*	
16	case TW5		*				*				*			*							*			*	
17	case TS1		*				*				*			*					*			*			
18	case TS2		*				*				*			*					*				*		
19	case TS3		*				*				*			*					*						*

CLSM Height

$y = -0.1184x + 0.8217$
$R^2 = 0.9969$

$y = -0.0304x + 0.223$
$R^2 = 0.9728$

Deflection, in — Deflection, mm — CLSM height, %

CLSM 30%   CLSM 50%   CLSM 70%   CLSM 100%
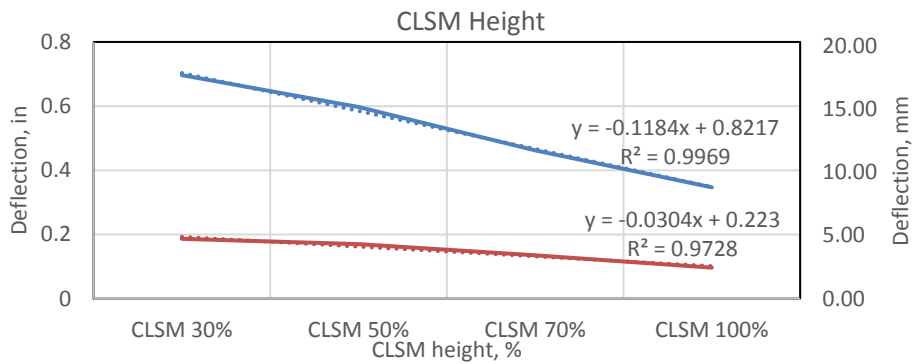
Figure 5-7 Effect of CLSM height to horizontal and vertical pipe deflection

Backfilling material

$y = 0.3989e^{0.1251x}$
$R^2 = 0.9159$

$y = 0.1046e^{0.1993x}$
$R^2 = 0.7992$

Deflection, in — Deflection, mm

Treated Soil   Select Fill Material   Native Soil
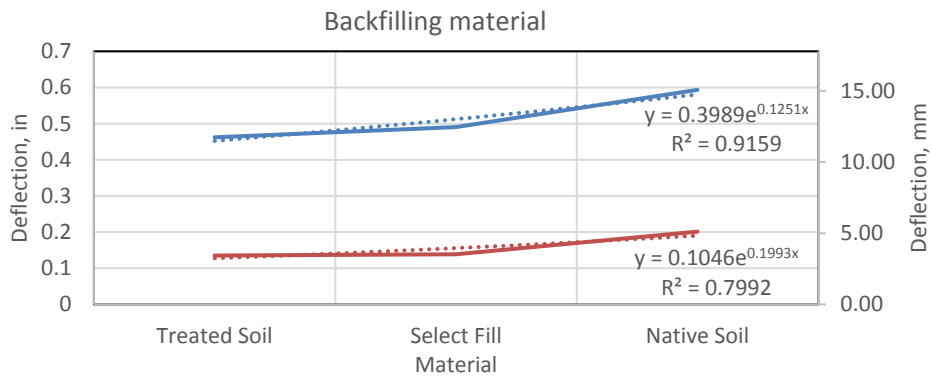
Figure 5-8 Effect of backfilling material to horizontal and vertical deflection

Trench Width

$y = 0.4577e^{0.0022x}$
$R^2 = 0.9644$

$y = 0.135x^{0.0005}$
$R^2 = 0.31$

Deflection, in — Deflection, mm — Trench width, 108 + in

OD+18   OD+24   OD+30   OD+36   OD+42   OD+48
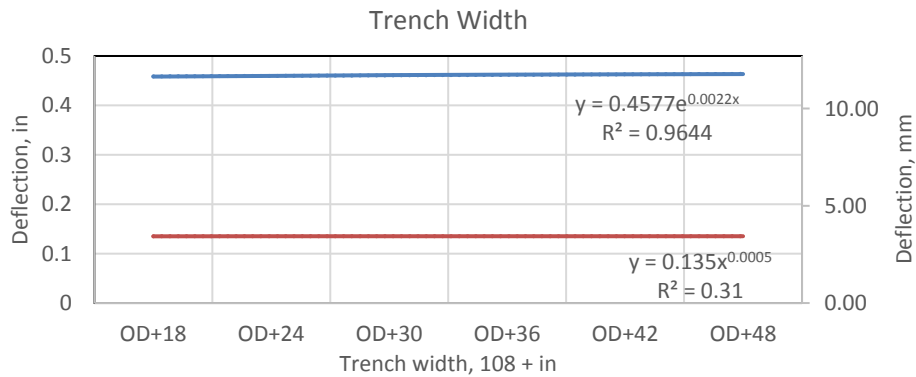
Figure 5-9 Effect of trench width to horizontal and vertical deflection

Trench Wall Stiffness

$y = 1.3136e^{-0.345x}$
$R^2 = 0.9897$

$y = 0.2723e^{-0.233x}$
$R^2 = 0.9931$
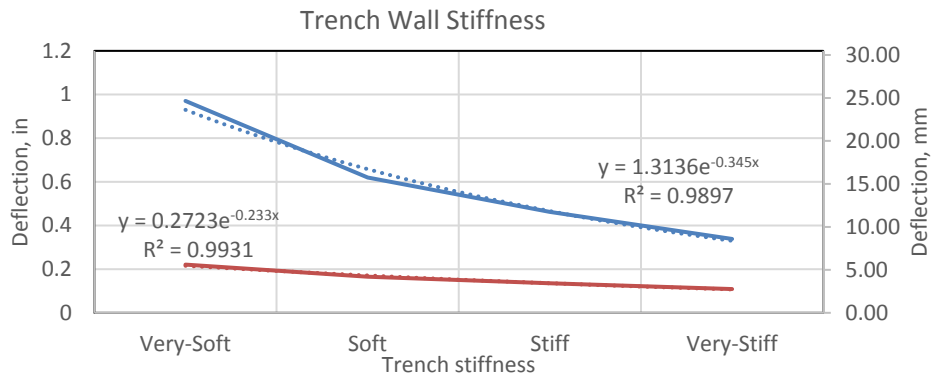
1

2   Figure 5-10 Effect of trench wall stiffness to horizontal and vertical deflection

3

Pipe Thickness

$y = 0.4593x^{0.0053}$
$R^2 = 0.6667$

$y = 0.1196e^{0.0632x}$
$R^2 = 0.9969$
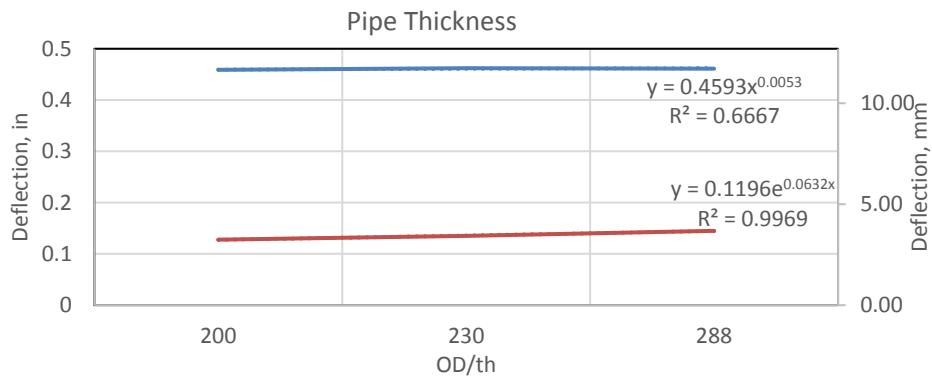
4

5   Figure 5-11 Effect of pipe thickness to horizontal and vertical deflection

6
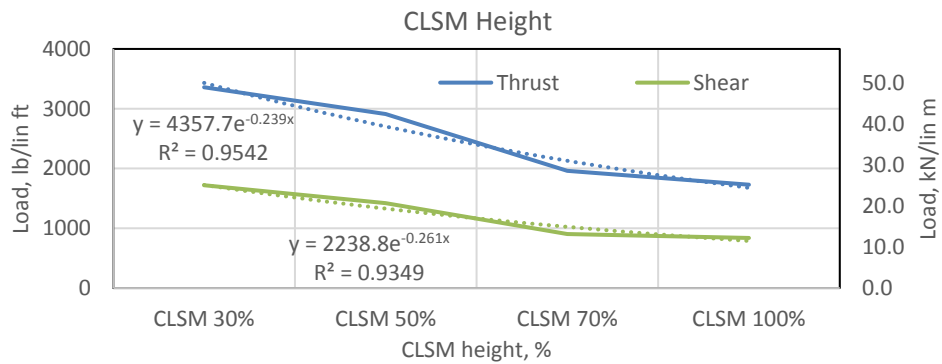
1

2   Figure 5-12 Effect of CLSM height to thrust and shear
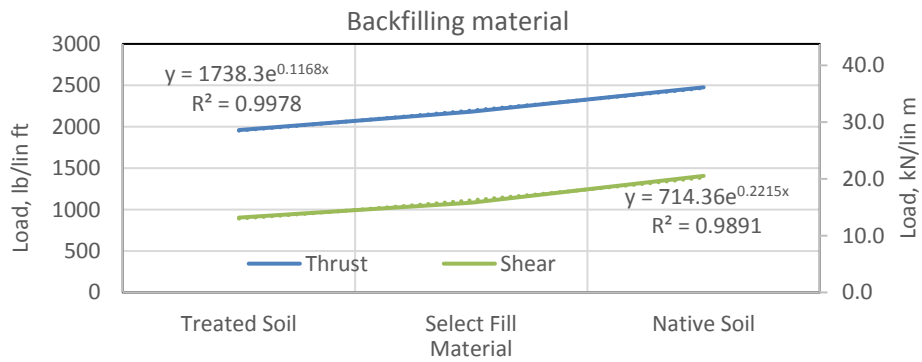
3

4   Figure 5-13 Effect of backfilling material to thrust and shear
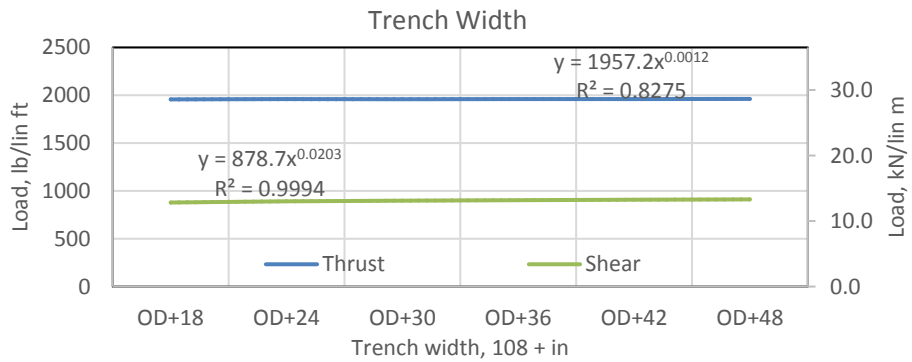
5

6   Figure 5-14 Effect of trench width to thrust and shear

1
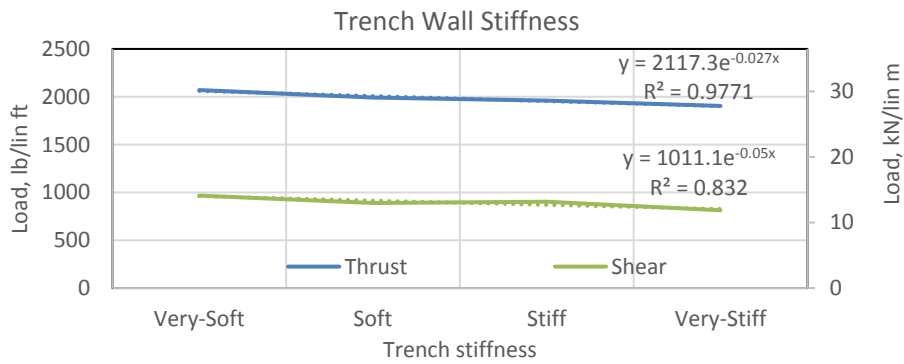
Figure 5-15 Effect of trench wall stiffness to thrust and shear

2

3
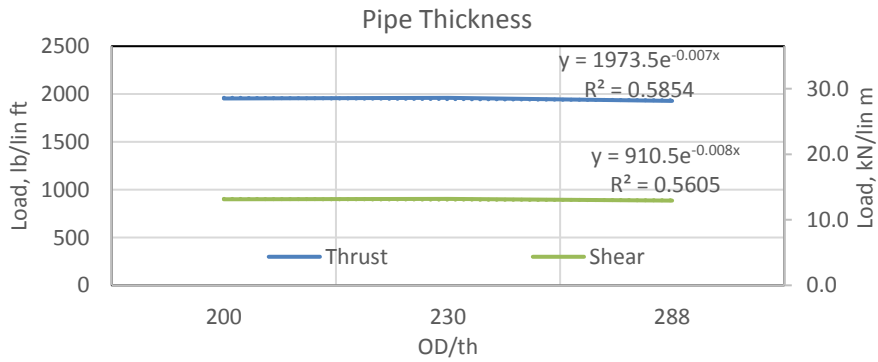
Figure 5-16 Effect of pipe thickness to thrust and shear

4

5
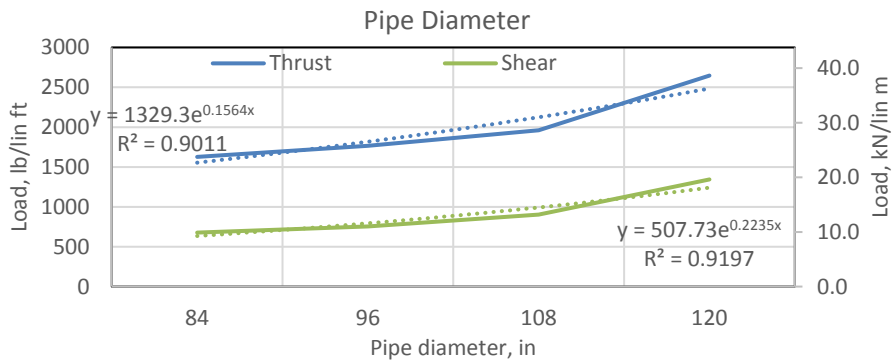
Figure 5-17 Effect of pipe diameter to thrust and shear

6

1

CLSM Height

$y = -638.2x + 5237$
$R^2 = 0.822$
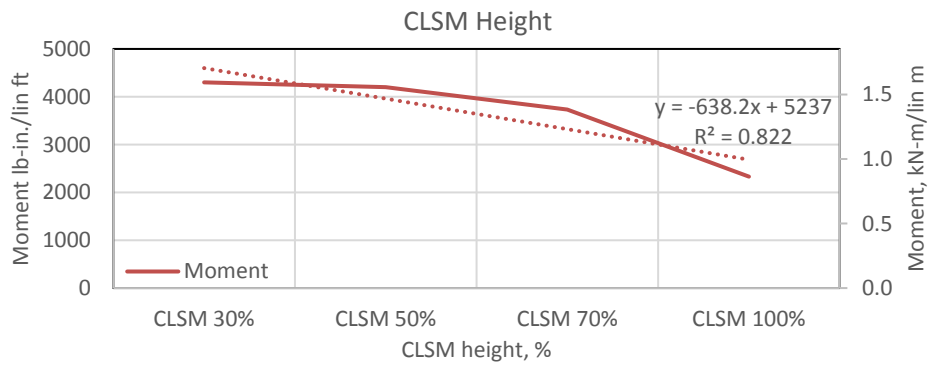
2   Figure 5-18 Effect of CLSM height to moment

3

Backfilling material

$y = 2352.7e^{0.3311x}$
$R^2 = 0.6821$
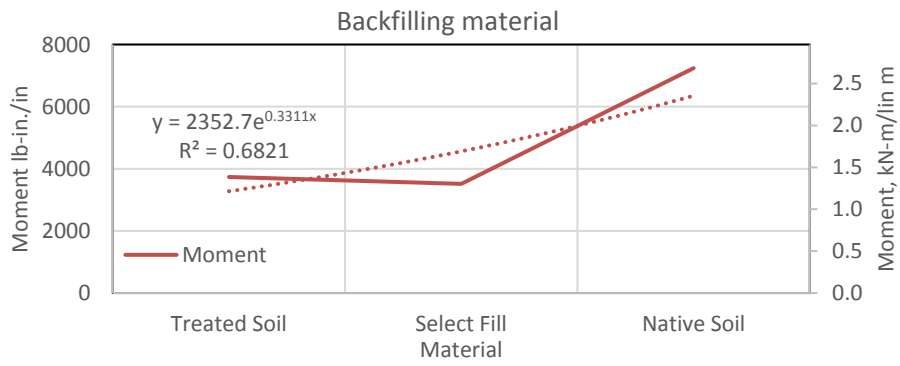
4

5   Figure 5-19 Effect of backfilling material to moment

1

Trench Width

$$y = 3887e^{-0.01x}$$
$$R^2 = 0.9947$$
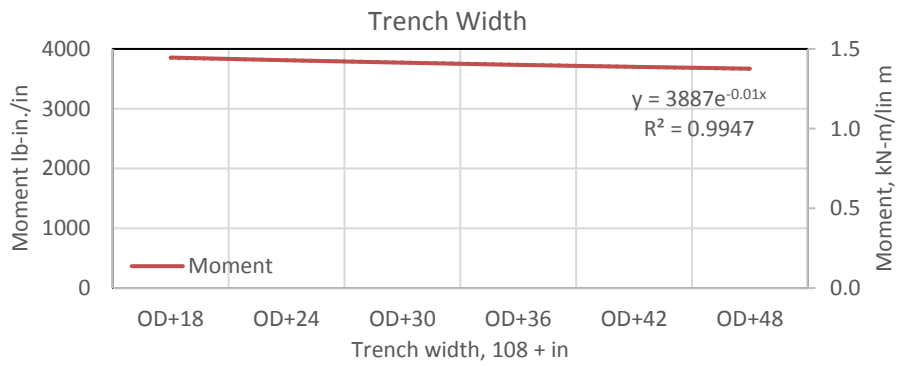
2

Figure 5-20 Effect of trench width to moment

3

Trench Wall Stiffness

$$y = 5916.3e^{-0.155x}$$
$$R^2 = 0.9929$$
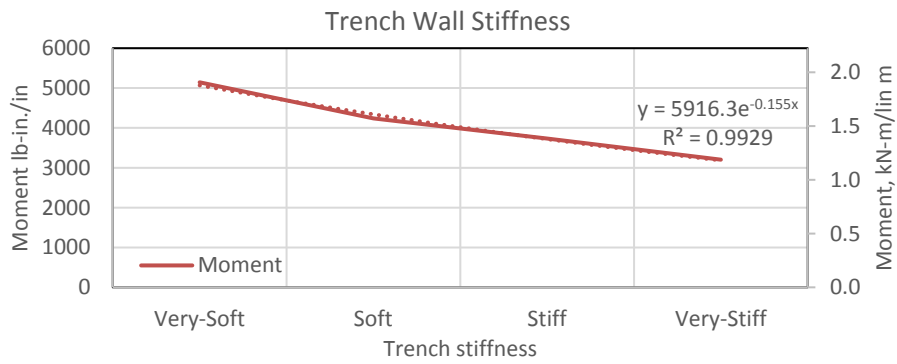
4

Figure 5-21 Effect of trench wall stiffness to moment

5

Pipe Thickness

$$y = 6014e^{-0.256x}$$
$$R^2 = 0.9861$$
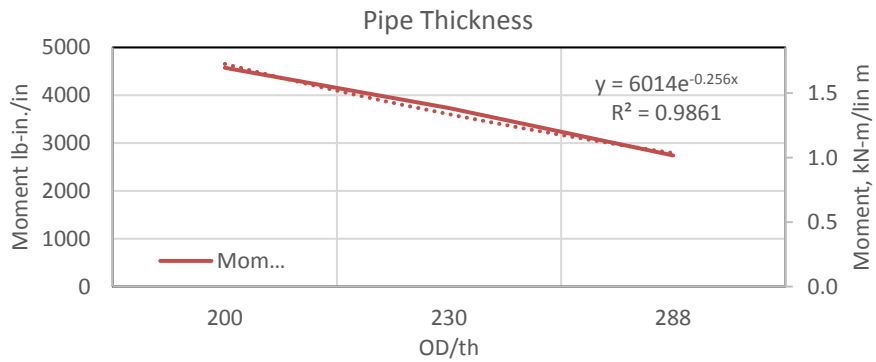
6

Figure 5-22 Effect of pipe thickness to moment

Pipe Diameter

$y = 2127e^{0.2239x}$

$R^2 = 0.9072$

Moment lb-in./in (left axis), Moment, kN-m/lin m (right axis)

Pipe diameter, in

1
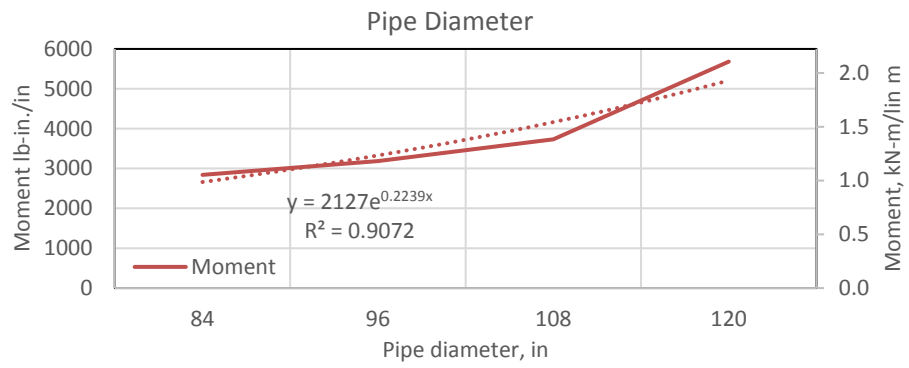
Figure 5-23 Effect of pipe diameter to moment

2

3

4

5.3   Multiple Linear Regression

5.3.1   Vertical Deflection

Multiple linear regression (MLR) analysis was performed by using the statistical software tool, SAS. The first approach was to define the relationship between the vertical deflection, expressed in percentage of the pipes diameter, and the independent variables. A linear formulation with intercept shown in Equation 11 was the first approach.

$$\Delta_y = C_0 + C_1(OD \times t) + C_2(a) + C_3(E_{backfill}) + C_3(\beta) + C_4(TW/OD) + C_5(E_{wall})$$

Equation (11)

Based on the regression analysis performed the equation proposed is shown in Equation 12 and it has a R^2 value equal to 0.5910 that means that 59% of the data are explained with this equation.

$$\delta_y(\%) = 0.34871 + 0.04369(OD \times t) + 0.12742(a) - 0.00412(E_{backfill}) - 0.13884(\beta) + 0.1328\left(\frac{TW}{OD}\right) - 0.33280(E_{wall})$$

Equation (12)

The signs of the parameter estimation show that: the vertical deflection of the pipe is increasing when the OD thickness, alfa and TWOD are increasing and when the Eback, beta and Ewall are decreasing.

The pair wise correlation between the response-predictor and predictor-predictor are shown in Table 5-3. The correlation matrix is symmetrical and the diagonal values are always one. A low correlation between the predictors is expected with a limit of 0.7. The correlation of the response variables is low for all the response variables except the alfa-beta and OD Thickness and TWOD which is around 0.4, which is considered accepted based on the 0.7 limit.

Table 5-3 Pearson Correlation Matrix

	ODThickness	alfa	Eback	beta	TWOD	Ewall
ODThickness	1.00000	0.00444	0.0033	-0.00223	-0.34345	-0.00159
alfa	0.00444	1.00000	0.00819	0.40489	0.00039	-0.00155
Eback	0.0033	0.00819	1.00000	0.00475	-0.00135	0.00586
beta	-0.00223	0.40489	0.00475	1.00000	0.0025	-0.00191
TWOD	-0.34345	0.00039	-0.00135	0.0025	1.00000	0.00236
Ewall	-0.00159	0.00155	0.00586	-0.00191	0.00236	1.00000

The p-values, shown in Table 5-4, shows that all the predictors are significant for explaining the linear model.

Table 5-4 p-values for the linear model with intercept

	p-values
Intercept	<0.0001
ODxThickness	<0.0001
alfa	<0.0001
$E_{backfill}$	<0.0001
beta	<0.0001
TW/OD	0.0764
E_{wall}	<0.0001

The experimental vs. predicted values are shown in Figure 5-24. It is observed that there is a good fit for almost all the data except for the experimental values that are above 0.8 %. These cases are the ones related to pipe diameter of 108 and 120, for very soft trench wall stiffness and CLSM height equal or higher than 0.7 of pipe diameter.
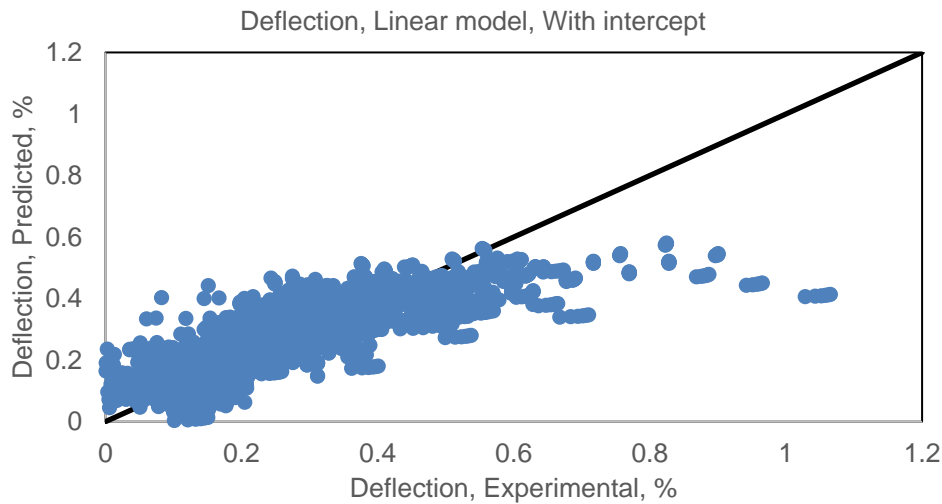
Figure 5-24 Predicted vs. experimental deflection values for linear model with intercept

5.3.2   Model Search Methods

The model search procedure is conducted so the potential good models are identified based on three methods, backward deletion, best subsets and stepwise regression.

5.3.2.1   Backward Deletion

In this method the full equation is input and one variable is removed from the model at each step, based on the higher p-value. The model with the remaining predictors is reanalyzed and the same procedure is followed until all remaining predictors are significant based on their p-value.

5.3.2.2   Best Subset Selection

In this method the analysis begin with the full model. The 'best' model is defined base on several criteria: i.e. high R^2 and low SSE (error sum of squares), high R_a^2 and low MSE (mean square of errors), Mallow's C_p value to be equal or close to the number of the independent variables used in the model, AIC (Akaike's information criterion) and SBC

(Schwarz' Bayesian Criterion) which are preferred to have a relatively low value. During this method the R^2 and R_a^2 will level off, which is an indication of achieving a good model.

5.3.2.3   Stepwise Regression

The third method used for defining the best model is based on backward and forward selection. The procedure starts with no predictors at the model, and based on the p-value each predictor will be added or removed from the model until reaching a point where no predictors can be added or removed from the model. A important point for this analysis is the input significance (a_{in}) should always be less or equal to the out significance level (a_{out}) to avoid deleting predictors that are just added at the model.

5.3.3   Model Search for Vertical Deflection

5.3.3.1   Backward Deletion

The best model from this analysis is the one that includes all the variables except the TWOD which is the ratio of trench width to pipe diameter. This predictor has a p-value of 0.0764 which is considered above the limit that was set for this analysis. The R^2 for the model with all the data but the TWOD is 0.5906 that means that 59% of the data is explained with the linear model.

Table 5-5 Backward deletion

Variable	Parameter Estimate	Standard Error	Type II SS	F Value	Pr>F
Intercept	0.37396	0.00815	17.77124	2107.19	<0.0001
ODThickness	0.04284	0.00131	8.99060	1066.04	<0.0001
alfa	0.12744	0.00669	3.06423	363.34	<0.0001
E_{back}	-0.00412	0.000264	2.05327	243.46	<0.0001
Beta	-0.13883	0.00667	3.65450	433.32	<0.0001
E_{wall}	-0.33277	0.00610	25.13885	2980.79	<0.0001

Table 5-6 Summary of backward deletion

	Summary of Backward Elimination						
Step	Variable Removed	Number Vars In	Partial R-Square	Model R-Square	C(p)	F value	Pr > F
1	TWOD	5	0.00054	0.5906	8.1410	3.14	0.0764

5.3.3.2   Best Subset Selection

The best subset selection is presented in Table 5-7. The selection of the best model is based on the high R^2 and R_a^2 and a Cp value close to the number of the predictors used for that specific model. The model that satisfies the requirements is the one shown on red box which has the highest R^2 and R_a^2 from all the models analyzed and a values very close to the number of predictors.

Table 5-7 Best Subset Selection summary


```
Number in  Adjusted
  Model    R-Square  R-Square     C(p)        AIC       SBC   Variables in Model

     1       0.3625    0.3627   1883.516  -14677.758  -14666  Ewall
     1       0.1302    0.1305   3802.310  -13625.519  -13613  ODThickness

     2       0.4922    0.4925    812.7546 -15447.223  -15429  ODThickness Ewall
     2       0.3912    0.3915   1647.183  -14832.611  -14814  Eback Ewall

     3       0.5213    0.5218    573.0565 -15646.277  -15622  ODThickness Eback Ewall
     3       0.5172    0.5176    607.2791 -15617.073  -15593  ODThickness beta Ewall

     4       0.5606    0.5611    249.7573 -15935.210  -15905  ODThickness alfa beta Ewall
     4       0.5461    0.5466    369.7064 -15825.003  -15794  ODThickness Eback beta Ewall


     6       0.5903    0.5910      7.0000 -16169.869  -16127  ODThickness alfa Eback beta TWOD
                                                             Ewall

     6       0.5903    0.5910      7.0000 -16169.869  -16127  ODThickness alfa Eback beta TWOD
                                                             Ewall
     5       0.5900    0.5906      8.1410 -16168.723  -16132  ODThickness alfa Eback beta Ewall

     6       0.5903    0.5910      7.0000 -16169.869  -16127  ODThickness alfa Eback beta TWOD
                                                             Ewall
     5       0.5900    0.5906      8.1410 -16168.723  -16132  ODThickness alfa Eback beta Ewal
```

5.3.3.3   Stepwise Regression

In this method both backward and forward selection was applied. The last step of the analysis is shown in the Figure 5-25 where one of the potential 'best' model is shown.

176

The predictors used in this method are five excluding the TWOD as in the method of backward deletion. The R^2 for this model is 0.5906 that means that 59% of the data are explained by this model.

```
                        Stepwise Selection: Step 5

          Variable alfa Entered: R-Square = 0.5906 and C(p) = 8.1410

                          Analysis of Variance

                                  Sum of          Mean
Source                   DF       Squares        Square      F Value    Pr > F

Model                     5      41.13544       8.22709       975.51    <.0001
Error                  3381      28.51406       0.00843
Corrected Total        3386      69.64950


                    Parameter      Standard
        Variable     Estimate        Error     Type II SS   F Value  Pr > F
        Intercept    0.37396       0.00815       17.77124   2107.19  <.0001
        ODThickness  0.04284       0.00131        8.99060   1066.04  <.0001
        alfa         0.12744       0.00669        3.06423    363.34  <.0001
        Eback       -0.00412    0.00026380        2.05327    243.46  <.0001
        beta        -0.13883       0.00667        3.65450    433.32  <.0001
        Ewall       -0.33277       0.00610       25.13885   2980.79  <.0001
```

Figure 5-25 Last step of the analysis with the significant predictors

5.3.3.4   Model Search Results and Discussion

Based on the model search procedure there are two 'best' models with R^2 of 59%. The first one is that that has 6 predictors and the second one had 5 predictors excluding the TWOD. Since the R^2 is equal for both models the model with the 6 predictors will be used.

Different transformations were performed based on the principals of the regression analysis method. The final results are shown for all the equations developed while the results from all the transformations are analytically presented at Appendix D.

A log-linear model shown in Equation 13 is proposed for predicting the vertical deflection of the large diameter steel pipe with CLSM. The R^2 is equal to 0.9299 which means that 93% of the data is explained through Equation 13.

$$Ln(\delta\_y) = 0.08011(OD \times t) + 0.56285(a) - 0.00768(E\_backfill) -$$
$$0.68987(\beta) - 0.39881(TW/OD) - 1.34824(E\_wall)$$

Equation (13)

The p-values are shown in Table 5-8 and it is concluded that all the variables are significant for the model. The experimental vs. predicted data for the log-linear model are shown in Figure 5-26. It is observed that there is a good match for the majority of data except several values. The deviated data are related to the models with CLSM height at 30% of the OD, backfilling material of Native Soil, and a very stiff trench wall.

Table 5-8 p-values for log-linear model without intercept

	p-values
ODxThickness	<0.0001
alfa	<0.0001
Ebackfill	<0.0001
beta	<0.0001
TW/OD	<0.0001
Ewall	<0.0001
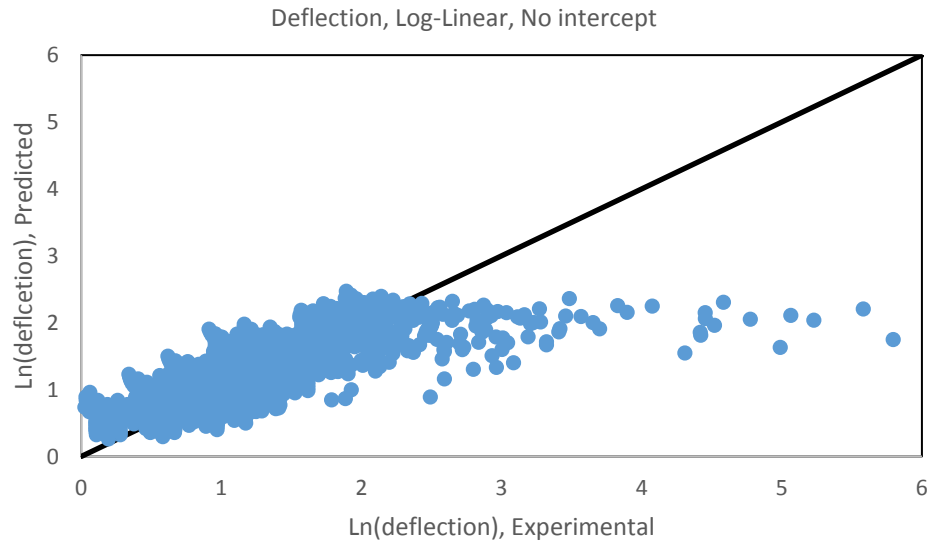
Figure 5-26 Experimental vs. predicted deflection for the log-linear model

5.3.4 Moment Log-Linear Model

A log-linear model shown in Equation 14 is proposed for predicting the maximum moment of the large diameter steel pipe with CLSM. The R^2 is equal to 0.9903 which means that 99% of the data is explained through Equation 14.

$$Ln(Moment) = 0.61840(OD \times t) + 1.08963(a) - 0.01006(E_{backfill}) - 0.14669(\beta) + 2.93179\left(\frac{TW}{OD}\right) + 0.50880(E_{wall})$$

Equation (14)

The p-values are shown in Table 5-9 and it is concluded that all the variables are significant for the model. The experimental vs. predicted data for the log-linear model are shown in Figure 5-27. It is observed that there is a good match for the majority of data except several values.

Table 5-9 p-values for log-linear model without intercept

	p-values
ODxThickness	<0.0001
alfa	<0.0001
Ebackfill	<0.0001
beta	0.0146
TW/OD	<0.0001
Ewall	<0.0001
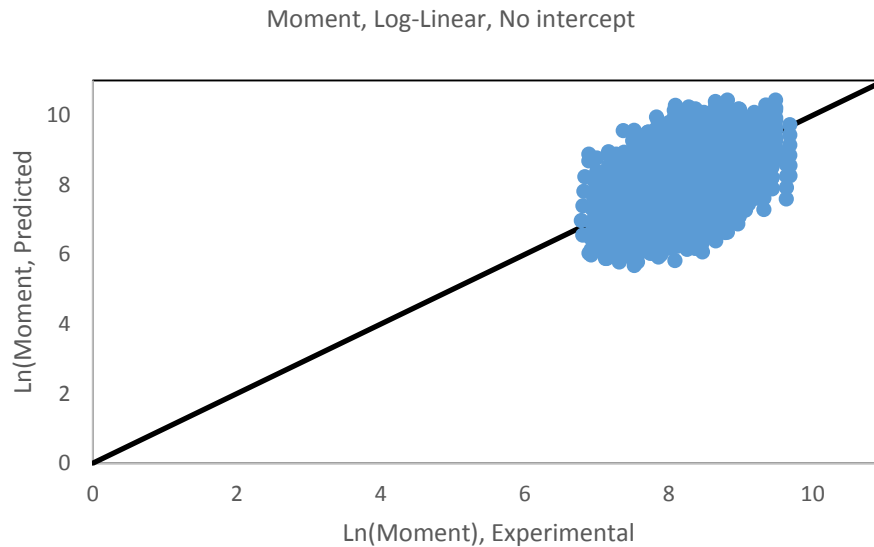
Figure 5-27 Log-linear model for moment without intercept

5.3.5   *Thrust Log-Linear Model*

A log-linear model shown in Equation 15 is proposed for predicting the maximum thrust of the large diameter steel pipe with CLSM. The R^2 is equal to 0.9907 which means that 99% of the data is explained through Equation 15.

$$Ln(Thrust) = 0.45087(OD \times t) + 0.76186(a) + 0.00624(E_{backfill}) +$$
$$0.43828(\beta) + 2.83147\left(\frac{TW}{OD}\right) + 0.59415(E_{wall})$$

Equation (15)

The p-values are shown in Table 5-10 and it is concluded that all the variables are significant for the model. The experimental vs. predicted data for the log-linear model are shown in Figure 5-28. It is observed that there is a good match for the majority of data.

Table 5-10 p-value for log-linear model without intercept

	p-values
ODxThickness	<0.0001
alfa	<0.0001
Ebackfill	0.0044
beta	<0.0001
TW/OD	<0.0001

180

Ewall	<0.0001

Thrust, Log-Lineare model, No intercept
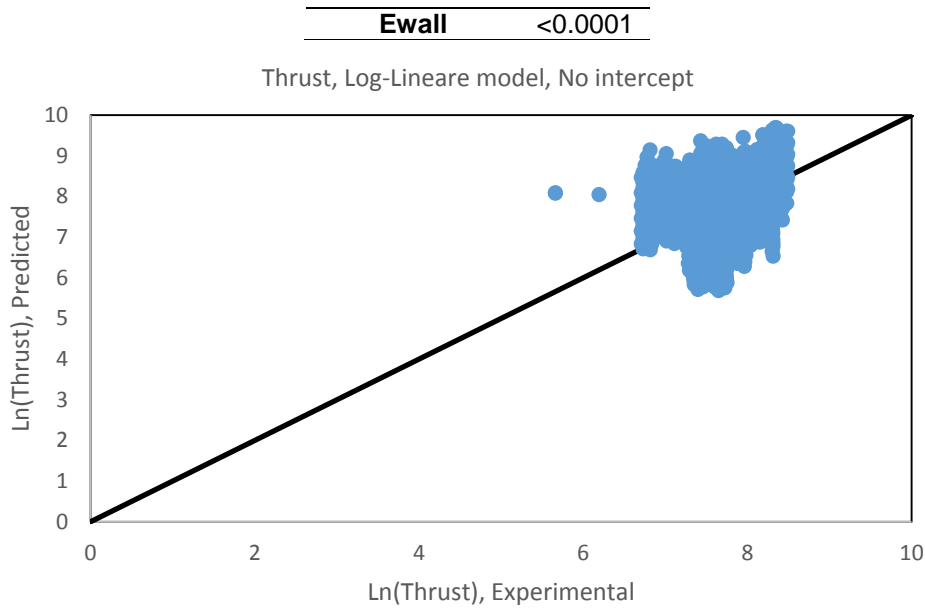
Figure 5-28 Log-linear model for the experimental vs. predicted thrust data

5.3.6 Shear Log-Linear Model

A log-linear model shown in Equation 16 is proposed for predicting the maximum thrust of the large diameter steel pipe with CLSM. The R^2 is equal to 0.99 which means that 99% of the data is explained through Equation 16.

$$Ln(Shear) = 0.49542(OD \times t) + 0.65269(a) - 0.00279(E_{backfill}) + 0.50930(\beta) + 2.47159\left(\frac{TW}{OD}\right) + 0.49600(E_{wall})$$

Equation (16)

The p-values are shown in Table 5-11 and it is concluded that all the variables are significant for the model. The experimental vs. predicted data for the log-linear model are shown in Figure 5-29. It is observed that there is a good match for the majority of data.

Table 5-11 p-values for log-linear shear equation without intercept

	p-values
ODxThickness	<0.0001
alfa	<0.0001
Ebackfill	0.1671
beta	<0.0001

TW/OD	<0.0001
Ewall	<0.0001

Shear, Log-Linear model, No intercept
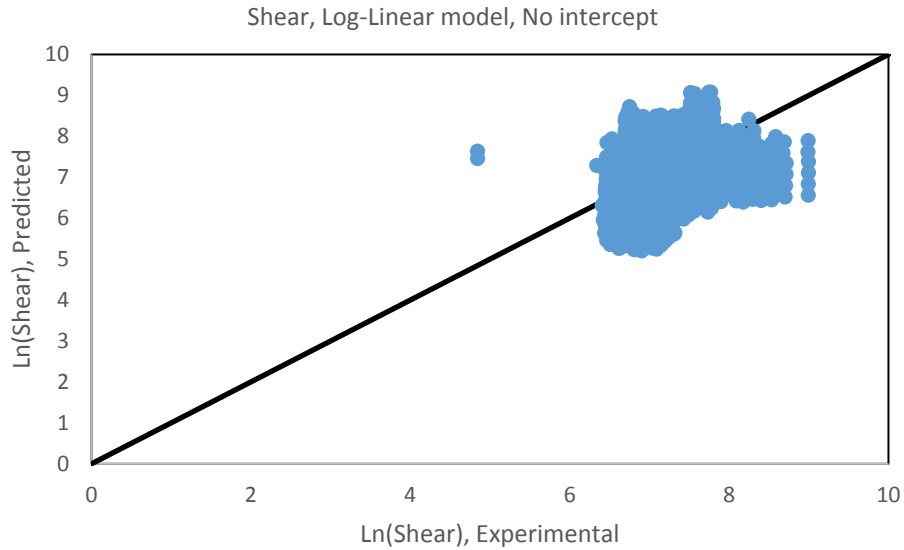
Figure 5-29 Log-linear experimental vs. predicted shear data

5.4   Multivariate Adaptive Regression Spline (MARS)

A multivariate adaptive regression spline (MARS) analysis, developed by Friedman (61), was also performed in this study. Mars is a nonlinear and nonparametric regression method that models the nonlinear responses between the inputs and the output of a system. The number of basis function (BF) as well as the parameters associated with each on are automatically determined. The main advantages of mars are its capability to produce simple and easy-to-interpret mathematical models based on Zhang et al. (62).

The MARS model f(X), is constructed as a linear combination of BFs, which are expressed similar to Equation 17, and their interactions, and is expressed through Equation 17. The coefficients β are constants, estimated using the least-squares method.

$$\max(0, x - t) = \begin{pmatrix} x - t, if \ x \geq t \\ 0, otherwise \end{pmatrix}$$

Equation

(1715)

182

where t is the point where the relationship between the predictor and the dependent variable changes, and is called knot point.

$$f(X) = \beta_0 + \sum_{m=1}^{M} \beta_m \lambda_m(X)$$ Equation (18)

where each $\lambda_m(X)$ is a basis function.

Two models were analyzed with MARS. The first analysis was performed by allowing no interaction between the predictors and the second one by allowing maximum two interactions between the predictors.

5.4.1.1   Model for horizontal deflection with no interaction between the predictors

The model obtained from this analysis is shown in Equation 19. The experimental vs. predicted data are shown in Figure 5-32. The outlying data are for pipe diameter of 108 and 120, for CLSM height equal to the pipe's diameter or 70% OD, and for very soft trench wall. The R^2 for this model equals to 0.70436.

```
Y = 0.353456 - 0.340018 * BF1 + 0.650097 * BF2 + 3.64067 *
BF3 - 0.0205816 * BF4 + 0.0878875 * BF5 - 0.354561 * BF6 +
0.00242576 * BF7 + 0.0154496 * BF8 - 0.302812 * BF9 -
0.101976 * BF11 + 0.225602 * BF13 - 3.85293 * BF15 +
0.601573 * BF17 - 0.169274 * BF19 - 0.522604 * BF21 -
1.14084 * BF22 + 0.133191 * BF23 - 0.0918309 * BF25 -
0.0833027 * BF27 + 0.554405 * BF29
```
                                                            Equation (19)

where the BFs are equal to:

```
BF1  = max( 0, EWALL - 0.5);
BF2  = max( 0, 0.5 - EWALL);
BF3  = max( 0, ODTH - 4.22609);
BF4  = max( 0, 4.22609 - ODTH);
BF5  = max( 0, ALFA - 0.7);
BF6  = max( 0, 0.7 - ALFA);
BF7  = max( 0, EBACK - 5);
BF8  = max( 0, 5 - EBACK);
BF9  = max( 0, ODTH - 3.375);
BF11 = max( 0, ODTH - 5.21739);
BF13 = max( 0, ODTH - 2.94);
BF15 = max( 0, ODTH - 4.16667);
BF17 = max( 0, ODTH - 3.84);
BF19 = max( 0, ALFA - 0.5);
BF21 = max( 0, TWOD - 1.33333);
BF22 = max( 0, 1.33333 - TWOD);
BF23 = max( 0, EWALL - 0.7);
BF25 = max( 0, ODTH - 4.86);
```

```
BF27 = max( 0, ODTH - 2.66667);
BF29 = max( 0, TWOD - 1.375);
```

The BF's are separated into different cased based on their relationship with the dependent variable. The relationship of the predictors with the horizontal deflection are shown in Figure 5-30.

(a)

(b)

(c)

(d)

(e)
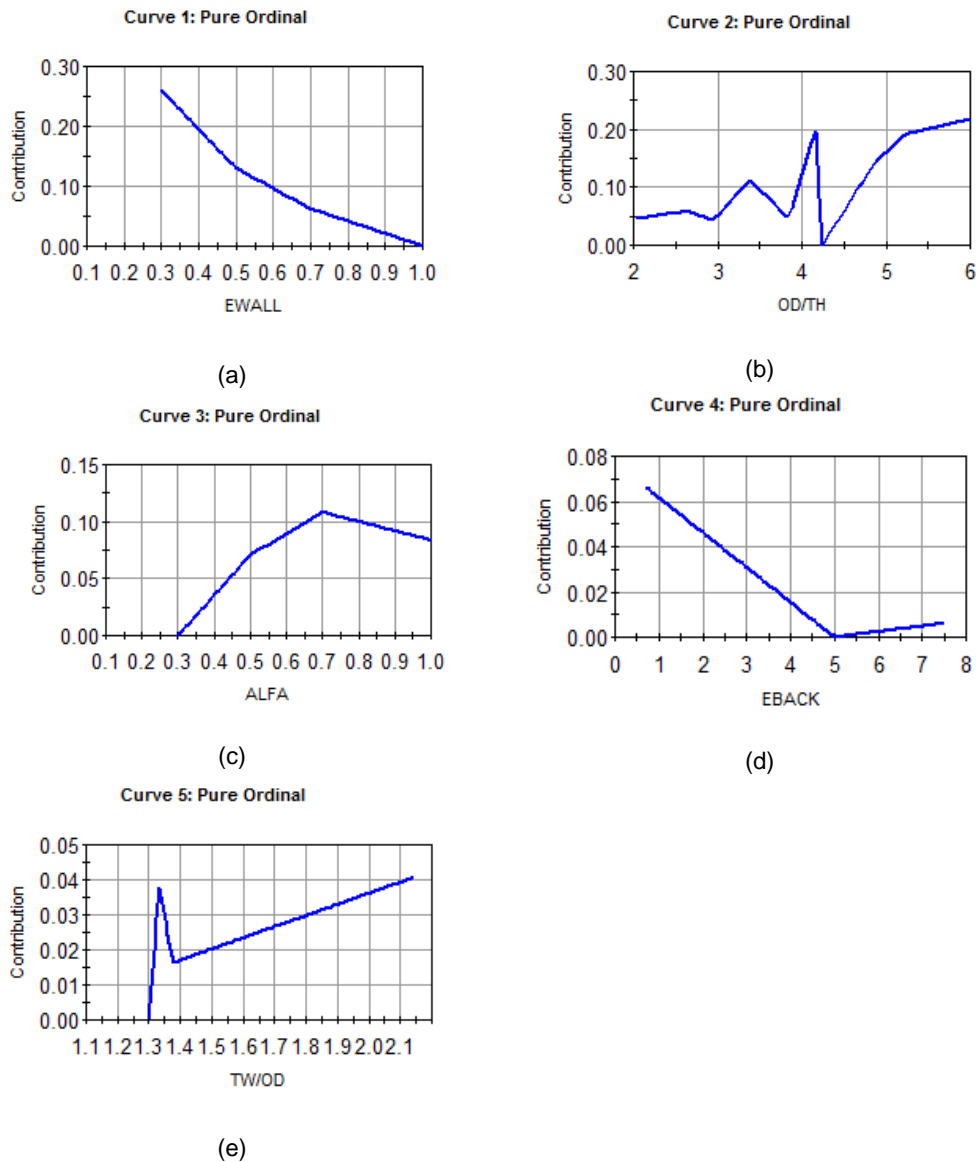
Figure 5-30 Predictors vs. contribution to the horizontal deflection

Another way of presenting the BFs is also shown in Figure 5-31. When selecting the BFs required for the model, those are then applied in the Equation 19 for calculating the predicted value of horizontal deflection.

$$Horizontal\ Deflection = \left\{ \begin{array}{l} E_{wall} \left\{ \begin{array}{l} < 0.5\ use\ BF2 \\ 0.5 - 0.7\ use\ BF1 \\ > 0.7\ use\ BF1\ and\ BF23 \end{array} \right\} \\ OD/Th \left\{ \begin{array}{l} < 2.667\ BF4 \\ 2.667 - 2.94\ use\ BF4, BF27 \\ 2.94 - 3.375\ use\ BF4, BF13, BF27 \\ 3.375\ - 3.84\ use\ BF4, BF9, BF13, BF27 \\ 3.84 - 4.17\ use\ BF4, BF9, BF13, BF17, BF27 \\ 4.17 - 4.226\ use\ BF4, BF9, BF13, BF15, BF17, BF27 \\ 4.226 - 4.86\ use\ BF3, BF9, BF13, BF15, BF17, BF27 \\ 4.86 - 5.2174\ use\ BF3, BF9, BF13, BF15, BF17, BF25, BF27 \\ > 5.2174\ useBF3, BF9, BF13, BF15, BF17, BF25, BF25, BF27 \end{array} \right\} \\ alfa \left\{ \begin{array}{l} < 0.7\ use\ BF6 \\ 0.5 - 0.7\ use\ BF19 \\ > 0.7\ use\ BF5\ and\ BF19 \end{array} \right\} \\ Eback \left\{ \begin{array}{l} < 5\ use\ BF8 \\ > 5\ use\ BF7 \end{array} \right\} \\ TW/OD \left\{ \begin{array}{l} < 1.3\ use\ BF22 \\ 1.3 - 1.375\ use\ BF21 \\ > 1.375\ use\ BF29\ and\ BF21 \end{array} \right\} \end{array} \right\}$$

Figure 5-31 Selection of Bfs based on predictors knots
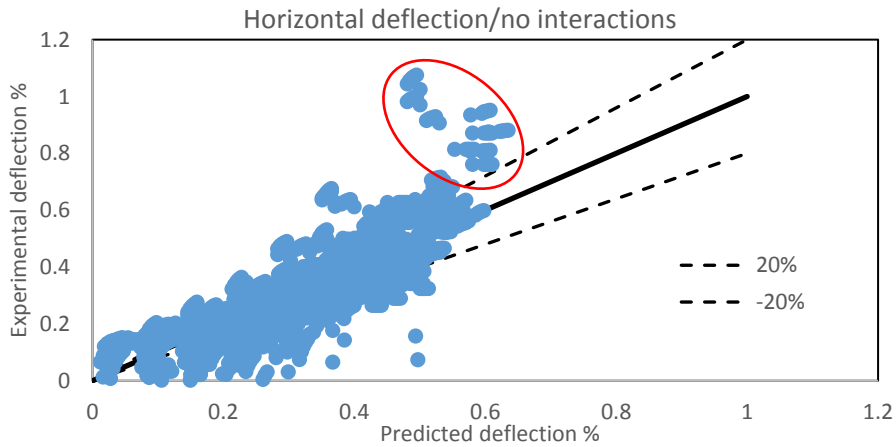
Figure 5-32 Predicted vs. Experimental data for horizontal deflection without interactions

5.4.1.2   Model for horizontal deflection with two interaction between the predictors

The model obtained from this analysis is shown in Equation 20. The experimental

vs. predicted data are shown in Figure 5-33. The R^2 value for this model was equal to

0.81427.

```
Y = 0.269166 - 0.238632 * BF1 + 0.674933 * BF2 - 0.00715188
* BF3 - 0.00962438 * BF4 + 0.470159 * BF5 + 0.207848 * BF6 -
0.0334225 * BF7 + 0.012993 * BF8 - 0.0175317 * BF9 -
0.0599597 * BF10 - 0.10682 * BF11 + 0.0241516 * BF12 -
0.822469 * BF13 - 0.525401 * BF14 + 0.00224416 * BF15 +
0.0504269 * BF16 + 0.0512314 * BF17 - 0.149626 * BF18 -
0.0182199 * BF19 + 0.0637275 * BF20 + 0.187367 * BF21 -
0.0409035 * BF22 - 0.109763 * BF23 - 0.0489505 * BF25 -
0.0158491 * BF26 + 0.0751849 * BF27 - 0.0360014 * BF29;
```
                                                    Equation (20)

where,

```
BF1 = max( 0, EWALL - 0.5);
BF2 = max( 0, 0.5 - EWALL);
BF3 = max( 0, ODTH - 4.22609);
BF4 = max( 0, 4.22609 - ODTH);
BF5 = max( 0, BETA - 0.7) * BF3;
BF6 = max( 0, 0.7 - BETA) * BF3;
BF7 = max( 0, EBACK - 5) * BF2;
BF8 = max( 0, 5 - EBACK) * BF2;
BF9 = max( 0, ALFA - 0.7) * BF4;
BF10 = max( 0, 0.7 - ALFA) * BF4;
BF11 = max( 0, ODTH - 5.21739) * BF1;
BF12 = max( 0, 5.21739 - ODTH) * BF1;
BF13 = max( 0, BETA - 0.5) * BF2;
BF14 = max( 0, 0.5 - BETA) * BF2;
BF15 = max( 0, EBACK - 5);
BF16 = max( 0, 5 - EBACK);
BF17 = max( 0, ALFA - 0.7) * BF16;
BF18 = max( 0, 0.7 - ALFA) * BF16;
BF19 = max( 0, EWALL - 0.7) * BF16;
BF20 = max( 0, 0.7 - EWALL) * BF16;
BF21 = max( 0, ODTH - 3.84) * BF2;
BF22 = max( 0, 3.84 - ODTH) * BF2;
BF23 = max( 0, ALFA - 0.5) * BF16;
BF25 = max( 0, ODTH - 3.375) * BF16;
BF26 = max( 0, 3.375 - ODTH) * BF16;
BF27 = max( 0, ODTH - 3.84) * BF16;
BF29 = max( 0, ODTH - 4.86) * BF16;
```
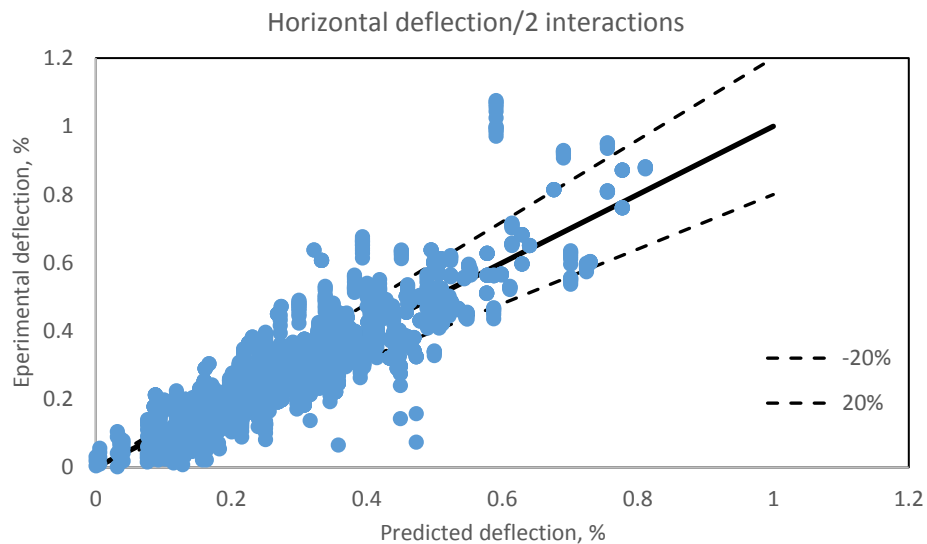
Figure 5-33 Predicted vs. Experimental data for horizontal deflection with two interactions

5.4.1.3 *Vertical deflection no interaction*

The model obtained from this analysis is shown in Equation 21. The experimental vs. predicted data are shown in Figure 5-34. The outlying data are for pipe diameter of 108 and 120, for CLSM height equal to the pipe's diameter or 70% OD, and for very soft trench wall. The R^2 for this model equals to 0.72162

$$Y = 0.339483 - 0.314408 * BF1 + 0.600634 * BF2 + 3.43512 * BF3 + 0.202712 * BF5 - 0.420739 * BF6 + 0.0170614 * BF8 - 0.307959 * BF9 - 0.333292 * BF11 + 0.6265 * BF13 - 3.70209 * BF15 - 0.102988 * BF17 + 0.289161 * BF19 + 0.127028 * BF21 - 0.0383371 * BF24 - 0.257048 * BF25 - 0.0682708 * BF27 + 0.14732 * BF29$$

Equation

(2116)

where,
```
BF1  = max( 0, EWALL - 0.5);
BF2  = max( 0, 0.5 - EWALL);
BF3  = max( 0, ODTH - 4.22609);
BF5  = max( 0, ALFA - 0.7);
BF6  = max( 0, 0.7 - ALFA);
BF8  = max( 0, 5 - EBACK);
BF9  = max( 0, ALFA - 0.5);
BF11 = max( 0, ODTH - 3.375);
BF13 = max( 0, ODTH - 3.84);
BF15 = max( 0, ODTH - 4.16667);
BF17 = max( 0, ODTH - 5.21739);
BF19 = max( 0, ODTH - 2.94);
```

```
BF21 = max( 0, EWALL - 0.7);
BF24 = max( 0, 1.77778 - TWOD);
BF25 = max( 0, ODTH - 2.66667);
BF27 = max( 0, ODTH - 4.86);
BF29 = max( 0, ODTH - 2.55652);
```
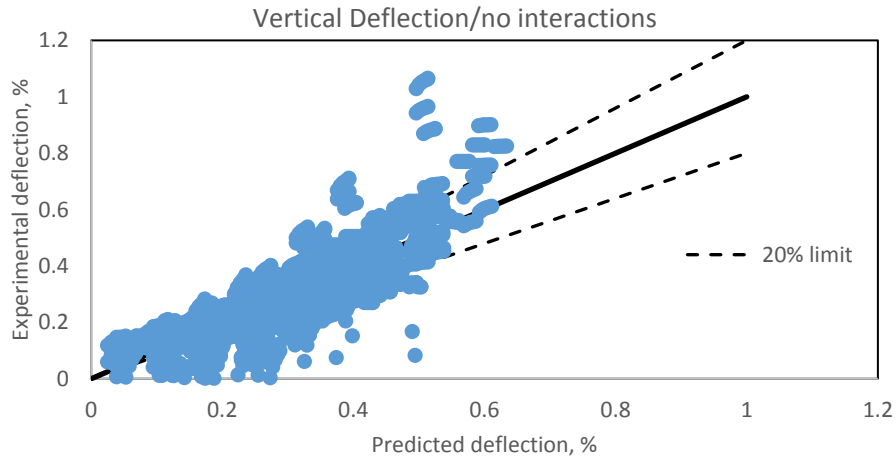

Figure 5-34 Predicted vs. Experimental data for vertical deflection with no interactions

5.4.1.4   Vertical deflection with two interactions

The model obtained from this analysis is shown in Equation 22. The experimental vs. predicted data are shown in Figure 5-35. The R^2 value for this model was equal to 0.82261.

```
Y = 0.316996 - 0.18858 * BF1 + 0.500873 * BF2 - 0.0103258 *
BF3 - 0.0349046 * BF4 - 0.478971 * BF5 - 0.108458 * BF6+
0.30059 * BF9 + 0.0238973 * BF12 - 0.0428832 * BF13  -
0.194707 * BF14 - 0.0518738 * BF15 + 0.155364 * BF16 -
2.21097 * BF17 + 0.14206 * BF18 + 0.21644 * BF19 - 0.698353
* BF20 + 1.99108 * BF21 + 0.0644344 * BF24 - 15.8861 * BF25
+ 13.4221 * BF27 + 2.24097 * BF29;
```
Equation (22)

where,
```
BF1 = max( 0, EWALL - 0.5);
BF2 = max( 0, 0.5 - EWALL);
BF3 = max( 0, ODTH - 4.22609);
BF4 = max( 0, 4.22609 - ODTH);
BF5 = max( 0, ALFA - 0.7);
BF6 = max( 0, 0.7 - ALFA);
BF9 = max( 0, ALFA - 0.5) * BF3;
BF12 = max( 0, 5 - EBACK);
BF13 = max( 0, ALFA - 0.5) * BF12;
BF14 = max( 0, 0.5 - ALFA) * BF12;
BF15 = max( 0, EWALL - 0.7) * BF3;
BF16 = max( 0, 0.7 - EWALL) * BF3;
BF17 = max( 0, ODTH - 5.21739) * BF5;
```

188

```
BF18 = max( 0, 5.21739 - ODTH) * BF5;
BF19 = max( 0, EWALL - 0.5) * BF5;
BF20 = max( 0, 0.5 - EWALL) * BF5;
BF21 = max( 0, ODTH - 4.86) * BF5;
BF24 = max( 0, 0.7 - EWALL) * BF12;
BF25 = max( 0, ODTH - 4.16667) * BF5;
BF27 = max( 0, ODTH - 4.22609) * BF5;
BF29 = max( 0, ODTH - 3.84) * BF5;
```
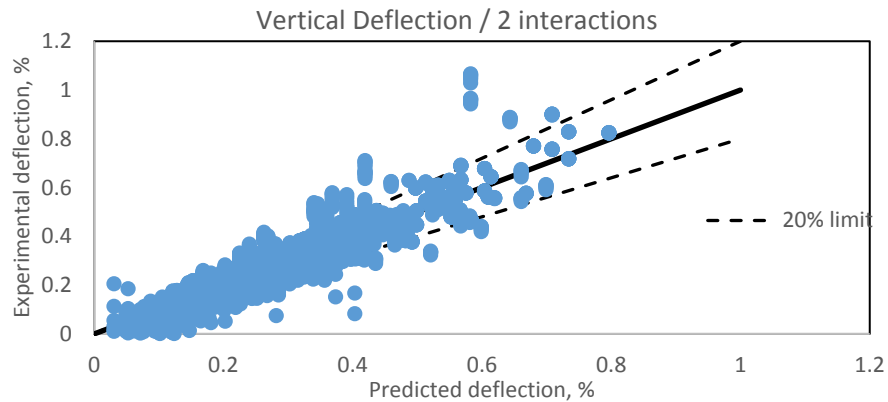

Figure 5-35 Predicted vs. Experimental data for vertical deflection with two interactions

5.4.1.5   Moment with two interactions

The model obtained from this analysis is shown in Equation 23. The experimental vs. predicted data are shown in Figure 5-36. The R^2 value for this model was equal to 0.65924.

```
 Y = 7090.13 + 2837.98 * BF1 - 1716.55 * BF2 - 88.8907 * BF3
 + 518.796 * BF4 - 3467.61 * BF5 - 9396.49 * BF6 - 50762 *
 BF7 - 16397.3 * BF8 - 9148.3 * BF9 + 3130.13 * BF10 +
 5105.59 * BF11 + 54478.7 * BF13 - 1875.43 * BF14 + 339.543 *
 BF15 + 215.202 * BF16 - 28096 * BF17 + 15316.2 * BF19 +
 1089.24 * BF20 - 875.481 * BF21 - 893.646 * BF22 + 5396.85 *
 BF23 + 20142.9 * BF25 + 6657.68 * BF28 - 5660.66 * BF29;
```

Equation (23)

```
BF1 = max( 0, ODTH - 5.21739);
BF2 = max( 0, 5.21739 - ODTH);
BF3 = max( 0, EBACK - 5);
BF4 = max( 0, 5 - EBACK);
BF5 = max( 0, ALFA - 0.7);
BF6 = max( 0, 0.7 - ALFA);
BF7 = max( 0, EWALL - 0.7) * BF1;
BF8 = max( 0, 0.7 - EWALL) * BF1;
BF9 = max( 0, ODTH - 4.86) * BF6;
BF10 = max( 0, 4.86 - ODTH) * BF6;
```

189

```
BF11 = max( 0, EWALL - 0.7);
BF12 = max( 0, 0.7 - EWALL);
BF13 = max( 0, ODTH - 4.86) * BF11;
BF14 = max( 0, 4.86 - ODTH) * BF11;
BF15 = max( 0, ALFA - 0.7) * BF3;
BF16 = max( 0, 0.7 - ALFA) * BF3;
BF17 = max( 0, ODTH - 4.16667);
BF19 = max( 0, ODTH - 4.86) * BF12;
BF20 = max( 0, 4.86 - ODTH) * BF12;
BF21 = max( 0, ALFA - 0.7) * BF4;
BF22 = max( 0, 0.7 - ALFA) * BF4;
BF23 = max( 0, ODTH - 3.84);
BF25 = max( 0, ODTH - 4.22609);
BF28 = max( 0, 0.7 - ALFA) * BF25;
BF29 = max( 0, ODTH - 3.375) * BF11;
```
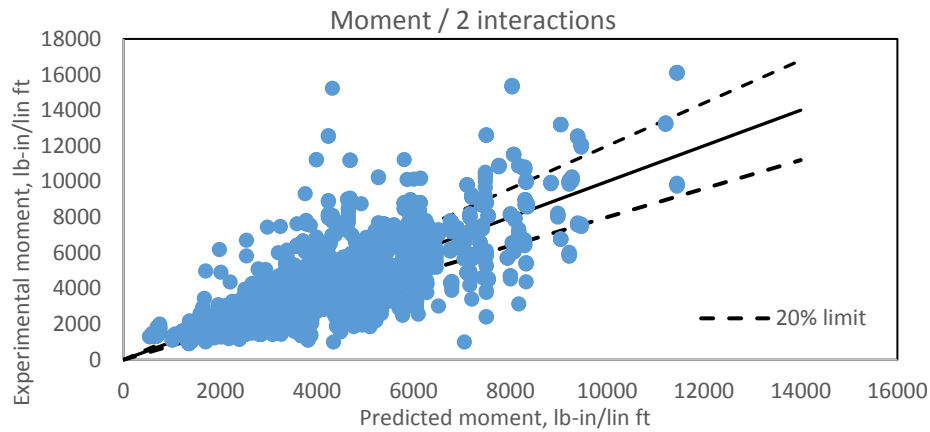

Figure 5-36 Predicted vs. Experimental data for moment with two interactions

5.4.1.6 *Thrust with two interactions*

The model obtained from this analysis is shown in Equation 24. The experimental

vs. predicted data are shown in Figure 5-37. The R^2 value for this model was equal to

0.87993.

$$
\begin{aligned}
Y = &\ 2001.52 + 5712.63 * BF1 + 6148.52 * BF4 - 3247.45 * BF5 \\
&- 19987.1 * BF7 + 19.9567 * BF9 + 90.3321 * BF10 - 54395 * \\
&BF11 + 82313.9 * BF12 - 5201.85 * BF13 - 7573.28 * BF14 + \\
&474.507 * BF15 + 59864.6 * BF16 + 5332.25 * BF18 - 21123.5 * \\
&BF21 + 470.555 * BF22 + 162.391 * BF23 + 1181.83 * BF24 - \\
&1447.83 * BF25 + 731.056 * BF26 - 700.133 * BF28 + 28.3358 * \\
&BF29 - 751.366 * BF30;
\end{aligned}
$$

Equation (174)

```
BF1 = max( 0, ODTH - 4.86);
BF2 = max( 0, 4.86 - ODTH);
```

```
BF4 = max( 0, 0.5 - ALFA) * BF1;
BF5 = max( 0, ODTH - 5.21739);
BF7 = max( 0, ODTH - 4.16667);
BF8 = max( 0, 4.16667 - ODTH);
BF9 = max( 0, EBACK - 5);
BF10 = max( 0, 5 - EBACK);
BF11 = max( 0, ALFA - 0.5) * BF7;
BF12 = max( 0, 0.5 - ALFA) * BF7;
BF13 = max( 0, ALFA - 0.5) * BF5;
BF14 = max( 0, 0.5 - ALFA) * BF5;
BF15 = max( 0, ALFA - 0.3);
BF16 = max( 0, ODTH - 4.22609) * BF15;
BF18 = max( 0, ODTH - 3.84);
BF21 = max( 0, 0.5 - ALFA) * BF18;
BF22 = max( 0, EWALL - 0.7) * BF18;
BF23 = max( 0, 0.7 - EWALL) * BF18;
BF24 = max( 0, BETA - 0.5) * BF8;
BF25 = max( 0, 0.5 - BETA) * BF8;
BF26 = max( 0, ODTH - 4.22609) * BF9;
BF28 = max( 0, EBACK - 5) * BF7;
BF29 = max( 0, 5 - EBACK) * BF7;
BF30 = max( 0, BETA - 0.3) * BF2;
```
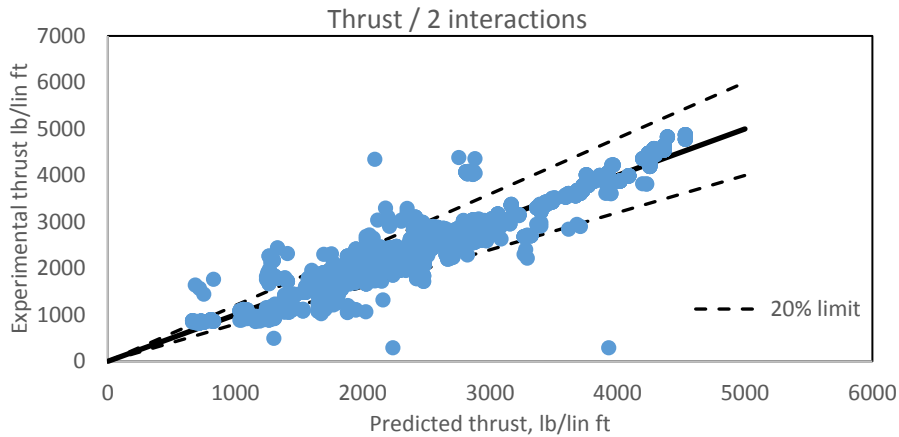

Figure 5-37 Predicted vs. Experimental data for thrust with two interactions

5.4.1.7   Shear with two interactions

The model obtained from this analysis is shown in Equation 25. The experimental vs. predicted data are shown in Figure 5-38.. The R^2 value for this model was equal to 0.76216, which shows a good overall trend except a small group of data which are shown inside the red circle. The common variables of these cases are the pipe diameter of 108

in. and CLSM height of 50% and 70% of the pipes diameter and very soft or soft trench

wall.

```
 Y = 874.857 - 5145.7 * BF1 + 85.0759 * BF4 + 1448.69 * BF5
+ 6070.77 * BF7 + 23135 * BF9 + 7034.09 * BF10 - 7134.03 *
BF11 - 2979.75 * BF13 - 19696.1 * BF14 + 560.228 * BF15 -
57121.4 * BF19 - 20030.9 * BF21 - 158.443 * BF22 + 15978 *
BF23 + 1632.86 * BF25 - 26531 * BF27 + 32716.7 * BF29;
```

Equation (25)

```
BF1  = max( 0, ODTH - 4.86);
BF4  = max( 0, 5 - EBACK);
BF5  = max( 0, ODTH - 3.84);
BF7  = max( 0, ODTH - 5.21739);
BF9  = max( 0, ALFA - 0.5) * BF1;
BF10 = max( 0, 0.5 - ALFA) * BF1;
BF11 = max( 0, BETA - 0.5) * BF5;
BF13 = max( 0, ALFA - 0.5) * BF7;
BF14 = max( 0, 0.5 - ALFA) * BF7;
BF15 = max( 0, BETA - 0.7);
BF16 = max( 0, 0.7 - BETA);
BF19 = max( 0, ODTH - 4.22609) * BF15;
BF21 = max( 0, ODTH - 4.86) * BF16;
BF22 = max( 0, 4.86 - ODTH) * BF16;
BF23 = max( 0, ODTH - 3.84) * BF15;
BF25 = max( 0, ODTH - 4.22609);
BF27 = max( 0, ODTH - 5.21739) * BF15;
BF29 = max( 0, ODTH - 4.16667) * BF15;
```
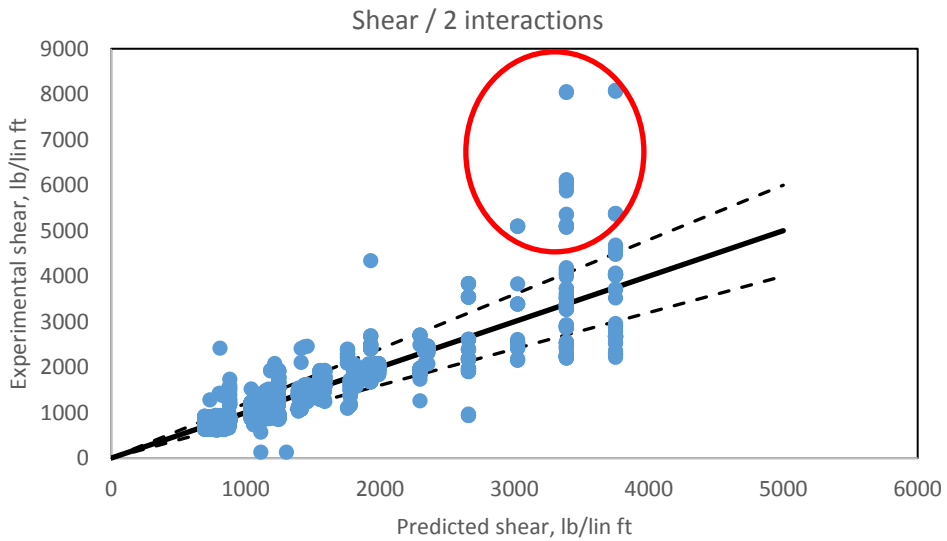

Figure 5-38 Predicted vs. Experimental data for shear with two interactions

5.5   Main Findings

A case study was conducted aiming to develop equations which predict the behavior of the buried large diameter steel pipes with CLSM. A sensitivity analysis was performed based on the FEA method, which investigates the relationship between every predictor and the dependent variables. It was observed that all the variables affected the deflection of the pipe with the variable "pipe thickness" and "trench width" having smaller effects on the deflection variable. While analyzing the effect of the independent variables to thrust and shear, it was observed that the all the variables had an important effect on the dependent variables.

To establish the equations, 33456 cases were created through the pre-processor DP and the post-processor was used to extract the data needed for the regression analysis. Six independent predictors: pipe diameter expressed in feet; pipe wall thickness expressed in inches; ratio of backfilling material to pipe diameter, alfa; modulus of elasticity of the backfilling materials expressed in ksi; ratio of embedment material to pipe diameter, beta; trench width expressed in feet; and modulus of elasticity of the trench wall expressed in ksi. The three model search methods applied, backward deletion, best subset selection, and stepwise regression, were capable of defining which independent variables were needed for creating the best model. The best model was selected from both linear and nonlinear models, based on the fundamentals of the regression analysis checks. Five equations were established, which successfully predict the maximum horizontal and vertical deflection, moment, thrust and shear, which are also called dependent variables.

The predicted vs. experimental values were also plotted. When observing the graph for the deflection variable, the predicted values calculated showed that only a few cases did not follow the trend of the majority of the data. For horizontal deflection, these cases were mainly for CLSM height up to 30% of the pipes diameter and a very stiff trench

wall. The few cases of the vertical deflection which did not follow the same trend as the majority of the data, were related to the cases which had CLSM height of 30% of the pipe's diameter, native soil backfilling material, and a very stiff trench wall. Overall it is concluded, based on the explained percentage, R^2, that more than 90% of the data is representative of the equations developed for all the predicted variables.

A multivariate adaptive regression spine (MARS) analysis was also performed and two sets of equations were proposed with no interaction between the predictors and with maximum of two interaction between the predictors.

Chapter 6

DISCUSSION OF RESULTS AND RECOMMENDATION FOR FUTURE WORK

6.1   Results and Discussion

The interaction of the pipe-soil system was investigated in this study embedded with controlled low strength material. The performance of this system was tested in the field and through the finite element analysis method. An extended analysis of the properties of the CSLM was performed in a controlled laboratory conditions. From this analysis a CSLM mix design was proposed along with material properties for compressive, tensile, and confined triaxial resistance of the CLSM. Through an extensive parametric study of 3456 cases, two studies were performed: the first one was a multilinear regression analysis and the second one a multivariate adaptive regression splines analysis. Based on these studies, five equations are proposed to predict the maximum horizontal and vertical deflection, the moment, shear, and thrust of the pipe.

This study funded by the Tarrant Regional Water District and the Water Research Foundation is a unique study which contributes to an ongoing research for the complex behavior of the buried large diameter pipes.

The deflection of a 108-diamter pipe, installed with the staged construction method, was investigated during every construction stage through two methods; 1) MOP-119, and 2) laser profiler method. Due to physical obstacles inside the pipe, during the construction, the laser profiler method was modified to a photo profiler method. When the installation was ended, the laser video profiler was applied for measuring the deflection. A 518 ft. section was measured during every construction stage and a 2-mile section was measured with the laser video profiler method at the end of the installation procedure. The main results obtained from the experimental measurements of the deflection of the pipe are presented.

1. The MOP-119 is an easily-applied method used for calculating the maximum deflection of the measured pipe section at every construction stage.

2. The laser video profiler is a method for continuous measurement of the deflection of pipes, and is very useful for identifying the deflections of any point along the length of the section measured.

3. The laser photo profiler is a method substituted for the continuous laser video profiler when physical obstacles are present inside the pipe.

4. In all cases, the MOP-119 method yielded larger deflections, which is relatively safe, but may result in rejection of otherwise acceptable pipe installations. These differences were attributed mainly to three factors: (1) the theoretical assumptions of a pipe buried in a homogeneous, isotropic, elastic material, (2) the use of empirical graph to define the maximum deflection which is based on empirical values and not realistic values, and (3) the lack of this method to account for the support provided by the mortar lining, which increases the stiffness of the pipe, and leads to lower deflection.

5. The laser video profiling method is more realistic because the calculations are based on data collected from the site of interest rather than calculated by using an empirical graph.

6. When comparing the accuracy of the results, the laser profiler methods were more accurate than the MOP-119 and gave a complete view of the inner condition of pipe, in contrast to the MOP-119, which provides only the maximum deflection of the pipe.

7. The photo laser profiler method is recommended when physical obstacles are present inside the pipe, while the video laser profiler is recommended for measurement after the pipe's installation procedure.

8. MOP-119 method was easier to apply at the site and post process while the video laser profile requires more equipment to be transferred inside the pipe.

A finite element analysis was performed for the 108-inch pipe to mimic the installation procedure applied at the site. The results obtained from this method are presented below.

1. The deflection of the pipe calculated with the FEA showed a good agreement when compared with the experimental calculations.

2. The concrete damage plasticity model was a good model for simulating the CLSM.

3. The use of the model change algorithm was used to simulate the staged construction.

4. The mortar lining was simulated with concrete damaged plasticity, which successfully predicted the cracks observed inside the pipe

The investigation of the properties of the CLSM were also investigated in this study. Three tests were performed, compression, splitting tensile or Brazilian test, and confined triaxial test. The main conclusions drawn are presented below.

1. A mix design for CLSM with a well-graded sand is proposed in this study

2. The w/c ratio, the flowability and the range of the compression strength were investigated

3. Ninety-six cylinders were tested with the compressive test. It was concluded that for specimens tested 1 day past the production the

compressive strength raged from 10 to 24 psi. For specimens tested 3 days past the production the compressive strength varied from 10 to 54 psi. For specimens tested 7 days past the production day the compressive strength of the specimens varied from 4 to 132 psi. For specimens tested 28 days past the production day the compressive strength varied from 7 to 192 psi.

4. Based on the results for the compressive strength of the specimens, it was observed that the mix designs with cement percentage from 1 to 3% showed a low strength, the specimens with cement percentage from 4 to 7% showed a higher compressive strength, and the specimens with cement percentage of 8% had a relative higher strength than the other mix designs.

5. The main fracture mode of the specimens were the shear, cone and shear, and columnar failure. When the shear failure happened, which was the most-often-observed failure mode, crushing at the top corner was happening at the same time. In other cases, not so often, small columnar cracks were observed along the circumference of the specimens, and small pieces were separated from the main body.

6. The tensile properties of the CLSM were tested based on the splitting tensile test, or Brazilian test, at 7th day past production.

7. The average tensile strength of the CLSM ranged from 1 psi to 53psi. For the tensile test, the average strength of the mix design with cement percentage 1 and 2 are relatively smaller than the stress of the mix with 3 until 7. The mix design with 8% cement percentage has a significantly higher stress than the rest of the mix designs.

8. A linear relationship was observed between the average compressive versus the average tensile strength of the CLSM mixes on 7th day.

9. To calculate the tensile properties that represent the behavior of the CSLM with 6% cement percentage analyzed with FEA, the inverse analysis was applied.

10. From the confined trixial test, the cohesion and the friction angle were defined for all the mix designs. The cohesion ranges from 4 to 10 psi. The highest values were observed for the mix designs with 1,5,and 8% cement, while the lowest values were observed for the mix design with 3and 4% cement.

11. The friction angle is observed to be constant, around 38-44 degrees for all the mix designs, except the mix design with 2% cement which is slowly smaller than the rest of the values (27 degrees).

12. When comparing the confined vs. the unconfined stress-strain graph, for three of the mixes, it was observed that not only the compressive strength increases with confinement but the material becomes more ductile, which was also the case during the testing procedure

From the parametric study, performed in 3456 cases, the conclusions are presented below.

1. A case study was conducted aiming to develop equations which predict the behavior of the buried large diameter steel pipes with CLSM.

2. The pre-processor and post-processor, previously developed as part of a previous research, were successfully modified and used for this study. The pre-processor was used to create the models and feed them into the finite element which analyzes it. The post processor accesses the result files

from every model and obtains the required data and creates the required graphs.

3. Six independent predictors were used for building equations which predict the maximum deflection, moment, shear and thrust of the pipe. The predictors used are: pipe diameter expressed in feet; pipe wall thickness expressed in inches; ratio of backfilling material to pipe diameter, alfa; modulus of elasticity of the backfilling materials expressed in ksi; ratio of embedment material to pipe diameter, beta; trench width expressed in feet; and modulus of elasticity of the trench wall expressed in ksi.

4. Two methods were applied: the multivariate adaptive regression spine and the multilinear regression analysis.

6.2   Recommendations for Future Work

Based on the work conducted in this research the future work recommended is presented below.

1. *An experimental measurement method which can more accurately measure the deflection of the pipe through the bents.* The restriction while applying the laser profiler method was that the laser and the camera, which record the path of the laser light, are not perpendicular and therefore the scaling factor applied should be defined based on a non-constant distance.

2. *Analysis of the bents for large diameter buried steel pipes with CLSM.* Bents are critical sections of the pipeline system and the investigation of the performance will be essential for the pipe design. Depending on the fluid velocity, the flow of the water through the bents will cause a negative

pressure in the inner radius of the bent. Thus, it will increase the pressure in the outer radius of the bent.

3. *The investigation of the compressive, tensile and confined compressive test while using different soil materials on the mix design proposed in this study.* This will provide a more comprehensive knowledge of the behavior of the CLSM.

4. *The accelerated aging of CLSM, with constant humidity and temperature, and chemicals.* This study will provide better understanding of how the material properties of the CLSM change with time and with exposure to chemicals transferred from the soil.

5. The material properties defined from the accelerated aging can be implemented in FEM and a parametric study can be performed and the design equations will be updated.

References

1. Cates, Walter H. *History of Steel Water Pipe; its Fabrication and Design Development.* 1971.

2. Watkins, Reynold K. *The story of buried steel pipes and tanks.* 2006.

3. William, Whidden, R. *Buried Flexible Steel Pipe: Design and Analysis.* Virginia : The task Committee on buried Flexible (Steel) Pipe Load Stability Criteria & Design of the Pipeline Divsion. American Society of Civil Engineers, 2009.

4. Howard, Amster K. *Modulus of Soil Reaction (E') Values for Buried Flexible Pipe.* Virginia : National Technical Information Service, 1977.

5. Krizek, R. J., et al. *Structural Analysis and Design of Pipe Culverts, Report No. 116.* Washington, D.C. : National Cooperative Highway Research Program, Highway Research Board, 1971.

6. *"E" and its Variation with Depth.* Hartley, James D. and Duncan, James M. 1987, Journal of Transportation , Vol. Division of ASCE.

7. *Composite E' (Modulus of Soil Reaction).* Howard, Amster. 2009, Pipelines, pp. 958-969.

8. (AWWA), American Water Work Association. *Steel Water Pipe: A Guide for Design and Intallation (M11).* Denver, CO : American Water Work Association, 2004.

9. Vipulanandan, C., Qiao, W. and Hovsepian, H. *Water Pipeline Failures in the Active Zone.* Houston, TX : Center for Innovative Grouting Materials and Technology (CIGMAT), 2010.

10. Doyle, G. *The Role of Soil in the External Corrosion of Cast-iron Water Mains in Toronto, Canada.* Ottawa, Canada : University of Toronto, Master Thesis of Applied Science, 2000.

11. Denise, Fort and Barry, Nelson. *Pipe Dreams: Water Supply Pipeline Projects in the West.* s.l. : Natural Resources Defence Council, 2012.

12. Whidden, William. *ASCE Manuals and Reports on Engineering Practice No. 119.* Reston, Virginia : s.n., 2009.

13. Martson, A. *The Theory of External Loads on Closed Conduits in the Light of the Latest Experiments.* Washington, DC : Transportation Research Board, 1930.

14. *Some Characteristics of the Modulus of Passive Resistance of Soil: A Study in Similitude.* Watkins, R. K. and and Spangler, M. G. s.l. : Proc., 37th Annu. Meeting, Hwy. Res. Board, 1958, Proc., 37th Annu. Meeting, Hwy. Res. Board, pp. 576-583.

15. *The Iowa Formula It's Use and Misuse when Designing Flexible Pipe.* Smith, Greg and Watkins, Reynold. 2004, Pipeline engineering and Construction.

16. *Laboratory Load Tests on Buried Flexible Pipe.* Howard, Amster K. 1972, American Water Works Association, Vol. 64, No. 10, pp. 655-662.

17. Kriezek, R.J, et al. *Structural Analysis and Design of Pipe* . s.l. : Report 116. HCHRP, 1971.

18. *Pipe zone bedding and backfill: A flexible pipe perspective.* Watkins, Reynold, et al. 2010, ASCE Pipelines.

19. *Some observations on flexible pipe response to load.* Rogers, C. D. F. 1129, 1988, Transportation Research Record, pp. 1-11.

20. Craig, R. *Craig's Soil Mechanics.* Lomdon : Spon Press, 1974.

21. *Field Measurememnt and numerical analysis for buried large diameter steel pipes.* Kawabata, T., et al. 2008, Pipelines, ASCE.

22. *Technical note: Soil-Based Controlled Low-Strength Materials.* Green, Brian H. and Schmitz, Darrel W. s.l. : Environmental & Engineering Geoscience 10.2 169-174., 2004.

23. ACI Committee, 229. *Controlled Low-Strength Materials.* s.l. : ACI Committee Reports, Guides, Standard Proactices, and Commentaries, 2005.

24. *Development of engineerign properties for regular and quick set flowable fill.* Pons, Femando, Landwermeyer, John S. and Kerns, Larry. 1998, American Society of Civil Engineers.

25. Mullarky, J.I. Long Term Strength Gain of Controlled Low-Strength Materials. *The Design and Application of Controlled Low-Strength Materials (Flowable Fill).* s.l. : ASTM, 1998, pp. 102-107.

26. *Performance of industrial by-products in controlled low-strength materials (CLSM).* Nataraja, M. C. and Nalanda, Y. 2007, Scinece Direct, p. 14.

27. *Alkali-activated, cementless, controlled low-strength materials (CLSM) utilizing industrial by-products.* Lee, N.K., et al. 2013, Journal of Construction and Buliding Materials, pp. 738-746.

28. Howard, A. K. Soil-cement slurry pipe embedment. [book auth.] Wayne S. Adaska. *Controlled low strength materials.* Detroit : American Concrete Institute, 1994.

29. Weng, Yinan and Vipulanandan, C. *A Study on Controlled Low Strength Material (CLSM).* Houston : Univeristy of Houston, 1998.

30. Abelleira, A., Berke, N. S. and Picker, D. G. Corrosion Activity of Seel in Cementitious Controlled 469 Low-Strength Materials vs. that in Soil. *The Design 470 and Application of Controlled Low-Strength Materials (Flowable-Fill).* s.l. : ASTM, 1998, pp. 124-134.

31. *Predicting performance of pipe culverts buried in soil.* Leonards, G. A., Roy, M. B. Purdue Universtiy : Indiana State Highway Commision, 1976.

32. *Stiffness and Deflection Analysis of Complex Structures.* Turner, M. J., Clough, R. W. and Topp, L. T. s.l. : Journal of the Aeronautical Sciences, 1956, Vol. 23.

33. *CANDE--A modern approach for the structural desing and analysis of buried culverts.* Katona, M G, et al. 1976, Transportation Research Board (TRB), p. 475.

34. *Kinematic hardening model for pipeline-soil interaction under various loading conditions.* Zhang, J., Stewart, D. P. and Randolph, M. F. s.l. : The International Journal of Geomechanics, 2002, Vol. 2.4.

35. *Modeling of pipe–soil interaction and its application in numerical simulation.* Tian, Yinghui and Cassidy, Mark J. s.l. : International Journal of Geomechanics, 2008, Vol. 8.4.

36. *Load settlement response of footing placed over buried flexible pipe through model plate load test.* Srivastava, Amit, Goyal, Chaitanya R. and Raghuvanshi, Abhishek. s.l. : International Journal of Geomechanics, 2012.

37. *Soil Structure Interaction of Flexible Pipe under Pressure.* Zarghamee, M.S. and Tigue, D. Washington D.C. : Transportation Research Board, National Research Council, 1986, Vol. No. 1087.

38. *. "Analysis of Deeply Buried Flexible Pipes.* Suleiman, M.T., R. A. Lohnes, T. J. Wipf and Klaiber, F. W. Washington D.C : Transportation Research Board, 2003, Vol. Record No. 1849. .

39. *Pipe-soil interactions during backfill placement.* McGrath, Timothy J. 1998.

40. Dezfooli, S. Mojtaba. *Staged construction modeling of large diameter steel pipes using 3-D nonlinear finite element analysis.* Arlington : Univeristy of Texas at Arlington, 2015.

41. *Testing and Evaluation of the Statically Loaded Large Diameter Steel Pipe with Native Backfill.* M., Najafi. Center for Underground Infrastructure Research and Education : s.n., 2012.

42. *Staged Consrtruction Modeling of Steel Pipes Buries in Controlled Low strength Material (CLSM) Using 3-D Nonlinear Finite Element Analysis.* Dezfooli, M. S., et al. s.l. : International Journal of Geomechanics, 2013, ASCE's Internaltiona Journal of Geomechanics.

43. Corp., Dassault Systèmes Simulia. *Abaqus Theory Manual.* Providence, RI : s.n., 2010.

44. *Plasticity in Reinforced Concrete.* Chen, Wai-Fah. s.l. : J. Ross, 2007.

45. *Analysis User's Manual.* Abaqus.

46. Chen, W.F. and Lui, E.M. *Structural Stability, Theory and Implementation .* New York : Elsevier, 1987.

47. *A Plastic-Damage Model for Concrete.* Lubliner, J., J. Oliver, S. Oller and Oñate, E. 1989, International Journal of Solids and Structures, pp. 299–329.

48. *Selection of soil models and parameters for geotechnical engineering application.* Brinkgreve, Ronald BJ. 2005, ASCE.

49. Lade, Poul V. *Overview of constitutive models for soils.* s.l. : ASCE, 2005.

50. Bathe, Klaus-Lurgen. *Finite elenment Procedures .* s.l. : Englewood Cliffs: Prentice hall, 1996.

51. *A medium-scale apparatus and procedure to measure interface shear for HDD design.* Chazli, G. El, et al. 2005, Proc. 2005 No-Dig Cof.

52. *A Plastic-Damage Model for Concrete.* Lubliner, J., et al. 1989, International Journal of Solids and Structures vol. 25, pp. 299–329.

53. *Tensile stress–crack width law for steel fibre reinforced self-compacting concrete obtained from indirect (splitting) tensile tests.* Abrishambaf, Amin, Barros, Joaquim A.O. and Cunha, Vítor M.C.F. s.l. : Cement & Concrete Composites, 2015.

54. *Angle of friction and dilantancy of sand.* Schanz, T. and Vermeer, P.A. s.l. : Geotechnique 46 , pg. 145-151, 1996, Vol. No. I.

55. *The strength and dilatancy of sands.* Bolton, M. D. s.l. : Geotechnique 36, pg. 65-78, 1986, Vol. No. 1.

56. Neville, A. *Properties of concrete.* s.l. : Prentice Hall, 1995.

57. C09, ASTM Committee. *Manual of aggregate and concrete testing.* s.l. : ASTM , 2016.

58. *The Brazilian test: a tool for measuring the toughness of a material and its brittle to ductile transition.* Proveti, J. R. C. and Michot, G. 3, s.l. : International Journal of Fracture, pg. 455-460, 2006, Vol. 139.

59. Indriyantho, B.R. and Nuroji. *finite element modeling of concrete fracture in tension with the Brazilian spitting test on the case of plane-stress and plane-strain.* s.l. : International Conference in Suistainable Civil Engineering Structures and Construction Materials , 2014.

60. *Concrete uniaxial tensile strength and cylinder splitting test.* Lin, Zhuhai and Wood, Laurence. s.l. : Journal of Structural Engineering , 2003.

61. *Multivariate adaptive regression splines.* Friedman, J. H. s.l. : Annals of Statistics, pg. 1-141, 1991, Vol. vol. 19.

62. *Multivaiate adaptive regression splines for analysis of geotechnical engineering systems.* Zhang, W. G. and Goh, A. T. C. s.l. : Coputers and Geotechnics, Elsevier, 2012.

63. Pons, F., Landwermeyer, J.S. and Kerns, L. Development of Engineering Properties for Regualr and Quick-Set Flowable Fill. *The Design and Application 505 of Cotreolled Low-Strength Materials (Flowable Fill).* s.l. : ASTM STP 1331, 1998, pp. 67-86.

64. Kaneshiro, J., et al. Controlled Low Strength Material For Pipeline Backfill - Specifications, Case Histories And Lessons Learned. *Pipeline Division Specialty Conference.* s.l. : American Society of Civil Engineers, 2001, pp. 1-13.

65. *Pipe zone bedding and backfill: A flexible pipe perspective.* Watkins, R., et al. 2010, Pipelines, ASCE, pp. 426-438.

66. *Staged construction modeling of large diameter steel pipe using 3-D nonlinear finite element analysis.* S.D., Mojtaba. Arlington : University of texas at Arlington , 2013.

Appendix A

Laser Video Profiler Measurement for the 2-mile section
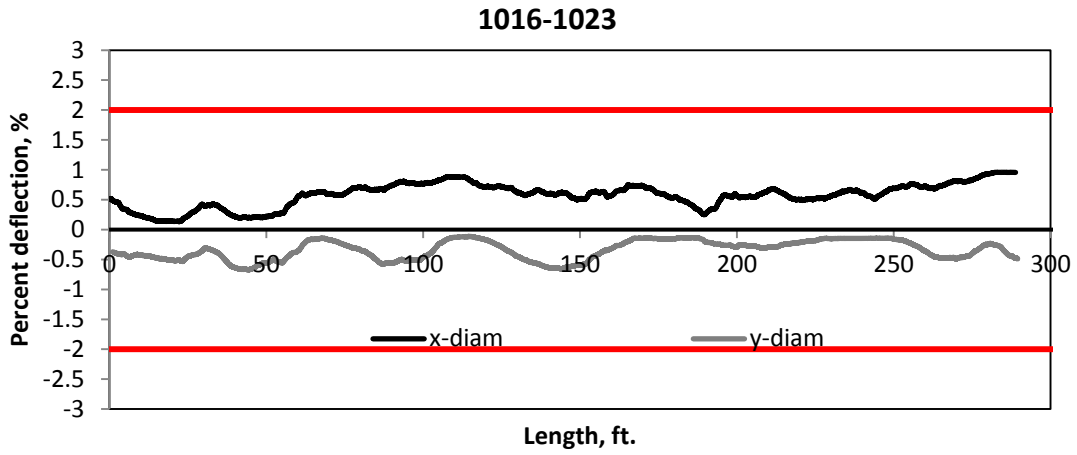
Figure 0-1 Laser video profiler for pipe 1016 to 1023
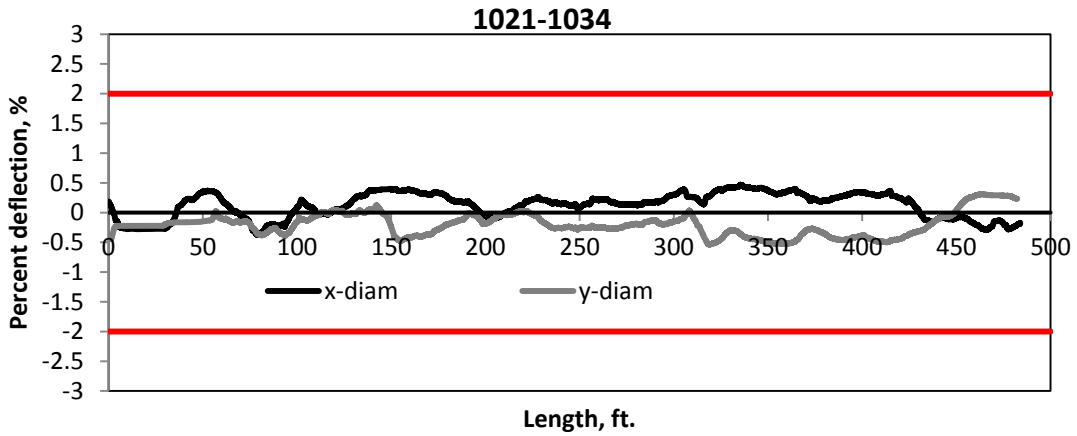
Figure 0-2 Laser video profiler for pipe 1021 to 1034
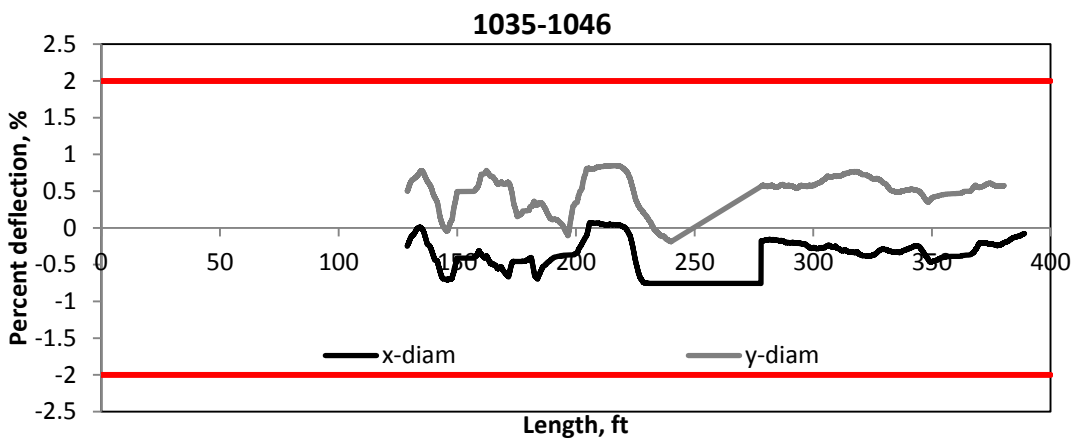
Figure 0-3 Laser video profiler for pipe 1035 to 1046
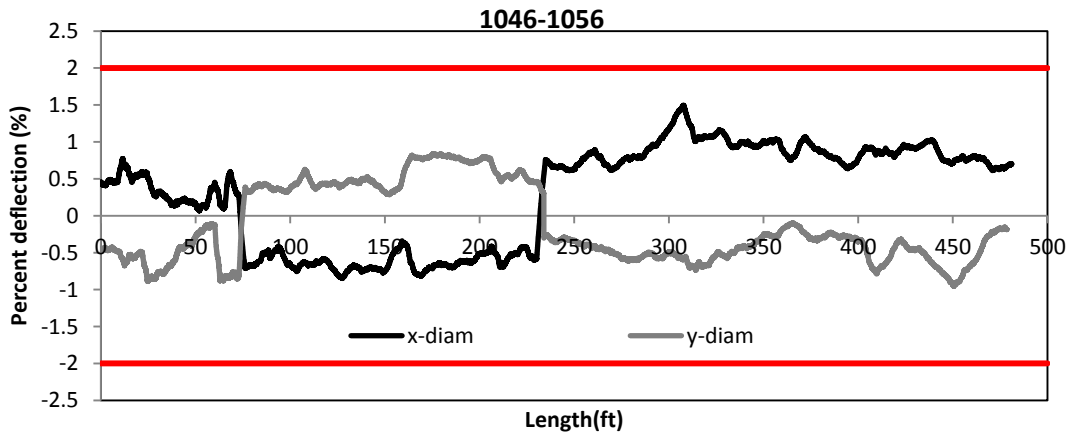
Figure 0-4 Laser video profiler for pipe 1046 to 1056
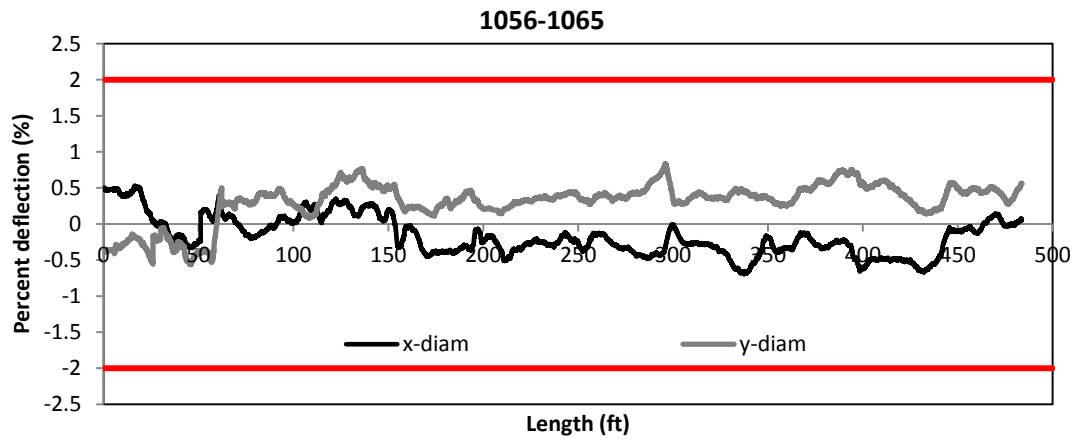
Figure 0-5 Laser video profiler for pipe 1056 to 1065
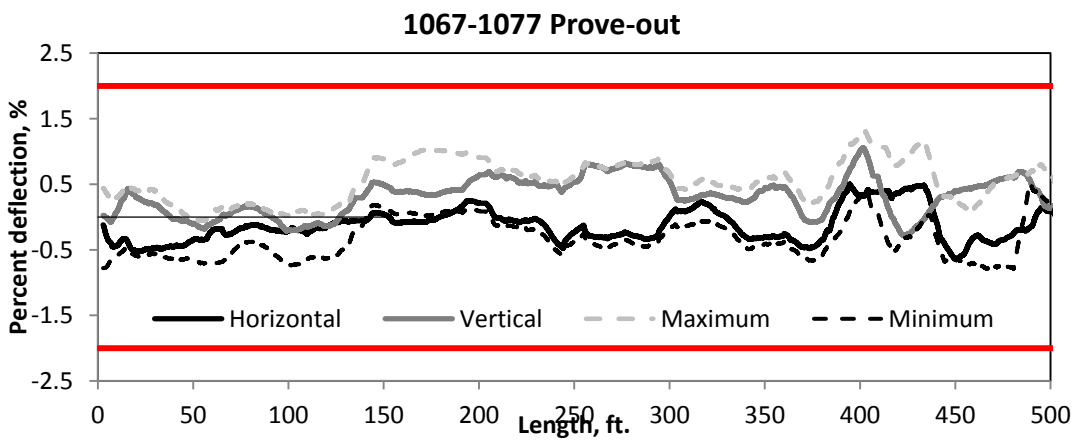
Figure 0-6 Laser video profiler for pipe 1067 to 1077

208
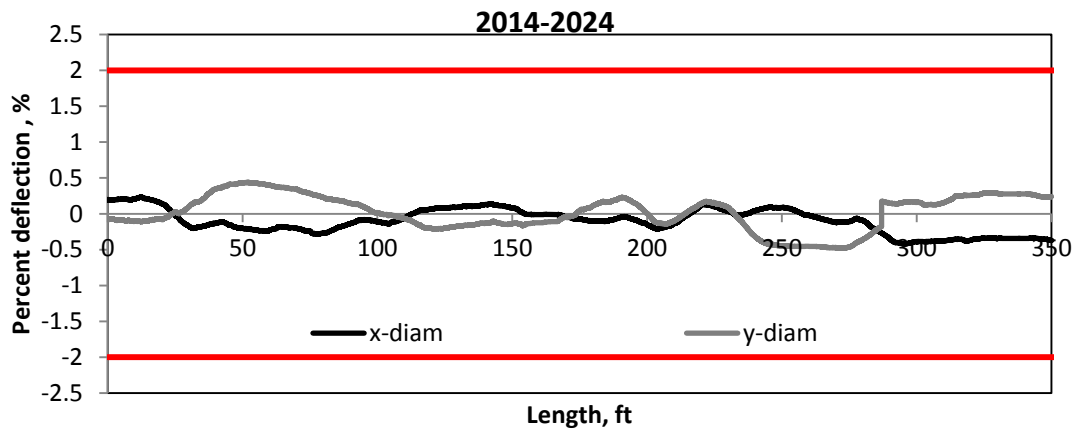
Figure 0-7 Laser video profiler for pipe 2014 to 2024
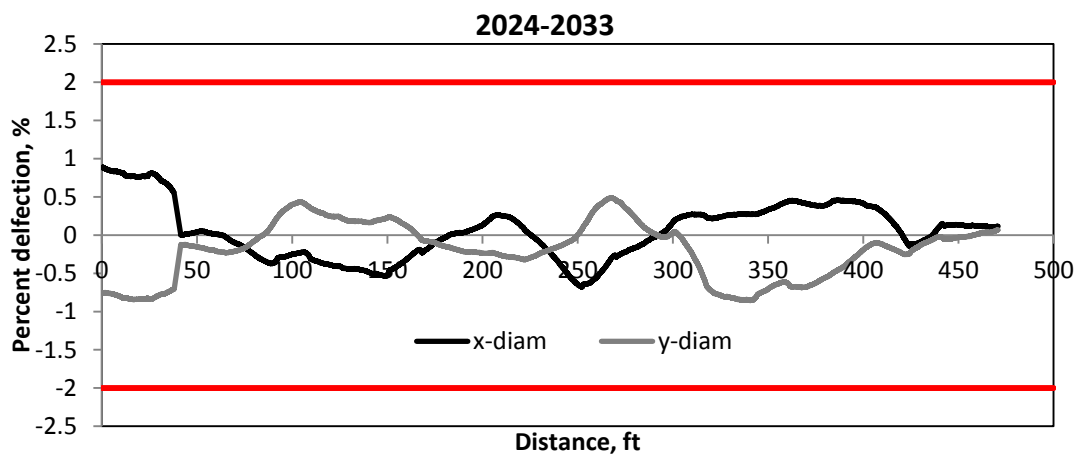
Figure 0-8 Laser video profiler for pipe 2024 to 2033
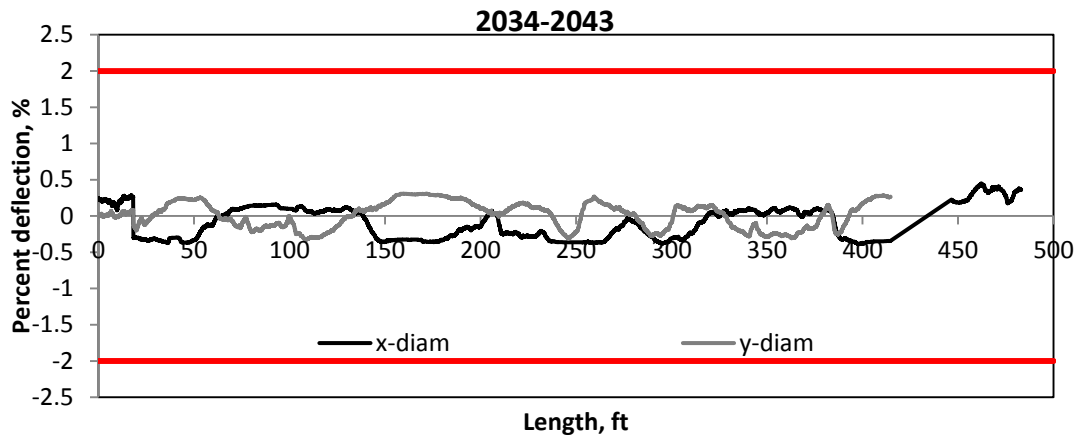
Figure 0-9 Laser video profiler for pipe 2034 to 2043
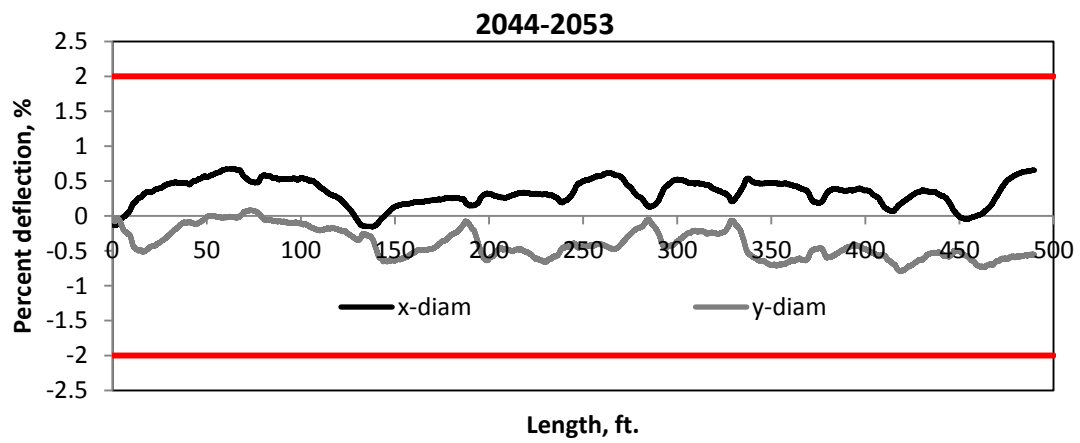
Figure 0-10 Laser video profiler for pipe 2044 to 2053

210
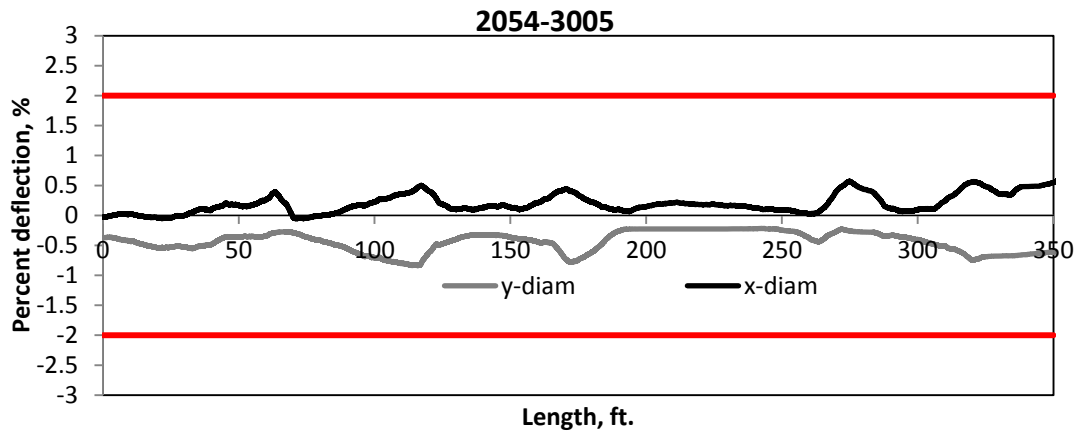
Figure 0-11 Laser video profiler for pipe 2054 to 3005
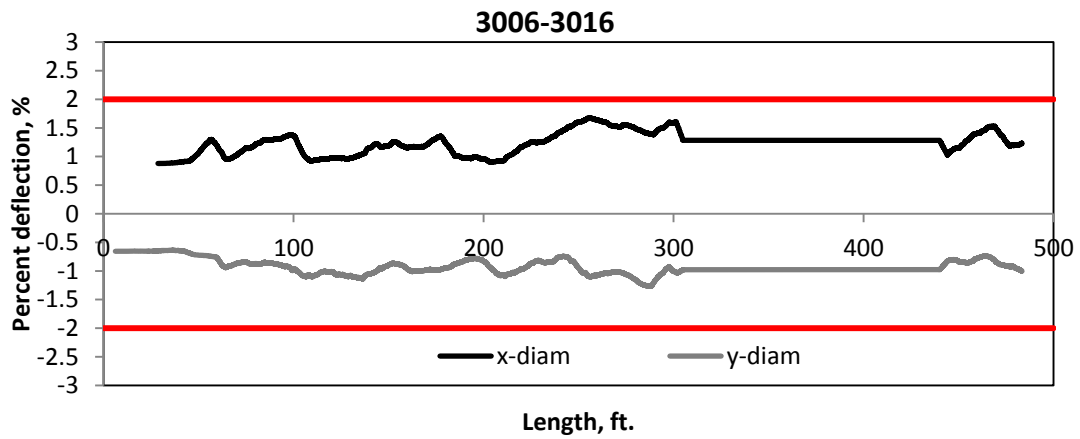
Figure 0-12 Laser video profiler for pipe 3006 to 3016

3017-3027
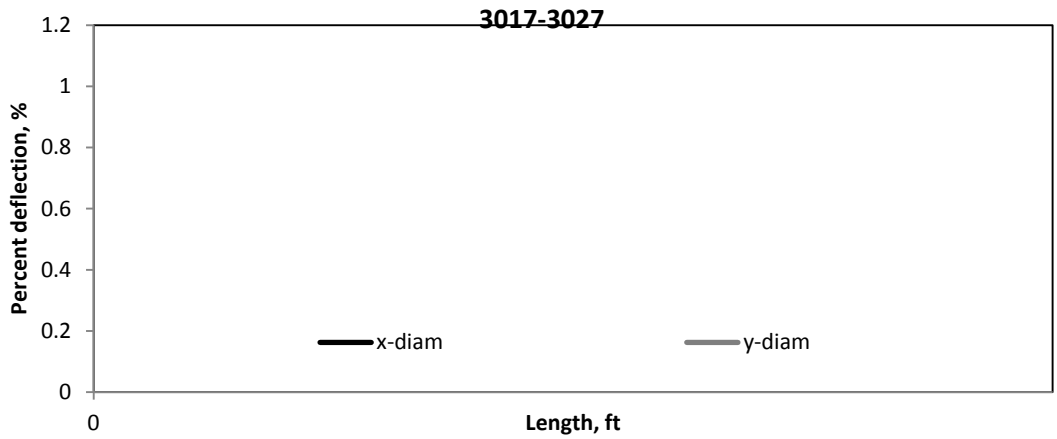
Figure 0-13 Laser video profiler for pipe 3017 to 3027

3027-3039
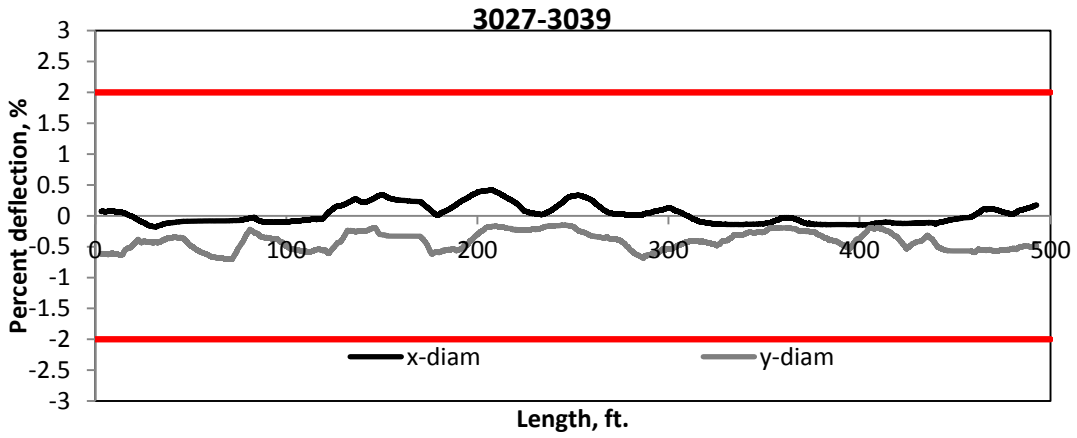
Figure 0-14 Laser video profiler for pipe 3027 to 3039

3039-3053
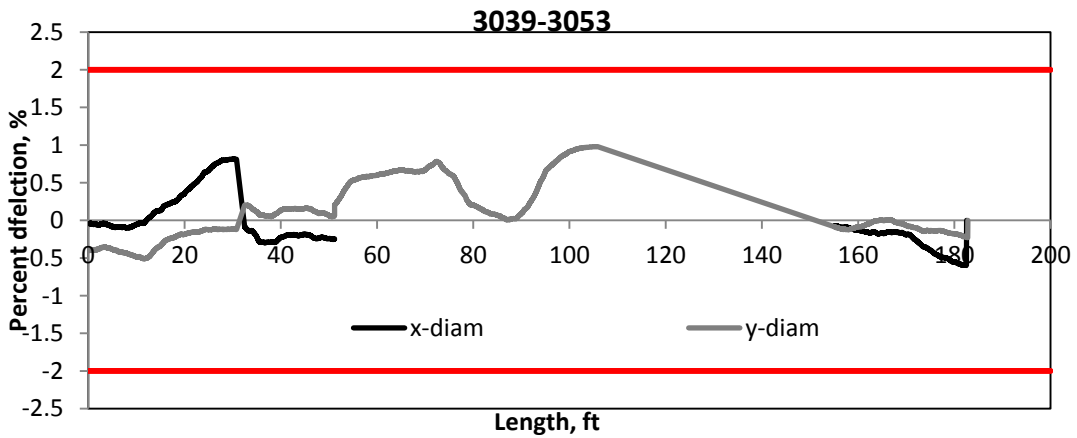
Figure 0-15 Laser video profiler for pipe 3039 to 3053

212
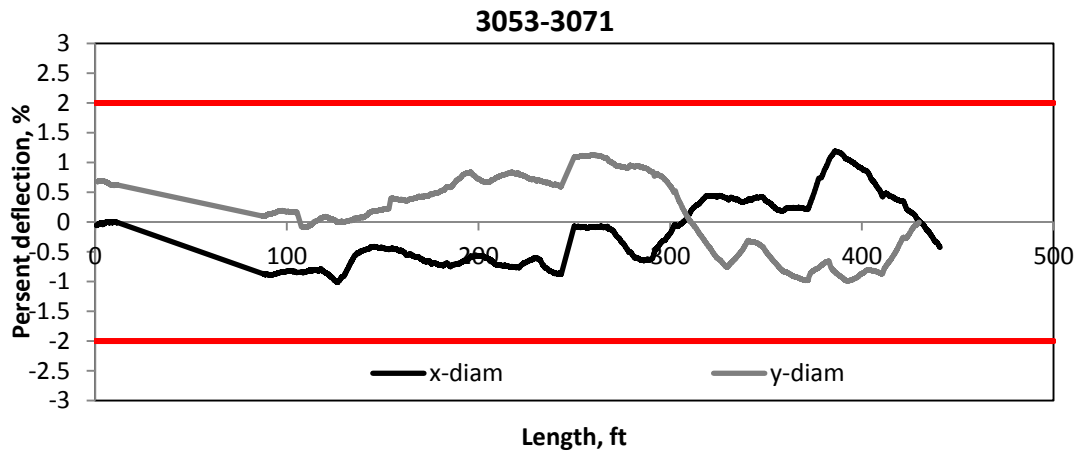
Figure 0-16 Laser video profiler for pipe 3053 to 3071
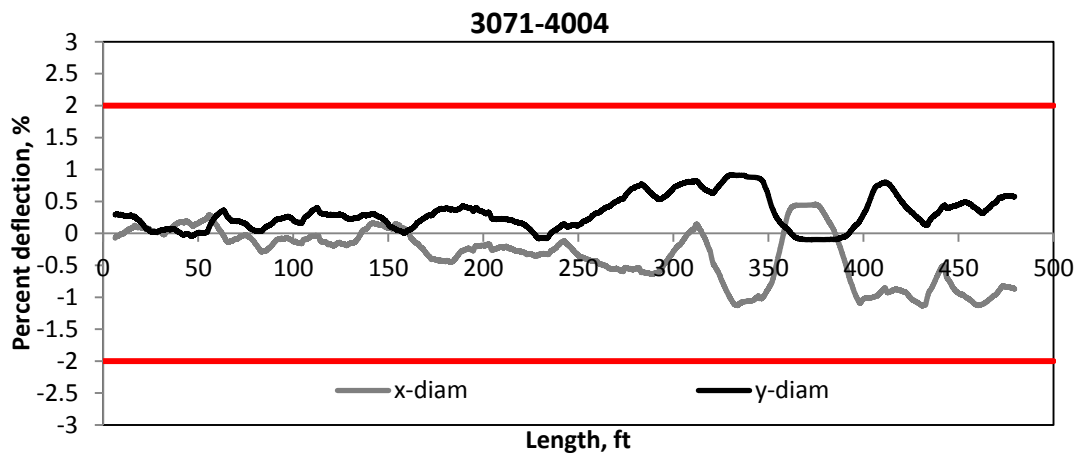
Figure 0-17 Laser video profiler for pipe 3071 to 4004
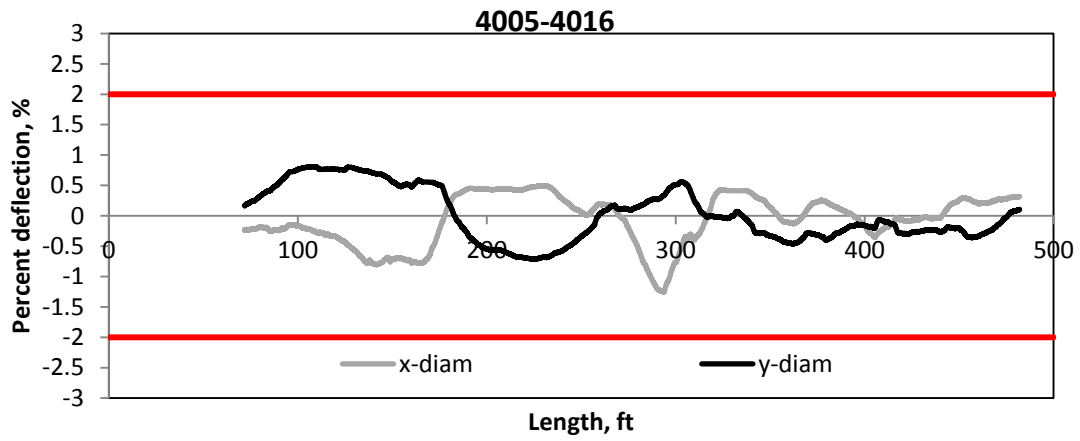
Figure 0-18 Laser video profiler for pipe 4005 to 4016
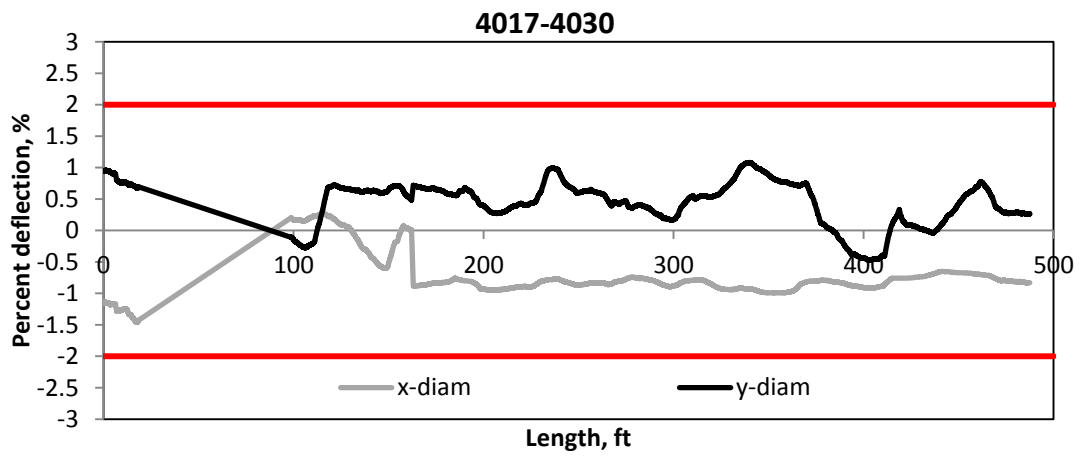
Figure 0-19 Laser video profiler for pipe 4017 to 4030
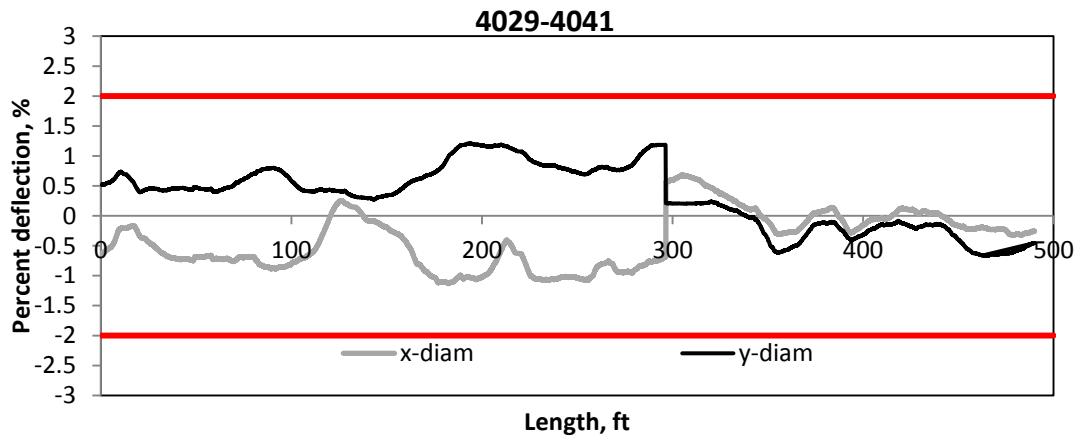
Figure 0-20 Laser video profiler for pipe 4029 to 4041
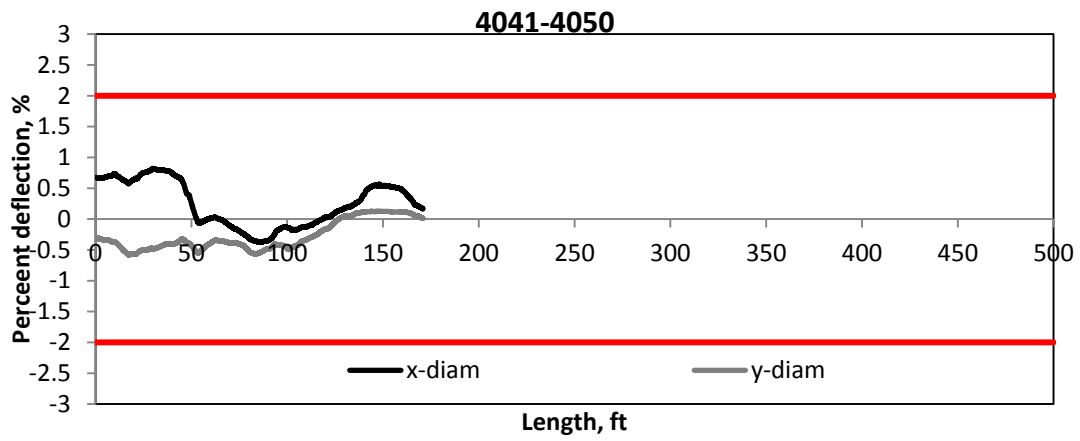
Figure 0-21 Laser video profiler for pipe 4041 to 4050

4051-4060
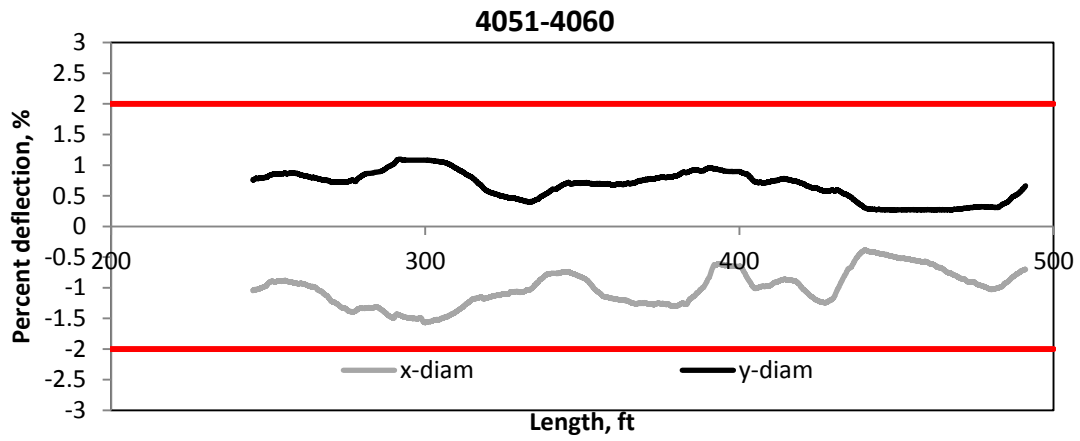
Figure 0-22 Laser video profiler for pipe 4051 to 4060

4061-4070
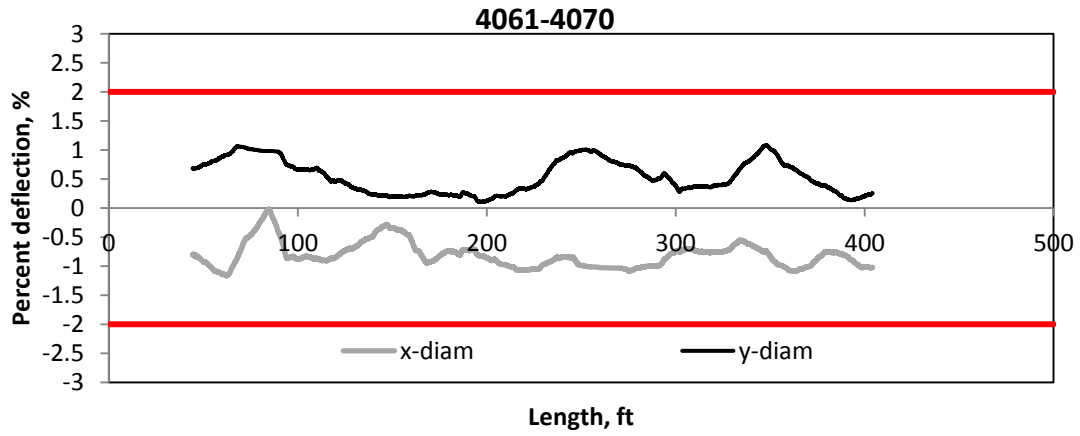
Figure 0-23 Laser video profiler for pipe 4061 to 4070

216

Appendix B

MOP-119 measurements

Table 0-1 Raw data – measurement of "e" with MOP-119 at 90º

	Pipe#	Section #	Distance	Installation	30% CLSM	70% CLSM	Full backfill
	66	**Joint**	0ft	1.50	1.44	1.30	1.36
	//	10ft	10ft	1.19	0.00	1.18	1.23
50ft	//	25ft	25ft	1.31	1.25	1.21	1.22
	//	40ft	40ft	1.25	1.22	0.00	0.00
	67	**Joint**	50ft	1.26	0.00	1.26	1.31
	//	10ft	60ft	1.25	1.25	1.21	1.25
50ft	//	25ft	75ft	1.32	1.28	1.23	1.25
	//	40ft	90ft	1.25	0.00	1.23	1.29
	68	**Joint**	100ft	1.31	1.29	1.22	1.25
	//	10ft	110ft	1.31	1.29	1.22	1.26
50ft	//	25ft	125ft	1.31	1.28	1.26	1.28
	//	40ft	140ft	1.31	0.00	1.25	1.27
	69	**Joint**	150ft	1.31	1.30	1.23	1.24
	//	10ft	160ft	1.25	0.00	1.19	1.22
50ft	//	25ft	175ft	1.28	1.27	1.20	1.23
	//	40ft	190ft	1.25	0.00	1.18	1.21
	70	**Joint**	200ft	1.25	0.00	1.19	1.35
	//	10ft	210ft	1.29	1.27	1.24	1.38
50ft	//	25ft	225ft	1.31	1.27	1.25	1.40
	//	40ft	240ft	1.20	1.20	1.18	1.32
	71	**Joint**	250ft	1.35	1.30	1.24	1.32
	//	10ft	260ft	1.31	1.26	1.18	1.33
50ft	//	25ft	275ft	1.25	0.00	1.24	1.38
	//	40ft	290ft	1.25	0.00	1.24	1.45
	72	**Joint**	300ft	1.25	0.00	1.28	0.00
	//	10ft	310ft	1.31	1.28	1.27	1.27
50ft	//	25ft	325ft	1.25	0.00	1.24	0.00
	//	40ft	340ft	1.25	1.25	1.24	0.00
	73	**Joint**	350ft	1.25	0.00	1.24	1.24
	//	10ft	360ft	1.31	1.31	1.25	0.00
44ft	//	22ft	372ft	1.33	1.26	1.20	0.00
	//	34ft	384ft	1.25	1.22	1.20	0.00
	74	**Joint**	394ft	1.23	0.00	1.26	1.27
	//	10ft	404ft	1.38	1.22	0.00	1.23
24ft	//	22ft	416ft	1.13	1.12	0.00	1.13
	75	**Joint**	418ft	1.25	1.14	0.00	1.21

50ft	//	10ft	428ft	1.25	1.21	0.00	1.27
	//	25ft	443ft	1.31	1.23	0.00	1.27
	//	40ft	458ft	1.31	1.26	1.24	1.26
	76	**Joint**	468ft	1.28	1.26	1.22	1.25
50ft	//	10ft	478ft	1.25	0.00	0.00	1.32
	//	28ft	496ft	1.25	1.22	1.21	1.23
	END	**Joint**	518ft	1.25	0.00	0.00	0.00

Table 0-2 Raw data – measurement of "e" with MOP-119 at 45º

	Pipe#	Section #	Distance	Installation	30% CLSM	70% CLSM	Full backfill
	66	**Joint**	0ft	1.31	1.31	1.29	1.29
	//	10ft	10ft	1.25	0.22	1.31	1.30
50 ft	//	25ft	25ft	1.25	1.20	1.29	1.30
	//	40ft	40ft	1.25	1.25	1.32	1.31
	67	**Joint**	50ft	1.25	1.19	1.25	1.28
	//	10ft	60ft	1.34	1.25	1.34	1.37
50ft	//	25ft	75ft	1.25	1.19	1.31	1.33
	//	40ft	90ft	1.25	1.19	1.33	1.33
	68	**Joint**	100ft	1.31	1.32	1.27	1.29
	//	10ft	110ft	1.13	1.32	1.24	1.28
50ft	//	25ft	125ft	1.19	1.31	1.23	1.25
	//	40ft	140ft	1.25	1.26	1.24	1.28
	69	**Joint**	150ft	1.25	1.28	1.32	1.33
	//	10ft	160ft	1.29	1.29	1.32	1.34
50ft	//	25ft	175ft	1.29	1.27	1.29	1.30
	//	40ft	190ft	1.29	1.28	1.32	1.33
	70	**Joint**	200ft	1.25	1.25	1.24	1.42
	//	10ft	210ft	1.25	1.27	1.28	1.43
50ft	//	25ft	225ft	1.29	1.25	1.25	1.40
	//	40ft	240ft	1.28	1.25	1.27	1.40
	71	**Joint**	250ft	1.19	1.21	1.26	1.39
	//	10ft	260ft	1.28	1.26	1.30	1.42
50ft	//	25ft	275ft	1.28	1.28	1.29	1.40
	//	40ft	290ft	1.21	1.28	1.27	1.42
	72	**Joint**	300ft	1.25	1.32	1.27	1.28
	//	10ft	310ft	1.25	1.30	1.28	1.27
50ft	//	25ft	325ft	1.25	1.32	1.29	1.28
	//	40ft	340ft	1.25	1.33	1.29	1.29
	73	**Joint**	350ft	1.36	1.30	1.26	1.28
	//	10ft	360ft	1.31	1.30	1.24	1.25
44ft	//	22ft	372ft	1.19	1.30	1.27	1.25
	//	34ft	384ft	1.19	1.28	1.27	1.28
	74	**Joint**	394ft	1.13	1.16	1.18	1.20
	//	10ft	404ft	1.19	1.21	1.20	1.25
24ft	//	22ft	416ft	1.22	1.07	1.10	1.09
	75	**Joint**	418ft	1.38	1.29	1.27	1.33
50ft	//	10ft	428ft	1.25	1.26	1.26	1.28
	//	25ft	443ft	1.20	1.28	1.25	1.29

	//	40ft	458ft	1.19	1.26	1.23	1.28
	76	Joint	468ft	1.28	1.41	1.16	1.17
	//	10ft	478ft	1.25	1.24	1.26	1.25
50ft	//	28ft	496ft	1.25	1.21	1.20	1.32
	END	Joint	518ft	1.22	1.17	1.24	1.30

Appendix C

Controlled Low Strength Material Experimental Testing

CLSM 1-76-23-1

Confined Compressive Stress

Stress, psi (y-axis)
Strain, % (x-axis)

Confinement = 15 psi
Confinement = 10 psi
Confinement = 5 psi
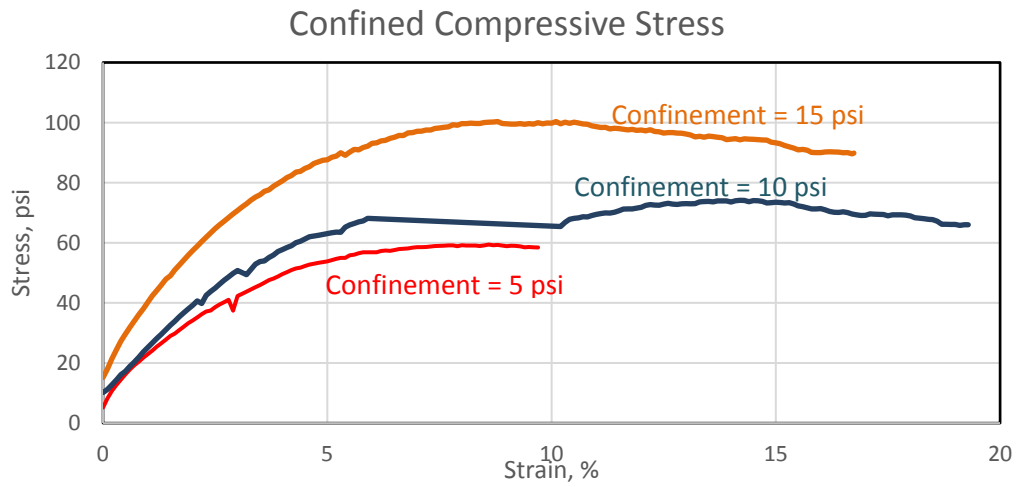
Figure A1 Stress-strain curve for 1%

Shear stress, psi (y-axis)
Principal stress, psi (x-axis)

c =10 psi
φ = 40 ^{0}
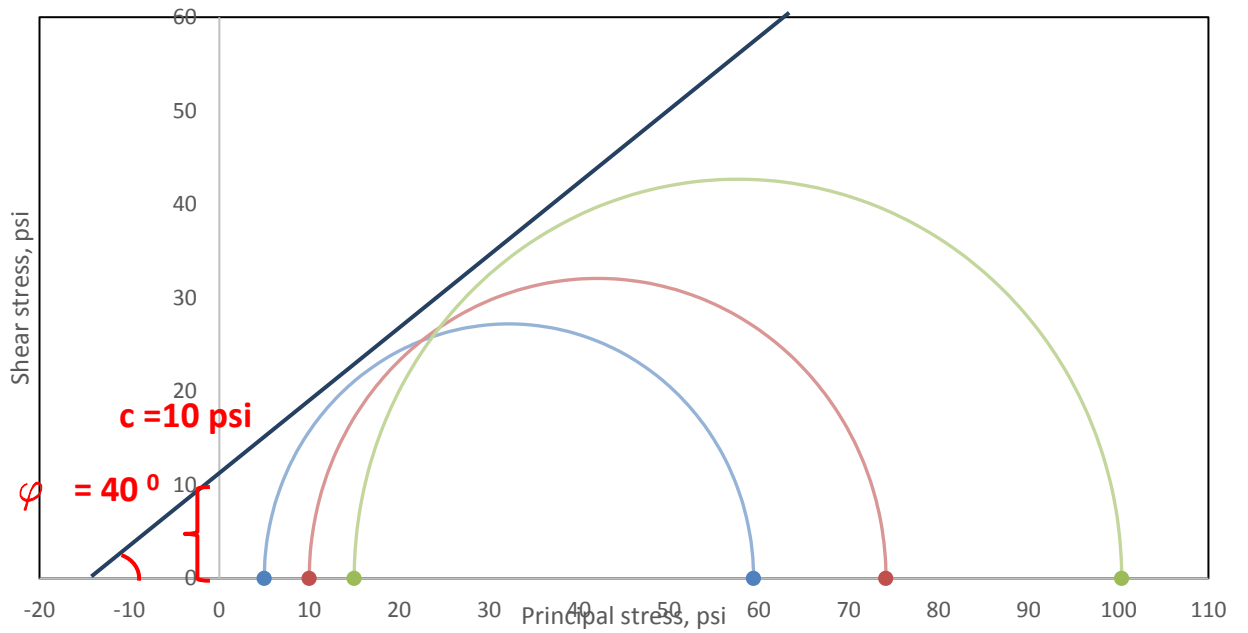
Figure A2 Calculation of cohesion and friction angle for 1%

CLSM 1-76-23-2
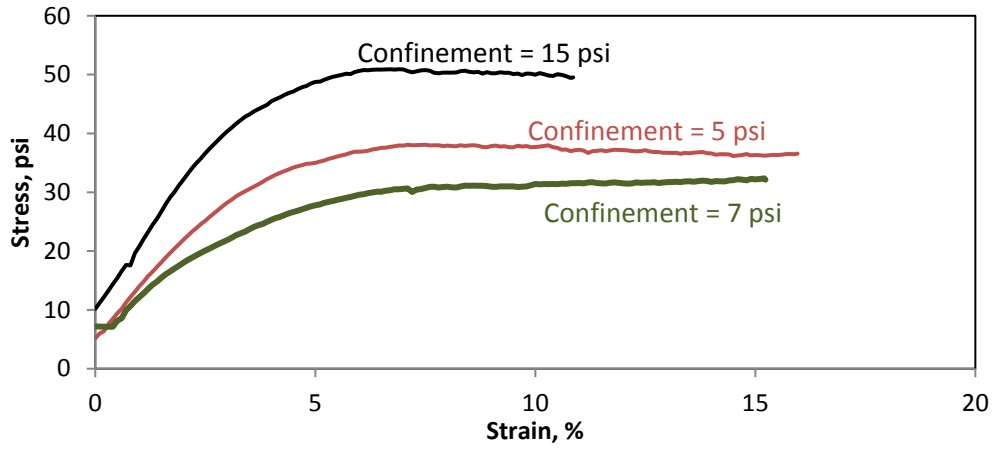
Figure A3 Stress-strain curve for 2%
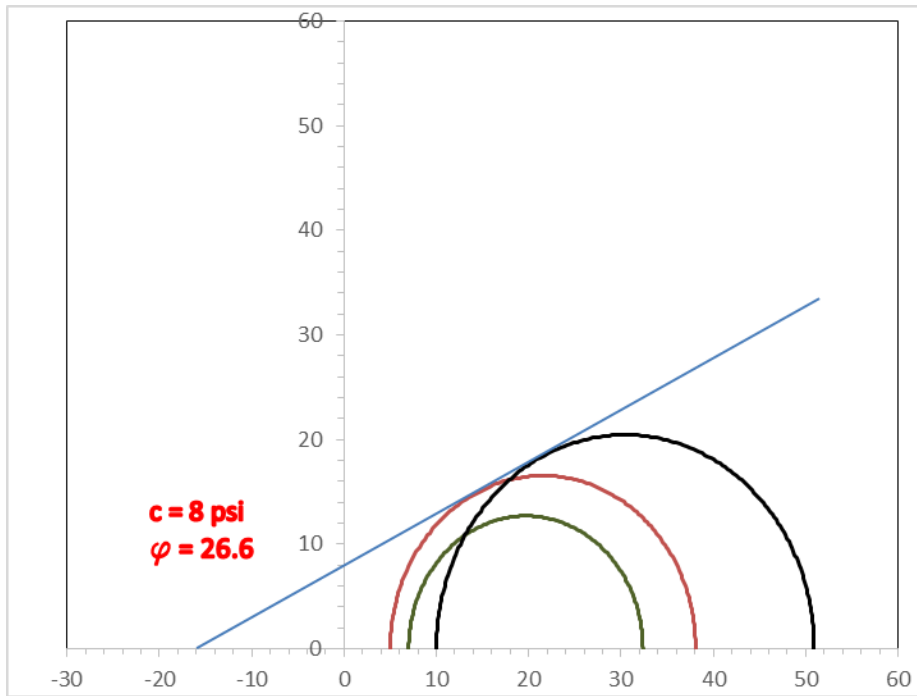
Figure A4 Calculation of cohesion and friction angle for 2%

CLSM 1-76-23-3
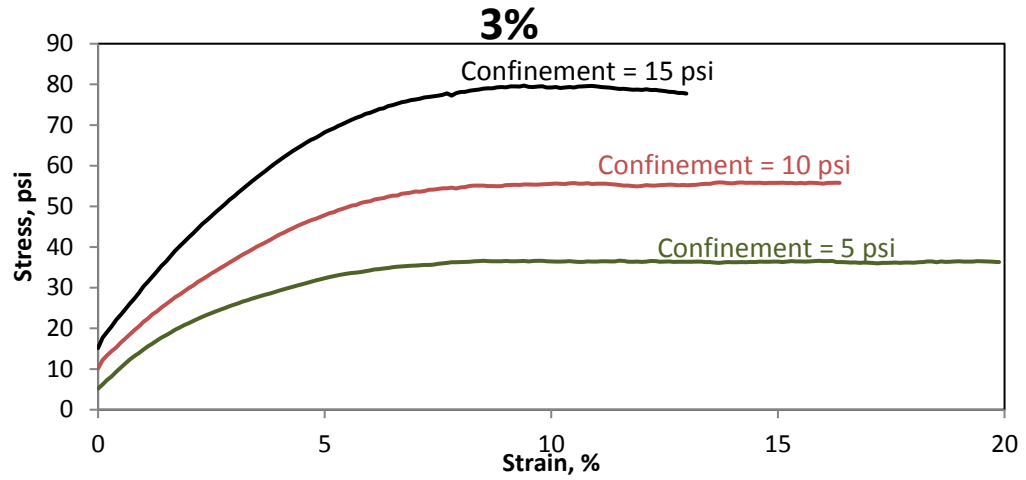
Figure A5 Stress-strain curve for 3%
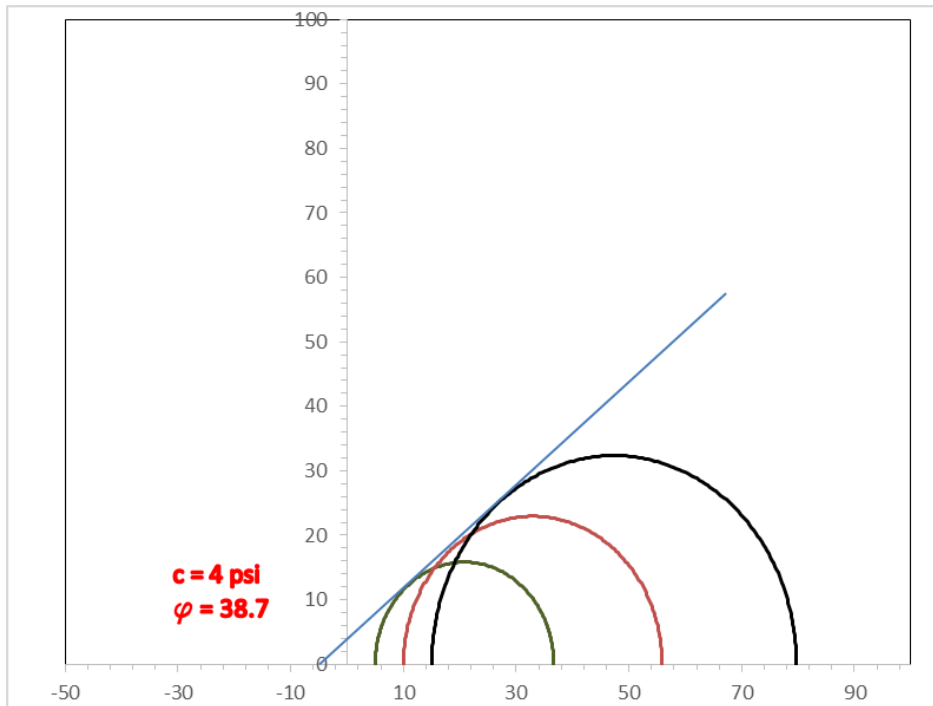
Figure A6 Calculation of cohesion and friction angle for 3%

CLSM 1-76-23-4
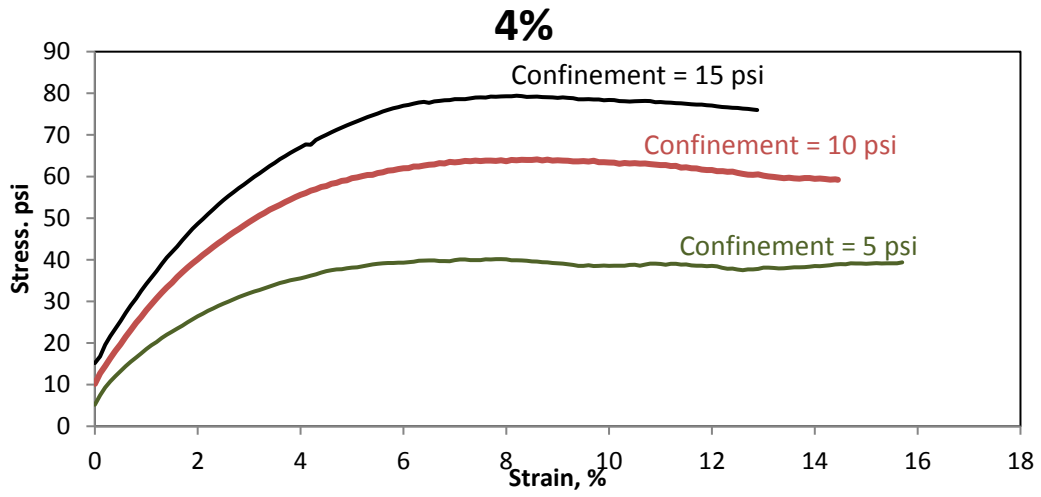
Figure A7 Stress-strain curve for 4%
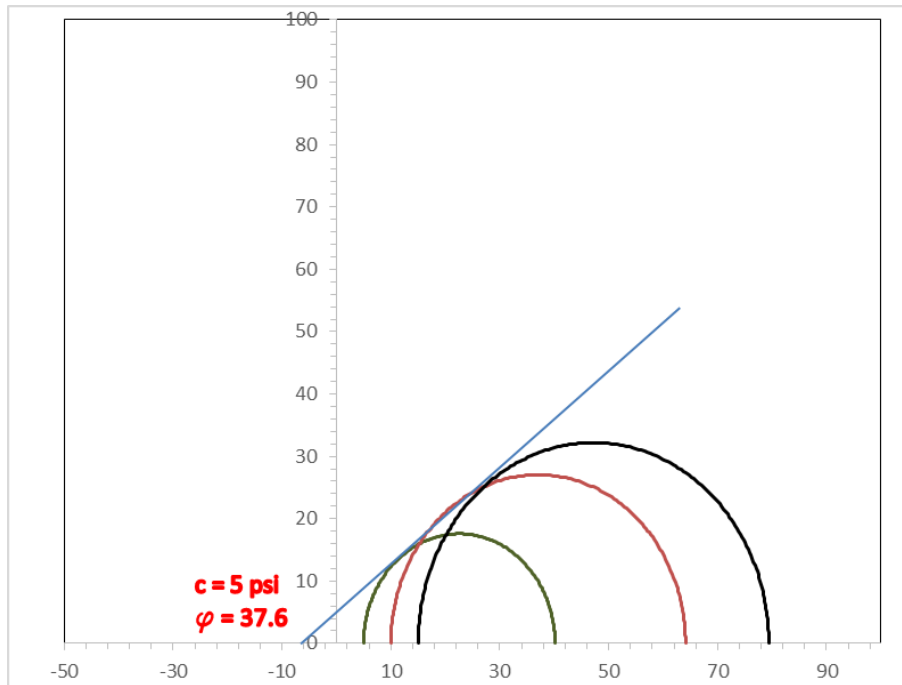
Figure A8 Calculation of cohesion and friction angle for 4%

CLSM 1-76-23-5

5%
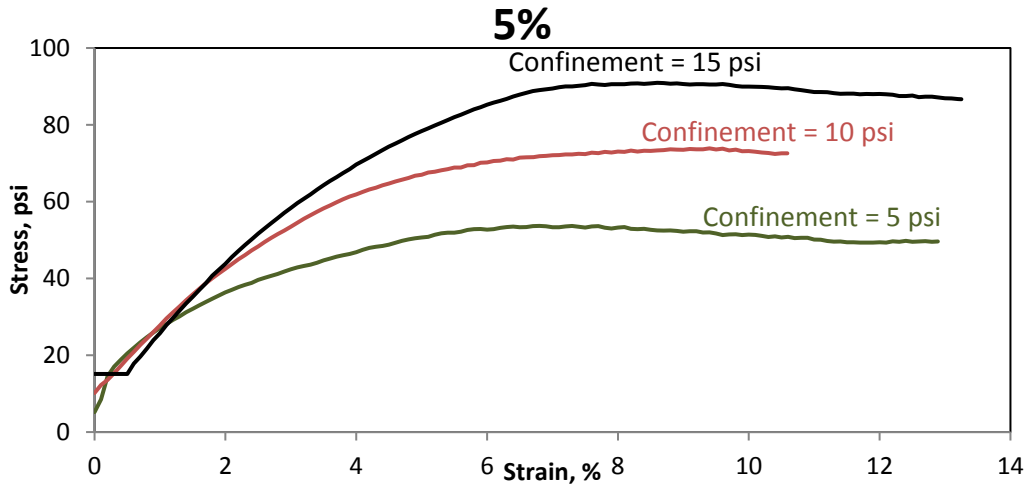
Figure A9 Stress-strain curve for 5%

c = 8.8 psi
φ = 37.4
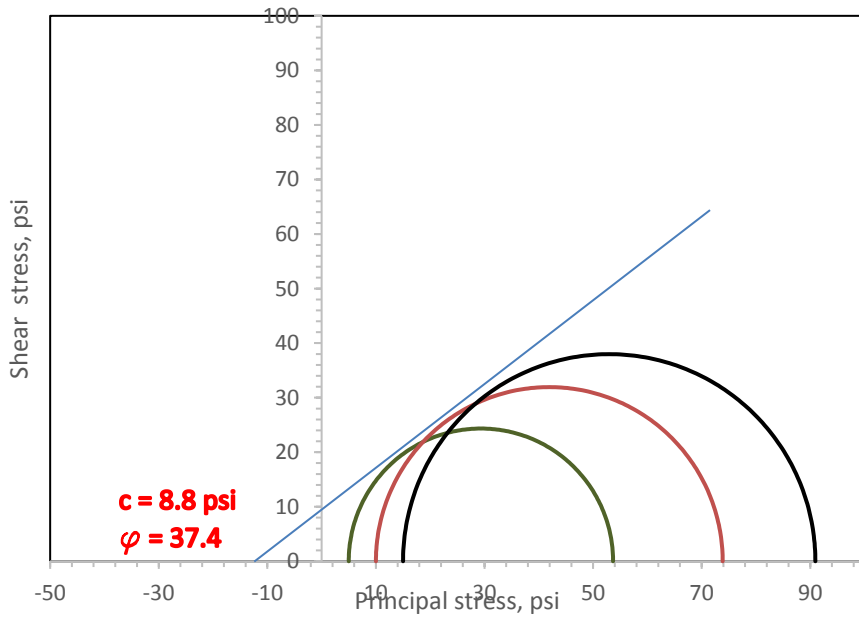
Figure A10 Calculation of cohesion and friction angle for 5%

CLSM 1-76-23-6

6%
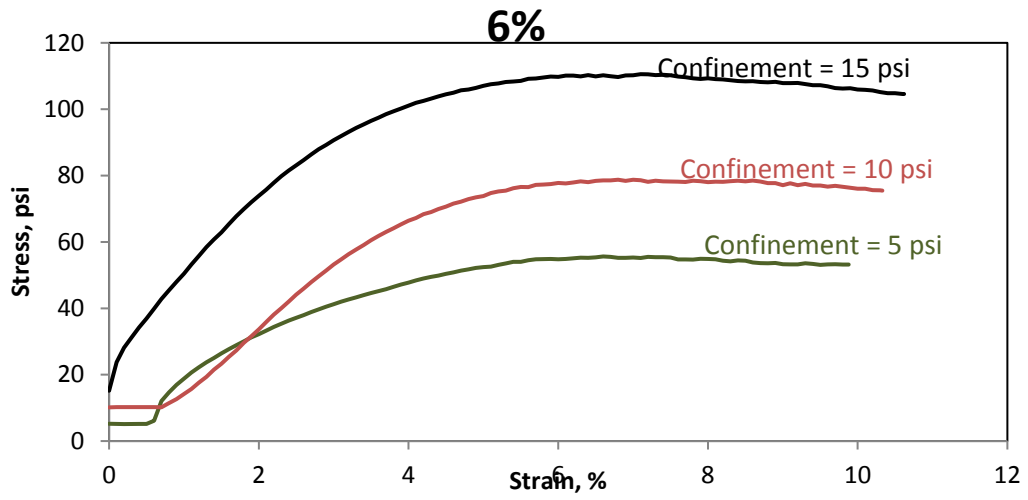
Figure A11 Stress-strain curve for 6%
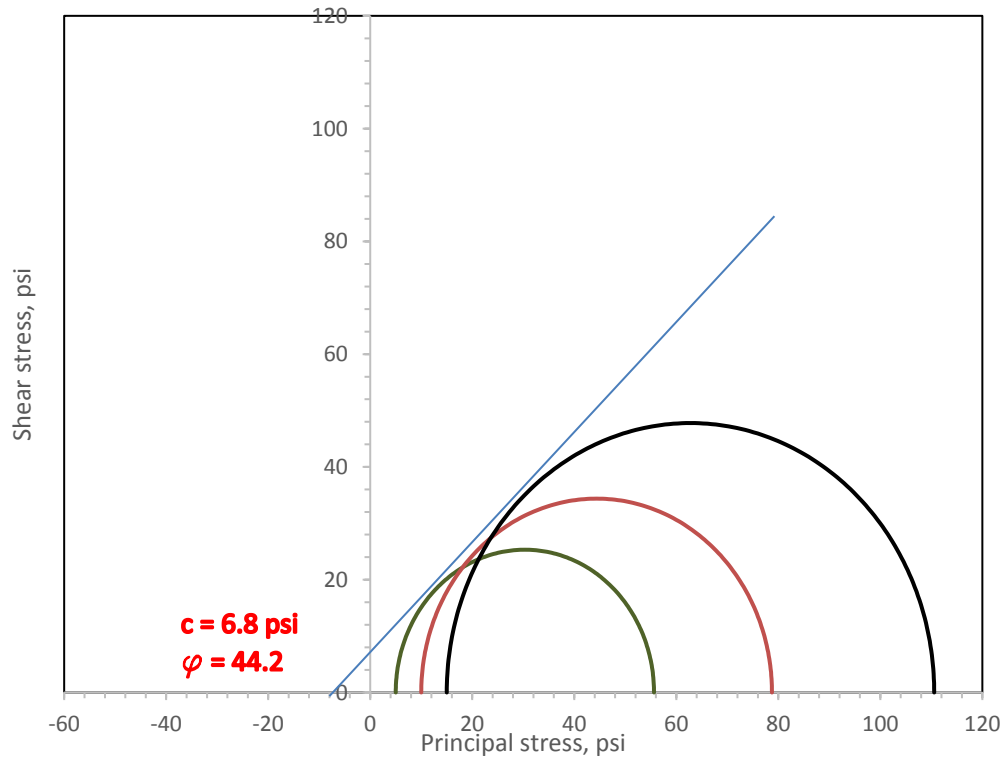
Figure A12 Calculation of cohesion and friction angle for 6%

CLSM 1-76-23-7

7%
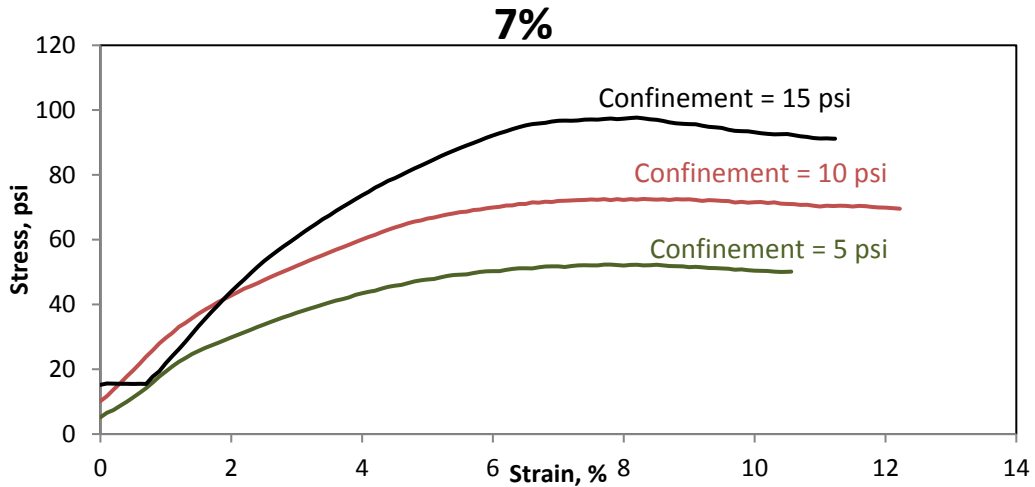
Figure A13 Stress-strain curve for 7%
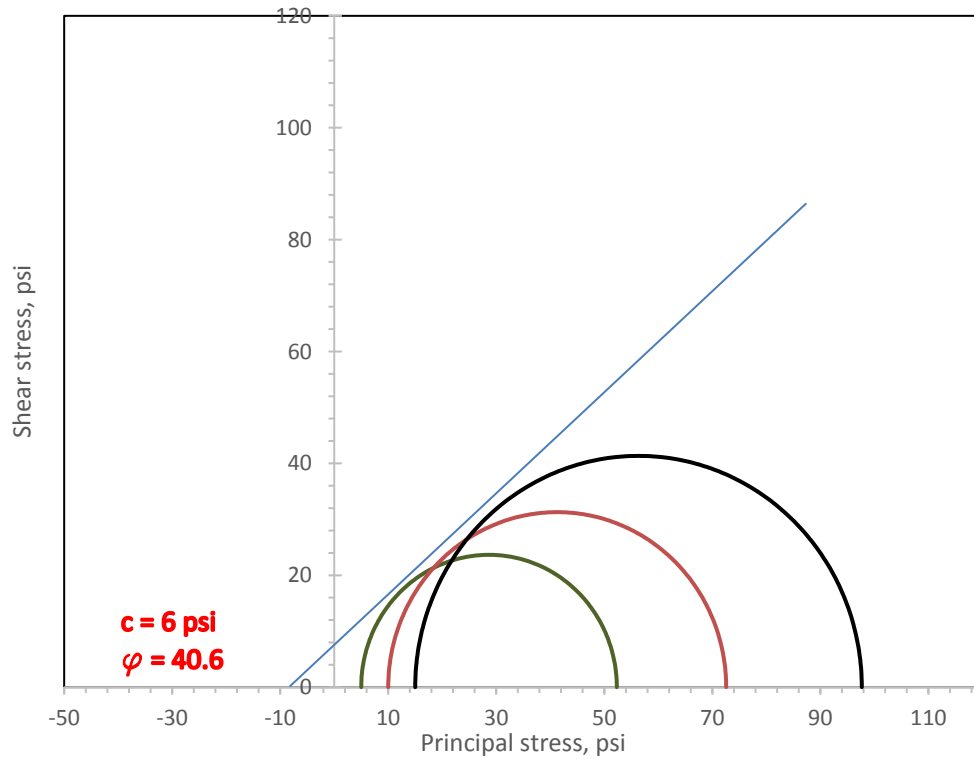
Figure A14 Calculation of cohesion and friction angle for 7%

CLSM 1-76-23-8

8%
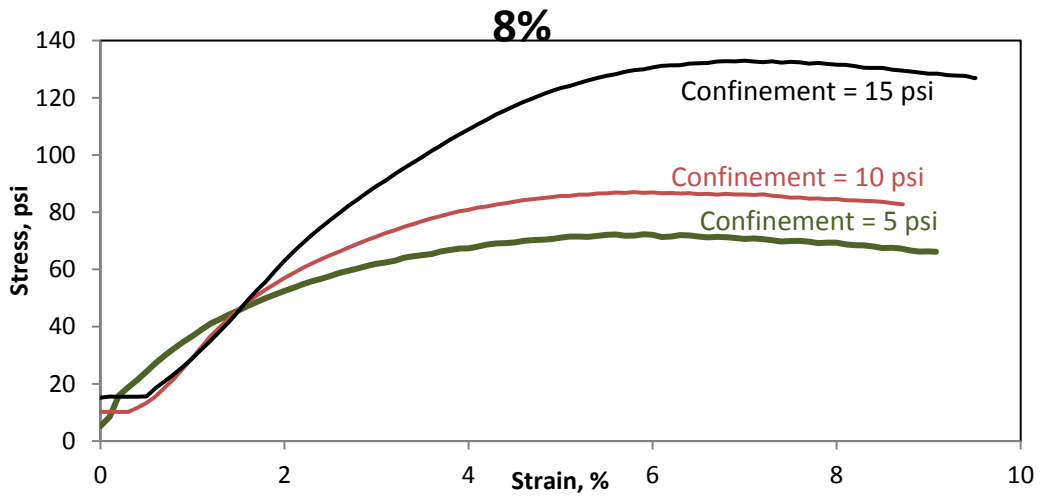
Figure A15 Stress-strain curve for 8%
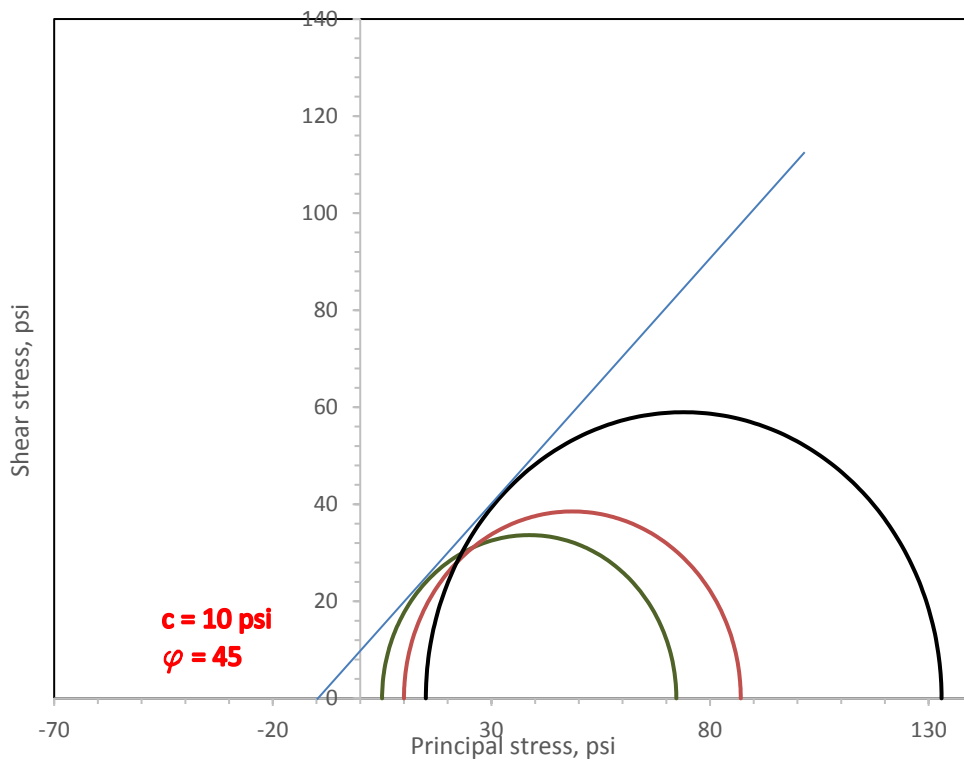
Figure A16 Calculation of cohesion and friction angle for 8%

Appendix D

Parametric Study Results

ODTh	alfa	Eback	beta	TWOD	Ewall	δy(%)	δx(%)	M(lb-in)	V (lb)	Th (lb)	ODTh	alfa	Eback	beta	TWOD	Ewall	δy(%)	δx(%)	M(lb-in)	V (lb)	Th (lb)
2.940	1	0.7	1	1.4286	1	0.1880	0.1901	3008	1256	2307	2.667	0.5	7.5	0.5	1.6250	0.7	0.2163	0.2060	1242	859.6	1957
2.940	1	0.7	1	1.4286	0.3	0.3098	0.3203	3634	1252	2533	2.667	0.5	7.5	0.5	1.7500	1	0.1734	0.1612	2373	865.9	2194
2.940	1	0.7	1	1.4286	0.5	0.2562	0.2622	3429	1249	2439	2.667	0.5	7.5	0.5	1.7500	0.3	0.3618	0.3594	1906	824.8	2092
2.940	1	0.7	1	1.4286	0.7	0.2217	0.2255	3244	1250	2378	2.667	0.5	7.5	0.5	1.7500	0.5	0.2663	0.2603	1600	839.6	2015
2.940	1	0.7	1	1.5714	1	0.1880	0.1901	3008	1256	2307	2.667	0.5	7.5	0.5	1.7500	0.7	0.2180	0.2088	1244	876.8	1941
2.940	1	0.7	1	1.5714	0.3	0.3098	0.3203	3634	1252	2533	2.667	0.5	7.5	0.5	1.8750	1	0.1755	0.1640	2345	872.6	2201
2.940	1	0.7	1	1.5714	0.5	0.2562	0.2622	3429	1249	2439	2.667	0.5	7.5	0.5	1.8750	0.3	0.3614	0.3595	1912	859.4	2059
2.940	1	0.7	1	1.5714	0.7	0.2217	0.2255	3244	1250	2378	2.667	0.5	7.5	0.5	1.8750	0.5	0.2725	0.2651	1602	849	2009
2.940	1	0.7	1	1.7143	1	0.1880	0.1901	3008	1256	2307	2.667	0.5	7.5	0.5	1.8750	0.7	0.2199	0.2111	1245	881.5	1945
2.940	1	0.7	1	1.7143	0.3	0.3098	0.3203	3634	1252	2533	2.667	0.5	7.5	0.5	2.0000	1	0.1765	0.1659	2324	878.8	2207
2.940	1	0.7	1	1.7143	0.5	0.2562	0.2622	3429	1249	2439	2.667	0.5	7.5	0.5	2.0000	0.3	0.3610	0.3595	1914	866.8	2058
2.940	1	0.7	1	1.7143	0.7	0.2217	0.2255	3244	1250	2378	2.667	0.5	7.5	0.5	2.0000	0.5	0.2743	0.2676	1602	853.6	2018
2.940	1	0.7	1	1.8571	1	0.1880	0.1901	3008	1256	2307	2.667	0.5	7.5	0.5	2.0000	0.7	0.2206	0.2124	1958	773.3	1789
2.940	1	0.7	1	1.8571	0.3	0.3098	0.3203	3634	1252	2533	2.667	0.5	5	0.5	1.3750	1	0.1262	0.0866	2585	649.9	1930
2.940	1	0.7	1	1.8571	0.5	0.2562	0.2622	3429	1249	2439	2.667	0.5	5	0.5	1.3750	0.3	0.3327	0.3248	2193	686.9	1829
2.940	1	0.7	1	1.8571	0.7	0.2217	0.2255	3244	1250	2378	2.667	0.5	5	0.5	1.3750	0.5	0.2365	0.2169	2023	733.1	1794
2.940	1	0.7	1	2.0000	1	0.1880	0.1901	3008	1256	2307	2.667	0.5	5	0.5	1.3750	0.7	0.1793	0.1512	1783	769.8	1750
2.940	1	0.7	1	2.0000	0.3	0.3098	0.3203	3634	1252	2533	2.667	0.5	5	0.5	1.5000	1	0.1409	0.1078	2571	644.9	1917
2.940	1	0.7	1	2.0000	0.5	0.2562	0.2622	3429	1249	2439	2.667	0.5	5	0.5	1.5000	0.3	0.3424	0.3358	2068	673.8	1830
2.940	1	0.7	1	2.0000	0.7	0.2217	0.2255	3244	1250	2378	2.667	0.5	5	0.5	1.5000	0.5	0.2450	0.2290	1906	725.8	1771
2.940	1	0.7	1	2.1429	1	0.1880	0.1901	3008	1256	2307	2.667	0.5	5	0.5	1.5000	0.7	0.1920	0.1681	1680	765.8	1727
2.940	1	0.7	1	2.1429	0.3	0.3098	0.3203	3634	1252	2533	2.667	0.5	5	0.5	1.6250	1	0.1497	0.1201	2527	644.2	1921
2.940	1	0.7	1	2.1429	0.5	0.2562	0.2622	3429	1249	2439	2.667	0.5	5	0.5	1.6250	0.3	0.3471	0.3423	2025	678.3	1815
2.940	1	0.7	1	2.1429	0.7	0.2217	0.2255	3244	1250	2378	2.667	0.5	5	0.5	1.6250	0.5	0.2516	0.2375	1816	721	1766
2.940	1	7.5	1	1.4286	1	0.1615	0.1592	2288	1105	2042	2.667	0.5	5	0.5	1.6250	0.7	0.1987	0.1777	1599	763.8	1713
2.940	1	7.5	1	1.4286	0.3	0.2584	0.2594	3164	1077	2231	2.667	0.5	5	0.5	1.7500	1	0.1554	0.1287	2547	640.4	1910
2.940	1	7.5	1	1.4286	0.5	0.2164	0.2152	2762	1090	2129	2.667	0.5	5	0.5	1.7500	0.3	0.3521	0.3476	2009	681.4	1804
2.940	1	7.5	1	1.4286	0.7	0.1889	0.1869	2539	1098	2086	2.667	0.5	5	0.5	1.7500	0.5	0.2566	0.2434	1745	719	1765
2.940	1	7.5	1	1.5714	1	0.1615	0.1592	2288	1105	2042	2.667	0.5	5	0.5	1.7500	0.7	0.2031	0.1844	1526	762.5	1711
2.940	1	7.5	1	1.5714	0.3	0.2584	0.2594	3164	1077	2231	2.667	0.5	5	0.5	1.8750	1	0.1591	0.1349	2570	653.3	1899
2.940	1	7.5	1	1.5714	0.5	0.2164	0.2152	2762	1090	2129	2.667	0.5	5	0.5	1.8750	0.3	0.3561	0.3517	1980	688.5	1803
2.940	1	7.5	1	1.5714	0.7	0.1889	0.1869	2539	1098	2086	2.667	0.5	5	0.5	1.8750	0.5	0.2593	0.2472	1692	715.2	1762
2.940	1	7.5	1	1.7143	1	0.1615	0.1592	2288	1105	2042	2.667	0.5	5	0.5	1.8750	0.7	0.2063	0.1894	1470	758.9	1710
2.940	1	7.5	1	1.7143	0.3	0.2584	0.2594	3164	1077	2231	2.667	0.5	5	0.5	2.0000	1	0.1620	0.1397	2544	656.3	1903
2.940	1	7.5	1	1.7143	0.5	0.2164	0.2152	2762	1090	2129	2.667	0.5	5	0.5	2.0000	0.3	0.3570	0.3534	1957	691.9	1804
2.940	1	7.5	1	1.7143	0.7	0.1889	0.1869	2539	1098	2086	2.667	0.5	5	0.5	2.0000	0.5	0.2614	0.2501	1647	716.6	1763
2.940	1	7.5	1	1.8571	1	0.1615	0.1592	2288	1105	2042	2.667	0.5	5	0.5	2.0000	0.7	0.2084	0.1930	4354	1420	2060
2.940	1	7.5	1	1.8571	0.3	0.2584	0.2594	3164	1077	2231	2.667	0.7	0.7	0.3	1.3750	1	0.2714	0.2058	5832	994.9	2454
2.940	1	7.5	1	1.8571	0.5	0.2164	0.2152	2762	1090	2129	2.667	0.7	0.7	0.3	1.3750	0.3	0.5525	0.5633	4975	1094	2306
2.940	1	7.5	1	1.8571	0.7	0.1889	0.1869	2539	1098	2086	2.667	0.7	0.7	0.3	1.3750	0.5	0.4105	0.3839	4639	1250	2186
2.940	1	7.5	1	2.0000	1	0.1615	0.1592	2288	1105	2042	2.667	0.7	0.7	0.3	1.3750	0.7	0.3379	0.2915	4215	1404	2065
2.940	1	7.5	1	2.0000	0.3	0.2584	0.2594	3164	1077	2231	2.667	0.7	0.7	0.3	1.5000	1	0.2716	0.2121	5798	994.1	2451
2.940	1	7.5	1	2.0000	0.5	0.2164	0.2152	2762	1090	2129	2.667	0.7	0.7	0.3	1.5000	0.3	0.5541	0.5683	4888	1087	2307
2.940	1	7.5	1	2.0000	0.7	0.1889	0.1869	2539	1098	2086	2.667	0.7	0.7	0.3	1.5000	0.5	0.4107	0.3889	4525	1237	2190
2.940	1	7.5	1	2.1429	1	0.1615	0.1592	2288	1105	2042	2.667	0.7	0.7	0.3	1.5000	0.7	0.3379	0.2968	4117	1393	2066
2.940	1	7.5	1	2.1429	0.3	0.2584	0.2594	3164	1077	2231	2.667	0.7	0.7	0.3	1.6250	1	0.2716	0.2166	5770	991.9	2448
2.940	1	7.5	1	2.1429	0.5	0.2164	0.2152	2762	1090	2129	2.667	0.7	0.7	0.3	1.6250	0.3	0.5551	0.5720	4827	1083	2308

ODTh	alfa	Eback	beta	TWOD	Ewall	δy(%)	δx(%)	M(lb-in)	V(lb)	Th(lb)	ODTh	alfa	Eback	beta	TWOD	Ewall	δy(%)	δx(%)	M(lb-in)	V(lb)	Th(lb)
2.940	1	7.5	1	2.1429	0.7	0.1889	0.1869	2539	1098	2086	2.667	0.7	0.7	0.3	1.6250	0.5	0.4109	0.3924	4442	1226	2189
2.940	1	5	1	1.4286	1	0.1542	0.1523	2228	1050	1941	2.667	0.7	0.7	0.3	1.6250	0.7	0.3378	0.3005	4040	1383	2067
2.940	1	5	1	1.4286	0.3	0.2461	0.2472	3007	1027	2125	2.667	0.7	0.7	0.3	1.7500	1	0.2715	0.2199	5749	990.2	2448
2.940	1	5	1	1.4286	0.5	0.2062	0.2053	2698	1037	2029	2.667	0.7	0.7	0.3	1.7500	0.3	0.5559	0.5750	4782	1079	2309
2.940	1	5	1	1.4286	0.7	0.1801	0.1785	2473	1043	1989	2.667	0.7	0.7	0.3	1.7500	0.5	0.4109	0.3951	4378	1218	2191
2.940	1	5	1	1.5714	1	0.1542	0.1523	2228	1050	1941	2.667	0.7	0.7	0.3	1.7500	0.7	0.3376	0.3033	3980	1376	2070
2.940	1	5	1	1.5714	0.3	0.2461	0.2472	3007	1027	2125	2.667	0.7	0.7	0.3	1.8750	1	0.2714	0.2225	5731	988.8	2446
2.940	1	5	1	1.5714	0.5	0.2062	0.2053	2698	1037	2029	2.667	0.7	0.7	0.3	1.8750	0.3	0.5565	0.5773	4746	1077	2310
2.940	1	5	1	1.5714	0.7	0.1801	0.1785	2473	1043	1989	2.667	0.7	0.7	0.3	1.8750	0.5	0.4110	0.3972	4328	1212	2193
2.940	1	5	1	1.7143	1	0.1542	0.1523	2228	1050	1941	2.667	0.7	0.7	0.3	1.8750	0.7	0.3374	0.3055	3931	1369	2071
2.940	1	5	1	1.7143	0.3	0.2461	0.2472	3007	1027	2125	2.667	0.7	0.7	0.3	2.0000	1	0.2713	0.2245	5720	987.4	2445
2.940	1	5	1	1.7143	0.5	0.2062	0.2053	2698	1037	2029	2.667	0.7	0.7	0.3	2.0000	0.3	0.5571	0.5792	4718	1075	2311
2.940	1	5	1	1.7143	0.7	0.1801	0.1785	2473	1043	1989	2.667	0.7	0.7	0.3	2.0000	0.5	0.4110	0.3990	4287	1207	2195
2.940	1	5	1	1.8571	1	0.1542	0.1523	2228	1050	1941	2.667	0.7	0.7	0.3	2.0000	0.7	0.3372	0.3073	1942	888.4	1963
2.940	1	5	1	1.8571	0.3	0.2461	0.2472	3007	1027	2125	2.667	0.7	7.5	0.3	1.3750	1	0.1876	0.1711	3034	817.5	2236
2.940	1	5	1	1.8571	0.5	0.2062	0.2053	2698	1037	2029	2.667	0.7	7.5	0.3	1.3750	0.3	0.3646	0.3635	2466	836.9	2089
2.940	1	5	1	1.8571	0.7	0.1801	0.1785	2473	1043	1989	2.667	0.7	7.5	0.3	1.3750	0.5	0.2793	0.2716	2180	859	2034
2.940	1	5	1	2.0000	1	0.1542	0.1523	2228	1050	1941	2.667	0.7	7.5	0.3	1.3750	0.7	0.2310	0.2192	1876	895.2	1966
2.940	1	5	1	2.0000	0.3	0.2461	0.2472	3007	1027	2125	2.667	0.7	7.5	0.3	1.5000	1	0.1877	0.1734	2993	833.2	2237
2.940	1	5	1	2.0000	0.5	0.2062	0.2053	2698	1037	2029	2.667	0.7	7.5	0.3	1.5000	0.3	0.3645	0.3636	2406	845.6	2095
2.940	1	5	1	2.0000	0.7	0.1801	0.1785	2473	1043	1989	2.667	0.7	7.5	0.3	1.5000	0.5	0.2789	0.2724	2124	867.9	2038
2.940	1	5	1	2.1429	1	0.1542	0.1523	2228	1050	1941	2.667	0.7	7.5	0.3	1.5000	0.7	0.2310	0.2208	1824	899.3	1971
2.940	1	5	1	2.1429	0.3	0.2461	0.2472	3007	1027	2125	2.667	0.7	7.5	0.3	1.6250	1	0.1877	0.1751	2931	831	2247
2.940	1	5	1	2.1429	0.5	0.2062	0.2053	2698	1037	2029	2.667	0.7	7.5	0.3	1.6250	0.3	0.3621	0.3619	2360	851.8	2101
2.940	1	5	1	2.1429	0.7	0.1801	0.1785	2473	1043	1989	2.667	0.7	7.5	0.3	1.6250	0.5	0.2784	0.2729	2080	876.3	2037
2.940	0	0.7	1	1.4286	1	-0.0396	-0.0195	2266	1473	2182	2.667	0.7	7.5	0.3	1.6250	0.7	0.2312	0.2220	1784	903.7	1973
2.940	0	0.7	1	1.4286	0.3	0.3243	0.3288	4482	1152	2155	2.667	0.7	7.5	0.3	1.7500	1	0.1877	0.1764	2912	838.8	2249
2.940	0	0.7	1	1.4286	0.5	0.1502	0.1593	2943	1264	2157	2.667	0.7	7.5	0.3	1.7500	0.3	0.3619	0.3620	2325	857.2	2104
2.940	0	0.7	1	1.4286	0.7	0.0496	0.0640	2371	1339	2172	2.667	0.7	7.5	0.3	1.7500	0.5	0.2782	0.2734	2048	883.2	2037
2.940	0	0.7	1	1.5714	1	0.0116	0.0185	1991	1455	2176	2.667	0.7	7.5	0.3	1.7500	0.7	0.2313	0.2229	1750	906.5	1977
2.940	0	0.7	1	1.5714	0.3	0.3557	0.3564	4814	1146	2160	2.667	0.7	7.5	0.3	1.8750	1	0.1876	0.1772	2879	842	2254
2.940	0	0.7	1	1.5714	0.5	0.1914	0.1916	3121	1253	2160	2.667	0.7	7.5	0.3	1.8750	0.3	0.3608	0.3612	2294	857.4	2108
2.940	0	0.7	1	1.5714	0.7	0.0965	0.0998	2459	1330	2180	2.667	0.7	7.5	0.3	1.8750	0.5	0.2774	0.2731	2017	888.3	2039
2.940	0	0.7	1	1.7143	1	0.0422	0.0420	2049	1442	2177	2.667	0.7	7.5	0.3	1.8750	0.7	0.2311	0.2233	1725	910.2	1978
2.940	0	0.7	1	1.7143	0.3	0.3728	0.3719	5050	1143	2166	2.667	0.7	7.5	0.3	2.0000	1	0.1875	0.1780	2872	853.8	2252
2.940	0	0.7	1	1.7143	0.5	0.2155	0.2109	3261	1245	2163	2.667	0.7	7.5	0.3	2.0000	0.3	0.3615	0.3619	2270	860.3	2111
2.940	0	0.7	1	1.7143	0.7	0.1244	0.1217	2508	1322	2182	2.667	0.7	7.5	0.3	2.0000	0.5	0.2770	0.2731	1990	891.9	2043
2.940	0	0.7	1	1.8571	1	0.0627	0.0580	2086	1433	2178	2.667	0.7	7.5	0.3	2.0000	0.7	0.2307	0.2236	2406	767.7	1722
2.940	0	0.7	1	1.8571	0.3	0.3833	0.3818	5227	1141	2171	2.667	0.7	5	0.3	1.3750	1	0.1849	0.1536	3394	669.4	1960
2.940	0	0.7	1	1.8571	0.5	0.2306	0.2235	3389	1241	2166	2.667	0.7	5	0.3	1.3750	0.3	0.3634	0.3623	2843	700.3	1830
2.940	0	0.7	1	1.8571	0.7	0.1426	0.1364	2577	1316	2183	2.667	0.7	5	0.3	1.3750	0.5	0.2759	0.2616	2594	744.9	1783
2.940	0	0.7	1	2.0000	1	0.0772	0.0698	2111	1427	2184	2.667	0.7	5	0.3	1.3750	0.7	0.2276	0.2050	2326	786.1	1728
2.940	0	0.7	1	2.0000	0.3	0.3908	0.3887	5356	1140	2175	2.667	0.7	5	0.3	1.5000	1	0.1852	0.1583	2791	708.7	1833
2.940	0	0.7	1	2.0000	0.5	0.2413	0.2324	3491	1237	2168	2.667	0.7	5	0.3	1.5000	0.5	0.2766	0.2651	2518	750.6	1788
2.940	0	0.7	1	2.0000	0.7	0.1554	0.1469	2643	1312	2185	2.667	0.7	5	0.3	1.5000	0.7	0.2280	0.2088	2255	794.1	1731
2.940	0	0.7	1	2.1429	1	0.0879	0.0786	2129	1422	2187	2.667	0.7	5	0.3	1.6250	1	0.1852	0.1613	2749	714.6	1835

ODTh	alfa	Eback	beta	TWOD	Ewall	δy(%)	δx(%)	M(lb-in)	V(lb)	Th(lb)	ODTh	alfa	Eback	beta	TWOD	Ewall	δy(%)	δx(%)	M(lb-in)	V(lb)	Th(lb)
2.940	0	0.7	1	2.1429	0.3	0.3964	0.3942	5450	1140	2179	2.667	0.7	5	0.3	1.6250	0.5	0.2771	0.2676	2468	754.3	1792
2.940	0	0.7	1	2.1429	0.5	0.2488	0.2389	3575	1233	2171	2.667	0.7	5	0.3	1.6250	0.7	0.2281	0.2117	2202	797.8	1736
2.940	0	0.7	1	2.1429	0.7	0.1648	0.1548	2695	1308	2187	2.667	0.7	5	0.3	1.7500	1	0.1850	0.1636	3332	677.5	1960
2.940	0	7.5	1	1.4286	1	0.1177	0.1204	1923	874	1749	3.840	0.7	5	0.3	1.7500	0.3	0.3669	0.3693	2709	718	1837
2.940	0	7.5	1	1.4286	0.3	0.2627	0.2681	3379	931	1987	3.840	0.7	5	0.3	1.7500	0.5	0.2769	0.2690	2426	758.8	1794
2.940	0	7.5	1	1.4286	0.5	0.1965	0.1997	2674	906	1903	3.840	0.7	5	0.3	1.7500	0.7	0.2284	0.2141	2150	799.8	1738
2.940	0	7.5	1	1.4286	0.7	0.1569	0.1599	2348	890	1837	3.840	0.7	5	0.3	1.8750	1	0.1849	0.1655	3298	682.4	1964
2.940	0	7.5	1	1.5714	1	0.1294	0.1308	1969	854	1770	3.840	0.7	5	0.3	1.8750	0.3	0.3662	0.3694	2679	722.5	1839
2.940	0	7.5	1	1.5714	0.3	0.2680	0.2729	3414	918	2006	3.840	0.7	5	0.3	1.8750	0.5	0.2770	0.2704	2393	761.5	1796
2.940	0	7.5	1	1.5714	0.5	0.2066	0.2083	2704	882	1901	3.840	0.7	5	0.3	1.8750	0.7	0.2284	0.2158	2113	803	1740
2.940	0	7.5	1	1.5714	0.7	0.1667	0.1687	2385	869	1857	3.840	0.7	5	0.3	2.0000	1	0.1850	0.1673	3273	686.6	1967
2.940	0	7.5	1	1.7143	1	0.1364	0.1371	1995	862	1793	3.840	0.7	5	0.3	2.0000	0.3	0.3659	0.3697	2654	727.2	1840
2.940	0	7.5	1	1.7143	0.3	0.2712	0.2758	3436	910	2018	3.840	0.7	5	0.3	2.0000	0.5	0.2771	0.2713	2357	763.4	1798
2.940	0	7.5	1	1.7143	0.5	0.2109	0.2124	2718	874	1922	3.840	0.7	5	0.3	2.0000	0.7	0.2285	0.2172	6991	2414	4344
2.940	0	7.5	1	1.7143	0.7	0.1746	0.1749	2414	848	1841	6.000	1	0.7	1	1.3000	1	0.3502	0.3594	13190	2319	4774
2.940	0	7.5	1	1.8571	1	0.1409	0.1411	2012	870	1806	6.000	1	0.7	1	1.3000	0.3	0.7172	0.7608	9808	2378	4543
2.940	0	7.5	1	1.8571	0.3	0.2733	0.2775	3452	906	2031	6.000	1	0.7	1	1.3000	0.5	0.5383	0.5630	7893	2398	4442
2.940	0	7.5	1	1.8571	0.5	0.2155	0.2168	2774	865	1924	6.000	1	0.7	1	1.3000	0.7	0.4387	0.4547	6991	2414	4344
2.940	0	7.5	1	1.8571	0.7	0.1786	0.1784	2428	855	1853	6.000	1	0.7	1	1.4000	1	0.3502	0.3594	13190	2319	4774
2.940	0	7.5	1	2.0000	1	0.1440	0.1438	2024	876	1820	6.000	1	0.7	1	1.4000	0.3	0.7172	0.7608	9808	2378	4543
2.940	0	7.5	1	2.0000	0.3	0.2748	0.2786	3470	903	2042	6.000	1	0.7	1	1.4000	0.5	0.5383	0.5630	7893	2398	4442
2.940	0	7.5	1	2.0000	0.5	0.2174	0.2183	2781	861	1934	6.000	1	0.7	1	1.4000	0.7	0.4387	0.4547	6991	2414	4344
2.940	0	7.5	1	2.0000	0.7	0.1819	0.1813	2440	869	1861	6.000	1	0.7	1	1.5000	1	0.3502	0.3594	13190	2319	4774
2.940	0	7.5	1	2.1429	1	0.1465	0.1459	2034	886	1825	6.000	1	0.7	1	1.5000	0.3	0.7172	0.7608	9808	2378	4543
2.940	0	7.5	1	2.1429	0.3	0.2747	0.2785	3461	903	2059	6.000	1	0.7	1	1.5000	0.5	0.5383	0.5630	7893	2398	4442
2.940	0	7.5	1	2.1429	0.5	0.2184	0.2193	2775	859	1948	6.000	1	0.7	1	1.5000	0.7	0.4387	0.4547	6991	2414	4344
2.940	0	7.5	1	2.1429	0.7	0.1843	0.1836	2449	895	1868	6.000	1	0.7	1	1.6000	1	0.3502	0.3594	13190	2319	4774
2.940	0	5	1	1.4286	1	0.0592	0.0661	1585	858	1484	6.000	1	0.7	1	1.6000	0.3	0.7172	0.7608	9808	2378	4543
2.940	0	5	1	1.4286	0.3	0.2382	0.2454	3382	863	1693	6.000	1	0.7	1	1.6000	0.5	0.5383	0.5630	7893	2398	4442
2.940	0	5	1	1.4286	0.5	0.1602	0.1660	2432	845	1586	6.000	1	0.7	1	1.6000	0.7	0.4387	0.4547	6991	2414	4344
2.940	0	5	1	1.4286	0.7	0.1096	0.1159	2025	842	1517	6.000	1	0.7	1	1.7000	1	0.3502	0.3594	13190	2319	4774
2.940	0	5	1	1.5714	1	0.0860	0.0886	1683	801	1486	6.000	1	0.7	1	1.7000	0.3	0.7172	0.7608	9808	2378	4543
2.940	0	5	1	1.5714	0.3	0.2554	0.2604	3563	827	1695	6.000	1	0.7	1	1.7000	0.5	0.5383	0.5630	7893	2398	4442
2.940	0	5	1	1.5714	0.5	0.1797	0.1829	2512	807	1605	6.000	1	0.7	1	1.7000	0.7	0.4387	0.4547	6991	2414	4344
2.940	0	5	1	1.5714	0.7	0.1328	0.1357	2129	799	1542	6.000	1	0.7	1	1.8000	1	0.3502	0.3594	13190	2319	4774
2.940	0	5	1	1.7143	1	0.1019	0.1022	1738	771	1502	6.000	1	0.7	1	1.8000	0.3	0.7172	0.7608	9808	2378	4543
2.940	0	5	1	1.7143	0.3	0.2643	0.2681	3641	809	1704	6.000	1	0.7	1	1.8000	0.5	0.5383	0.5630	7893	2398	4442
2.940	0	5	1	1.7143	0.5	0.1910	0.1929	2645	788	1622	6.000	1	0.7	1	1.8000	0.7	0.4387	0.4547	5738	2069	3813
2.940	0	5	1	1.7143	0.7	0.1462	0.1472	2188	776	1557	6.000	1	7.5	1	1.3000	1	0.2985	0.2914	11510	1932	4188
2.940	0	5	1	1.8571	1	0.1123	0.1111	1773	772	1517	6.000	1	7.5	1	1.3000	0.3	0.5854	0.5965	8805	1997	3992
2.940	0	5	1	1.8571	0.3	0.2699	0.2727	3683	799	1712	6.000	1	7.5	1	1.3000	0.5	0.4472	0.4475	7212	2034	3873
2.940	0	5	1	1.8571	0.5	0.1982	0.1990	2723	776	1634	6.000	1	7.5	1	1.3000	0.7	0.3692	0.3648	5738	2069	3813
2.940	0	5	1	1.8571	0.7	0.1549	0.1548	2222	762	1572	6.000	1	7.5	1	1.4000	1	0.2985	0.2914	11510	1932	4188
2.940	0	5	1	2.0000	1	0.1197	0.1177	1798	781	1530	6.000	1	7.5	1	1.4000	0.3	0.5854	0.5965	8805	1997	3992
2.940	0	5	1	2.0000	0.3	0.2727	0.2751	3680	793	1723	6.000	1	7.5	1	1.4000	0.5	0.4472	0.4475	7212	2034	3873
2.940	0	5	1	2.0000	0.5	0.2032	0.2034	2789	768	1643	6.000	1	7.5	1	1.4000	0.7	0.3692	0.3648	5738	2069	3813
2.940	0	5	1	2.0000	0.7	0.1611	0.1602	2245	752	1584	6.000	1	7.5	1	1.5000	1	0.2985	0.2914	11510	1932	4188

ODTh	alfa	Eback	beta	TWOD	Ewall	δy(%)	δx(%)	M(lb-in)	V(lb)	Th(lb)	ODTh	alfa	Eback	beta	TWOD	Ewall	δy(%)	δx(%)	M(lb-in)	V(lb)	Th(lb)
2.940	0	5	1	2.1429	1	0.1251	0.1224	1816	787	1542	6.000	1	7.5	1	1.5000	0.3	0.5854	0.5965	8805	1997	3992
2.940	0	5	1	2.1429	0.3	0.2753	0.2775	3689	789	1733	6.000	1	7.5	1	1.5000	0.5	0.4472	0.4475	7212	2034	3873
2.940	0	5	1	2.1429	0.5	0.2067	0.2064	2831	763	1655	6.000	1	7.5	1	1.5000	0.7	0.3692	0.3648	5738	2069	3813
2.940	0	5	1	2.1429	0.7	0.1654	0.1640	2274	746	1593	6.000	1	7.5	1	1.6000	1	0.2985	0.2914	11510	1932	4188
2.940	1	0.7	1	1.4286	1	0.1680	0.1235	4410	1478	2208	6.000	1	7.5	1	1.6000	0.3	0.5854	0.5965	8805	1997	3992
2.940	1	0.7	1	1.4286	0.3	0.4419	0.4343	6565	1097	2275	6.000	1	7.5	1	1.6000	0.5	0.4472	0.4475	7212	2034	3873
2.940	1	0.7	1	1.4286	0.5	0.3067	0.2823	5194	1212	2239	6.000	1	7.5	1	1.6000	0.7	0.3692	0.3648	5738	2069	3813
2.940	1	0.7	1	1.4286	0.7	0.2325	0.1990	4665	1314	2231	6.000	1	7.5	1	1.7000	1	0.2985	0.2914	11510	1932	4188
2.940	1	0.7	1	1.5714	1	0.1799	0.1390	4186	1457	2209	6.000	1	7.5	1	1.7000	0.3	0.5854	0.5965	8805	1997	3992
2.940	1	0.7	1	1.5714	0.3	0.4496	0.4432	6620	1096	2263	6.000	1	7.5	1	1.7000	0.5	0.4472	0.4475	7212	2034	3873
2.940	1	0.7	1	1.5714	0.5	0.3163	0.2935	5159	1206	2226	6.000	1	7.5	1	1.7000	0.7	0.3692	0.3648	5738	2069	3813
2.940	1	0.7	1	1.5714	0.7	0.2433	0.2124	4527	1303	2233	6.000	1	7.5	1	1.8000	1	0.2985	0.2914	11510	1932	4188
2.940	1	0.7	1	1.7143	1	0.1871	0.1488	4047	1443	2210	6.000	1	7.5	1	1.8000	0.3	0.5854	0.5965	8805	1997	3992
2.940	1	0.7	1	1.7143	0.3	0.4540	0.4483	6646	1096	2256	6.000	1	7.5	1	1.8000	0.5	0.4472	0.4475	7212	2034	3873
2.940	1	0.7	1	1.7143	0.5	0.3220	0.3002	5144	1204	2219	6.000	1	7.5	1	1.8000	0.7	0.3692	0.3648	5641	1944	3604
2.940	1	0.7	1	1.7143	0.7	0.2496	0.2204	4451	1296	2234	5.217	1	5	1	1.3000	1	0.2836	0.2774	10880	1826	3978
2.940	1	0.7	1	1.8571	1	0.1917	0.1554	3951	1432	2212	5.217	1	5	1	1.3000	0.3	0.5556	0.5674	8334	1883	3779
2.940	1	0.7	1	1.8571	0.3	0.4563	0.4512	6650	1096	2253	5.217	1	5	1	1.3000	0.5	0.4245	0.4256	6839	1914	3665
2.940	1	0.7	1	1.8571	0.5	0.3256	0.3047	5130	1203	2214	5.217	1	5	1	1.3000	0.7	0.3505	0.3470	5641	1944	3604
2.940	1	0.7	1	1.8571	0.7	0.2538	0.2259	4401	1292	2233	5.217	1	5	1	1.4000	1	0.2836	0.2774	10880	1826	3978
2.940	1	0.7	1	2.0000	1	0.1949	0.1600	3883	1426	2214	5.217	1	5	1	1.4000	0.3	0.5556	0.5674	8334	1883	3779
2.940	1	0.7	1	2.0000	0.3	0.4577	0.4531	6648	1096	2252	5.217	1	5	1	1.4000	0.5	0.4245	0.4256	6839	1914	3665
2.940	1	0.7	1	2.0000	0.5	0.3280	0.3079	5121	1203	2211	5.217	1	5	1	1.4000	0.7	0.3505	0.3470	5641	1944	3604
2.940	1	0.7	1	2.0000	0.7	0.2567	0.2298	4370	1288	2232	5.217	1	5	1	1.5000	1	0.2836	0.2774	10880	1826	3978
2.940	1	0.7	1	2.1429	1	0.1971	0.1634	3832	1420	2217	5.217	1	5	1	1.5000	0.3	0.5556	0.5674	8334	1883	3779
2.940	1	0.7	1	2.1429	0.3	0.4590	0.4548	6646	1099	2251	5.217	1	5	1	1.5000	0.5	0.4245	0.4256	6839	1914	3665
2.940	1	0.7	1	2.1429	0.5	0.3297	0.3101	5116	1202	2209	5.217	1	5	1	1.5000	0.7	0.3505	0.3470	5641	1944	3604
2.940	1	0.7	1	2.1429	0.7	0.2588	0.2327	4346	1286	2232	5.217	1	5	1	1.6000	1	0.2836	0.2774	10880	1826	3978
2.940	1	7.5	1	1.4286	1	0.1581	0.1500	2123	823	1829	5.217	1	5	1	1.6000	0.3	0.5556	0.5674	8334	1883	3779
2.940	1	7.5	1	1.4286	0.3	0.2913	0.2927	3551	843	2035	5.217	1	5	1	1.6000	0.5	0.4245	0.4256	6839	1914	3665
2.940	1	7.5	1	1.4286	0.5	0.2289	0.2266	2822	801	1968	5.217	1	5	1	1.6000	0.7	0.3505	0.3470	5641	1944	3604
2.940	1	7.5	1	1.4286	0.7	0.1932	0.1877	2504	768	1907	5.217	1	5	1	1.7000	1	0.2836	0.2774	10880	1826	3978
2.940	1	7.5	1	1.5714	1	0.1614	0.1542	2126	844	1832	5.217	1	5	1	1.7000	0.3	0.5556	0.5674	8334	1883	3779
2.940	1	7.5	1	1.5714	0.3	0.2904	0.2921	3504	848	2044	5.217	1	5	1	1.7000	0.5	0.4245	0.4256	6839	1914	3665
2.940	1	7.5	1	1.5714	0.5	0.2326	0.2304	2829	800	1962	5.217	1	5	1	1.7000	0.7	0.3505	0.3470	5641	1944	3604
2.940	1	7.5	1	1.5714	0.7	0.1960	0.1912	2508	802	1909	5.217	1	5	1	1.8000	1	0.2836	0.2774	10880	1826	3978
2.940	1	7.5	1	1.7143	1	0.1630	0.1564	2126	858	1840	5.217	1	5	1	1.8000	0.3	0.5556	0.5674	8334	1883	3779
2.940	1	7.5	1	1.7143	0.3	0.2889	0.2908	3461	853	2059	5.217	1	5	1	1.8000	0.5	0.4245	0.4256	6839	1914	3665
2.940	1	7.5	1	1.7143	0.5	0.2341	0.2315	2838	815	1957	5.217	1	5	1	1.8000	0.7	0.3505	0.3470	3817	1941	2941
2.940	1	7.5	1	1.7143	0.7	0.1973	0.1931	2509	822	1915	5.217	0.3	0.7	0.7	1.3000	1	0.0493	0.0431	9148	1504	2918
2.940	1	7.5	1	1.8571	1	0.1639	0.1577	2126	872	1848	5.217	0.3	0.7	0.7	1.3000	0.3	0.4504	0.4520	5388	1652	2909
2.940	1	7.5	1	1.8571	0.3	0.2873	0.2894	3422	858	2074	5.217	0.3	0.7	0.7	1.3000	0.5	0.2525	0.2454	4703	1784	2935
2.940	1	7.5	1	1.8571	0.5	0.2339	0.2314	2824	831	1963	5.217	0.3	0.7	0.7	1.3000	0.7	0.1453	0.1384	3892	1923	2933
2.940	1	7.5	1	1.8571	0.7	0.1976	0.1939	2509	841	1926	5.217	0.3	0.7	0.7	1.4000	1	0.0828	0.0690	9673	1493	2917
2.940	1	7.5	1	2.0000	1	0.1642	0.1585	2125	884	1859	5.217	0.3	0.7	0.7	1.4000	0.3	0.4712	0.4716	5842	1634	2906
2.940	1	7.5	1	2.0000	0.3	0.2874	0.2894	3413	860	2080	5.217	0.3	0.7	0.7	1.4000	0.5	0.2766	0.2662	4762	1767	2931
2.940	1	7.5	1	2.0000	0.5	0.2334	0.2312	2800	843	1972	5.217	0.3	0.7	0.7	1.4000	0.7	0.1747	0.1624	3936	1910	2930

ODTh	alfa	Eback	beta	TWOD	Ewall	δy(%)	δx(%)	M(lb-in)	V (lb)	Th (lb)	ODTh	alfa	Eback	beta	TWOD	Ewall	δy(%)	δx(%)	M(lb-in)	V (lb)	Th (lb)
2.940	1	7.5	1	2.0000	0.7	0.1977	0.1942	2509	854	1929	5.217	0.3	0.7	0.7	1.5000	1	0.1030	0.0852	10000	1488	2914
2.940	1	7.5	1	2.1429	1	0.1644	0.1591	2124	894	1867	5.217	0.3	0.7	0.7	1.5000	0.3	0.4844	0.4840	6225	1623	2904
2.940	1	7.5	1	2.1429	0.3	0.2868	0.2887	3412	863	2088	5.217	0.3	0.7	0.7	1.5000	0.5	0.2912	0.2790	4798	1754	2930
2.940	1	7.5	1	2.1429	0.5	0.2335	0.2313	2794	863	1978	5.217	0.3	0.7	0.7	1.5000	0.7	0.1921	0.1773	3965	1899	2931
2.940	1	7.5	1	2.1429	0.7	0.1996	0.1954	2516	887	1911	5.217	0.3	0.7	0.7	1.6000	1	0.1163	0.0967	10230	1486	2910
2.940	1	5	1	1.4286	1	0.1430	0.1281	2337	669	1592	5.217	0.3	0.7	0.7	1.6000	0.3	0.4935	0.4927	6491	1615	2903
2.940	1	5	1	1.4286	0.3	0.2945	0.2946	3880	711	1727	5.217	0.3	0.7	0.7	1.6000	0.5	0.3012	0.2878	4821	1745	2928
2.940	1	5	1	1.4286	0.5	0.2268	0.2198	3184	665	1665	5.217	0.3	0.7	0.7	1.6000	0.7	0.2036	0.1874	3985	1892	2930
2.940	1	5	1	1.4286	0.7	0.1848	0.1740	2747	634	1618	5.217	0.3	0.7	0.7	1.7000	1	0.1259	0.1049	10390	1483	2910
2.940	1	5	1	1.5714	1	0.1509	0.1369	2351	689	1579	5.217	0.3	0.7	0.7	1.7000	0.3	0.5001	0.4990	6684	1609	2902
2.940	1	5	1	1.5714	0.3	0.2970	0.2976	3858	716	1737	5.217	0.3	0.7	0.7	1.7000	0.5	0.3085	0.2943	4838	1737	2928
2.940	1	5	1	1.5714	0.5	0.2313	0.2249	3167	669	1669	5.217	0.3	0.7	0.7	1.7000	0.7	0.2119	0.1947	4001	1899	2928
2.940	1	5	1	1.5714	0.7	0.1908	0.1806	2742	637	1616	5.217	0.3	0.7	0.7	1.8000	1	0.1333	0.1119	10510	1481	2909
2.940	1	5	1	1.7143	1	0.1551	0.1419	2336	709	1579	5.217	0.3	0.7	0.7	1.8000	0.3	0.5051	0.5039	6833	1606	2901
2.940	1	5	1	1.7143	0.3	0.2977	0.2985	3836	721	1749	5.217	0.3	0.7	0.7	1.8000	0.5	0.3140	0.2991	4961	1732	2927
2.940	1	5	1	1.7143	0.5	0.2332	0.2271	3149	674	1676	5.217	0.3	0.7	0.7	1.8000	0.7	0.2181	0.2002	3681	1284	2497
2.940	1	5	1	1.7143	0.7	0.1938	0.1842	2724	646	1621	5.217	0.3	7.5	0.7	1.3000	1	0.1704	0.1687	7554	1151	2836
2.940	1	5	1	1.8571	1	0.1576	0.1452	2310	724	1583	5.217	0.3	7.5	0.7	1.3000	0.3	0.4045	0.4129	5654	1198	2647
2.940	1	5	1	1.8571	0.3	0.2998	0.2999	3872	720	1746	5.217	0.3	7.5	0.7	1.3000	0.5	0.2924	0.2929	4588	1240	2547
2.940	1	5	1	1.8571	0.5	0.2342	0.2284	3127	678	1684	5.217	0.3	7.5	0.7	1.3000	0.7	0.2288	0.2268	3723	1287	2481
2.940	1	5	1	1.8571	0.7	0.1955	0.1865	2701	667	1626	5.217	0.3	7.5	0.7	1.4000	1	0.1803	0.1766	7644	1143	2848
2.940	1	5	1	2.0000	1	0.1591	0.1473	2288	740	1587	5.217	0.3	7.5	0.7	1.4000	0.3	0.4090	0.4172	5779	1196	2655
2.940	1	5	1	2.0000	0.3	0.2990	0.2992	3834	725	1756	5.217	0.3	7.5	0.7	1.4000	0.5	0.2993	0.2992	4713	1238	2555
2.940	1	5	1	2.0000	0.5	0.2348	0.2294	3100	681	1689	5.217	0.3	7.5	0.7	1.4000	0.7	0.2368	0.2339	3790	1288	2477
2.940	1	5	1	2.0000	0.7	0.1965	0.1879	2679	688	1631	5.217	0.3	7.5	0.7	1.5000	1	0.1860	0.1816	7703	1139	2858
2.940	1	5	1	2.1429	1	0.1602	0.1490	2266	752	1592	5.217	0.3	7.5	0.7	1.5000	0.3	0.4120	0.4200	5855	1197	2660
2.940	1	5	1	2.1429	0.3	0.2983	0.2985	3800	728	1764	5.217	0.3	7.5	0.7	1.5000	0.5	0.3035	0.3030	4801	1245	2555
2.940	1	5	1	2.1429	0.5	0.2350	0.2298	3071	684	1694	5.217	0.3	7.5	0.7	1.5000	0.7	0.2418	0.2383	3872	1287	2480
2.940	1	5	1	2.1429	0.7	0.1972	0.1889	2659	708	1636	5.217	0.3	7.5	0.7	1.6000	1	0.1898	0.1850	7751	1135	2864
2.940	1	0.7	0	1.4286	1	0.2615	0.2443	5239	1236	2017	5.217	0.3	7.5	0.7	1.6000	0.3	0.4141	0.4219	5898	1197	2663
2.940	1	0.7	0	1.4286	0.3	0.4800	0.5094	7811	866	2279	5.217	0.3	7.5	0.7	1.6000	0.5	0.3064	0.3056	4855	1245	2558
2.940	1	0.7	0	1.4286	0.5	0.3772	0.3823	6590	949	2148	5.217	0.3	7.5	0.7	1.6000	0.7	0.2451	0.2412	3925	1288	2484
2.940	1	0.7	0	1.4286	0.7	0.3183	0.3106	5929	1086	2083	5.217	0.3	7.5	0.7	1.7000	1	0.1925	0.1873	7786	1132	2866
2.940	1	0.7	0	1.5714	1	0.2610	0.2453	5178	1228	2018	5.217	0.3	7.5	0.7	1.7000	0.3	0.4156	0.4232	5928	1197	2665
2.940	1	0.7	0	1.5714	0.3	0.4797	0.5101	7776	868	2282	5.217	0.3	7.5	0.7	1.7000	0.5	0.3085	0.3074	4895	1246	2563
2.940	1	0.7	0	1.5714	0.5	0.3764	0.3827	6534	947	2151	5.217	0.3	7.5	0.7	1.7000	0.7	0.2474	0.2434	3962	1290	2486
2.940	1	0.7	0	1.5714	0.7	0.3176	0.3113	5871	1081	2086	5.217	0.3	7.5	0.7	1.8000	1	0.1946	0.1891	7794	1130	2869
2.940	1	0.7	0	1.7143	1	0.2605	0.2459	5132	1223	2021	5.217	0.3	7.5	0.7	1.8000	0.3	0.4166	0.4242	5963	1198	2664
2.940	1	0.7	0	1.7143	0.3	0.4793	0.5104	7743	869	2283	5.217	0.3	7.5	0.7	1.8000	0.5	0.3102	0.3089	4919	1247	2561
2.940	1	0.7	0	1.7143	0.5	0.3757	0.3830	6490	946	2154	5.217	0.3	7.5	0.7	1.8000	0.7	0.2492	0.2449	3163	1169	2223
2.940	1	0.7	0	1.7143	0.7	0.3169	0.3117	5822	1079	2090	5.217	0.3	5	0.7	1.3000	1	0.1154	0.1168	7164	1062	2401
2.940	1	0.7	0	1.8571	1	0.2601	0.2463	5094	1218	2024	5.217	0.3	5	0.7	1.3000	0.3	0.3666	0.3740	4884	1077	2298
2.940	1	0.7	0	1.8571	0.3	0.4789	0.5106	7717	870	2283	5.217	0.3	5	0.7	1.3000	0.5	0.2440	0.2455	4096	1097	2255
2.940	1	0.7	0	1.8571	0.5	0.3751	0.3832	6453	946	2155	5.217	0.3	5	0.7	1.3000	0.7	0.1767	0.1777	3243	1159	2221
2.940	1	0.7	0	1.8571	0.7	0.3164	0.3121	5786	1077	2092	5.217	0.3	5	0.7	1.4000	1	0.1343	0.1330	7387	1031	2397
2.940	1	0.7	0	2.0000	1	0.2597	0.2467	5063	1215	2025	5.217	0.3	5	0.7	1.4000	0.3	0.3797	0.3859	5203	1042	2308
2.940	1	0.7	0	2.0000	0.3	0.4787	0.5108	7695	871	2283	5.217	0.3	5	0.7	1.4000	0.5	0.2592	0.2593	4176	1088	2261

ODTh	alfa	Eback	beta	TWOD	Ewall	δy(%)	δx(%)	M(lb-in)	V (lb)	Th (lb)	ODTh	alfa	Eback	beta	TWOD	Ewall	δy(%)	δx(%)	M(lb-in)	V (lb)	Th (lb)
2.940	1	0.7	0	2.0000	0.5	0.3745	0.3832	6420	947	2157	5.217	0.3	5	0.7	1.4000	0.7	0.1933	0.1920	3292	1153	2224
2.940	1	0.7	0	2.0000	0.7	0.3159	0.3123	5754	1075	2094	5.217	0.3	5	0.7	1.5000	1	0.1459	0.1430	7541	1014	2402
2.940	1	0.7	0	2.1429	1	0.2594	0.2469	5037	1213	2027	5.217	0.3	5	0.7	1.5000	0.3	0.3875	0.3932	5413	1042	2311
2.940	1	0.7	0	2.1429	0.3	0.4783	0.5107	7675	872	2283	5.217	0.3	5	0.7	1.5000	0.5	0.2690	0.2682	4224	1092	2257
2.940	1	0.7	0	2.1429	0.5	0.3740	0.3832	6393	947	2158	5.217	0.3	5	0.7	1.5000	0.7	0.2042	0.2014	3326	1154	2222
2.940	1	0.7	0	2.1429	0.7	0.3155	0.3124	5727	1074	2096	5.217	0.3	5	0.7	1.6000	1	0.1542	0.1501	7627	1005	2407
2.940	1	7.5	0	1.4286	1	0.1752	0.1678	2639	779	1816	5.217	0.3	5	0.7	1.6000	0.3	0.3925	0.3979	5567	1052	2306
2.940	1	7.5	0	1.4286	0.3	0.2958	0.2975	3894	866	2075	5.217	0.3	5	0.7	1.6000	0.5	0.2759	0.2744	4337	1094	2261
2.940	1	7.5	0	1.4286	0.5	0.2427	0.2397	3303	805	1942	5.217	0.3	5	0.7	1.6000	0.7	0.2115	0.2079	3351	1159	2220
2.940	1	7.5	0	1.4286	0.7	0.2085	0.2032	2965	773	1881	5.217	0.3	5	0.7	1.7000	1	0.1600	0.1551	7675	999.5	2414
2.940	1	7.5	0	1.5714	1	0.1744	0.1680	2570	802	1826	5.217	0.3	5	0.7	1.7000	0.3	0.3958	0.4012	5646	1058	2307
2.940	1	7.5	0	1.5714	0.3	0.2938	0.2957	3815	870	2087	5.217	0.3	5	0.7	1.7000	0.5	0.2807	0.2785	4449	1099	2266
2.940	1	7.5	0	1.5714	0.5	0.2413	0.2387	3227	809	1954	5.217	0.3	5	0.7	1.7000	0.7	0.2167	0.2125	3411	1160	2223
2.940	1	7.5	0	1.5714	0.7	0.2074	0.2028	2893	779	1892	5.217	0.3	5	0.7	1.8000	1	0.1645	0.1591	7713	1001	2424
2.940	1	7.5	0	1.7143	1	0.1737	0.1679	2517	819	1837	5.217	0.3	5	0.7	1.8000	0.3	0.3981	0.4036	5704	1070	2299
2.940	1	7.5	0	1.7143	0.3	0.2922	0.2943	3757	873	2097	5.217	0.3	5	0.7	1.8000	0.5	0.2845	0.2817	4530	1102	2270
2.940	1	7.5	0	1.7143	0.5	0.2400	0.2378	3168	813	1964	5.217	0.3	5	0.7	1.8000	0.7	0.2205	0.2159	6699	1913	3037
2.940	1	7.5	0	1.7143	0.7	0.2062	0.2022	2832	794	1901	5.217	0.5	0.7	0.5	1.3000	1	0.2027	0.1585	11920	1466	3030
2.940	1	7.5	0	1.8571	1	0.1730	0.1677	2472	833	1845	5.217	0.5	0.7	0.5	1.3000	0.3	0.5421	0.5368	8768	1593	3027
2.940	1	7.5	0	1.8571	0.3	0.2907	0.2930	3707	876	2105	5.217	0.5	0.7	0.5	1.3000	0.5	0.3637	0.3386	7437	1738	3060
2.940	1	7.5	0	1.8571	0.5	0.2389	0.2370	3122	816	1973	5.217	0.5	0.7	0.5	1.3000	0.7	0.2765	0.2426	6555	1895	3039
2.940	1	7.5	0	1.8571	0.7	0.2055	0.2018	2793	809	1907	5.217	0.5	0.7	0.5	1.4000	1	0.2096	0.1672	11990	1462	3017
2.940	1	7.5	0	2.0000	1	0.1724	0.1675	2437	844	1852	5.217	0.5	0.7	0.5	1.4000	0.3	0.5482	0.5438	8821	1585	3009
2.940	1	7.5	0	2.0000	0.3	0.2894	0.2918	3665	878	2111	5.217	0.5	0.7	0.5	1.4000	0.5	0.3701	0.3456	7411	1727	3048
2.940	1	7.5	0	2.0000	0.5	0.2380	0.2363	3086	818	1979	5.217	0.5	0.7	0.5	1.4000	0.7	0.2832	0.2506	6474	1885	3039
2.940	1	7.5	0	2.0000	0.7	0.2048	0.2013	2757	821	1913	5.217	0.5	0.7	0.5	1.5000	1	0.2139	0.1726	12020	1460	3009
2.940	1	7.5	0	2.1429	1	0.1719	0.1673	2407	853	1859	5.217	0.5	0.7	0.5	1.5000	0.3	0.5521	0.5484	8849	1579	2997
2.940	1	7.5	0	2.1429	0.3	0.2884	0.2909	3634	880	2117	5.217	0.5	0.7	0.5	1.5000	0.5	0.3742	0.3502	7398	1719	3039
2.940	1	7.5	0	2.1429	0.5	0.2373	0.2357	3056	820	1986	5.217	0.5	0.7	0.5	1.5000	0.7	0.2874	0.2557	6411	1878	3037
2.940	1	7.5	0	2.1429	0.7	0.2042	0.2009	2726	831	1920	5.217	0.5	0.7	0.5	1.6000	1	0.2168	0.1768	12040	1458	3003
2.940	1	5	0	1.4286	1	0.1773	0.1654	3133	628	1562	5.217	0.5	0.7	0.5	1.6000	0.3	0.5549	0.5518	8865	1576	2989
2.940	1	5	0	1.4286	0.3	0.3082	0.3117	4565	740	1755	5.217	0.5	0.7	0.5	1.6000	0.5	0.3770	0.3535	7389	1713	3032
2.940	1	5	0	1.4286	0.5	0.2496	0.2458	3849	683	1645	5.217	0.5	0.7	0.5	1.6000	0.7	0.2902	0.2591	6365	1872	3036
2.940	1	5	0	1.4286	0.7	0.2123	0.2044	3468	656	1605	5.217	0.5	0.7	0.5	1.7000	1	0.2190	0.1799	12060	1457	2999
2.557	1	5	0	1.5714	1	0.1768	0.1664	3062	633	1570	5.217	0.5	0.7	0.5	1.7000	0.3	0.5568	0.5540	8874	1573	2984
2.557	1	5	0	1.5714	0.3	0.3059	0.3098	4481	746	1772	5.217	0.5	0.7	0.5	1.7000	0.5	0.3790	0.3559	7381	1709	3026
2.557	1	5	0	1.5714	0.5	0.2485	0.2455	3812	688	1656	5.217	0.5	0.7	0.5	1.7000	0.7	0.2922	0.2617	6329	1867	3034
2.557	1	5	0	1.5714	0.7	0.2116	0.2050	3418	661	1614	5.217	0.5	0.7	0.5	1.8000	1	0.2207	0.1823	12070	1456	2997
2.557	1	5	0	1.7143	1	0.1762	0.1669	3013	637	1578	5.217	0.5	0.7	0.5	1.8000	0.3	0.5583	0.5559	8884	1571	2979
2.557	1	5	0	1.7143	0.3	0.3038	0.3080	4404	750	1785	5.217	0.5	0.7	0.5	1.8000	0.5	0.3805	0.3576	7373	1706	3023
2.557	1	5	0	1.7143	0.5	0.2472	0.2449	3752	692	1667	5.217	0.5	0.7	0.5	1.8000	0.7	0.2938	0.2636	4095	1298	2551
2.557	1	5	0	1.7143	0.7	0.2109	0.2052	3378	664	1622	5.217	0.5	7.5	0.5	1.3000	1	0.2002	0.1896	8078	1133	2848
2.557	1	5	0	1.8571	1	0.1756	0.1671	2967	640	1586	5.217	0.5	7.5	0.5	1.3000	0.3	0.4233	0.4284	6209	1204	2672
2.557	1	5	0	1.8571	0.3	0.3018	0.3062	4339	754	1795	5.217	0.5	7.5	0.5	1.3000	0.5	0.3161	0.3115	5119	1248	2583
2.557	1	5	0	1.8571	0.5	0.2458	0.2440	3685	697	1677	5.217	0.5	7.5	0.5	1.3000	0.7	0.2553	0.2467	4113	1297	2525
2.557	1	5	0	1.8571	0.7	0.2099	0.2048	3318	668	1632	5.217	0.5	7.5	0.5	1.4000	1	0.2035	0.1930	8074	1131	2848
2.557	1	5	0	2.0000	1	0.1749	0.1672	2920	644	1594	5.217	0.5	7.5	0.5	1.4000	0.3	0.4244	0.4299	6210	1206	2668

ODTh	alfa	Eback	beta	TWOD	Ewall	δy(%)	δx(%)	M(lb-in)	V(lb)	Th(lb)	ODTh	alfa	Eback	beta	TWOD	Ewall	δy(%)	δx(%)	M(lb-in)	V(lb)	Th(lb)
2.557	1	5	0	2.0000	0.3	0.3000	0.3046	4278	758	1806	5.217	0.5	7.5	0.5	1.4000	0.5	0.3181	0.3138	5113	1247	2580
2.557	1	5	0	2.0000	0.5	0.2446	0.2431	3630	700	1687	5.217	0.5	7.5	0.5	1.4000	0.7	0.2576	0.2493	4101	1298	2520
2.557	1	5	0	2.0000	0.7	0.2090	0.2045	3267	672	1640	5.217	0.5	7.5	0.5	1.5000	1	0.2052	0.1950	8070	1133	2850
2.557	1	0.7	1	1.4286	1	0.1966	0.1999	2482	1271	2315	5.217	0.5	7.5	0.5	1.5000	0.3	0.4251	0.4306	6200	1207	2668
2.557	1	0.7	1	1.4286	0.3	0.3300	0.3425	3015	1259	2583	5.217	0.5	7.5	0.5	1.5000	0.5	0.3191	0.3151	5107	1253	2577
2.557	1	0.7	1	1.4286	0.5	0.2702	0.2780	2842	1256	2479	5.217	0.5	7.5	0.5	1.5000	0.7	0.2590	0.2510	4093	1298	2517
2.557	1	0.7	1	1.4286	0.7	0.2327	0.2380	2691	1259	2405	5.217	0.5	7.5	0.5	1.6000	1	0.2063	0.1964	8064	1134	2855
2.557	1	0.7	1	1.5714	1	0.1966	0.1999	2482	1271	2315	5.217	0.5	7.5	0.5	1.6000	0.3	0.4254	0.4311	6195	1207	2669
2.557	1	0.7	1	1.5714	0.3	0.3300	0.3425	3015	1259	2583	5.217	0.5	7.5	0.5	1.6000	0.5	0.3199	0.3160	5096	1253	2577
2.557	1	0.7	1	1.5714	0.5	0.2702	0.2780	2842	1256	2479	5.217	0.5	7.5	0.5	1.6000	0.7	0.2599	0.2521	4081	1298	2517
2.557	1	0.7	1	1.5714	0.7	0.2327	0.2380	2691	1259	2405	5.217	0.5	7.5	0.5	1.7000	1	0.2070	0.1974	8052	1134	2858
2.557	1	0.7	1	1.7143	1	0.1966	0.1999	2482	1271	2315	5.217	0.5	7.5	0.5	1.7000	0.3	0.4256	0.4314	6194	1207	2669
2.557	1	0.7	1	1.7143	0.3	0.3300	0.3425	3015	1259	2583	5.217	0.5	7.5	0.5	1.7000	0.5	0.3204	0.3166	5086	1254	2578
2.557	1	0.7	1	1.7143	0.5	0.2702	0.2780	2842	1256	2479	5.217	0.5	7.5	0.5	1.7000	0.7	0.2605	0.2529	4072	1298	2519
2.557	1	0.7	1	1.7143	0.7	0.2327	0.2380	2691	1259	2405	5.217	0.5	7.5	0.5	1.8000	1	0.2076	0.1981	8053	1135	2860
2.557	1	0.7	1	1.8571	1	0.1966	0.1999	2482	1271	2315	5.217	0.5	7.5	0.5	1.8000	0.3	0.4257	0.4315	6190	1205	2669
2.557	1	0.7	1	1.8571	0.3	0.3300	0.3425	3015	1259	2583	5.217	0.5	7.5	0.5	1.8000	0.5	0.3208	0.3170	5079	1254	2578
2.557	1	0.7	1	1.8571	0.5	0.2702	0.2780	2842	1256	2479	5.217	0.5	7.5	0.5	1.8000	0.7	0.2610	0.2535	4130	1132	2302
2.557	1	0.7	1	1.8571	0.7	0.2327	0.2380	2691	1259	2405	5.217	0.5	5	0.5	1.3000	1	0.1766	0.1609	8120	956.9	2453
2.557	1	0.7	1	2.0000	1	0.1966	0.1999	2482	1271	2315	5.217	0.5	5	0.5	1.3000	0.3	0.4060	0.4083	6080	1023	2361
2.557	1	0.7	1	2.0000	0.3	0.3300	0.3425	3015	1259	2583	5.217	0.5	5	0.5	1.3000	0.5	0.2931	0.2855	5028	1073	2318
2.557	1	0.7	1	2.0000	0.5	0.2702	0.2780	2842	1256	2479	5.217	0.5	5	0.5	1.3000	0.7	0.2315	0.2193	4133	1138	2281
2.557	1	0.7	1	2.0000	0.7	0.2327	0.2380	2691	1259	2405	5.217	0.5	5	0.5	1.4000	1	0.1825	0.1678	8178	975	2446
2.557	1	0.7	1	2.1429	1	0.1966	0.1999	2482	1271	2315	5.217	0.5	5	0.5	1.4000	0.3	0.4100	0.4125	6138	1031	2344
2.557	1	0.7	1	2.1429	0.3	0.3300	0.3425	3015	1259	2583	5.217	0.5	5	0.5	1.4000	0.5	0.2977	0.2906	5047	1082	2307
2.557	1	0.7	1	2.1429	0.5	0.2702	0.2780	2842	1256	2479	5.217	0.5	5	0.5	1.4000	0.7	0.2365	0.2249	4127	1144	2274
2.557	1	0.7	1	2.1429	0.7	0.2327	0.2380	2691	1259	2405	5.217	0.5	5	0.5	1.5000	1	0.1859	0.1718	8169	980.6	2449
2.557	1	7.5	1	1.4286	1	0.1685	0.1668	1850	1106	2048	5.217	0.5	5	0.5	1.5000	0.3	0.4117	0.4145	6144	1037	2340
2.557	1	7.5	1	1.4286	0.3	0.2753	0.2771	2488	1072	2251	5.217	0.5	5	0.5	1.5000	0.5	0.3004	0.2938	5074	1090	2292
2.557	1	7.5	1	1.4286	0.5	0.2283	0.2278	2258	1086	2145	5.217	0.5	5	0.5	1.5000	0.7	0.2397	0.2285	4125	1152	2266
2.557	1	7.5	1	1.4286	0.7	0.1981	0.1968	2061	1095	2103	5.217	0.5	5	0.5	1.6000	1	0.1883	0.1749	8151	987.9	2453
2.557	1	7.5	1	1.5714	1	0.1685	0.1668	1850	1106	2048	5.217	0.5	5	0.5	1.6000	0.3	0.4127	0.4158	6144	1045	2339
2.557	1	7.5	1	1.5714	0.3	0.2753	0.2771	2488	1072	2251	5.217	0.5	5	0.5	1.6000	0.5	0.3022	0.2960	5072	1093	2287
2.557	1	7.5	1	1.5714	0.5	0.2283	0.2278	2258	1086	2145	5.217	0.5	5	0.5	1.6000	0.7	0.2417	0.2309	4125	1158	2256
2.557	1	7.5	1	1.5714	0.7	0.1981	0.1968	2061	1095	2103	5.217	0.5	5	0.5	1.7000	1	0.1901	0.1770	8139	998.9	2456
2.557	1	7.5	1	1.7143	1	0.1685	0.1668	1850	1106	2048	5.217	0.5	5	0.5	1.7000	0.3	0.4137	0.4170	6159	1054	2330
2.557	1	7.5	1	1.7143	0.3	0.2753	0.2771	2488	1072	2251	5.217	0.5	5	0.5	1.7000	0.5	0.3039	0.2975	5061	1098	2286
2.557	1	7.5	1	1.7143	0.5	0.2283	0.2278	2258	1086	2145	5.217	0.5	5	0.5	1.7000	0.7	0.2431	0.2327	4111	1160	2253
2.557	1	7.5	1	1.7143	0.7	0.1981	0.1968	2061	1095	2103	5.217	0.5	5	0.5	1.8000	1	0.1913	0.1786	8119	1003	2461
2.557	1	7.5	1	1.8571	1	0.1685	0.1668	1850	1106	2048	5.217	0.5	5	0.5	1.8000	0.3	0.4139	0.4173	6169	1062	2326
2.557	1	7.5	1	1.8571	0.3	0.2753	0.2771	2488	1072	2251	5.217	0.5	5	0.5	1.8000	0.5	0.3050	0.2987	5045	1100	2286
2.557	1	7.5	1	1.8571	0.5	0.2283	0.2278	2258	1086	2145	5.217	0.5	5	0.5	1.8000	0.7	0.2441	0.2340	9313	1987	3288
2.557	1	7.5	1	1.8571	0.7	0.1981	0.1968	2061	1095	2103	5.217	0.7	0.7	0.3	1.3000	1	0.3419	0.3247	16120	1595	3568
2.557	1	7.5	1	2.0000	1	0.1685	0.1668	1850	1106	2048	5.217	0.7	0.7	0.3	1.3000	0.3	0.7558	0.8066	12550	1736	3433
2.557	1	7.5	1	2.0000	0.3	0.2753	0.2771	2488	1072	2251	5.217	0.7	0.7	0.3	1.3000	0.5	0.5428	0.5583	10810	1816	3372
2.557	1	7.5	1	2.0000	0.5	0.2283	0.2278	2258	1086	2145	5.217	0.7	0.7	0.3	1.3000	0.7	0.4349	0.4331	9258	1981	3289
2.557	1	7.5	1	2.0000	0.7	0.1981	0.1968	2061	1095	2103	5.217	0.7	0.7	0.3	1.4000	1	0.3419	0.3261	16100	1596	3571

ODTh	alfa	Eback	beta	TWOD	Ewall	δy(%)	δx(%)	M(lb-in)	V (lb)	Th (lb)	ODTh	alfa	Eback	beta	TWOD	Ewall	δy(%)	δx(%)	M(lb-in)	V (lb)	Th (lb)
2.557	1	7.5	1	2.1429	1	0.1685	0.1668	1850	1106	2048	5.217	0.7	0.7	0.3	1.4000	0.3	0.7561	0.8079	12530	1733	3429
2.557	1	7.5	1	2.1429	0.3	0.2753	0.2771	2488	1072	2251	5.217	0.7	0.7	0.3	1.4000	0.5	0.5437	0.5607	10780	1813	3371
2.557	1	7.5	1	2.1429	0.5	0.2283	0.2278	2258	1086	2145	5.217	0.7	0.7	0.3	1.4000	0.7	0.4352	0.4346	9206	1976	3291
2.557	1	7.5	1	2.1429	0.7	0.1981	0.1968	2061	1095	2103	5.217	0.7	0.7	0.3	1.5000	1	0.3419	0.3272	16090	1594	3569
2.557	1	5	1	1.4286	1	0.1610	0.1598	1810	1051	1949	5.217	0.7	0.7	0.3	1.5000	0.3	0.7565	0.8088	12510	1731	3426
2.557	1	5	1	1.4286	0.3	0.2623	0.2645	2448	1022	2146	5.217	0.7	0.7	0.3	1.5000	0.5	0.5440	0.5618	10740	1813	3372
2.557	1	5	1	1.4286	0.5	0.2178	0.2177	2212	1034	2048	5.217	0.7	0.7	0.3	1.5000	0.7	0.4353	0.4357	9161	1971	3294
2.557	1	5	1	1.4286	0.7	0.1891	0.1883	2015	1041	2004	5.217	0.7	0.7	0.3	1.6000	1	0.3418	0.3279	16090	1592	3567
2.557	1	5	1	1.5714	1	0.1610	0.1598	1810	1051	1949	5.217	0.7	0.7	0.3	1.6000	0.3	0.7568	0.8095	12500	1730	3424
2.557	1	5	1	1.5714	0.3	0.2623	0.2645	2448	1022	2146	5.217	0.7	0.7	0.3	1.6000	0.5	0.5443	0.5628	10720	1816	3372
2.557	1	5	1	1.5714	0.5	0.2178	0.2177	2212	1034	2048	5.217	0.7	0.7	0.3	1.6000	0.7	0.4354	0.4367	9125	1967	3297
2.557	1	5	1	1.5714	0.7	0.1891	0.1883	2015	1041	2004	5.217	0.7	0.7	0.3	1.7000	1	0.3417	0.3286	16080	1591	3567
2.557	1	5	1	1.7143	1	0.1610	0.1598	1810	1051	1949	5.217	0.7	0.7	0.3	1.7000	0.3	0.7570	0.8101	12490	1728	3421
2.557	1	5	1	1.7143	0.3	0.2623	0.2645	2448	1022	2146	5.217	0.7	0.7	0.3	1.7000	0.5	0.5445	0.5635	10690	1817	3373
2.557	1	5	1	1.7143	0.5	0.2178	0.2177	2212	1034	2048	5.217	0.7	0.7	0.3	1.7000	0.7	0.4354	0.4374	9108	1965	3296
2.557	1	5	1	1.7143	0.7	0.1891	0.1883	2015	1041	2004	5.217	0.7	0.7	0.3	1.8000	1	0.3417	0.3291	16080	1589	3565
2.557	1	5	1	1.8571	1	0.1610	0.1598	1810	1051	1949	5.217	0.7	0.7	0.3	1.8000	0.3	0.7572	0.8105	12480	1728	3420
2.557	1	5	1	1.8571	0.3	0.2623	0.2645	2448	1022	2146	5.217	0.7	0.7	0.3	1.8000	0.5	0.5447	0.5641	10670	1815	3374
2.557	1	5	1	1.8571	0.5	0.2178	0.2177	2212	1034	2048	5.217	0.7	0.7	0.3	1.8000	0.7	0.4354	0.4379	5698	1584	2981
2.557	1	5	1	1.8571	0.7	0.1891	0.1883	2015	1041	2004	5.217	0.7	7.5	0.3	1.3000	1	0.2579	0.2469	9937	1456	3373
2.557	1	5	1	2.0000	1	0.1610	0.1598	1810	1051	1949	5.217	0.7	7.5	0.3	1.3000	0.3	0.5177	0.5241	7638	1515	3160
2.557	1	5	1	2.0000	0.3	0.2623	0.2645	2448	1022	2146	5.217	0.7	7.5	0.3	1.3000	0.5	0.3924	0.3887	6632	1549	3048
2.557	1	5	1	2.0000	0.5	0.2178	0.2177	2212	1034	2048	5.217	0.7	7.5	0.3	1.3000	0.7	0.3213	0.3130	5655	1593	2985
2.557	1	5	1	2.0000	0.7	0.1891	0.1883	2015	1041	2004	5.217	0.7	7.5	0.3	1.4000	1	0.2577	0.2469	9966	1467	3373
2.557	1	5	1	2.1429	1	0.1610	0.1598	1810	1051	1949	5.217	0.7	7.5	0.3	1.4000	0.3	0.5180	0.5241	7581	1522	3168
2.557	1	5	1	2.1429	0.3	0.2623	0.2645	2448	1022	2146	5.217	0.7	7.5	0.3	1.4000	0.5	0.3918	0.3883	5612	1597	2991
2.557	1	5	1	2.1429	0.5	0.2178	0.2177	2212	1034	2048	5.217	0.7	7.5	0.3	1.5000	1	0.2576	0.2470	9976	1469	3372
2.557	1	5	1	2.1429	0.7	0.1891	0.1883	2015	1041	2004	5.217	0.7	7.5	0.3	1.5000	0.3	0.5181	0.5242	7550	1527	3166
2.557	0	0.7	1	1.4286	1	-0.0935	-0.0684	2344	1470	2174	5.217	0.7	7.5	0.3	1.5000	0.5	0.3917	0.3880	6546	1563	3061
2.557	0	0.7	1	1.4286	0.3	0.3257	0.3318	3861	1174	2134	5.217	0.7	7.5	0.3	1.5000	0.7	0.3208	0.3129	5579	1601	2995
2.557	0	0.7	1	1.4286	0.5	0.1212	0.1353	2748	1274	2134	5.217	0.7	7.5	0.3	1.6000	1	0.2574	0.2470	10040	1480	3361
2.557	0	0.7	1	1.4286	0.7	0.0068	0.0263	2294	1341	2160	5.217	0.7	7.5	0.3	1.6000	0.3	0.5189	0.5243	7562	1534	3162
2.557	0	0.7	1	1.5714	1	-0.0282	-0.0206	1957	1454	2165	5.217	0.7	7.5	0.3	1.6000	0.5	0.3921	0.3883	6496	1563	3065
2.557	0	0.7	1	1.5714	0.3	0.3711	0.3692	4075	1164	2139	5.217	0.7	7.5	0.3	1.6000	0.7	0.3203	0.3127	5549	1604	3000
2.557	0	0.7	1	1.5714	0.5	0.1764	0.1775	2818	1267	2138	5.217	0.7	7.5	0.3	1.7000	1	0.2572	0.2471	10030	1474	3358
2.557	0	0.7	1	1.5714	0.7	0.0670	0.0713	2324	1331	2156	5.217	0.7	7.5	0.3	1.7000	0.3	0.5187	0.5241	7533	1538	3165
2.557	0	0.7	1	1.7143	1	0.0116	0.0093	1973	1442	2160	5.217	0.7	7.5	0.3	1.7000	0.5	0.3917	0.3878	6469	1565	3069
2.557	0	0.7	1	1.7143	0.5	0.2089	0.2031	2886	1263	2137	5.217	0.7	7.5	0.3	1.7000	0.7	0.3201	0.3126	5517	1606	3005
2.557	0	0.7	1	1.7143	0.7	0.1037	0.0997	2348	1329	2161	5.217	0.7	7.5	0.3	1.8000	1	0.2570	0.2471	10040	1477	3360
2.557	0	0.7	1	1.8571	1	0.0380	0.0298	1992	1434	2162	5.217	0.7	7.5	0.3	1.8000	0.3	0.5187	0.5240	7522	1545	3167
2.557	0	0.7	1	1.8571	0.3	0.4134	0.4066	4386	1163	2147	5.217	0.7	7.5	0.3	1.8000	0.5	0.3916	0.3877	6443	1568	3071
2.557	0	0.7	1	1.8571	0.5	0.2302	0.2203	2951	1259	2140	5.217	0.7	7.5	0.3	1.8000	0.7	0.3198	0.3124	6167	1360	2630
2.557	0	0.7	1	1.8571	0.7	0.1281	0.1189	2372	1325	2163	5.217	0.7	5	0.3	1.3000	1	0.2490	0.2356	10060	1216	2917
2.557	0	0.7	1	2.0000	1	0.0565	0.0444	1999	1427	2163	5.217	0.7	5	0.3	1.3000	0.3	0.5131	0.5250	8186	1268	2759
2.557	0	0.7	1	2.0000	0.3	0.4244	0.4170	4494	1163	2151	5.217	0.7	5	0.3	1.3000	0.5	0.3842	0.3825	7125	1319	2678

ODTh	alfa	Eback	beta	TWOD	Ewall	δy(%)	δx(%)	M(lb-in)	V (lb)	Th (lb)	ODTh	alfa	Eback	beta	TWOD	Ewall	δy(%)	δx(%)	M(lb-in)	V (lb)	Th (lb)
2.557	0	0.7	1	2.0000	0.5	0.2451	0.2326	3005	1256	2144	5.217	0.7	5	0.3	1.3000	0.7	0.3127	0.3048	6105	1365	2633
2.557	0	0.7	1	2.0000	0.7	0.1452	0.1328	2398	1321	2164	5.217	0.7	5	0.3	1.4000	1	0.2492	0.2372	10000	1223	2923
2.557	0	0.7	1	2.1429	1	0.0706	0.0558	2005	1423	2162	5.217	0.7	5	0.3	1.4000	0.3	0.5123	0.5243	8128	1277	2762
2.557	0	0.7	1	2.1429	0.3	0.4322	0.4244	4579	1163	2155	5.217	0.7	5	0.3	1.4000	0.5	0.3840	0.3829	7066	1327	2684
2.557	0	0.7	1	2.1429	0.5	0.2559	0.2417	3057	1253	2147	5.217	0.7	5	0.3	1.4000	0.7	0.3126	0.3057	6047	1371	2635
2.557	0	0.7	1	2.1429	0.7	0.1578	0.1433	2424	1318	2166	5.217	0.7	5	0.3	1.5000	1	0.2493	0.2384	9958	1230	2929
2.557	0	7.5	1	1.4286	1	0.1135	0.1178	1492	887	1726	5.217	0.7	5	0.3	1.5000	0.3	0.5118	0.5238	8079	1284	2766
2.557	0	7.5	1	1.4286	0.3	0.2731	0.2797	2685	958	1992	5.217	0.7	5	0.3	1.5000	0.5	0.3836	0.3829	7025	1330	2684
2.557	0	7.5	1	1.4286	0.5	0.1992	0.2051	2134	929	1810	5.217	0.7	5	0.3	1.5000	0.7	0.3128	0.3065	5990	1376	2636
2.557	0	7.5	1	1.4286	0.7	0.1572	0.1619	1854	903	1810	5.217	0.7	5	0.3	1.6000	1	0.2492	0.2390	9921	1237	2938
2.557	0	7.5	1	1.5714	1	0.1284	0.1307	1529	858	1746	5.217	0.7	5	0.3	1.6000	0.3	0.5110	0.5229	8036	1289	2771
2.557	0	7.5	1	1.5714	0.3	0.2835	0.2903	2760	941	2007	5.217	0.7	5	0.3	1.6000	0.5	0.3833	0.3828	6986	1334	2684
2.557	0	7.5	1	1.5714	0.5	0.2138	0.2170	2182	900	1899	5.217	0.7	5	0.3	1.6000	0.7	0.3128	0.3070	5949	1380	2638
2.557	0	7.5	1	1.5714	0.7	0.1694	0.1729	1888	881	1832	5.217	0.7	5	0.3	1.7000	1	0.2492	0.2395	9883	1238	2939
2.557	0	7.5	1	1.7143	1	0.1371	0.1386	1551	843	1770	5.217	0.7	5	0.3	1.7000	0.3	0.5105	0.5226	8000	1293	2774
2.557	0	7.5	1	1.7143	0.3	0.2880	0.2941	2784	932	2019	5.217	0.7	5	0.3	1.7000	0.5	0.3830	0.3827	6945	1340	2688
2.557	0	7.5	1	1.7143	0.5	0.2216	0.2233	2197	884	1892	5.217	0.7	5	0.3	1.7000	0.7	0.3126	0.3070	5913	1384	2641
2.557	0	7.5	1	1.7143	0.7	0.1765	0.1792	1906	870	1853	5.217	0.7	5	0.3	1.8000	1	0.2491	0.2398	9843	1242	2945
2.557	0	7.5	1	1.8571	1	0.1427	0.1436	1564	836	1792	5.217	0.7	5	0.3	1.8000	0.3	0.5097	0.5218	7962	1299	2778
2.557	0	7.5	1	1.8571	0.3	0.2905	0.2963	2806	929	2038	5.217	0.7	5	0.3	1.8000	0.5	0.3826	0.3824	6910	1345	2691
2.557	0	7.5	1	1.8571	0.5	0.2257	0.2273	2236	878	1907	5.217	0.7	5	0.3	1.8000	0.7	0.3123	0.3069	5643	2445	4358
2.557	0	7.5	1	1.8571	0.7	0.1819	0.1836	1920	859	1858	5.217	1	0.7	1	1.3000	1	0.3658	0.3754	10180	2345	4824
2.557	0	7.5	1	2.0000	1	0.1464	0.1470	1574	843	1810	5.217	1	0.7	1	1.3000	0.3	0.7699	0.8139	7377	2410	4574
2.557	0	7.5	1	2.0000	0.3	0.2915	0.2970	2806	927	2056	5.217	1	0.7	1	1.3000	0.5	0.5694	0.5940	6063	2424	4474
2.557	0	7.5	1	2.0000	0.5	0.2298	0.2314	2274	872	1914	5.217	1	0.7	1	1.3000	0.7	0.4605	0.4765	5643	2445	4358
2.557	0	7.5	1	2.0000	0.7	0.1877	0.1879	1933	845	1844	5.217	1	0.7	1	1.4000	1	0.3658	0.3754	10180	2345	4824
2.557	0	7.5	1	2.1429	1	0.1496	0.1496	1583	857	1812	5.217	1	0.7	1	1.4000	0.3	0.7699	0.8139	7377	2410	4574
2.557	0	7.5	1	2.1429	0.3	0.2937	0.2987	2826	924	2062	5.217	1	0.7	1	1.4000	0.5	0.5694	0.5940	6063	2424	4474
2.557	0	7.5	1	2.1429	0.5	0.2312	0.2327	2279	871	1932	5.217	1	0.7	1	1.4000	0.7	0.4605	0.4765	5643	2445	4358
2.557	0	7.5	1	2.1429	0.7	0.1909	0.1906	1941	856	1849	5.217	1	0.7	1	1.5000	1	0.3658	0.3754	10180	2345	4824
2.557	0	5	1	1.4286	1	0.0435	0.0514	1223	875	1475	5.217	1	0.7	1	1.5000	0.3	0.7699	0.8139	7377	2410	4574
2.557	0	5	1	1.4286	0.3	0.2442	0.2547	2729	891	1688	5.217	1	0.7	1	1.5000	0.5	0.5694	0.5940	6063	2424	4474
2.557	0	5	1	1.4286	0.5	0.1560	0.1645	1916	862	1543	5.217	1	0.7	1	1.5000	0.7	0.4605	0.4765	5643	2445	4358
2.557	0	5	1	1.4286	0.7	0.0990	0.1074	1564	859	1474	5.217	1	0.7	1	1.6000	1	0.3658	0.3754	10180	2345	4824
2.557	0	5	1	1.5714	1	0.0756	0.0786	1300	814	1453	5.217	1	0.7	1	1.6000	0.3	0.7699	0.8139	7377	2410	4574
2.557	0	5	1	1.5714	0.3	0.2635	0.2719	2856	858	1707	5.217	1	0.7	1	1.6000	0.5	0.5694	0.5940	6063	2424	4474
2.557	0	5	1	1.5714	0.5	0.1805	0.1858	1988	823	1575	5.217	1	0.7	1	1.6000	0.7	0.4605	0.4765	5643	2445	4358
2.557	0	5	1	1.5714	0.7	0.1280	0.1321	1661	808	1489	5.217	1	0.7	1	1.7000	1	0.3658	0.3754	10180	2345	4824
2.557	0	5	1	1.7143	1	0.0957	0.0957	1346	777	1454	5.217	1	0.7	1	1.7000	0.3	0.7699	0.8139	7377	2410	4574
2.557	0	5	1	1.7143	0.3	0.2752	0.2820	2931	839	1719	5.217	1	0.7	1	1.7000	0.5	0.5694	0.5940	6063	2424	4474
2.557	0	5	1	1.7143	0.5	0.1952	0.1984	2088	801	1592	5.217	1	0.7	1	1.7000	0.7	0.4605	0.4765	5643	2445	4358
2.557	0	5	1	1.7143	0.7	0.1452	0.1471	1711	784	1515	5.217	1	0.7	1	1.8000	1	0.3658	0.3754	10180	2345	4824
2.557	0	5	1	1.8571	1	0.1089	0.1071	1375	757	1468	5.217	1	0.7	1	1.8000	0.3	0.7699	0.8139	7377	2410	4574
2.557	0	5	1	1.8571	0.3	0.2849	0.2896	3023	823	1718	5.217	1	0.7	1	1.8000	0.5	0.5694	0.5940	6063	2424	4474
2.557	0	5	1	1.8571	0.5	0.2045	0.2068	2181	789	1609	5.217	1	0.7	1	1.8000	0.7	0.4605	0.4765	4579	2070	3818
2.557	0	5	1	1.8571	0.7	0.1563	0.1564	1743	768	1533	5.217	1	7.5	1	1.3000	1	0.3119	0.3036	8966	1932	4220
2.557	0	5	1	2.0000	1	0.1179	0.1152	1394	750	1491	5.217	1	7.5	1	1.3000	0.3	0.6287	0.6371	6718	2004	3996

ODTh	alfa	Eback	beta	TWOD	Ewall	δy(%)	δx(%)	M(lb-in)	V(lb)	Th(lb)	ODTh	alfa	Eback	beta	TWOD	Ewall	δy(%)	δx(%)	M(lb-in)	V(lb)	Th(lb)
2.557	0	5	1	2.0000	0.3	0.2908	0.2943	3061	814	1722	5.217	1	7.5	1	1.3000	0.5	0.4739	0.4716	5423	2045	3868
2.557	0	5	1	2.0000	0.5	0.2108	0.2121	2240	781	1623	5.217	1	7.5	1	1.3000	0.7	0.3886	0.3819	4579	2070	3818
2.557	0	5	1	2.0000	0.7	0.1638	0.1632	1765	759	1550	5.217	1	7.5	1	1.4000	1	0.3119	0.3036	8966	1932	4220
2.557	0	5	1	2.1429	1	0.1246	0.1212	1409	758	1507	5.217	1	7.5	1	1.4000	0.3	0.6287	0.6371	6718	2004	3996
2.557	0	5	1	2.1429	0.3	0.2942	0.2971	3061	809	1729	5.217	1	7.5	1	1.4000	0.5	0.4739	0.4716	5423	2045	3868
2.557	0	5	1	2.1429	0.5	0.2154	0.2161	2276	776	1636	5.217	1	7.5	1	1.4000	0.7	0.3886	0.3819	4579	2070	3818
2.557	1	0.7	1	1.4286	1	0.1649	0.0986	4373	1485	2225	5.217	1	7.5	1	1.5000	1	0.3119	0.3036	8966	1932	4220
2.557	1	0.7	1	1.4286	0.3	0.4808	0.4636	5742	1118	2267	5.217	1	7.5	1	1.5000	0.3	0.6287	0.6371	6718	2004	3996
2.557	1	0.7	1	1.4286	0.5	0.3226	0.2850	4736	1232	2234	5.217	1	7.5	1	1.5000	0.5	0.4739	0.4716	5423	2045	3868
2.557	1	0.7	1	1.4286	0.7	0.2372	0.1865	4432	1324	2239	5.217	1	7.5	1	1.5000	0.7	0.3886	0.3819	4579	2070	3818
2.557	1	0.7	1	1.5714	1	0.1808	0.1200	4041	1465	2220	5.217	1	7.5	1	1.6000	1	0.3119	0.3036	8966	1932	4220
2.557	1	0.7	1	1.5714	0.3	0.4918	0.4769	5741	1120	2252	5.217	1	7.5	1	1.6000	0.3	0.6287	0.6371	6718	2004	3996
2.557	1	0.7	1	1.5714	0.5	0.3362	0.3017	4612	1229	2219	5.217	1	7.5	1	1.6000	0.5	0.4739	0.4716	5423	2045	3868
2.557	1	0.7	1	1.5714	0.7	0.2519	0.2055	4202	1315	2236	5.217	1	7.5	1	1.6000	0.7	0.3886	0.3819	4579	2070	3818
2.557	1	0.7	1	1.7143	1	0.1901	0.1334	3840	1452	2218	4.167	1	7.5	1	1.7000	1	0.3119	0.3036	8966	1932	4220
2.557	1	0.7	1	1.7143	0.3	0.4979	0.4843	5740	1121	2244	4.167	1	7.5	1	1.7000	0.3	0.6287	0.6371	6718	2004	3996
2.557	1	0.7	1	1.7143	0.5	0.3440	0.3115	4543	1228	2213	4.167	1	7.5	1	1.7000	0.5	0.4739	0.4716	5423	2045	3868
2.557	1	0.7	1	1.7143	0.7	0.2605	0.2172	4061	1310	2234	4.167	1	7.5	1	1.7000	0.7	0.3886	0.3819	4579	2070	3818
2.557	1	0.7	1	1.8571	1	0.1962	0.1426	3704	1442	2217	4.167	1	7.5	1	1.8000	1	0.3119	0.3036	8966	1932	4220
2.557	1	0.7	1	1.8571	0.3	0.5018	0.4892	5737	1123	2238	4.167	1	7.5	1	1.8000	0.3	0.6287	0.6371	6718	2004	3996
2.557	1	0.7	1	1.8571	0.5	0.3489	0.3179	4495	1226	2210	4.167	1	7.5	1	1.8000	0.5	0.4739	0.4716	5423	2045	3868
2.557	1	0.7	1	1.8571	0.7	0.2661	0.2250	3968	1308	2233	4.167	1	7.5	1	1.8000	0.7	0.3886	0.3819	4504	1947	3610
2.557	1	0.7	1	2.0000	1	0.2005	0.1494	3603	1435	2216	4.167	1	5	1	1.3000	1	0.2965	0.2894	8475	1832	4011
2.557	1	0.7	1	2.0000	0.3	0.5042	0.4923	5730	1123	2233	4.167	1	5	1	1.3000	0.3	0.5972	0.6068	6359	1893	3784
2.557	1	0.7	1	2.0000	0.5	0.3523	0.3223	4460	1226	2208	4.167	1	5	1	1.3000	0.5	0.4503	0.4493	5143	1926	3661
2.557	1	0.7	1	2.0000	0.7	0.2700	0.2307	3902	1305	2232	4.167	1	5	1	1.3000	0.7	0.3693	0.3639	4504	1947	3610
2.557	1	0.7	1	2.1429	1	0.2036	0.1546	3521	1429	2217	4.167	1	5	1	1.4000	1	0.2965	0.2894	8475	1832	4011
2.557	1	0.7	1	2.1429	0.3	0.5055	0.4943	5716	1123	2231	4.167	1	5	1	1.4000	0.3	0.5972	0.6068	6359	1893	3784
2.557	1	0.7	1	2.1429	0.5	0.3547	0.3256	4437	1227	2206	4.167	1	5	1	1.4000	0.5	0.4503	0.4493	5143	1926	3661
2.557	1	0.7	1	2.1429	0.7	0.2729	0.2350	3853	1304	2231	4.167	1	5	1	1.4000	0.7	0.3693	0.3639	4504	1947	3610
2.557	1	7.5	1	1.4286	1	0.1635	0.1526	1727	788	1803	4.167	1	5	1	1.5000	1	0.2965	0.2894	8475	1832	4011
2.557	1	7.5	1	1.4286	0.3	0.3101	0.3124	2837	868	2050	4.167	1	5	1	1.5000	0.3	0.5972	0.6068	6359	1893	3784
2.557	1	7.5	1	1.4286	0.5	0.2400	0.2368	2243	818	1970	4.167	1	5	1	1.5000	0.5	0.4503	0.4493	5143	1926	3661
2.557	1	7.5	1	1.4286	0.7	0.2020	0.1948	1990	774	1881	4.167	1	5	1	1.5000	0.7	0.3693	0.3639	4504	1947	3610
2.557	1	7.5	1	1.5714	1	0.1674	0.1579	1662	805	1809	4.167	1	5	1	1.6000	1	0.2965	0.2894	8475	1832	4011
2.557	1	7.5	1	1.5714	0.3	0.3140	0.3154	2876	865	2033	4.167	1	5	1	1.6000	0.3	0.5972	0.6068	6359	1893	3784
2.557	1	7.5	1	1.5714	0.5	0.2428	0.2408	2230	821	1976	4.167	1	5	1	1.6000	0.5	0.4503	0.4493	5143	1926	3661
2.557	1	7.5	1	1.5714	0.7	0.2051	0.1991	1988	778	1890	4.167	1	5	1	1.6000	0.7	0.3693	0.3639	4504	1947	3610
2.557	1	7.5	1	1.7143	1	0.1693	0.1610	1656	819	1818	4.167	1	5	1	1.7000	1	0.2965	0.2894	8475	1832	4011
2.557	1	7.5	1	1.7143	0.3	0.3122	0.3140	2812	871	2050	4.167	1	5	1	1.7000	0.3	0.5972	0.6068	6359	1893	3784
2.557	1	7.5	1	1.7143	0.5	0.2447	0.2433	2290	822	1976	4.167	1	5	1	1.7000	0.5	0.4503	0.4493	5143	1926	3661
2.557	1	7.5	1	1.7143	0.7	0.2062	0.2011	1989	783	1902	4.167	1	5	1	1.7000	0.7	0.3693	0.3639	4504	1947	3610
2.557	1	7.5	1	1.8571	1	0.1702	0.1627	1656	834	1831	4.167	1	5	1	1.8000	1	0.2965	0.2894	8475	1832	4011
2.557	1	7.5	1	1.8571	0.3	0.3101	0.3123	2764	877	2070	4.167	1	5	1	1.8000	0.3	0.5972	0.6068	6359	1893	3784
2.557	1	7.5	1	1.8571	0.5	0.2466	0.2447	2290	820	1970	4.167	1	5	1	1.8000	0.5	0.4503	0.4493	5143	1926	3661
2.557	1	7.5	1	1.8571	0.7	0.2071	0.2024	1990	796	1908	4.167	1	5	1	1.8000	0.7	0.3693	0.3639	2957	1943	2896

ODTh	alfa	Eback	beta	TWOD	Ewall	δy(%)	δx(%)	M(lb-in)	V (lb)	Th (lb)
2.557	1	7.5	1	2.0000	1	0.1706	0.1637	1655	847	1850
2.557	1	7.5	1	2.0000	0.3	0.3098	0.3120	2782	880	2080
2.557	1	7.5	1	2.0000	0.5	0.2484	0.2458	2284	819	1963
2.557	1	7.5	1	2.0000	0.7	0.2076	0.2033	1990	809	1914
2.557	1	7.5	1	2.1429	1	0.1708	0.1645	1654	855	1862
2.557	1	7.5	1	2.1429	0.3	0.3098	0.3118	2805	882	2087
2.557	1	7.5	1	2.1429	0.5	0.2481	0.2455	2281	823	1972
2.557	1	7.5	1	2.1429	0.7	0.2085	0.2046	1992	844	1914
2.557	1	5	1	1.4286	1	0.1450	0.1242	2059	628	1576
2.557	1	5	1	1.4286	0.3	0.3168	0.3163	3216	730	1724
2.557	1	5	1	1.4286	0.5	0.2405	0.2306	2694	672	1635
2.557	1	5	1	1.4286	0.7	0.1930	0.1778	2368	637	1583
2.557	1	5	1	1.5714	1	0.1559	0.1365	2041	658	1548
2.557	1	5	1	1.5714	0.3	0.3190	0.3190	3166	736	1739
2.557	1	5	1	1.5714	0.5	0.2458	0.2370	2637	676	1642
2.557	1	5	1	1.5714	0.7	0.2000	0.1864	2315	640	1584
2.557	1	5	1	1.7143	1	0.1613	0.1433	2002	679	1544
2.557	1	5	1	1.7143	0.3	0.3199	0.3204	3125	742	1754
2.557	1	5	1	1.7143	0.5	0.2484	0.2405	2592	681	1652
2.557	1	5	1	1.7143	0.7	0.2039	0.1913	2267	644	1591
2.557	1	5	1	1.8571	1	0.1643	0.1475	1954	695	1549
2.557	1	5	1	1.8571	0.3	0.3205	0.3216	3098	745	1766
2.557	1	5	1	2.0000	1	0.1663	0.1505	1912	712	1554
2.557	1	5	1	2.0000	0.3	0.3218	0.3225	3104	746	1768
2.557	1	5	1	2.0000	0.5	0.2500	0.2430	2524	690	1674
2.557	1	5	1	2.0000	0.7	0.2073	0.1963	2188	656	1605
2.557	1	5	1	2.1429	1	0.1675	0.1527	1875	725	1561
2.557	1	5	1	2.1429	0.3	0.3226	0.3229	3103	747	1769
2.557	1	5	1	2.1429	0.5	0.2502	0.2437	2495	694	1683
2.557	1	5	1	2.1429	0.7	0.2080	0.1975	2157	675	1612
2.557	1	0.7	0	1.4286	1	0.2757	0.2523	4592	1266	2042
2.557	1	0.7	0	1.4286	0.3	0.5190	0.5525	6751	893	2308
2.557	1	0.7	0	1.4286	0.5	0.4028	0.4069	5709	967	2209
2.557	1	0.7	0	1.4286	0.7	0.3370	0.3256	5148	1110	2136
2.557	1	0.7	0	1.5714	1	0.2750	0.2542	4509	1257	2048
2.557	1	0.7	0	1.5714	0.3	0.5191	0.5543	6710	894	2307
2.557	1	0.7	0	1.5714	0.5	0.4018	0.4079	5643	966	2212
2.557	1	0.7	0	1.5714	0.7	0.3362	0.3271	5077	1104	2138
2.557	1	0.7	0	1.7143	1	0.2744	0.2553	4450	1250	2051
2.557	1	0.7	0	1.7143	0.3	0.5192	0.5555	6678	895	2307
2.557	1	0.7	0	1.7143	0.5	0.4010	0.4084	5592	965	2213
2.557	1	0.7	0	1.7143	0.7	0.3356	0.3282	5022	1100	2141
2.557	1	0.7	0	1.8571	1	0.2739	0.2562	4404	1245	2053
2.557	1	0.7	0	1.8571	0.3	0.5188	0.5561	6649	895	2307
2.557	1	0.7	0	1.8571	0.5	0.4002	0.4088	5552	964	2216
2.557	1	0.7	0	1.8571	0.7	0.3350	0.3288	4974	1098	2139

ODTh	alfa	Eback	beta	TWOD	Ewall	δy(%)	δx(%)	M(lb-in)	V (lb)	Th (lb)
4.167	0.3	0.7	0.7	1.3000	1	0.0120	-0.0004	7199	1550	2879
4.167	0.3	0.7	0.7	1.3000	0.3	0.4776	0.4722	4263	1685	2879
4.167	0.3	0.7	0.7	1.3000	0.5	0.2436	0.2313	3686	1794	2896
4.167	0.3	0.7	0.7	1.3000	0.7	0.1191	0.1056	3003	1929	2893
4.167	0.3	0.7	0.7	1.4000	1	0.0557	0.0320	7712	1540	2877
4.167	0.3	0.7	0.7	1.4000	0.3	0.5051	0.4977	4657	1672	2876
4.167	0.3	0.7	0.7	1.4000	0.5	0.2782	0.2598	3729	1775	2897
4.167	0.3	0.7	0.7	1.4000	0.7	0.1592	0.1375	3033	1919	2890
4.167	0.3	0.7	0.7	1.5000	1	0.0826	0.0527	8034	1535	2877
4.167	0.3	0.7	0.7	1.5000	0.3	0.5225	0.5138	4963	1663	2874
4.167	0.3	0.7	0.7	1.5000	0.5	0.2986	0.2776	3754	1776	2892
4.167	0.3	0.7	0.7	1.5000	0.7	0.1834	0.1579	3052	1910	2885
4.167	0.3	0.7	0.7	1.6000	1	0.1006	0.0675	8257	1532	2874
4.167	0.3	0.7	0.7	1.6000	0.3	0.5346	0.5251	5188	1656	2872
4.167	0.3	0.7	0.7	1.6000	0.5	0.3123	0.2897	3849	1767	2891
4.167	0.3	0.7	0.7	1.6000	0.7	0.1992	0.1716	3116	1902	2883
4.167	0.3	0.7	0.7	1.7000	1	0.1135	0.0783	8414	1529	2873
4.167	0.3	0.7	0.7	1.7000	0.3	0.5433	0.5333	5357	1650	2872
4.167	0.3	0.7	0.7	1.7000	0.5	0.3220	0.2984	3992	1762	2890
4.167	0.3	0.7	0.7	1.7000	0.7	0.2105	0.1815	3199	1896	2883
4.167	0.3	0.7	0.7	1.8000	1	0.1231	0.0866	8532	1527	2873
4.167	0.3	0.7	0.7	1.8000	0.3	0.5500	0.5396	5485	1646	2871
4.167	0.3	0.7	0.7	1.8000	0.5	0.3295	0.3052	4103	1757	2890
4.167	0.3	0.7	0.7	1.8000	0.7	0.2189	0.1891	2783	1278	2476
4.167	0.3	7.5	0.7	1.3000	1	0.1721	0.1700	5930	1183	2834
4.167	0.3	7.5	0.7	1.3000	0.3	0.4352	0.4426	4412	1193	2622
4.167	0.3	7.5	0.7	1.3000	0.5	0.3071	0.3064	3543	1243	2519
4.167	0.3	7.5	0.7	1.3000	0.7	0.2361	0.2333	2814	1302	2447
4.167	0.3	7.5	0.7	1.4000	1	0.1849	0.1800	6002	1173	2848
4.167	0.3	7.5	0.7	1.4000	0.3	0.4415	0.4486	4527	1201	2629
4.167	0.3	7.5	0.7	1.4000	0.5	0.3161	0.3146	3648	1237	2524
4.167	0.3	7.5	0.7	1.4000	0.7	0.2464	0.2423	2944	1290	2454
4.167	0.3	7.5	0.7	1.5000	1	0.1917	0.1860	6063	1167	2854
4.167	0.3	7.5	0.7	1.5000	0.3	0.4456	0.4523	4596	1203	2629
4.167	0.3	7.5	0.7	1.5000	0.5	0.3216	0.3196	3747	1243	2535
4.167	0.3	7.5	0.7	1.5000	0.7	0.2526	0.2480	3008	1292	2453
4.167	0.3	7.5	0.7	1.6000	1	0.1964	0.1901	6102	1164	2863
6.000	0.3	7.5	0.7	1.6000	0.3	0.4483	0.4547	4647	1204	2635
6.000	0.3	7.5	0.7	1.6000	0.5	0.3252	0.3229	3794	1246	2528
6.000	0.3	7.5	0.7	1.6000	0.7	0.2568	0.2517	3048	1289	2455
6.000	0.3	7.5	0.7	1.7000	1	0.1998	0.1933	6125	1162	2869
6.000	0.3	7.5	0.7	1.7000	0.3	0.4501	0.4563	4670	1205	2640
6.000	0.3	7.5	0.7	1.7000	0.5	0.3277	0.3252	3833	1248	2531
6.000	0.3	7.5	0.7	1.7000	0.7	0.2598	0.2544	3077	1292	2459
6.000	0.3	7.5	0.7	1.8000	1	0.2024	0.1957	6152	1160	2870
6.000	0.3	7.5	0.7	1.8000	0.3	0.4515	0.4576	4692	1205	2644

ODTh	alfa	Eback	beta	TWOD	Ewall	δy(%)	δx(%)	M(lb-in)	V (lb)	Th (lb)	ODTh	alfa	Eback	beta	TWOD	Ewall	δy(%)	δx(%)	M(lb-in)	V (lb)	Th (lb)
2.557	1	0.7	0	2.0000	1	0.2734	0.2567	4365	1241	2055	6.000	0.3	7.5	0.7	1.8000	0.5	0.3295	0.3268	3857	1249	2531
2.557	1	0.7	0	2.0000	0.3	0.5187	0.5567	6626	896	2307	6.000	0.3	7.5	0.7	1.8000	0.7	0.2621	0.2564	2398	1156	2184
2.557	1	0.7	0	2.0000	0.5	0.3996	0.4090	5518	964	2218	6.000	0.3	5	0.7	1.3000	1	0.1065	0.1073	5676	1099	2394
2.557	1	0.7	0	2.0000	0.7	0.3346	0.3293	4940	1096	2139	6.000	0.3	5	0.7	1.3000	0.3	0.3896	0.3968	3797	1107	2287
2.557	1	0.7	0	2.1429	1	0.2730	0.2572	4332	1238	2057	6.000	0.3	5	0.7	1.3000	0.5	0.2487	0.2506	3140	1119	2228
2.557	1	0.7	0	2.1429	0.3	0.5184	0.5569	6605	897	2308	6.000	0.3	5	0.7	1.3000	0.7	0.1739	0.1751	2453	1149	2180
2.557	1	0.7	0	2.1429	0.5	0.3990	0.4091	5490	964	2219	6.000	0.3	5	0.7	1.4000	1	0.1300	0.1275	2486	1147	2184
2.557	1	0.7	0	2.1429	0.7	0.3341	0.3296	4910	1094	2141	6.000	0.3	5	0.7	1.5000	1	0.1448	0.1405	6035	1044	2385
2.557	1	7.5	0	1.4286	1	0.1839	0.1742	2241	746	1806	6.000	0.3	5	0.7	1.5000	0.3	0.4176	0.4219	4211	1043	2290
2.557	1	7.5	0	1.4286	0.3	0.3206	0.3218	3257	879	2048	6.000	0.3	5	0.7	1.5000	0.5	0.2805	0.2788	3246	1081	2230
2.557	1	7.5	0	1.4286	0.5	0.2601	0.2561	2814	815	1927	6.000	0.3	5	0.7	1.5000	0.7	0.2084	0.2049	2510	1145	2192
2.557	1	7.5	0	1.4286	0.7	0.2206	0.2143	2513	782	1869	6.000	0.3	5	0.7	1.6000	1	0.1546	0.1491	6117	1034	2391
2.557	1	7.5	0	1.5714	1	0.1830	0.1748	2163	760	1817	6.000	0.3	5	0.7	1.6000	0.3	0.4245	0.4283	4378	1055	2277
2.557	1	7.5	0	1.5714	0.3	0.3183	0.3198	3179	883	2061	6.000	0.3	5	0.7	1.6000	0.5	0.2899	0.2868	3341	1087	2232
2.557	1	7.5	0	1.5714	0.5	0.2583	0.2550	2730	820	1942	6.000	0.3	5	0.7	1.6000	0.7	0.2177	0.2132	2527	1152	2185
2.557	1	7.5	0	1.5714	0.7	0.2193	0.2141	2433	786	1881	6.000	0.3	5	0.7	1.7000	1	0.1621	0.1555	6148	1026	2394
2.557	1	7.5	0	1.7143	1	0.1823	0.1751	2105	778	1826	6.000	0.3	5	0.7	1.7000	0.3	0.4292	0.4326	4458	1066	2274
2.557	1	7.5	0	1.7143	0.3	0.3163	0.3181	3119	888	2075	6.000	0.3	5	0.7	1.7000	0.5	0.2963	0.2924	3455	1092	2238
2.557	1	7.5	0	1.7143	0.5	0.2567	0.2538	2666	824	1954	6.000	0.3	5	0.7	1.7000	0.7	0.2244	0.2192	2618	1153	2187
2.557	1	7.5	0	1.7143	0.7	0.2181	0.2136	2371	790	1891	6.000	0.3	5	0.7	1.8000	1	0.1677	0.1606	6160	1022	2401
2.557	1	7.5	0	1.8571	1	0.1816	0.1752	2059	796	1836	6.000	0.3	5	0.7	1.8000	0.3	0.4321	0.4357	4528	1075	2271
2.557	1	7.5	0	1.8571	0.3	0.3147	0.3166	3069	891	2084	6.000	0.3	5	0.7	1.8000	0.5	0.3012	0.2965	3537	1101	2238
2.557	1	7.5	0	1.8571	0.5	0.2556	0.2530	2622	827	1962	6.000	0.3	5	0.7	1.8000	0.7	0.2295	0.2237	6174	1926	3034
2.557	1	7.5	0	1.8571	0.7	0.2171	0.2131	2323	793	1900	6.000	0.5	0.7	0.5	1.3000	1	0.2047	0.1364	9865	1512	3019
2.557	1	7.5	0	2.0000	1	0.1810	0.1751	2024	810	1843	6.000	0.5	0.7	0.5	1.3000	0.3	0.5905	0.5732	7395	1631	3013
2.557	1	7.5	0	2.0000	0.3	0.3133	0.3153	3029	893	2091	6.000	0.5	0.7	0.5	1.3000	0.5	0.3855	0.3447	6533	1769	3040
2.557	1	7.5	0	2.0000	0.5	0.2543	0.2521	2581	830	1971	6.000	0.5	0.7	0.5	1.3000	0.7	0.2870	0.2335	5923	1913	3028
2.557	1	7.5	0	2.0000	0.7	0.2163	0.2125	2288	796	1905	6.000	0.5	0.7	0.5	1.4000	1	0.2141	0.1493	9901	1508	3004
2.557	1	7.5	0	2.1429	1	0.1805	0.1750	1994	821	1850	6.000	0.5	0.7	0.5	1.4000	0.3	0.5985	0.5825	7364	1623	2993
2.557	1	7.5	0	2.1429	0.3	0.3122	0.3143	2998	895	2097	6.000	0.5	0.7	0.5	1.4000	0.5	0.3941	0.3550	6404	1758	3024
2.557	1	7.5	0	2.1429	0.5	0.2534	0.2513	2549	833	1977	6.000	0.5	0.7	0.5	1.4000	0.7	0.2961	0.2451	5767	1904	3020
2.557	1	7.5	0	2.1429	0.7	0.2155	0.2120	2255	798	1913	6.000	0.5	0.7	0.5	1.5000	1	0.2200	0.1578	9921	1505	2995
2.557	1	5	0	1.4286	1	0.1871	0.1713	2748	631	1550	6.000	0.5	0.7	0.5	1.5000	0.3	0.6034	0.5882	7348	1617	2981
2.557	1	5	0	1.4286	0.3	0.3371	0.3401	3897	749	1721	6.000	0.5	0.7	0.5	1.5000	0.5	0.3994	0.3614	6337	1748	3017
2.557	1	5	0	1.4286	0.5	0.2673	0.2619	3324	694	1640	6.000	0.5	0.7	0.5	1.5000	0.7	0.3014	0.2519	5678	1898	3014
2.557	1	5	0	1.4286	0.7	0.2250	0.2147	3006	665	1600	6.000	0.5	0.7	0.5	1.6000	1	0.2239	0.1630	9928	1504	2989
2.557	1	5	0	1.5714	1	0.1864	0.1729	2664	636	1560	6.000	0.5	0.7	0.5	1.6000	0.3	0.6068	0.5925	7339	1614	2972
2.557	1	5	0	1.5714	0.3	0.3341	0.3378	3810	755	1740	6.000	0.5	0.7	0.5	1.6000	0.5	0.4030	0.3659	6285	1742	3011
2.042	1	5	0	1.5714	0.5	0.2659	0.2620	3268	700	1652	6.000	0.5	0.7	0.5	1.6000	0.7	0.3052	0.2569	5601	1889	3011
2.042	1	5	0	1.5714	0.7	0.2240	0.2152	2940	669	1609	6.000	0.5	0.7	0.5	1.7000	1	0.2267	0.1671	9938	1504	2985
2.042	1	5	0	1.7143	1	0.1857	0.1737	2601	641	1570	6.000	0.5	0.7	0.5	1.7000	0.3	0.6095	0.5958	7327	1612	2966
2.042	1	5	0	1.7143	0.3	0.3316	0.3357	3737	761	1755	6.000	0.5	0.7	0.5	1.7000	0.5	0.4058	0.3694	6249	1740	3003
2.042	1	5	0	1.7143	0.5	0.2648	0.2617	3215	704	1663	6.000	0.5	0.7	0.5	1.7000	0.7	0.3080	0.2609	5544	1885	3008
2.042	1	5	0	1.7143	0.7	0.2231	0.2156	2896	673	1618	6.000	0.5	0.7	0.5	1.8000	1	0.2289	0.1705	9941	1503	2982
2.042	1	5	0	1.8571	1	0.1849	0.1741	2548	645	1578	6.000	0.5	0.7	0.5	1.8000	0.3	0.6114	0.5983	7317	1610	2962
2.042	1	5	0	1.8571	0.3	0.3292	0.3337	3669	765	1767	6.000	0.5	0.7	0.5	1.8000	0.5	0.4078	0.3720	6212	1738	2997
2.042	1	5	0	1.8571	0.5	0.2633	0.2610	3150	708	1673	6.000	0.5	0.7	0.5	1.8000	0.7	0.3103	0.2643	3164	1294	2541

ODTh	alfa	Eback	beta	TWOD	Ewall	δy(%)	δx(%)	M(lb-in)	V (lb)	Th (lb)	ODTh	alfa	Eback	beta	TWOD	Ewall	δy(%)	δx(%)	M(lb-in)	V (lb)	Th (lb)
2.042	1	5	0	1.8571	0.7	0.2222	0.2156	2840	677	1627	6.000	0.5	7.5	0.5	1.3000	1	0.2085	0.1945	6440	1164	2848
2.042	1	5	0	2.0000	1	0.1842	0.1744	2498	648	1586	6.000	0.5	7.5	0.5	1.3000	0.3	0.4594	0.4619	4878	1213	2640
2.042	1	5	0	2.0000	0.3	0.3271	0.3318	3611	769	1779	6.000	0.5	7.5	0.5	1.3000	0.5	0.3372	0.3291	3980	1256	2552
2.042	1	5	0	2.0000	0.5	0.2619	0.2602	3091	712	1684	6.000	0.5	7.5	0.5	1.3000	0.7	0.2693	0.2572	3141	1296	2524
2.042	1	5	0	2.0000	0.7	0.2211	0.2155	2785	681	1637	6.000	0.5	7.5	0.5	1.4000	1	0.2122	0.1988	6418	1168	2850
2.042	1	5	0	2.1429	1	0.1834	0.1744	2451	652	1594	6.000	0.5	7.5	0.5	1.4000	0.3	0.4611	0.4640	4852	1217	2640
2.042	1	5	0	2.1429	0.3	0.3252	0.3301	3558	773	1790	6.000	0.5	7.5	0.5	1.4000	0.5	0.3395	0.3321	3970	1255	2541
2.042	1	5	0	2.1429	0.5	0.2606	0.2593	3044	715	1692	6.000	0.5	7.5	0.5	1.4000	0.7	0.2723	0.2607	3169	1309	2493
2.042	1	5	0	2.1429	0.7	0.2204	0.2155	2740	684	1645	6.000	0.5	7.5	0.5	1.5000	1	0.2150	0.2015	6416	1170	2852
2.042	1	0.7	1	1.4286	1	0.2067	0.2121	1820	1275	2334	6.000	0.5	7.5	0.5	1.5000	0.3	0.4620	0.4650	4835	1216	2641
2.042	1	0.7	1	1.4286	0.3	0.3523	0.3686	2238	1251	2670	6.000	0.5	7.5	0.5	1.5000	0.5	0.3408	0.3337	3947	1254	2541
2.042	1	0.7	1	1.4286	0.5	0.2858	0.2969	2103	1245	2546	6.000	0.5	7.5	0.5	1.5000	0.7	0.2739	0.2628	3142	1305	2492
2.042	1	0.7	1	1.4286	0.7	0.2459	0.2536	1984	1261	2439	6.000	0.5	7.5	0.5	1.6000	1	0.2164	0.2036	6412	1173	2855
2.042	1	0.7	1	1.5714	1	0.2067	0.2121	1820	1275	2334	6.000	0.5	7.5	0.5	1.6000	0.3	0.4625	0.4656	4823	1219	2643
2.042	1	0.7	1	1.5714	0.3	0.3523	0.3686	2238	1251	2670	6.000	0.5	7.5	0.5	1.6000	0.5	0.3417	0.3350	3924	1253	2542
2.042	1	0.7	1	1.5714	0.5	0.2858	0.2969	2103	1245	2546	6.000	0.5	7.5	0.5	1.6000	0.7	0.2749	0.2643	3122	1306	2494
2.042	1	0.7	1	1.5714	0.7	0.2459	0.2536	1984	1261	2439	6.000	0.5	7.5	0.5	1.7000	1	0.2174	0.2050	6404	1175	2857
2.042	1	0.7	1	1.7143	1	0.2067	0.2121	1820	1275	2334	6.000	0.5	7.5	0.5	1.7000	0.3	0.4628	0.4659	4812	1220	2644
2.042	1	0.7	1	1.7143	0.3	0.3523	0.3686	2238	1251	2670	6.000	0.5	7.5	0.5	1.7000	0.5	0.3423	0.3358	3909	1254	2545
2.042	1	0.7	1	1.7143	0.5	0.2858	0.2969	2103	1245	2546	6.000	0.5	7.5	0.5	1.7000	0.7	0.2756	0.2654	3105	1305	2495
2.042	1	0.7	1	1.7143	0.7	0.2459	0.2536	1984	1261	2439	6.000	0.5	7.5	0.5	1.8000	1	0.2180	0.2060	6400	1176	2860
2.042	1	0.7	1	1.8571	1	0.2067	0.2121	1820	1275	2334	6.000	0.5	7.5	0.5	1.8000	0.3	0.4630	0.4662	4807	1221	2645
2.042	1	0.7	1	1.8571	0.3	0.3523	0.3686	2238	1251	2670	6.000	0.5	7.5	0.5	1.8000	0.5	0.3429	0.3365	3898	1255	2546
2.042	1	0.7	1	1.8571	0.5	0.2858	0.2969	2103	1245	2546	6.000	0.5	7.5	0.5	1.8000	0.7	0.2762	0.2662	3369	1140	2273
2.042	1	0.7	1	1.8571	0.7	0.2459	0.2536	1984	1261	2439	6.000	0.5	5	0.5	1.3000	1	0.1816	0.1590	6487	977.5	2457
2.042	1	0.7	1	2.0000	1	0.2067	0.2121	1820	1275	2334	6.000	0.5	5	0.5	1.3000	0.3	0.4398	0.4392	4816	1023	2339
2.042	1	0.7	1	2.0000	0.3	0.3523	0.3686	2238	1251	2670	6.000	0.5	5	0.5	1.3000	0.5	0.3105	0.2984	4011	1078	2290
2.042	1	0.7	1	2.0000	0.5	0.2858	0.2969	2103	1245	2546	6.000	0.5	5	0.5	1.3000	0.7	0.2418	0.2243	3330	1139	2261
2.042	1	0.7	1	2.0000	0.7	0.2459	0.2536	1984	1261	2439	6.000	0.5	5	0.5	1.4000	1	0.1888	0.1680	6570	982.4	2439
2.042	1	0.7	1	2.1429	1	0.2067	0.2121	1820	1275	2334	6.000	0.5	5	0.5	1.4000	0.3	0.4459	0.4452	4849	1032	2325
2.042	1	0.7	1	2.1429	0.3	0.3523	0.3686	2238	1251	2670	6.000	0.5	5	0.5	1.4000	0.5	0.3164	0.3052	3995	1084	2275
2.042	1	0.7	1	2.1429	0.5	0.2858	0.2969	2103	1245	2546	6.000	0.5	5	0.5	1.4000	0.7	0.2485	0.2323	3288	1140	2253
2.042	1	0.7	1	2.1429	0.7	0.2459	0.2536	1984	1261	2439	6.000	0.5	5	0.5	1.5000	1	0.1934	0.1739	6558	991.1	2443
2.042	1	7.5	1	1.4286	1	0.1773	0.1766	1314	1098	2053	6.000	0.5	5	0.5	1.5000	0.3	0.4482	0.4481	4836	1040	2322
2.042	1	7.5	1	1.4286	0.3	0.2941	0.2981	1806	1047	2281	6.000	0.5	5	0.5	1.5000	0.5	0.3199	0.3097	3998	1090	2261
2.042	1	7.5	1	1.4286	0.5	0.2416	0.2430	1615	1061	2186	6.000	0.5	5	0.5	1.5000	0.7	0.2525	0.2371	3256	1140	2248
2.042	1	7.5	1	1.4286	0.7	0.2085	0.2090	1466	1075	2132	6.000	0.5	5	0.5	1.6000	1	0.1963	0.1780	6538	996.8	2445
2.042	1	7.5	1	1.5714	1	0.1773	0.1766	1314	1098	2053	6.000	0.5	5	0.5	1.6000	0.3	0.4497	0.4500	4821	1043	2325
2.042	1	7.5	1	1.5714	0.3	0.2941	0.2981	1806	1047	2281	6.000	0.5	5	0.5	1.6000	0.5	0.3220	0.3126	3980	1098	2258
2.042	1	7.5	1	1.5714	0.5	0.2416	0.2430	1615	1061	2186	6.000	0.5	5	0.5	1.6000	0.7	0.2551	0.2405	3252	1147	2237
2.042	1	7.5	1	1.7143	1	0.1773	0.1766	1314	1098	2053	6.000	0.5	5	0.5	1.7000	1	0.1985	0.1808	6524	1006	2447
2.042	1	7.5	1	1.7143	0.3	0.2941	0.2981	1806	1047	2281	6.000	0.5	5	0.5	1.7000	0.3	0.4507	0.4513	4854	1059	2310
2.042	1	7.5	1	1.7143	0.5	0.2416	0.2430	1615	1061	2186	6.000	0.5	5	0.5	1.7000	0.5	0.3246	0.3149	3964	1102	2257
2.042	1	7.5	1	1.7143	0.7	0.2085	0.2090	1466	1075	2132	6.000	0.5	5	0.5	1.7000	0.7	0.2569	0.2428	3226	1152	2236
2.042	1	7.5	1	1.8571	1	0.1773	0.1766	1314	1098	2053	6.000	0.5	5	0.5	1.8000	1	0.2000	0.1830	6524	1017	2445
2.042	1	7.5	1	1.8571	0.3	0.2941	0.2981	1806	1047	2281	6.000	0.5	5	0.5	1.8000	0.3	0.4519	0.4525	4867	1069	2300
											6.000	0.5	5	0.5	1.8000	0.5	0.3264	0.3166	3942	1105	2259

ODTh	alfa	Eback	beta	TWOD	Ewall	δy(%)	δx(%)	M(lb-in)	V (lb)	Th (lb)	ODTh	alfa	Eback	beta	TWOD	Ewall	δy(%)	δx(%)	M(lb-in)	V (lb)	Th (lb)
2.042	1	7.5	1	1.8571	0.5	0.2416	0.2430	1615	1061	2186	6.000	0.5	5	0.5	1.8000	0.7	0.2581	0.2446	7618	2022	3295
2.042	1	7.5	1	1.8571	0.7	0.2085	0.2090	1466	1075	2132	6.000	0.7	0.7	0.3	1.3000	1	0.3593	0.3349	13280	1683	3558
2.042	1	7.5	1	2.0000	1	0.1773	0.1766	1314	1098	2053	6.000	0.7	0.7	0.3	1.3000	0.3	0.8228	0.8751	10250	1764	3483
2.042	1	7.5	1	2.0000	0.3	0.2941	0.2981	1806	1047	2281	6.000	0.7	0.7	0.3	1.3000	0.5	0.5772	0.5856	8775	1855	3419
2.042	1	7.5	1	2.0000	0.5	0.2416	0.2430	1615	1061	2186	6.000	0.7	0.7	0.3	1.3000	0.7	0.4589	0.4508	7529	2017	3297
2.042	1	7.5	1	2.0000	0.7	0.2085	0.2090	1466	1075	2132	6.000	0.7	0.7	0.3	1.4000	1	0.3593	0.3370	13270	1681	3560
2.042	1	7.5	1	2.1429	1	0.1773	0.1766	1314	1098	2053	6.000	0.7	0.7	0.3	1.4000	0.3	0.8234	0.8770	10190	1766	3488
2.042	1	7.5	1	2.1429	0.3	0.2941	0.2981	1806	1047	2281	6.000	0.7	0.7	0.3	1.4000	0.5	0.5776	0.5885	8705	1850	3420
2.042	1	7.5	1	2.1429	0.5	0.2416	0.2430	1615	1061	2186	6.000	0.7	0.7	0.3	1.4000	0.7	0.4590	0.4530	7460	2012	3298
2.042	1	7.5	1	2.1429	0.7	0.2085	0.2090	1466	1075	2132	6.000	0.7	0.7	0.3	1.5000	1	0.3591	0.3385	13250	1680	3559
2.042	1	5	1	1.4286	1	0.1694	0.1694	1294	1044	1954	6.000	0.7	0.7	0.3	1.5000	0.3	0.8238	0.8783	10140	1770	3497
2.042	1	5	1	1.4286	0.3	0.2807	0.2853	1784	1002	2175	6.000	0.7	0.7	0.3	1.5000	0.5	0.5779	0.5912	8652	1845	3422
2.042	1	5	1	1.4286	0.5	0.2306	0.2328	1588	1011	2090	6.000	0.7	0.7	0.3	1.5000	0.7	0.4589	0.4544	7406	2007	3300
2.042	1	5	1	1.4286	0.7	0.1992	0.2004	1442	1024	2032	6.000	0.7	0.7	0.3	1.6000	1	0.3590	0.3397	13230	1680	3558
2.042	1	5	1	1.5714	1	0.1694	0.1694	1294	1044	1954	6.000	0.7	0.7	0.3	1.6000	0.3	0.8242	0.8794	10100	1778	3505
2.042	1	5	1	1.5714	0.3	0.2807	0.2853	1784	1002	2175	6.000	0.7	0.7	0.3	1.6000	0.5	0.5777	0.5923	8611	1842	3423
2.042	1	5	1	1.5714	0.5	0.2306	0.2328	1588	1011	2090	6.000	0.7	0.7	0.3	1.6000	0.7	0.4589	0.4556	7363	2005	3302
2.042	1	5	1	1.5714	0.7	0.1992	0.2004	1442	1024	2032	6.000	0.7	0.7	0.3	1.7000	1	0.3590	0.3407	13220	1679	3557
2.042	1	5	1	1.7143	1	0.1694	0.1694	1294	1044	1954	6.000	0.7	0.7	0.3	1.7000	0.3	0.8244	0.8803	10040	1791	3513
2.042	1	5	1	1.7143	0.3	0.2807	0.2853	1784	1002	2175	6.000	0.7	0.7	0.3	1.7000	0.5	0.5773	0.5941	8584	1841	3422
2.042	1	5	1	1.7143	0.5	0.2306	0.2328	1588	1011	2090	6.000	0.7	0.7	0.3	1.7000	0.7	0.4589	0.4567	7328	2003	3303
2.042	1	5	1	1.7143	0.7	0.1992	0.2004	1442	1024	2032	6.000	0.7	0.7	0.3	1.8000	1	0.3589	0.3414	13210	1678	3556
2.042	1	5	1	1.8571	1	0.1694	0.1694	1294	1044	1954	6.000	0.7	0.7	0.3	1.8000	0.3	0.8246	0.8810	10020	1790	3512
2.042	1	5	1	1.8571	0.3	0.2807	0.2853	1784	1002	2175	6.000	0.7	0.7	0.3	1.8000	0.5	0.5776	0.5952	8564	1841	3421
2.042	1	5	1	1.8571	0.5	0.2306	0.2328	1588	1011	2090	6.000	0.7	0.7	0.3	1.8000	0.7	0.4590	0.4576	4605	1584	2945
2.042	1	5	1	1.8571	0.7	0.1992	0.2004	1442	1024	2032	6.000	0.7	7.5	0.3	1.3000	1	0.2711	0.2567	7833	1466	3375
2.042	1	5	1	2.0000	1	0.1694	0.1694	1294	1044	1954	6.000	0.7	7.5	0.3	1.3000	0.3	0.5598	0.5625	6136	1519	3131
2.042	1	5	1	2.0000	0.3	0.2807	0.2853	1784	1002	2175	6.000	0.7	7.5	0.3	1.3000	0.5	0.4183	0.4107	4544	1590	2952
2.042	1	5	1	2.0000	0.5	0.2306	0.2328	1588	1011	2090	6.000	0.7	7.5	0.3	1.4000	1	0.2709	0.2571	7934	1482	3356
2.042	1	5	1	2.0000	0.7	0.1992	0.2004	1442	1024	2032	6.000	0.7	7.5	0.3	1.4000	0.3	0.5622	0.5633	6075	1526	3142
2.042	1	5	1	2.1429	1	0.1694	0.1694	1294	1044	1954	6.000	0.7	7.5	0.3	1.4000	0.5	0.4178	0.4106	4509	1600	2956
2.042	1	5	1	2.1429	0.3	0.2807	0.2853	1784	1002	2175	6.000	0.7	7.5	0.3	1.5000	1	0.2707	0.2572	7929	1483	3361
2.042	1	5	1	2.1429	0.5	0.2306	0.2328	1588	1011	2090	6.000	0.7	7.5	0.3	1.5000	0.3	0.5609	0.5621	6028	1534	3151
2.042	1	5	1	2.1429	0.7	0.1992	0.2004	1442	1024	2032	6.000	0.7	7.5	0.3	1.5000	0.5	0.4172	0.4102	5243	1566	3027
2.042	0	0.7	1	1.4286	1	-0.2050	-0.1748	2988	1459	2187	6.000	0.7	7.5	0.3	1.5000	0.7	0.3394	0.3281	4471	1604	2963
2.042	0	0.7	1	1.4286	0.3	0.2965	0.3079	3258	1203	2102	6.000	0.7	7.5	0.3	1.6000	1	0.2705	0.2573	7947	1489	3357
2.042	0	0.7	1	1.4286	0.5	0.0457	0.0666	2592	1276	2115	6.000	0.7	7.5	0.3	1.6000	0.3	0.5612	0.5622	5992	1538	3151
2.042	0	0.7	1	1.4286	0.7	-0.0893	-0.0627	2313	1334	2146	6.000	0.7	7.5	0.3	1.6000	0.5	0.4169	0.4100	5196	1571	3037
2.042	0	0.7	1	1.5714	1	-0.1123	-0.1074	2468	1442	2166	6.000	0.7	7.5	0.3	1.6000	0.7	0.3386	0.3276	4440	1608	2967
2.042	0	0.7	1	1.5714	0.3	0.3655	0.3611	3290	1194	2102	6.000	0.7	7.5	0.3	1.7000	1	0.2703	0.2574	7950	1492	3363
2.042	0	0.7	1	1.5714	0.5	0.1268	0.1273	2547	1269	2109	6.000	0.7	7.5	0.3	1.7000	0.3	0.5609	0.5618	6012	1542	3144
2.042	0	0.7	1	1.5714	0.7	-0.0012	0.0016	2264	1331	2144	6.000	0.7	7.5	0.3	1.7000	0.5	0.4174	0.4099	5159	1574	3043
2.042	0	0.7	1	1.7143	1	-0.0551	-0.0651	2134	1432	2155	6.000	0.7	7.5	0.3	1.7000	0.7	0.3384	0.3278	4411	1611	2972

ODTh	alfa	Eback	beta	TWOD	Ewall	δy(%)	δx(%)	M(lb-in)	V(lb)	Th(lb)	ODTh	alfa	Eback	beta	TWOD	Ewall	δy(%)	δx(%)	M(lb-in)	V(lb)	Th(lb)
2.042	0	0.7	1	1.7143	0.3	0.4062	0.3934	3341	1186	2109	6.000	0.7	7.5	0.3	1.8000	1	0.2701	0.2575	7950	1486	3360
2.042	0	0.7	1	1.7143	0.5	0.1766	0.1665	2520	1274	2113	6.000	0.7	7.5	0.3	1.8000	0.3	0.5607	0.5617	5998	1550	3145
2.042	0	0.7	1	1.7143	0.7	0.0517	0.0415	2216	1325	2141	6.000	0.7	7.5	0.3	1.8000	0.5	0.4174	0.4099	5134	1575	3047
2.042	0	0.7	1	1.8571	1	-0.0170	-0.0361	1967	1425	2150	6.000	0.7	7.5	0.3	1.8000	0.7	0.3382	0.3277	5038	1372	2629
2.042	0	0.7	1	1.8571	0.3	0.4335	0.4159	3399	1182	2112	6.000	0.7	5	0.3	1.3000	1	0.2618	0.2450	8215	1234	2906
2.042	0	0.7	1	1.8571	0.5	0.2092	0.1921	2512	1273	2117	6.000	0.7	5	0.3	1.3000	0.3	0.5578	0.5666	6692	1287	2729
2.042	0	0.7	1	2.0000	1	0.0102	-0.0148	1938	1419	2150	6.000	0.7	5	0.3	1.3000	0.5	0.4113	0.4061	5824	1328	2653
2.042	0	0.7	1	2.0000	0.3	0.4525	0.4323	3453	1184	2116	6.000	0.7	5	0.3	1.3000	0.7	0.3313	0.3197	4961	1372	2627
2.042	0	0.7	1	2.0000	0.5	0.2321	0.2106	2509	1272	2118	6.000	0.7	5	0.3	1.4000	1	0.2620	0.2472	8161	1243	2912
2.042	0	0.7	1	2.0000	0.7	0.1122	0.0892	2170	1319	2139	6.000	0.7	5	0.3	1.4000	0.3	0.5573	0.5665	6637	1296	2732
2.042	0	0.7	1	2.1429	1	0.0307	0.0016	1916	1415	2150	6.000	0.7	5	0.3	1.4000	0.5	0.4114	0.4071	5775	1336	2648
2.042	0	0.7	1	2.1429	0.3	0.4671	0.4459	3505	1190	2120	6.000	0.7	5	0.3	1.4000	0.7	0.3317	0.3210	4897	1375	2626
2.042	0	0.7	1	2.1429	0.5	0.2490	0.2245	2516	1272	2120	6.000	0.7	5	0.3	1.5000	1	0.2620	0.2484	8112	1251	2916
2.042	0	0.7	1	2.1429	0.7	0.1313	0.1047	2155	1320	2136	6.000	0.7	5	0.3	1.5000	0.3	0.5566	0.5662	6585	1301	2734
2.042	0	7.5	1	1.4286	1	0.1015	0.1067	987.9	911	1671	6.000	0.7	5	0.3	1.5000	0.5	0.4111	0.4076	5721	1340	2647
2.042	0	7.5	1	1.4286	0.3	0.2789	0.2897	1852	998	2000	6.000	0.7	5	0.3	1.5000	0.7	0.3318	0.3220	4850	1381	2621
2.042	0	7.5	1	1.4286	0.5	0.1958	0.2068	1504	964	1905	6.000	0.7	5	0.3	1.6000	1	0.2620	0.2493	8071	1257	2925
2.042	0	7.5	1	1.4286	0.7	0.1489	0.1576	1242	932	1778	6.000	0.7	5	0.3	1.6000	0.3	0.5557	0.5654	6543	1308	2738
2.042	0	7.5	1	1.5714	1	0.1213	0.1250	1015	876	1702	6.000	0.7	5	0.3	1.6000	0.5	0.4108	0.4077	5682	1344	2647
2.042	0	7.5	1	1.5714	0.3	0.2884	0.2988	1862	983	2037	6.000	0.7	5	0.3	1.6000	0.7	0.3318	0.3227	4835	1390	2604
2.042	0	7.5	1	1.5714	0.5	0.2130	0.2213	1512	932	1901	6.000	0.7	5	0.3	1.7000	1	0.2624	0.2499	8036	1262	2929
2.042	0	7.5	1	1.5714	0.7	0.1658	0.1727	1271	907	1819	6.000	0.7	5	0.3	1.7000	0.3	0.5550	0.5648	5645	1347	2647
2.042	0	7.5	1	1.7143	1	0.1328	0.1355	1029	860	1736	6.000	0.7	5	0.3	1.7000	0.7	0.3317	0.3231	4806	1395	2601
2.042	0	7.5	1	1.7143	0.3	0.3044	0.3147	1972	963	2027	6.000	0.7	5	0.3	1.8000	1	0.2625	0.2504	7999	1270	2938
2.042	0	7.5	1	1.7143	0.5	0.2233	0.2298	1526	915	1743	6.000	0.7	5	0.3	1.8000	0.3	0.5540	0.5637	6477	1316	2743
2.042	0	7.5	1	1.7143	0.7	0.1756	0.1816	1290	892	1841	6.000	0.7	5	0.3	1.8000	0.5	0.4101	0.4075	5608	1353	2652
2.042	0	7.5	1	1.8571	1	0.1402	0.1427	1039	850	1768	6.000	0.7	5	0.3	1.8000	0.7	0.3315	0.3232	4140	2456	4380
2.042	0	7.5	1	1.8571	0.3	0.3070	0.3168	1975	959	2048	6.000	1	0.7	1	1.3000	1	0.3836	0.3940	6761	2370	4875
2.042	0	7.5	1	1.8571	0.5	0.2337	0.2373	1549	897	1884	6.000	1	0.7	1	1.3000	0.3	0.8284	0.8714	4873	2404	4644
2.042	0	7.5	1	1.8571	0.7	0.1839	0.1882	1306	876	1834	6.000	1	0.7	1	1.3000	0.5	0.6030	0.6272	4325	2434	4524
2.042	0	7.5	1	2.0000	1	0.1457	0.1478	1046	843	1791	6.000	1	0.7	1	1.3000	0.7	0.4849	0.5012	4140	2456	4380
2.042	0	7.5	1	2.0000	0.3	0.3099	0.3190	1986	955	2060	6.000	1	0.7	1	1.4000	1	0.3836	0.3940	6761	2370	4875
2.042	0	7.5	1	2.0000	0.5	0.2374	0.2403	1570	893	1902	6.000	1	0.7	1	1.4000	0.3	0.8284	0.8714	4873	2404	4644
2.042	0	7.5	1	2.0000	0.7	0.1882	0.1921	1313	871	1856	6.000	1	0.7	1	1.4000	0.5	0.6030	0.6272	4325	2434	4524
2.042	0	7.5	1	2.1429	1	0.1506	0.1516	1054	831	1775	6.000	1	0.7	1	1.4000	0.7	0.4849	0.5012	4140	2456	4380
2.042	0	7.5	1	2.1429	0.3	0.3132	0.3216	2008	951	2069	6.000	1	0.7	1	1.5000	1	0.3836	0.3940	6761	2370	4875
2.042	0	7.5	1	2.1429	0.5	0.2420	0.2444	1602	887	1909	6.000	1	0.7	1	1.5000	0.3	0.8284	0.8714	4873	2404	4644
2.042	0	7.5	1	2.1429	0.7	0.1911	0.1947	1318	869	1875	6.000	1	0.7	1	1.5000	0.5	0.6030	0.6272	4325	2434	4524
2.042	0	5	1	1.4286	1	0.0063	0.0129	1017	929	1602	6.000	1	0.7	1	1.5000	0.7	0.4849	0.5012	4140	2456	4380
2.042	0	5	1	1.4286	0.3	0.2424	0.2589	1936	920	1636	6.000	1	0.7	1	1.6000	1	0.3836	0.3940	6761	2370	4875
2.042	0	5	1	1.4286	0.5	0.1356	0.1491	1263	899	1564	6.000	1	0.7	1	1.6000	0.3	0.8284	0.8714	4873	2404	4644
2.042	0	5	1	1.4286	0.7	0.0735	0.0836	1016	897	1555	6.000	1	0.7	1	1.6000	0.5	0.6030	0.6272	4325	2434	4524
2.042	0	5	1	1.5714	1	0.0511	0.0529	905.7	848	1462	6.000	1	0.7	1	1.6000	0.7	0.4849	0.5012	4140	2456	4380
2.042	0	5	1	1.5714	0.3	0.2654	0.2808	2000	894	1689	6.000	1	0.7	1	1.7000	1	0.3836	0.3940	6761	2370	4875
2.042	0	5	1	1.5714	0.5	0.1712	0.1802	1354	848	1506	6.000	1	0.7	1	1.7000	0.3	0.8284	0.8714	4873	2404	4644

ODTh	alfa	Eback	beta	TWOD	Ewall	δy(%)	δx(%)	M(lb-in)	V (lb)	Th (lb)	ODTh	alfa	Eback	beta	TWOD	Ewall	δy(%)	δx(%)	M(lb-in)	V (lb)	Th (lb)
2.042	0	5	1	1.5714	0.7	0.1101	0.1166	1093	841	1455	6.000	1	0.7	1	1.7000	0.5	0.6030	0.6272	4325	2434	4524
2.042	0	5	1	1.7143	1	0.0783	0.0771	886.3	802	1411	6.000	1	0.7	1	1.7000	0.7	0.4849	0.5012	4140	2456	4380
2.042	0	5	1	1.7143	0.3	0.2818	0.2948	2063	873	1719	6.000	1	0.7	1	1.8000	1	0.3836	0.3940	6761	2370	4875
2.042	0	5	1	1.7143	0.5	0.1916	0.1984	1392	821	1539	6.000	1	0.7	1	1.8000	0.3	0.8284	0.8714	4873	2404	4644
2.042	0	5	1	1.7143	0.7	0.1335	0.1371	1134	808	1473	6.000	1	0.7	1	1.8000	0.5	0.6030	0.6272	4325	2434	4524
2.042	0	5	1	1.8571	1	0.0958	0.0927	906.4	775	1421	6.000	1	0.7	1	1.8000	0.7	0.4849	0.5012	3280	2071	3811
2.042	0	5	1	1.8571	0.3	0.2925	0.3038	2117	861	1739	6.000	1	7.5	1	1.3000	1	0.3285	0.3185	6052	1939	4249
2.042	0	5	1	1.8571	0.5	0.2041	0.2091	1469	809	1573	6.000	1	7.5	1	1.3000	0.3	0.6776	0.6819	4409	1983	3981
2.042	0	5	1	1.8571	0.7	0.1499	0.1512	1162	784	1476	6.000	1	7.5	1	1.3000	0.5	0.5042	0.4983	3550	2031	3880
2.042	0	5	1	2.0000	1	0.1078	0.1034	920	758	1435	6.000	1	7.5	1	1.3000	0.7	0.4104	0.4015	3280	2071	3811
2.042	0	5	1	2.0000	0.3	0.2994	0.3095	2138	854	1754	6.000	1	7.5	1	1.4000	1	0.3285	0.3185	6052	1939	4249
2.042	0	5	1	2.0000	0.5	0.2133	0.2175	1540	801	1595	6.000	1	7.5	1	1.4000	0.3	0.6776	0.6819	4409	1983	3981
2.042	0	5	1	2.0000	0.7	0.1605	0.1606	1180	771	1494	6.000	1	7.5	1	1.4000	0.5	0.5042	0.4983	3550	2031	3880
2.042	0	5	1	2.1429	1	0.1173	0.1121	931.1	746	1447	6.000	1	7.5	1	1.4000	0.7	0.4104	0.4015	3280	2071	3811
2.042	0	5	1	2.1429	0.3	0.3040	0.3130	2151	849	1766	6.000	1	7.5	1	1.5000	1	0.3285	0.3185	6052	1939	4249
2.042	0	5	1	2.1429	0.5	0.2200	0.2232	1574	793	1608	6.000	1	7.5	1	1.5000	0.3	0.6776	0.6819	4409	1983	3981
2.042	0	5	1	2.1429	0.7	0.1685	0.1676	1231	764	1517	6.000	1	7.5	1	1.5000	0.5	0.5042	0.4983	3550	2031	3880
2.042	1	0.7	1	1.4286	1	0.1491	0.0311	4461	1483	2254	6.000	1	7.5	1	1.5000	0.7	0.4104	0.4015	3280	2071	3811
2.042	1	0.7	1	1.4286	0.3	0.5226	0.4787	4778	1140	2267	6.000	1	7.5	1	1.6000	1	0.3285	0.3185	6052	1939	4249
2.042	1	0.7	1	1.4286	0.5	0.3301	0.2589	4314	1238	2243	6.000	1	7.5	1	1.6000	0.3	0.6776	0.6819	4409	1983	3981
2.042	1	0.7	1	1.4286	0.7	0.2290	0.1368	4283	1328	2263	6.000	1	7.5	1	1.6000	0.5	0.5042	0.4983	3550	2031	3880
2.042	1	0.7	1	1.5714	1	0.1723	0.0646	3977	1464	2241	6.000	1	7.5	1	1.6000	0.7	0.4104	0.4015	3280	2071	3811
2.042	1	0.7	1	1.5714	0.3	0.5416	0.5026	4646	1144	2244	6.000	1	7.5	1	1.7000	1	0.3285	0.3185	6052	1939	4249
2.042	1	0.7	1	1.5714	0.5	0.3533	0.2881	4042	1244	2213	6.000	1	7.5	1	1.7000	0.3	0.6776	0.6819	4409	1983	3981
2.042	1	0.7	1	1.5714	0.7	0.2531	0.1684	3905	1323	2244	6.000	1	7.5	1	1.7000	0.5	0.5042	0.4983	3550	2031	3880
2.042	1	0.7	1	1.7143	1	0.1864	0.0857	3676	1452	2231	6.000	1	7.5	1	1.7000	0.7	0.4104	0.4015	3280	2071	3811
2.042	1	0.7	1	1.7143	0.3	0.5521	0.5161	4577	1146	2231	6.000	1	7.5	1	1.8000	1	0.3285	0.3185	6052	1939	4249
2.042	1	0.7	1	1.7143	0.5	0.3663	0.3057	3881	1248	2203	6.000	1	7.5	1	1.8000	0.3	0.6776	0.6819	4409	1983	3981
2.042	1	0.7	1	1.7143	0.7	0.2674	0.1883	3675	1321	2231	6.000	1	7.5	1	1.8000	0.5	0.5042	0.4983	3550	2031	3880
2.042	1	0.7	1	1.8571	1	0.1958	0.1009	3464	1446	2225	6.000	1	7.5	1	1.8000	0.7	0.4104	0.4015	3225	1946	3608
2.042	1	0.7	1	1.8571	0.3	0.5583	0.5249	4525	1148	2225	6.000	1	5	1	1.3000	1	0.3124	0.3041	5714	1841	4043
2.042	1	0.7	1	1.8571	0.5	0.3744	0.3174	3772	1250	2197	6.000	1	5	1	1.3000	0.3	0.6440	0.6501	4171	1876	3771
2.042	1	0.7	1	1.8571	0.7	0.2765	0.2020	3521	1319	2224	6.000	1	5	1	1.3000	0.5	0.4793	0.4752	3503	1914	3677
2.042	1	0.7	1	2.0000	1	0.2023	0.1118	3314	1439	2220	6.000	1	5	1	1.3000	0.7	0.3903	0.3831	3225	1946	3608
2.042	1	0.7	1	2.0000	0.3	0.5628	0.5310	4494	1151	2220	6.000	1	5	1	1.4000	1	0.3124	0.3041	5714	1841	4043
2.042	1	0.7	1	2.0000	0.5	0.3798	0.3254	3690	1250	2194	6.000	1	5	1	1.4000	0.3	0.6440	0.6501	4171	1876	3771
2.042	1	0.7	1	2.0000	0.7	0.2828	0.2117	3411	1319	2220	6.000	1	5	1	1.4000	0.5	0.4793	0.4752	3503	1914	3677
2.042	1	0.7	1	2.1429	1	0.2073	0.1207	3200	1435	2216	6.000	1	5	1	1.4000	0.7	0.3903	0.3831	3225	1946	3608
2.042	1	0.7	1	2.1429	0.3	0.5657	0.5354	4468	1154	2217	6.000	1	5	1	1.5000	1	0.3124	0.3041	5714	1841	4043
2.042	1	0.7	1	2.1429	0.5	0.3838	0.3316	3629	1251	2192	6.000	1	5	1	1.5000	0.3	0.6440	0.6501	4171	1876	3771
2.042	1	0.7	1	2.1429	0.7	0.2874	0.2192	3327	1319	2217	6.000	1	5	1	1.5000	0.5	0.4793	0.4752	3503	1914	3677
2.042	1	7.5	1	1.4286	1	0.1693	0.1517	1314	730	1760	6.000	1	5	1	1.5000	0.7	0.3903	0.3831	3225	1946	3608
2.042	1	7.5	1	1.4286	0.3	0.3232	0.3275	1853	906	2099	6.000	1	5	1	1.6000	1	0.3124	0.3041	5714	1841	4043
2.042	1	7.5	1	1.4286	0.5	0.2532	0.2478	1585	832	1962	6.000	1	5	1	1.6000	0.3	0.6440	0.6501	4171	1876	3771
2.042	1	7.5	1	1.4286	0.7	0.2111	0.1998	1440	778	1851	6.000	1	5	1	1.6000	0.5	0.4793	0.4752	3503	1914	3677
2.042	1	7.5	1	1.5714	1	0.1740	0.1593	1225	735	1771	6.000	1	5	1	1.6000	0.7	0.3903	0.3831	3225	1946	3608
2.042	1	7.5	1	1.5714	0.3	0.3336	0.3377	1918	898	2074	6.000	1	5	1	1.7000	1	0.3124	0.3041	5714	1841	4043

ODTh	alfa	Eback	beta	TWOD	Ewall	δy(%)	δx(%)	M(lb-in)	V (lb)	Th (lb)
2.042	1	7.5	1	1.5714	0.5	0.2555	0.2523	1563	838	1981
2.042	1	7.5	1	1.5714	0.7	0.2139	0.2053	1368	787	1871
2.042	1	7.5	1	1.7143	1	0.1761	0.1638	1149	742	1790
2.042	1	7.5	1	1.7143	0.3	0.3389	0.3412	1964	894	2054
2.042	1	7.5	1	1.7143	0.5	0.2558	0.2539	1563	844	1996
2.042	1	7.5	1	1.7143	0.7	0.2153	0.2085	1368	793	1891
2.042	1	7.5	1	1.8571	1	0.1771	0.1665	1101	749	1809
2.042	1	7.5	1	1.8571	0.5	0.2583	0.2562	1576	843	1989
2.042	1	7.5	1	1.8571	0.7	0.2149	0.2096	1366	802	1916
2.042	1	7.5	1	2.0000	1	0.1775	0.1684	1101	757	1840
2.042	1	7.5	1	2.0000	0.3	0.3355	0.3387	1954	904	2085
2.042	1	7.5	1	2.0000	0.5	0.2596	0.2581	1610	843	1990
2.042	1	7.5	1	2.0000	0.7	0.2161	0.2112	1368	803	1919
2.042	1	7.5	1	2.1429	1	0.1778	0.1697	1100	771	1859
2.042	1	7.5	1	2.1429	0.3	0.3339	0.3373	1963	908	2099
2.042	1	7.5	1	2.1429	0.5	0.2609	0.2605	1674	845	1995
2.042	1	7.5	1	2.1429	0.7	0.2168	0.2119	1369	804	1919
2.042	1	5	1	1.4286	1	0.1370	0.1015	1773	640	1602
2.042	1	5	1	1.4286	0.3	0.3423	0.3399	2401	751	1737
2.042	1	5	1	1.4286	0.5	0.2558	0.2391	2106	673	1586
2.042	1	5	1	1.4286	0.7	0.1979	0.1726	1915	642	1555
2.042	1	5	1	1.5714	1	0.1563	0.1249	1671	616	1534
2.042	1	5	1	1.5714	0.3	0.3461	0.3454	2305	757	1749
2.042	1	5	1	1.5714	0.5	0.2627	0.2484	2010	678	1597
2.042	1	5	1	1.5714	0.7	0.2104	0.1879	1826	637	1535
2.042	1	5	1	1.7143	1	0.1663	0.1373	1608	607	1506
2.042	1	5	1	1.7143	0.3	0.3468	0.3468	2246	763	1765
2.042	1	5	1	1.7143	0.5	0.2656	0.2530	1933	685	1616
2.042	1	5	1	1.7143	0.7	0.2153	0.1953	1742	641	1544
2.042	1	5	1	1.8571	1	0.1714	0.1446	1547	632	1502
2.042	1	5	1	1.8571	0.3	0.3463	0.3472	2192	769	1784
2.042	1	5	1	1.8571	0.5	0.2675	0.2563	1877	690	1632
2.042	1	5	1	1.8571	0.7	0.2180	0.1998	1677	647	1557
2.042	1	5	1	2.0000	1	0.1742	0.1494	1490	647	1507
2.042	1	5	1	2.0000	0.3	0.3458	0.3470	2156	773	1796
2.042	1	5	1	2.0000	0.5	0.2681	0.2579	1829	696	1647
2.042	1	5	1	2.0000	0.7	0.2195	0.2028	1622	652	1571
2.042	1	5	1	2.1429	1	0.1757	0.1525	1437	660	1515
2.042	1	5	1	2.1429	0.3	0.3467	0.3483	2151	775	1802
2.042	1	5	1	2.1429	0.5	0.2681	0.2587	1791	701	1661
2.042	1	5	1	2.1429	0.7	0.2202	0.2049	1574	658	1584
2.042	1	0.7	0	1.4286	1	0.1693	0.1517	1314	730	1760
2.042	1	0.7	0	1.4286	0.3	0.3232	0.3275	1853	906	2099
2.042	1	0.7	0	1.4286	0.5	0.2532	0.2478	1585	832	1962

ODTh	alfa	Eback	beta	TWOD	Ewall	δy(%)	δx(%)	M(lb-in)	V (lb)	Th (lb)
6.000	1	5	1	1.7000	0.3	0.6440	0.6501	4171	1876	3771
6.000	1	5	1	1.7000	0.5	0.4793	0.4752	3503	1914	3677
6.000	1	5	1	1.7000	0.7	0.3903	0.3831	3225	1946	3608
6.000	1	5	1	1.8000	1	0.3124	0.3041	5714	1841	4043
6.000	1	5	1	1.8000	0.3	0.6440	0.6501	4171	1876	3771
6.000	1	5	1	1.8000	0.5	0.4793	0.4752	3503	1914	3677
6.000	1	5	1	1.8000	0.7	0.3903	0.3831	3946	1939	2840
6.000	0.3	0.7	0.7	1.3000	1	-0.0586	-0.0891	5179	1601	2820
6.000	0.3	0.7	0.7	1.3000	0.3	0.4874	0.4663	3529	1711	2835
6.000	0.3	0.7	0.7	1.3000	0.5	0.2045	0.1769	3049	1800	2846
6.000	0.3	0.7	0.7	1.3000	0.7	0.0608	0.0309	3464	1925	2837
6.000	0.3	0.7	0.7	1.4000	1	0.0030	-0.0444	5515	1591	2817
6.000	0.3	0.7	0.7	1.4000	0.3	0.5303	0.5036	3664	1702	2831
6.000	0.3	0.7	0.7	1.4000	0.5	0.2571	0.2185	3093	1790	2840
6.000	0.3	0.7	0.7	1.4000	0.7	0.1186	0.0745	3139	1914	2833
6.000	0.3	0.7	0.7	1.5000	1	0.0411	-0.0155	5773	1584	2820
6.000	0.3	0.7	0.7	1.5000	0.3	0.5560	0.5270	3813	1697	2827
6.000	0.3	0.7	0.7	1.5000	0.5	0.2889	0.2449	3153	1782	2837
6.000	0.3	0.7	0.7	1.5000	0.7	0.1541	0.1023	2907	1907	2827
6.000	0.3	0.7	0.7	1.6000	1	0.0667	0.0043	5960	1578	2822
6.000	0.3	0.7	0.7	1.6000	0.3	0.5735	0.5434	3946	1693	2826
6.000	0.3	0.7	0.7	1.6000	0.5	0.3103	0.2632	3224	1776	2834
6.000	0.3	0.7	0.7	1.6000	0.7	0.1776	0.1215	2864	1901	2826
6.000	0.3	0.7	0.7	1.7000	1	0.0852	0.0194	6100	1576	2821
6.000	0.3	0.7	0.7	1.7000	0.3	0.5864	0.5555	4054	1689	2825
6.000	0.3	0.7	0.7	1.7000	0.5	0.3254	0.2768	3283	1761	2837
6.000	0.3	0.7	0.7	1.7000	0.7	0.1942	0.1361	2893	1896	2824
6.000	0.3	0.7	0.7	1.8000	1	0.0992	0.0309	6212	1576	2819
6.000	0.3	0.7	0.7	1.8000	0.3	0.5964	0.5647	4144	1687	2824
6.000	0.3	0.7	0.7	1.8000	0.5	0.3366	0.2870	3337	1757	2839
6.000	0.3	0.7	0.7	1.8000	0.7	0.2069	0.1475	1847	1243	2458
6.000	0.3	7.5	0.7	1.3000	1	0.1690	0.1661	4100	1203	2802
6.000	0.3	7.5	0.7	1.3000	0.3	0.4680	0.4727	2978	1210	2579
6.000	0.3	7.5	0.7	1.3000	0.5	0.3193	0.3163	2417	1239	2489
6.000	0.3	7.5	0.7	1.3000	0.7	0.2401	0.2356	1861	1277	2404
6.000	0.3	7.5	0.7	1.4000	1	0.1860	0.1793	4176	1191	2818
6.000	0.3	7.5	0.7	1.4000	0.3	0.4772	0.4811	3089	1208	2586
6.000	0.3	7.5	0.7	1.4000	0.5	0.3320	0.3281	2456	1241	2489
6.000	0.3	7.5	0.7	1.4000	0.7	0.2534	0.2474	1978	1278	2409
6.000	0.3	7.5	0.7	1.5000	1	0.1956	0.1878	4228	1185	2831
6.000	0.3	7.5	0.7	1.5000	0.3	0.4826	0.4862	3159	1215	2594
6.000	0.3	7.5	0.7	1.5000	0.5	0.3394	0.3349	2559	1245	2492
6.000	0.3	7.5	0.7	1.5000	0.7	0.2626	0.2553	2048	1275	2411
6.000	0.3	7.5	0.7	1.6000	1	0.2020	0.1931	4259	1182	2843

ODTh	alfa	Eback	beta	TWOD	Ewall	δy(%)	δx(%)	M(lb-in)	V (lb)	Th (lb)
2.042	1	0.7	0	1.4286	0.7	0.2111	0.1998	1440	778	1851
2.042	1	0.7	0	1.5714	1	0.1740	0.1593	1225	735	1771
2.042	1	0.7	0	1.5714	0.3	0.3336	0.3377	1918	898	2074
2.042	1	0.7	0	1.5714	0.5	0.2555	0.2523	1563	838	1981
2.042	1	0.7	0	1.5714	0.7	0.2139	0.2053	1368	787	1871
2.042	1	0.7	0	1.7143	1	0.1761	0.1638	1149	742	1790
2.042	1	0.7	0	1.7143	0.3	0.3389	0.3412	1964	894	2054
2.042	1	0.7	0	1.7143	0.5	0.2558	0.2539	1563	844	1996
2.042	1	0.7	0	1.7143	0.7	0.2153	0.2085	1368	793	1891
2.042	1	0.7	0	1.8571	1	0.1771	0.1665	1101	749	1809
2.042	1	0.7	0	1.8571	0.5	0.2583	0.2562	1576	843	1989
2.042	1	0.7	0	1.8571	0.7	0.2149	0.2096	1366	802	1916
2.042	1	0.7	0	2.0000	1	0.1775	0.1684	1101	757	1840
2.042	1	0.7	0	2.0000	0.3	0.3355	0.3387	1954	904	2085
2.042	1	0.7	0	2.0000	0.5	0.2596	0.2581	1610	843	1990
2.042	1	0.7	0	2.0000	0.7	0.2161	0.2112	1368	803	1919
2.042	1	0.7	0	2.1429	1	0.1778	0.1697	1100	771	1859
2.042	1	0.7	0	2.1429	0.3	0.3339	0.3373	1963	908	2099
2.042	1	0.7	0	2.1429	0.5	0.2609	0.2605	1674	845	1995
2.042	1	0.7	0	2.1429	0.7	0.2168	0.2119	1369	804	1919
2.042	1	7.5	0	1.4286	1	0.1973	0.1823	1828	741	1774
2.042	1	7.5	0	1.4286	0.3	0.3513	0.3527	2500	900	2053
2.042	1	7.5	0	1.4286	0.5	0.2806	0.2747	2175	825	1912
2.042	1	7.5	0	1.4286	0.7	0.2362	0.2257	1991	784	1841
2.042	1	7.5	0	1.5714	1	0.1957	0.1828	1731	746	1790
2.042	1	7.5	0	1.5714	0.3	0.3480	0.3498	2418	906	2069
2.042	1	7.5	0	1.5714	0.5	0.2786	0.2742	2089	831	1928
2.042	1	7.5	0	1.5714	0.7	0.2348	0.2260	1900	789	1855
2.042	1	7.5	0	1.7143	1	0.1945	0.1831	1658	751	1802
2.042	1	7.5	0	1.7143	0.3	0.3454	0.3476	2357	910	2081
2.042	1	7.5	0	1.7143	0.5	0.2769	0.2734	2022	835	1941
2.042	1	7.5	0	1.7143	0.7	0.2333	0.2261	1829	794	1867
2.042	1	7.5	0	1.8571	1	0.1933	0.1831	1601	756	1815
2.042	1	7.5	0	1.8571	0.3	0.3436	0.3460	2308	913	2090
2.042	1	7.5	0	1.8571	0.5	0.2751	0.2724	1968	839	1951
2.042	1	7.5	0	1.8571	0.7	0.2325	0.2265	1779	798	1877
2.042	1	7.5	0	2.0000	1	0.1925	0.1831	1557	759	1824
2.042	1	7.5	0	2.0000	0.3	0.3425	0.3448	2274	915	2096
2.042	1	7.5	0	2.0000	0.5	0.2736	0.2713	1925	842	1960
2.042	1	7.5	0	2.0000	0.7	0.2314	0.2263	1737	801	1885
2.042	1	7.5	0	2.1429	1	0.1919	0.1835	1522	762	1832
2.042	1	7.5	0	2.1429	0.3	0.3408	0.3433	2241	918	2105
2.042	1	7.5	0	2.1429	0.5	0.2724	0.2704	1891	845	1967
2.042	1	7.5	0	2.1429	0.7	0.2305	0.2259	1702	804	1893
2.042	1	5	0	1.4286	1	0.2006	0.1741	2392	627	1541
2.042	1	5	0	1.4286	0.3	0.3696	0.3726	3056	770	1738
2.042	1	5	0	1.4286	0.5	0.2904	0.2799	2703	701	1627

ODTh	alfa	Eback	beta	TWOD	Ewall	δy(%)	δx(%)	M(lb-in)	V (lb)	Th (lb)
6.000	0.3	7.5	0.7	1.6000	0.3	0.4863	0.4898	3215	1217	2607
6.000	0.3	7.5	0.7	1.6000	0.5	0.3441	0.3392	2615	1245	2497
6.000	0.3	7.5	0.7	1.6000	0.7	0.2680	0.2603	2097	1284	2411
6.000	0.3	7.5	0.7	1.7000	1	0.2068	0.1976	4286	1183	2849
6.000	0.3	7.5	0.7	1.7000	0.3	0.4890	0.4923	3230	1220	2602
5.217	0.3	7.5	0.7	1.7000	0.5	0.3476	0.3423	2651	1246	2493
5.217	0.3	7.5	0.7	1.7000	0.7	0.2722	0.2645	2126	1283	2419
5.217	0.3	7.5	0.7	1.8000	1	0.2100	0.2006	4304	1184	2859
5.217	0.3	7.5	0.7	1.8000	0.3	0.4907	0.4939	3244	1219	2604
5.217	0.3	7.5	0.7	1.8000	0.5	0.3502	0.3448	2663	1250	2491
5.217	0.3	7.5	0.7	1.8000	0.7	0.2753	0.2673	1605	1159	2152
5.217	0.3	5	0.7	1.3000	1	0.0862	0.0825	3890	1117	2357
5.217	0.3	5	0.7	1.3000	0.3	0.4072	0.4107	2615	1127	2268
5.217	0.3	5	0.7	1.3000	0.5	0.2448	0.2465	2092	1136	2201
5.217	0.3	5	0.7	1.3000	0.7	0.1605	0.1602	1632	1132	2140
5.217	0.3	5	0.7	1.4000	1	0.1172	0.1105	4085	1086	2349
5.217	0.3	5	0.7	1.4000	0.3	0.4318	0.4330	2664	1086	2261
5.217	0.3	5	0.7	1.4000	0.5	0.2708	0.2694	2143	1089	2201
5.217	0.3	5	0.7	1.4000	0.7	0.1888	0.1855	1649	1129	2145
5.217	0.3	5	0.7	1.5000	1	0.1369	0.1283	4210	1066	2348
5.217	0.3	5	0.7	1.5000	0.3	0.4465	0.4475	2826	1062	2268
5.217	0.3	5	0.7	1.5000	0.5	0.2874	0.2840	2173	1073	2207
5.217	0.3	5	0.7	1.5000	0.7	0.2066	0.2017	1661	1130	2154
5.217	0.3	5	0.7	1.6000	1	0.1505	0.1408	4309	1054	2358
5.217	0.3	5	0.7	1.6000	0.3	0.4565	0.4570	2916	1043	2259
5.217	0.3	5	0.7	1.6000	0.5	0.2991	0.2941	2207	1075	2204
5.217	0.3	5	0.7	1.6000	0.7	0.2194	0.2126	1670	1136	2149
5.217	0.3	5	0.7	1.7000	1	0.1605	0.1497	4352	1046	2364
5.217	0.3	5	0.7	1.7000	0.3	0.4632	0.4631	3063	1040	2247
5.217	0.3	5	0.7	1.7000	0.5	0.3089	0.3019	2298	1076	2205
5.217	0.3	5	0.7	1.7000	0.7	0.2283	0.2207	1726	1135	2156
5.217	0.3	5	0.7	1.8000	1	0.1678	0.1565	4391	1042	2375
5.217	0.3	5	0.7	1.8000	0.3	0.4684	0.4679	3134	1052	2246
5.217	0.3	5	0.7	1.8000	0.5	0.3158	0.3081	2370	1080	2202
5.217	0.3	5	0.7	1.8000	0.7	0.2354	0.2268	5818	1929	3013
5.217	0.5	0.7	0.5	1.3000	1	0.2025	0.0813	7606	1561	3004
5.217	0.5	0.7	0.5	1.3000	0.3	0.6434	0.5951	6165	1676	2975
5.217	0.5	0.7	0.5	1.3000	0.5	0.4054	0.3254	5828	1791	3006
5.217	0.5	0.7	0.5	1.3000	0.7	0.2929	0.1926	5446	1917	2986
5.217	0.5	0.7	0.5	1.4000	1	0.2159	0.1009	7549	1560	2982
5.217	0.5	0.7	0.5	1.4000	0.3	0.6554	0.6107	5982	1668	2955
5.217	0.5	0.7	0.5	1.4000	0.5	0.4183	0.3428	5542	1782	2984
5.217	0.5	0.7	0.5	1.4000	0.7	0.3062	0.2110	5195	1909	2972
5.217	0.5	0.7	0.5	1.5000	1	0.2241	0.1140	7518	1553	2982
5.217	0.5	0.7	0.5	1.5000	0.3	0.6617	0.6189	5871	1663	2944
5.217	0.5	0.7	0.5	1.5000	0.5	0.4263	0.3541	5373	1776	2969
5.217	0.5	0.7	0.5	1.5000	0.7	0.3144	0.2230	5026	1903	2961

ODTh	alfa	Eback	beta	TWOD	Ewall	δy(%)	δx(%)	M(lb-in)	V (lb)	Th (lb)	ODTh	alfa	Eback	beta	TWOD	Ewall	δy(%)	δx(%)	M(lb-in)	V (lb)	Th (lb)
2.042	1	5	0	1.4286	0.7	0.2443	0.2270	2543	662	1575	5.217	0.5	0.7	0.5	1.6000	1	0.2297	0.1231	7497	1551	2973
2.042	1	5	0	1.5714	1	0.2007	0.1784	2282	629	1539	5.217	0.5	0.7	0.5	1.6000	0.3	0.6669	0.6257	5802	1661	2933
2.042	1	5	0	1.5714	0.3	0.3668	0.3713	2966	775	1754	5.217	0.5	0.7	0.5	1.6000	0.5	0.4318	0.3620	5252	1771	2960
2.940	1	5	0	1.5714	0.5	0.2882	0.2799	2612	707	1640	5.217	0.5	0.7	0.5	1.6000	0.7	0.3199	0.2315	4903	1900	2953
2.940	1	5	0	1.5714	0.7	0.2425	0.2282	2433	668	1587	5.217	0.5	0.7	0.5	1.7000	1	0.2339	0.1302	7484	1550	2967
2.940	1	5	0	1.7143	1	0.2001	0.1805	2195	633	1546	5.217	0.5	0.7	0.5	1.7000	0.3	0.6705	0.6307	5751	1661	2926
2.940	1	5	0	1.7143	0.3	0.3637	0.3691	2894	781	1769	5.217	0.5	0.7	0.5	1.7000	0.5	0.4359	0.3679	5164	1767	2954
2.940	1	5	0	1.7143	0.5	0.2862	0.2797	2542	712	1652	5.217	0.5	0.7	0.5	1.7000	0.7	0.3239	0.2379	4809	1896	2948
2.940	1	5	0	1.7143	0.7	0.2409	0.2287	2353	673	1596	5.217	0.5	0.7	0.5	1.8000	1	0.2370	0.1356	7472	1549	2964
2.940	1	5	0	1.8571	1	0.1990	0.1816	2115	638	1555	5.217	0.5	0.7	0.5	1.8000	0.3	0.6734	0.6347	5710	1658	2922
2.940	1	5	0	1.8571	0.3	0.3611	0.3672	2833	786	1782	5.217	0.5	0.7	0.5	1.8000	0.5	0.4388	0.3724	5097	1764	2949
2.940	1	5	0	1.8571	0.5	0.2843	0.2792	2474	717	1665	5.217	0.5	0.7	0.5	1.8000	0.7	0.3271	0.2429	2184	1259	2542
2.940	1	5	0	1.8571	0.7	0.2395	0.2288	2289	678	1607	5.217	0.5	7.5	0.5	1.3000	1	0.2167	0.1956	4563	1186	2828
2.940	1	5	0	2.0000	1	0.1980	0.1824	2050	642	1563	5.217	0.5	7.5	0.5	1.3000	0.3	0.5011	0.4972	3398	1228	2609
2.940	1	5	0	2.0000	0.3	0.3586	0.3650	2776	790	1794	5.217	0.5	7.5	0.5	1.3000	0.5	0.3597	0.3448	2651	1219	2595
2.940	1	5	0	2.0000	0.5	0.2830	0.2792	2415	721	1675	5.217	0.5	7.5	0.5	1.3000	0.7	0.2802	0.2637	2130	1262	2535
2.940	1	5	0	2.0000	0.7	0.2379	0.2285	2223	682	1617	5.217	0.5	7.5	0.5	1.4000	1	0.2211	0.2022	4529	1192	2833
2.940	1	5	0	2.1429	1	0.1971	0.1828	1994	646	1573	5.217	0.5	7.5	0.5	1.4000	0.3	0.5032	0.5002	3357	1229	2606
2.940	1	5	0	2.1429	0.3	0.3562	0.3630	2725	794	1804	5.217	0.5	7.5	0.5	1.4000	0.5	0.3634	0.3499	2740	1263	2513
2.940	1	5	0	2.1429	0.5	0.2815	0.2786	2361	725	1686	5.217	0.5	7.5	0.5	1.4000	0.7	0.2880	0.2697	2144	1283	2494
2.940	1	5	0	2.1429	0.7	0.2365	0.2280	2169	686	1627	5.217	0.5	7.5	0.5	1.5000	1	0.2251	0.2062	4504	1194	2838
3.840	1	0.7	1	1.3750	1	0.1816	0.1781	3041	1283	2304	5.217	0.5	7.5	0.5	1.5000	0.3	0.5043	0.5019	3329	1231	2607
3.840	1	0.7	1	1.3750	0.3	0.3156	0.3178	4550	1268	2547	5.217	0.5	7.5	0.5	1.5000	0.5	0.3652	0.3526	2701	1263	2515
3.840	1	0.7	1	1.3750	0.5	0.2547	0.2531	3710	1273	2414	5.217	0.5	7.5	0.5	1.5000	0.7	0.2904	0.2733	2148	1297	2463
3.840	1	0.7	1	1.3750	0.7	0.2172	0.2142	3405	1277	2359	5.217	0.5	7.5	0.5	1.6000	1	0.2279	0.2089	4494	1197	2842
3.840	1	0.7	1	1.5000	1	0.1816	0.1781	3041	1283	2304	5.217	0.5	7.5	0.5	1.6000	0.3	0.5050	0.5030	3308	1232	2610
3.840	1	0.7	1	1.5000	0.3	0.3156	0.3178	4550	1268	2547	5.217	0.5	7.5	0.5	1.6000	0.5	0.3663	0.3544	2676	1263	2515
3.840	1	0.7	1	1.5000	0.5	0.2547	0.2531	3710	1273	2414	5.217	0.5	7.5	0.5	1.6000	0.7	0.2921	0.2760	2120	1297	2463
3.840	1	0.7	1	1.5000	0.7	0.2172	0.2142	3405	1277	2359	5.217	0.5	7.5	0.5	1.7000	1	0.2291	0.2109	4484	1201	2844
3.840	1	0.7	1	1.6250	1	0.1816	0.1781	3041	1283	2304	5.217	0.5	7.5	0.5	1.7000	0.3	0.5056	0.5037	3293	1232	2613
3.840	1	0.7	1	1.6250	0.3	0.3156	0.3178	4550	1268	2547	5.217	0.5	7.5	0.5	1.7000	0.5	0.3670	0.3556	2653	1264	2519
3.840	1	0.7	1	1.6250	0.5	0.2547	0.2531	3710	1273	2414	5.217	0.5	7.5	0.5	1.7000	0.7	0.2933	0.2780	2097	1297	2464
3.840	1	0.7	1	1.6250	0.7	0.2172	0.2142	3405	1277	2359	5.217	0.5	7.5	0.5	1.8000	1	0.2300	0.2124	4473	1204	2847
3.840	1	0.7	1	1.7500	1	0.1816	0.1781	3041	1283	2304	5.217	0.5	7.5	0.5	1.8000	0.3	0.5058	0.5041	3277	1234	2616
3.840	1	0.7	1	1.7500	0.3	0.3156	0.3178	4550	1268	2547	5.217	0.5	7.5	0.5	1.8000	0.5	0.3675	0.3564	2635	1264	2521
3.840	1	0.7	1	1.7500	0.5	0.2547	0.2531	3710	1273	2414	5.217	0.5	7.5	0.5	1.8000	0.7	0.2940	0.2793	2635	1142	2240
3.840	1	0.7	1	1.7500	0.7	0.2172	0.2142	3405	1277	2359	5.217	0.5	5	0.5	1.3000	1	0.1848	0.1466	4525	1007	2489
3.840	1	0.7	1	1.8750	1	0.1816	0.1781	3041	1283	2304	5.217	0.5	5	0.5	1.3000	0.3	0.4724	0.4664	3439	1016	2328
3.840	1	0.7	1	1.8750	0.3	0.3156	0.3178	4550	1268	2547	5.217	0.5	5	0.5	1.3000	0.5	0.3265	0.3050	2969	1086	2261
3.840	1	0.7	1	1.8750	0.5	0.2547	0.2531	3710	1273	2414	5.217	0.5	5	0.5	1.3000	0.7	0.2506	0.2208	2525	1135	2234
3.840	1	0.7	1	1.8750	0.7	0.2172	0.2142	3405	1277	2359	5.217	0.5	5	0.5	1.4000	1	0.1943	0.1596	4657	993.5	2439
3.840	1	0.7	1	2.0000	1	0.1816	0.1781	3041	1283	2304	5.217	0.5	5	0.5	1.4000	0.3	0.4852	0.4783	3423	1023	2312
3.840	1	0.7	1	2.0000	0.3	0.3156	0.3178	4550	1268	2547	5.217	0.5	5	0.5	1.4000	0.5	0.3347	0.3152	2882	1083	2249
3.840	1	0.7	1	2.0000	0.5	0.2547	0.2531	3710	1273	2414	5.217	0.5	5	0.5	1.4000	0.7	0.2596	0.2334	2437	1133	2225
3.840	1	0.7	1	2.0000	0.7	0.2172	0.2142	3405	1277	2359	5.217	0.5	5	0.5	1.5000	1	0.2007	0.1693	4703	1008	2423
3.840	1	7.5	1	1.3750	1	0.1723	0.1681	2801	1221	2196	5.217	0.5	5	0.5	1.5000	0.3	0.4903	0.4833	3387	1029	2310
3.840	1	7.5	1	1.3750	0.3	0.2987	0.2991	4345	1197	2424	5.217	0.5	5	0.5	1.5000	0.5	0.3398	0.3221	2842	1076	2244

ODTh	alfa	Eback	beta	TWOD	Ewall	δy(%)	δx(%)	M(lb-in)	V(lb)	Th(lb)	ODTh	alfa	Eback	beta	TWOD	Ewall	δy(%)	δx(%)	M(lb-in)	V(lb)	Th(lb)
3.840	1	7.5	1	1.3750	0.5	0.2414	0.2385	3499	1207	2300	5.217	0.5	5	0.5	1.5000	0.7	0.2649	0.2405	2370	1127	2229
3.840	1	7.5	1	1.3750	0.7	0.2060	0.2019	3177	1215	2247	5.217	0.5	5	0.5	1.6000	1	0.2044	0.1752	4704	1014	2420
3.840	1	7.5	1	1.5000	1	0.1723	0.1681	2801	1221	2196	5.217	0.5	5	0.5	1.6000	0.3	0.4925	0.4861	3351	1031	2313
3.840	1	7.5	1	1.5000	0.3	0.2987	0.2991	4345	1197	2424	5.217	0.5	5	0.5	1.6000	0.5	0.3428	0.3266	2799	1081	2242
3.840	1	7.5	1	1.5000	0.5	0.2414	0.2385	3499	1207	2300	5.217	0.5	5	0.5	1.6000	0.7	0.2686	0.2459	2336	1128	2221
3.840	1	7.5	1	1.5000	0.7	0.2060	0.2019	3177	1215	2247	5.217	0.5	5	0.5	1.7000	1	0.2075	0.1799	4681	1020	2421
3.840	1	7.5	1	1.6250	1	0.1723	0.1681	2801	1221	2196	5.217	0.5	5	0.5	1.7000	0.3	0.4939	0.4882	3328	1035	2315
3.840	1	7.5	1	1.6250	0.3	0.2987	0.2991	4345	1197	2424	5.217	0.5	5	0.5	1.7000	0.5	0.3448	0.3296	2767	1089	2241
3.840	1	7.5	1	1.6250	0.5	0.2414	0.2385	3499	1207	2300	5.217	0.5	5	0.5	1.7000	0.7	0.2713	0.2500	2299	1132	2217
3.840	1	7.5	1	1.6250	0.7	0.2060	0.2019	3177	1215	2247	5.217	0.5	5	0.5	1.8000	1	0.2098	0.1836	4657	1027	2424
3.840	1	7.5	1	1.7500	1	0.1723	0.1681	2801	1221	2196	5.217	0.5	5	0.5	1.8000	0.3	0.4949	0.4898	3379	1054	2291
3.840	1	7.5	1	1.7500	0.3	0.2987	0.2991	4345	1197	2424	5.217	0.5	5	0.5	1.8000	0.5	0.3483	0.3323	2737	1091	2245
3.840	1	7.5	1	1.7500	0.5	0.2414	0.2385	3499	1207	2300	5.217	0.5	5	0.5	1.8000	0.7	0.2730	0.2529	6038	2075	3208
3.840	1	7.5	1	1.7500	0.7	0.2060	0.2019	3177	1215	2247	5.217	0.7	0.7	0.3	1.3000	1	0.3812	0.3295	9890	1781	3531
3.840	1	7.5	1	1.8750	1	0.1723	0.1681	2801	1221	2196	5.217	0.7	0.7	0.3	1.3000	0.3	0.8965	0.9349	7664	1842	3504
3.840	1	7.5	1	1.8750	0.3	0.2987	0.2991	4345	1197	2424	5.217	0.7	0.7	0.3	1.3000	0.5	0.6176	0.6055	6728	1915	3377
3.840	1	7.5	1	1.8750	0.5	0.2414	0.2385	3499	1207	2300	5.217	0.7	0.7	0.3	1.3000	0.7	0.4878	0.4536	5911	2067	3211
3.840	1	7.5	1	1.8750	0.7	0.2060	0.2019	3177	1215	2247	5.217	0.7	0.7	0.3	1.4000	1	0.3810	0.3334	9858	1780	3526
3.840	1	7.5	1	2.0000	1	0.1723	0.1681	2801	1221	2196	5.217	0.7	0.7	0.3	1.4000	0.3	0.8985	0.9407	7598	1842	3502
3.840	1	7.5	1	2.0000	0.3	0.2987	0.2991	4345	1197	2424	5.217	0.7	0.7	0.3	1.4000	0.5	0.6183	0.6102	6624	1912	3378
3.840	1	7.5	1	2.0000	0.5	0.2414	0.2385	3499	1207	2300	5.217	0.7	0.7	0.3	1.4000	0.7	0.4880	0.4580	5816	2059	3214
3.840	1	7.5	1	2.0000	0.7	0.2060	0.2019	3177	1215	2247	5.217	0.7	0.7	0.3	1.5000	1	0.3808	0.3364	9831	1780	3525
3.840	1	5	1	1.3750	1	0.1688	0.1646	2746	1193	2146	5.217	0.7	0.7	0.3	1.5000	0.3	0.9001	0.9463	7578	1844	3487
3.840	1	5	1	1.3750	0.3	0.2922	0.2924	4252	1170	2371	5.217	0.7	0.7	0.3	1.5000	0.5	0.6194	0.6135	6545	1910	3379
3.840	1	5	1	1.3750	0.5	0.2362	0.2332	3446	1179	2251	5.217	0.7	0.7	0.3	1.5000	0.7	0.4881	0.4612	5741	2055	3216
3.840	1	5	1	1.3750	0.7	0.2017	0.1976	3116	1186	2197	5.217	0.7	0.7	0.3	1.6000	1	0.3806	0.3386	9773	1787	3536
3.840	1	5	1	1.5000	1	0.1688	0.1646	2746	1193	2146	5.217	0.7	0.7	0.3	1.6000	0.3	0.8994	0.9474	7579	1847	3471
3.840	1	5	1	1.5000	0.3	0.2922	0.2924	4252	1170	2371	5.217	0.7	0.7	0.3	1.6000	0.5	0.6207	0.6163	6484	1908	3380
3.840	1	5	1	1.5000	0.5	0.2362	0.2332	3446	1179	2251	5.217	0.7	0.7	0.3	1.6000	0.7	0.4881	0.4638	5682	2052	3218
3.840	1	5	1	1.5000	0.7	0.2017	0.1976	3116	1186	2197	5.217	0.7	0.7	0.3	1.7000	1	0.3805	0.3404	9760	1785	3534
3.840	1	5	1	1.6250	1	0.1688	0.1646	2746	1193	2146	5.217	0.7	0.7	0.3	1.7000	0.3	0.9002	0.9497	7562	1847	3463
3.840	1	5	1	1.6250	0.3	0.2922	0.2924	4252	1170	2371	5.217	0.7	0.7	0.3	1.7000	0.5	0.6214	0.6188	6434	1907	3382
3.840	1	5	1	1.6250	0.5	0.2362	0.2332	3446	1179	2251	5.217	0.7	0.7	0.3	1.7000	0.7	0.4881	0.4658	5628	2047	3221
3.840	1	5	1	1.6250	0.7	0.2017	0.1976	3116	1186	2197	5.217	0.7	0.7	0.3	1.8000	1	0.3803	0.3419	9745	1783	3533
3.840	1	5	1	1.7500	1	0.1688	0.1646	2746	1193	2146	5.217	0.7	0.7	0.3	1.8000	0.3	0.9006	0.9512	7578	1850	3447
3.840	1	5	1	1.7500	0.3	0.2922	0.2924	4252	1170	2371	5.217	0.7	0.7	0.3	1.8000	0.5	0.6226	0.6208	6395	1906	3382
3.840	1	5	1	1.7500	0.5	0.2362	0.2332	3446	1179	2251	5.217	0.7	0.7	0.3	1.8000	0.7	0.4882	0.4676	3393	1546	2907
3.840	1	5	1	1.7500	0.7	0.2017	0.1976	3116	1186	2197	5.217	0.7	7.5	0.3	1.3000	1	0.2861	0.2650	5366	1450	3351
3.840	1	5	1	1.8750	1	0.1688	0.1646	2746	1193	2146	5.217	0.7	7.5	0.3	1.3000	0.3	0.6081	0.6042	4414	1491	3099
3.840	1	5	1	1.8750	0.3	0.2922	0.2924	4252	1170	2371	5.217	0.7	7.5	0.3	1.3000	0.5	0.4477	0.4338	3874	1521	2973
3.840	1	5	1	1.8750	0.5	0.2362	0.2332	3446	1179	2251	5.217	0.7	7.5	0.3	1.3000	0.7	0.3614	0.3434	3323	1554	2916
3.840	1	5	1	1.8750	0.7	0.2017	0.1976	3116	1186	2197	5.217	0.7	7.5	0.3	1.4000	1	0.2861	0.2665	4361	1503	3109
3.840	1	5	1	2.0000	1	0.1688	0.1646	2746	1193	2146	5.217	0.7	7.5	0.3	1.4000	0.5	0.4471	0.4339	3812	1529	2981
3.840	1	5	1	2.0000	0.3	0.2922	0.2924	4252	1170	2371	5.217	0.7	7.5	0.3	1.4000	0.7	0.3610	0.3439	3269	1562	2920
3.840	1	5	1	2.0000	0.5	0.2362	0.2332	3446	1179	2251	5.217	0.7	7.5	0.3	1.5000	1	0.2858	0.2673	5387	1438	3358
3.840	1	5	1	2.0000	0.7	0.2017	0.1976	3116	1186	2197	5.217	0.7	7.5	0.3	1.5000	0.3	0.6055	0.6006	3760	1534	2990

ODTh	alfa	Eback	beta	TWOD	Ewall	δy(%)	δx(%)	M(lb-in)	V(lb)	Th(lb)
3.840	0	0.7	1	1.3750	1	-0.0328	-0.0214	2706	1528	2238
3.840	0	0.7	1	1.3750	0.3	0.3159	0.3153	4933	1160	2229
3.840	0	0.7	1	1.3750	0.5	0.1487	0.1512	3379	1281	2233
3.840	0	0.7	1	1.3750	0.7	0.0532	0.0601	2815	1389	2233
3.840	0	0.7	1	1.5000	1	0.0109	0.0113	2299	1510	2234
3.840	0	0.7	1	1.5000	0.3	0.3412	0.3384	5385	1147	2227
3.840	0	0.7	1	1.5000	0.5	0.1838	0.1794	3459	1267	2228
3.840	0	0.7	1	1.5000	0.7	0.0933	0.0913	2917	1375	2234
3.840	0	0.7	1	1.6250	1	0.0376	0.0320	2357	1497	2231
3.840	0	0.7	1	1.6250	0.3	0.3566	0.3527	5687	1141	2225
3.840	0	0.7	1	1.6250	0.5	0.2042	0.1966	3504	1256	2226
3.840	0	0.7	1	1.6250	0.7	0.1172	0.1105	2977	1364	2231
3.840	0	0.7	1	1.7500	1	0.0555	0.0463	2395	1488	2232
3.840	0	0.7	1	1.7500	0.3	0.3669	0.3626	5887	1136	2225
3.840	0	0.7	1	1.7500	0.5	0.2173	0.2080	3584	1249	2225
3.840	0	0.7	1	1.7500	0.7	0.1330	0.1236	3018	1355	2229
3.840	0	0.7	1	1.8750	1	0.0681	0.0567	2423	1480	2232
3.840	0	0.7	1	1.8750	0.3	0.3745	0.3697	6031	1134	2225
3.840	0	0.7	1	1.8750	0.5	0.2264	0.2160	3732	1243	2224
3.840	0	0.7	1	1.8750	0.7	0.1441	0.1329	3046	1349	2228
3.840	0	0.7	1	2.0000	1	0.0779	0.0650	2444	1473	2231
3.840	0	0.7	1	2.0000	0.3	0.3802	0.3752	6137	1131	2224
3.840	0	0.7	1	2.0000	0.5	0.2331	0.2220	3849	1239	2224
3.840	0	0.7	1	2.0000	0.7	0.1522	0.1399	3067	1343	2227
3.840	0	7.5	1	1.3750	1	0.1174	0.1199	2237	901	1927
3.840	0	7.5	1	1.3750	0.3	0.2811	0.2855	4138	842	2128
3.840	0	7.5	1	1.3750	0.5	0.2059	0.2073	3310	859	2010
3.840	0	7.5	1	1.3750	0.7	0.1587	0.1614	2817	856	1993
3.840	0	7.5	1	1.5000	1	0.1290	0.1299	2288	910	1932
3.840	0	7.5	1	1.5000	0.3	0.2860	0.2901	4194	836	2148
3.840	0	7.5	1	1.5000	0.5	0.2153	0.2162	3345	866	2013
3.840	0	7.5	1	1.5000	0.7	0.1705	0.1712	2872	882	1967
3.840	0	7.5	1	1.6250	1	0.1360	0.1362	2318	914	1934
3.840	0	7.5	1	1.6250	0.3	0.2898	0.2936	4235	841	2156
3.840	0	7.5	1	1.6250	0.5	0.2206	0.2211	3364	874	2019
3.840	0	7.5	1	1.6250	0.7	0.1768	0.1767	2901	886	1968
3.840	0	7.5	1	1.7500	1	0.1408	0.1404	2340	918	1935
3.840	0	7.5	1	1.7500	0.5	0.2244	0.2245	3378	883	2024
3.840	0	7.5	1	1.7500	0.7	0.1813	0.1809	2922	897	1970
3.840	0	7.5	1	1.8750	1	0.1443	0.1434	2356	925	1934
3.840	0	7.5	1	1.8750	0.3	0.2939	0.2973	4264	850	2173
3.840	0	7.5	1	1.8750	0.5	0.2270	0.2268	3387	888	2029
3.840	0	7.5	1	1.8750	0.7	0.1850	0.1839	2938	913	1966
3.840	0	7.5	1	2.0000	1	0.1469	0.1456	2368	932	1933
3.840	0	7.5	1	2.0000	0.3	0.2949	0.2982	4263	851	2180
3.840	0	7.5	1	2.0000	0.5	0.2289	0.2284	3394	897	2035

Right table:

ODTh	alfa	Eback	beta	TWOD	Ewall	δy(%)	δx(%)	M(lb-in)	V(lb)	Th(lb)
5.217	0.7	7.5	0.3	1.5000	0.7	0.3605	0.3441	3227	1568	2928
5.217	0.7	7.5	0.3	1.6000	1	0.2856	0.2679	5412	1416	3352
5.217	0.7	7.5	0.3	1.6000	0.3	0.6052	0.5991	4257	1507	3130
5.217	0.7	7.5	0.3	1.6000	0.5	0.4453	0.4334	3729	1545	3002
5.217	0.7	7.5	0.3	1.6000	0.7	0.3602	0.3441	3198	1577	2934
5.217	0.7	7.5	0.3	1.7000	1	0.2854	0.2681	5429	1433	3350
5.217	0.7	7.5	0.3	1.7000	0.3	0.6060	0.5998	4233	1510	3130
5.217	0.7	7.5	0.3	1.7000	0.5	0.4445	0.4322	3691	1549	3014
5.217	0.7	7.5	0.3	1.7000	0.7	0.3596	0.3439	3167	1579	2942
5.217	0.7	7.5	0.3	1.8000	1	0.2850	0.2681	5425	1453	3355
5.217	0.7	7.5	0.3	1.8000	0.3	0.6054	0.5996	4251	1532	3121
5.217	0.7	7.5	0.3	1.8000	0.5	0.4458	0.4330	3660	1555	3022
5.217	0.7	7.5	0.3	1.8000	0.7	0.3591	0.3440	3875	1343	2588
5.217	0.7	5	0.3	1.3000	1	0.2762	0.2457	6019	1251	2878
5.217	0.7	5	0.3	1.3000	0.3	0.6096	0.6107	4945	1282	2691
5.217	0.7	5	0.3	1.3000	0.5	0.4408	0.4259	4390	1330	2602
5.217	0.7	5	0.3	1.3000	0.7	0.3523	0.3296	3796	1349	2580
5.217	0.7	5	0.3	1.4000	1	0.2764	0.2487	5960	1259	2884
5.217	0.7	5	0.3	1.4000	0.3	0.6088	0.6112	4890	1292	2692
5.217	0.7	5	0.3	1.4000	0.5	0.4412	0.4283	4308	1331	2601
5.217	0.7	5	0.3	1.4000	0.7	0.3529	0.3333	3744	1364	2571
5.217	0.7	5	0.3	1.5000	1	0.2768	0.2509	5917	1266	2890
5.217	0.7	5	0.3	1.5000	0.3	0.6083	0.6115	4840	1301	2694
5.217	0.7	5	0.3	1.5000	0.5	0.4413	0.4298	4243	1335	2601
5.217	0.7	5	0.3	1.5000	0.7	0.3530	0.3354	3700	1383	2561
5.217	0.7	5	0.3	1.6000	1	0.2780	0.2559	5873	1273	2894
5.217	0.7	5	0.3	1.6000	0.3	0.6075	0.6112	4187	1337	2601
5.217	0.7	5	0.3	1.6000	0.7	0.3528	0.3366	3645	1388	2561
5.217	0.7	5	0.3	1.7000	1	0.2781	0.2579	5836	1282	2900
5.217	0.7	5	0.3	1.7000	0.3	0.6065	0.6104	4758	1316	2699
5.217	0.7	5	0.3	1.7000	0.5	0.4409	0.4312	4149	1341	2600
5.217	0.7	5	0.3	1.7000	0.7	0.3528	0.3375	3599	1391	2562
5.217	0.7	5	0.3	1.8000	1	0.2781	0.2590	5804	1288	2908
5.217	0.7	5	0.3	1.8000	0.3	0.6057	0.6097	4724	1323	2703
5.217	0.7	5	0.3	1.8000	0.5	0.4405	0.4313	4119	1346	2600
5.217	0.7	5	0.3	1.8000	0.7	0.3529	0.3384	985.2	127.2	287.7
4.226	1	0.7	1	1.4444	1	0.0361	0.0333	985.2	127.2	287.7
4.226	1	0.7	1	1.5556	1	0.0361	0.0333	2835	962	1851
4.226	1	0.7	1	1.3333	1	0.1519	0.1465	4794	896.3	2085
4.226	1	0.7	1	1.3333	0.3	0.2752	0.2744	3814	919.2	1973
4.226	1	0.7	1	1.3333	0.5	0.2172	0.2129	3294	939.4	1904
4.226	1	0.7	1	1.3333	0.7	0.1834	0.1784	4338	791.6	1856
4.226	1	0.7	1	1.4444	0.3	0.2437	0.2398	2795	567.4	1319
4.226	1	0.7	1	1.4444	0.5	0.1453	0.1370	3296	938.7	1904
4.226	1	0.7	1	1.4444	0.7	0.1834	0.1784	2835	961.9	1852
4.226	1	0.7	1	1.6667	1	0.1519	0.1465	2835	962	1851

ODTh	alfa	Eback	beta	TWOD	Ewall	δy(%)	δx(%)	M(lb-in)	V(lb)	Th(lb)	ODTh	alfa	Eback	beta	TWOD	Ewall	δy(%)	δx(%)	M(lb-in)	V(lb)	Th(lb)
3.840	0	7.5	1	2.0000	0.7	0.1873	0.1859	2949	919	1968	4.226	1	0.7	1	1.7778	1	0.1519	0.1465	3294	939.4	1904
3.840	0	5	1	1.3750	1	0.0575	0.0632	1834	815	1690	4.226	1	0.7	1	1.7778	0.7	0.1834	0.1784	4794	896.2	2085
3.840	0	5	1	1.3750	0.3	0.2490	0.2535	3888	660	1807	4.226	1	0.7	1	1.8889	0.3	0.2752	0.2744	3814	919.2	1973
3.840	0	5	1	1.3750	0.5	0.1598	0.1648	2929	694	1766	4.226	1	0.7	1	1.8889	0.5	0.2172	0.2129	3294	939.4	1904
3.840	0	5	1	1.3750	0.7	0.1081	0.1134	2362	754	1721	4.226	1	0.7	1	1.8889	0.7	0.1834	0.1784	2578	890.8	1743
3.840	0	5	1	1.5000	1	0.0815	0.0842	1929	799	1690	4.226	1	7.5	1	1.3333	1	0.1431	0.1366	4552	832.9	1954
3.840	0	5	1	1.5000	0.3	0.2643	0.2675	4075	676	1808	4.226	1	7.5	1	1.3333	0.3	0.2569	0.2534	3644	847.8	1858
3.840	0	5	1	1.5000	0.5	0.1784	0.1811	3028	703	1765	4.226	1	7.5	1	1.3333	0.5	0.2040	0.1981	3087	868.8	1796
3.840	0	5	1	1.5000	0.7	0.1290	0.1318	2475	751	1728	4.226	1	7.5	1	1.3333	0.7	0.1726	0.1663	2578	890.8	1743
3.840	0	5	1	1.6250	1	0.0962	0.0972	1989	804	1688	4.226	1	7.5	1	1.4444	1	0.1431	0.1366	4552	832.9	1954
3.840	0	5	1	1.6250	0.3	0.2739	0.2766	4181	689	1806	4.226	1	7.5	1	1.4444	0.3	0.2569	0.2534	3644	847.8	1858
3.840	0	5	1	1.6250	0.5	0.1895	0.1908	3083	707	1769	4.226	1	7.5	1	1.4444	0.5	0.2040	0.1981	3087	869.4	1796
3.840	0	5	1	1.6250	0.7	0.1420	0.1432	2544	754	1727	4.226	1	7.5	1	1.4444	0.7	0.1726	0.1663	2578	890.8	1743
3.840	0	5	1	1.7500	1	0.1063	0.1062	2029	812	1687	4.226	1	7.5	1	1.5556	1	0.1431	0.1365	4552	832.9	1954
3.840	0	5	1	1.7500	0.3	0.2790	0.2812	4211	692	1813	4.226	1	7.5	1	1.5556	0.3	0.2569	0.2534	3644	847.8	1858
3.840	0	5	1	1.7500	0.5	0.1970	0.1975	3119	713	1775	4.226	1	7.5	1	1.5556	0.5	0.2040	0.1981	3087	868.6	1796
3.840	0	5	1	1.7500	0.7	0.1510	0.1510	2594	763	1723	4.226	1	7.5	1	1.5556	0.7	0.1726	0.1663	2578	890.8	1743
3.840	0	5	1	1.8750	1	0.1137	0.1127	2058	818	1684	4.226	1	7.5	1	1.6667	1	0.1431	0.1365	4552	832.9	1954
3.840	0	5	1	1.8750	0.3	0.2828	0.2847	4249	698	1823	4.226	1	7.5	1	1.6667	0.3	0.2569	0.2534	3644	847.8	1858
3.840	0	5	1	1.8750	0.5	0.2021	0.2020	3143	719	1780	4.226	1	7.5	1	1.6667	0.5	0.2040	0.1981	3087	868.6	1796
3.840	0	5	1	1.8750	0.7	0.1574	0.1566	2627	770	1726	4.226	1	7.5	1	1.6667	0.7	0.1726	0.1663	2578	890.8	1743
3.840	0	5	1	2.0000	1	0.1192	0.1175	2079	822	1684	4.226	1	7.5	1	1.7778	1	0.1431	0.1365	4553	832.8	1954
3.840	0	5	1	2.0000	0.3	0.2858	0.2875	4278	709	1831	4.226	1	7.5	1	1.7778	0.3	0.2570	0.2534	3644	847.7	1858
3.840	0	5	1	2.0000	0.5	0.2060	0.2056	3177	725	1784	4.226	1	7.5	1	1.7778	0.5	0.2040	0.1981	3087	868.6	1796
3.840	0	5	1	2.0000	0.7	0.1620	0.1607	2652	774	1730	4.226	1	7.5	1	1.7778	0.7	0.1726	0.1663	4552	832.9	1954
3.840	1	0.7	1	1.3750	1	0.1591	0.1139	5012	1520	2282	4.226	1	7.5	1	1.8889	0.3	0.2569	0.2534	3644	847.8	1858
3.840	1	0.7	1	1.3750	0.3	0.4191	0.4083	7458	1095	2341	4.226	1	7.5	1	1.8889	0.7	0.1726	0.1663	3087	868.6	1796
3.840	1	0.7	1	1.3750	0.5	0.2883	0.2633	5803	1222	2324	4.226	1	5	1	1.3333	1	0.1392	0.1326	2523	857.3	1690
3.840	1	0.7	1	1.3750	0.7	0.2197	0.1858	5229	1359	2311	4.226	1	5	1	1.3333	0.3	0.2493	0.2453	4432	809.5	1897
3.840	1	0.7	1	1.5000	1	0.1687	0.1268	4777	1501	2280	4.226	1	5	1	1.3333	0.5	0.1982	0.1922	3556	816	1804
3.840	1	0.7	1	1.5000	0.3	0.4273	0.4174	7530	1092	2326	4.226	1	5	1	1.3333	0.7	0.1678	0.1614	3017	836	1744
3.840	1	0.7	1	1.5000	0.5	0.2970	0.2731	5805	1214	2306	4.226	1	5	1	1.4444	1	0.1392	0.1326	2523	857.2	1690
3.840	1	0.7	1	1.5000	0.7	0.2288	0.1972	5111	1345	2306	4.226	1	5	1	1.4444	0.3	0.2493	0.2453	4432	809.5	1897
3.840	1	0.7	1	1.6250	1	0.1745	0.1349	4630	1487	2280	4.226	1	5	1	1.4444	0.5	0.1982	0.1922	3556	816	1804
3.840	1	0.7	1	1.6250	0.3	0.4324	0.4233	7566	1090	2317	4.226	1	5	1	1.4444	0.7	0.1678	0.1614	3017	836	1744
3.840	1	0.7	1	1.6250	0.5	0.3023	0.2792	5812	1208	2293	4.226	1	5	1	1.5556	1	0.1392	0.1326	2523	857.2	1690
3.840	1	0.7	1	1.6250	0.7	0.2344	0.2043	5042	1335	2302	4.226	1	5	1	1.5556	0.3	0.2493	0.2453	4432	809.5	1897
3.840	1	0.7	1	1.7500	1	0.1784	0.1406	4532	1478	2280	4.226	1	5	1	1.5556	0.5	0.1982	0.1922	3556	816	1804
3.840	1	0.7	1	1.7500	0.3	0.4360	0.4274	7592	1090	2311	4.226	1	5	1	1.5556	0.7	0.1678	0.1614	3017	836	1744
3.840	1	0.7	1	1.7500	0.5	0.3058	0.2833	5819	1204	2284	4.226	1	5	1	1.6667	1	0.1392	0.1326	2523	857.2	1690
3.840	1	0.7	1	1.7500	0.7	0.2382	0.2092	5001	1328	2298	4.226	1	5	1	1.6667	0.3	0.2493	0.2453	4432	809.5	1897
3.840	1	0.7	1	1.8750	1	0.1812	0.1446	4461	1470	2280	4.226	1	5	1	1.6667	0.5	0.1982	0.1922	3556	816	1804
3.840	1	0.7	1	1.8750	0.3	0.4385	0.4304	7609	1089	2307	4.226	1	5	1	1.6667	0.7	0.1678	0.1614	3017	836	1744
3.840	1	0.7	1	1.8750	0.5	0.3084	0.2863	5829	1201	2275	4.226	1	5	1	1.7778	1	0.1392	0.1326	2523	857.3	1690
3.840	1	0.7	1	1.8750	0.7	0.2409	0.2127	4975	1323	2294	4.226	1	5	1	1.7778	0.3	0.2493	0.2453	4432	809.5	1897
3.840	1	0.7	1	2.0000	1	0.1832	0.1477	4409	1464	2280	4.226	1	5	1	1.7778	0.5	0.1982	0.1922	3556	816	1804
3.840	1	0.7	1	2.0000	0.3	0.4403	0.4326	7618	1089	2304	4.226	1	5	1	1.7778	0.7	0.1678	0.1614	3017	836	1744

ODTh	alfa	Eback	beta	TWOD	Ewall	δy(%)	δx(%)	M(lb-in)	V (lb)	Th (lb)	ODTh	alfa	Eback	beta	TWOD	Ewall	δy(%)	δx(%)	M(lb-in)	V (lb)	Th (lb)
3.840	1	0.7	1	2.0000	0.5	0.3103	0.2885	5831	1199	2271	4.226	1	5	1	1.8889	1	0.1392	0.1326	2523	857.2	1690
3.840	1	0.7	1	2.0000	0.7	0.2429	0.2153	4957	1319	2290	4.226	1	5	1	1.8889	0.3	0.2493	0.2453	4432	809.5	1897
3.840	1	7.5	1	1.3750	1	0.1534	0.1454	2443	895	1987	4.226	1	5	1	1.8889	0.5	0.1982	0.1922	3556	816	1804
3.840	1	7.5	1	1.3750	0.3	0.3056	0.3056	4403	834	2161	4.226	1	5	1	1.8889	0.7	0.1678	0.1614	3017	836	1744
3.840	1	7.5	1	1.3750	0.5	0.2341	0.2303	3435	837	2068	4.226	1	0.7	1	1.3333	1	0.1600	0.1541	2269	1840	968.7
3.840	1	7.5	1	1.3750	0.7	0.1922	0.1861	3006	862	2021	4.226	1	0.7	1	1.3333	0.3	0.2972	0.2965	3773	2697	914.3
3.840	1	7.5	1	1.5000	1	0.1574	0.1499	2452	916	1969	4.226	1	0.7	1	1.3333	0.5	0.2317	0.2273	3034	1971	927.6
3.840	1	7.5	1	1.5000	0.3	0.3064	0.3070	4362	844	2170	4.226	1	0.7	1	1.3333	0.7	0.1944	0.1890	2639	1900	946.9
3.840	1	7.5	1	1.5000	0.5	0.2388	0.2345	3498	870	2046	4.226	1	0.7	1	1.4444	1	0.1599	0.1541	2268	1842	967.7
3.840	1	7.5	1	1.5000	0.7	0.1955	0.1898	3015	878	2009	4.226	1	0.7	1	1.4444	0.3	0.2972	0.2965	3773	2697	914.3
3.840	1	7.5	1	1.6250	1	0.1598	0.1526	2457	928	1959	4.226	1	0.7	1	1.4444	0.5	0.2317	0.2273	3034	1971	927.6
3.840	1	7.5	1	1.6250	0.3	0.3068	0.3077	4335	849	2176	4.226	1	0.7	1	1.4444	0.7	0.1944	0.1890	2639	1900	946.9
3.840	1	7.5	1	1.6250	0.5	0.2404	0.2364	3491	880	2044	4.226	1	0.7	1	1.5556	0.3	0.2972	0.2965	3773	2697	914.3
3.840	1	7.5	1	1.6250	0.7	0.1975	0.1923	3020	883	2007	4.226	1	0.7	1	1.5556	0.5	0.2317	0.2273	3034	1971	927.6
3.840	1	7.5	1	1.7500	1	0.1610	0.1544	2459	930	1958	4.226	1	0.7	1	1.5556	0.7	0.1944	0.1890	2639	1900	946.9
3.840	1	7.5	1	1.7500	0.3	0.3066	0.3077	4311	853	2184	4.226	1	0.7	1	1.6667	1	0.1599	0.1541	2268	1842	967.7
3.840	1	7.5	1	1.7500	0.5	0.2414	0.2375	3484	888	2045	4.226	1	0.7	1	1.6667	0.3	0.1515	0.1429	2199	1255	490.5
3.840	1	7.5	1	1.7500	0.7	0.1999	0.1945	3026	903	1994	4.226	1	0.7	1	1.6667	0.7	0.1945	0.1891	2644	1899	948.7
3.840	1	7.5	1	1.8750	1	0.1619	0.1556	2460	932	1963	4.226	1	0.7	1	1.7778	1	0.1599	0.1541	2269	1842	967.8
3.840	1	7.5	1	1.8750	0.3	0.3061	0.3075	4283	854	2192	4.226	1	0.7	1	1.7778	0.5	0.2317	0.2273	3034	1971	927.6
3.840	1	7.5	1	1.8750	0.5	0.2418	0.2381	3469	892	2049	4.226	1	0.7	1	1.7778	0.7	0.1944	0.1890	2639	1900	946.9
3.840	1	7.5	1	1.8750	0.7	0.2012	0.1957	3030	917	1988	4.226	1	0.7	1	1.8889	1	0.1599	0.1541	2268	1842	967.9
3.840	1	7.5	1	2.0000	1	0.1627	0.1567	2461	940	1962	4.226	1	0.7	1	1.8889	0.3	0.2972	0.2965	3773	2697	914.3
3.840	1	7.5	1	2.0000	0.5	0.2421	0.2385	3458	898	2052	4.226	1	0.7	1	1.8889	0.5	0.2317	0.2273	3034	1971	927.6
3.840	1	7.5	1	2.0000	0.7	0.2018	0.1965	3031	923	1989	4.226	1	0.7	1	1.8889	0.7	0.1944	0.1890	2639	1900	946.9
3.840	1	5	1	1.3750	1	0.1314	0.1173	2611	783	1786	4.226	1	7.5	1	1.3333	1	0.1507	0.1434	2036	1730	893.3
3.840	1	5	1	1.3750	0.3	0.2962	0.2940	4584	625	1859	4.226	1	7.5	1	1.3333	0.3	0.2776	0.2736	3594	2489	861.7
3.840	1	5	1	1.3750	0.5	0.2196	0.2115	3593	689	1798	4.226	1	7.5	1	1.3333	0.5	0.2176	0.2113	2833	1852	852.1
3.840	1	5	1	1.3750	0.7	0.1735	0.1627	3038	732	1796	4.226	1	7.5	1	1.4444	1	0.1507	0.1434	2036	1730	893.3
3.840	1	5	1	1.5000	1	0.1394	0.1265	2580	774	1765	4.226	1	7.5	1	1.4444	0.3	0.2776	0.2736	3594	2489	861.7
3.840	1	5	1	1.5000	0.3	0.3012	0.2994	4612	643	1854	4.226	1	7.5	1	1.4444	0.5	0.2176	0.2113	2833	1852	852.1
3.840	1	5	1	1.5000	0.5	0.2248	0.2173	3602	686	1787	4.226	1	7.5	1	1.4444	0.7	0.1828	0.1759	2385	1782	871.5
3.840	1	5	1	1.5000	0.7	0.1801	0.1703	3011	722	1784	4.226	1	7.5	1	1.5556	1	0.1507	0.1434	2036	1730	893.3
3.840	1	5	1	1.6250	1	0.1441	0.1322	2539	769	1754	4.226	1	7.5	1	1.5556	0.3	0.2776	0.2736	3594	2489	861.7
3.840	1	5	1	1.6250	0.3	0.3040	0.3025	4622	663	1850	4.226	1	7.5	1	1.5556	0.5	0.2176	0.2113	2833	1852	852.1
3.840	1	5	1	1.6250	0.5	0.2279	0.2209	3590	692	1790	4.226	1	7.5	1	1.5556	0.7	0.1828	0.1759	2385	1782	871.5
3.840	1	5	1	1.6250	0.7	0.1843	0.1751	3004	727	1775	4.226	1	7.5	1	1.6667	1	0.1507	0.1434	2036	1730	893.3
3.840	1	5	1	1.7500	1	0.1474	0.1362	2513	786	1745	4.226	1	7.5	1	1.6667	0.3	0.2776	0.2736	3594	2489	861.7
3.840	1	5	1	1.7500	0.3	0.3051	0.3038	4617	676	1851	4.226	1	7.5	1	1.6667	0.5	0.2176	0.2113	2833	1852	852.1
3.840	1	5	1	1.7500	0.5	0.2301	0.2237	3579	704	1790	4.226	1	7.5	1	1.6667	0.7	0.1828	0.1759	2385	1782	871.5
3.840	1	5	1	1.7500	0.7	0.1873	0.1784	3019	745	1759	4.226	1	7.5	1	1.7778	1	0.1507	0.1434	2036	1730	893.3
3.840	1	5	1	1.8750	1	0.1496	0.1390	2488	795	1741	4.226	1	7.5	1	1.7778	0.3	0.2776	0.2736	3594	2489	861.7
3.840	1	5	1	1.8750	0.3	0.3058	0.3046	4606	687	1852	4.226	1	7.5	1	1.7778	0.5	0.2176	0.2113	2833	1852	852.1
3.840	1	5	1	1.8750	0.5	0.2315	0.2257	3560	714	1790	4.226	1	7.5	1	1.7778	0.7	0.1828	0.1759	2385	1782	871.5
3.840	1	5	1	1.8750	0.7	0.1891	0.1806	3008	755	1756	4.226	1	7.5	1	1.8889	1	0.1507	0.1434	2036	1730	893.3
3.840	1	5	1	2.0000	1	0.1513	0.1411	2472	804	1739	4.226	1	7.5	1	1.8889	0.3	0.2776	0.2736	3594	2489	861.7
3.840	1	5	1	2.0000	0.3	0.3058	0.3049	4582	694	1859	4.226	1	7.5	1	1.8889	0.5	0.2176	0.2113	2833	1852	852.1

ODTh	alfa	Eback	beta	TWOD	Ewall	δy(%)	δx(%)	M(lb-in)	V(lb)	Th(lb)	ODTh	alfa	Eback	beta	TWOD	Ewall	δy(%)	δx(%)	M(lb-in)	V(lb)	Th(lb)
3.840	1	5	1	2.0000	0.5	0.2326	0.2271	3545	723	1793	4.226	1	7.5	1	1.8889	0.7	0.1828	0.1759	2385	1782	871.5
3.840	1	5	1	2.0000	0.7	0.1907	0.1825	3006	765	1752	4.226	1	5	1	1.3333	1	0.1466	0.1393	1989	1676	859.3
3.840	1	0.7	0	1.3750	1	0.2418	0.2186	5702	1338	2068	4.226	1	5	1	1.3333	0.3	0.2696	0.2652	3502	2401	836.8
3.840	1	0.7	0	1.3750	0.3	0.4625	0.4800	8692	880	2357	4.226	1	5	1	1.3333	0.5	0.2115	0.2050	2766	1798	819.9
3.840	1	0.7	0	1.3750	0.5	0.3546	0.3510	7179	1025	2227	4.226	1	5	1	1.3333	0.7	0.1777	0.1708	2330	1729	838.1
3.840	1	0.7	0	1.3750	0.7	0.2958	0.2809	6420	1167	2150	4.226	1	5	1	1.4444	1	0.1466	0.1393	1989	1676	859.3
3.840	1	0.7	0	1.5000	1	0.2417	0.2200	5646	1326	2072	3.375	1	5	1	1.4444	0.3	0.2694	0.2651	3500	2400	837.3
3.840	1	0.7	0	1.5000	0.3	0.4634	0.4821	8695	878	2356	3.375	1	5	1	1.4444	0.5	0.2115	0.2050	2766	1798	819.9
3.840	1	0.7	0	1.5000	0.5	0.3548	0.3527	7152	1020	2228	3.375	1	5	1	1.4444	0.7	0.1777	0.1708	2330	1729	838.1
3.840	1	0.7	0	1.5000	0.7	0.2956	0.2822	6372	1158	2153	3.375	1	5	1	1.5556	1	0.1466	0.1393	1989	1676	859.3
3.840	1	0.7	0	1.6250	1	0.2415	0.2211	5603	1316	2075	3.375	1	5	1	1.5556	0.3	0.2694	0.2651	3500	2400	837.3
3.840	1	0.7	0	1.6250	0.3	0.4641	0.4836	8695	876	2355	3.375	1	5	1	1.5556	0.5	0.2115	0.2050	2766	1798	819.9
3.840	1	0.7	0	1.6250	0.5	0.3550	0.3539	7132	1018	2228	3.375	1	5	1	1.5556	0.7	0.1777	0.1708	2330	1729	838.1
3.840	1	0.7	0	1.6250	0.7	0.2953	0.2831	6336	1151	2157	3.375	1	5	1	1.6667	1	0.1466	0.1393	1989	1676	859.3
3.840	1	0.7	0	1.7500	1	0.2413	0.2218	5569	1309	2077	3.375	1	5	1	1.6667	0.3	0.2694	0.2651	3500	2400	837.3
3.840	1	0.7	0	1.7500	0.3	0.4646	0.4848	8694	875	2354	3.375	1	5	1	1.6667	0.5	0.2115	0.2050	2766	1798	819.9
3.840	1	0.7	0	1.7500	0.5	0.3552	0.3549	7118	1015	2229	3.375	1	5	1	1.6667	0.7	0.1777	0.1708	2330	1729	838.1
3.840	1	0.7	0	1.7500	0.7	0.2951	0.2838	6308	1145	2160	3.375	1	5	1	1.7778	1	0.1466	0.1393	1989	1676	859.3
3.840	1	0.7	0	1.8750	1	0.2411	0.2224	5542	1303	2079	3.375	1	5	1	1.7778	0.3	0.2694	0.2651	3500	2400	837.3
3.840	1	0.7	0	1.8750	0.3	0.4650	0.4857	8690	874	2353	3.375	1	5	1	1.7778	0.5	0.2115	0.2050	2766	1798	819.9
3.840	1	0.7	0	1.8750	0.5	0.3553	0.3556	7106	1014	2229	3.375	1	5	1	1.7778	0.7	0.1777	0.1708	2330	1729	838.1
3.840	1	0.7	0	1.8750	0.7	0.2950	0.2843	6283	1141	2162	3.375	1	5	1	1.8889	1	0.1466	0.1393	1989	1676	859.3
3.840	1	0.7	0	2.0000	1	0.2410	0.2228	5520	1298	2081	3.375	1	5	1	1.8889	0.3	0.2694	0.2651	3500	2400	837.3
3.840	1	0.7	0	2.0000	0.3	0.4653	0.4864	8687	873	2352	3.375	1	5	1	1.8889	0.5	0.2115	0.2050	2766	1798	819.9
3.840	1	0.7	0	2.0000	0.5	0.3554	0.3563	7096	1013	2229	3.375	1	5	1	1.8889	0.7	0.1777	0.1708	2330	1729	838.1
3.840	1	0.7	0	2.0000	0.7	0.2948	0.2847	6264	1137	2164	3.375	0.3	0.7	0.7	1.3333	1	-0.0331	-0.0202	2956	2683	1762
3.840	1	7.5	0	1.3750	1	0.1710	0.1630	3043	916	1956	3.375	0.3	0.7	0.7	1.3333	0.3	0.4355	0.4405	5995	4338	1443
3.840	1	7.5	0	1.3750	0.3	0.3091	0.3107	4801	824	2198	3.375	0.3	0.7	0.7	1.3333	0.5	0.2018	0.2070	3681	2666	1565
3.840	1	7.5	0	1.3750	0.5	0.2451	0.2418	3989	853	2076	3.375	0.3	0.7	0.7	1.3333	0.7	0.0760	0.0849	3046	2683	1638
3.840	1	7.5	0	1.3750	0.7	0.2065	0.2006	3483	881	2012	3.375	0.3	0.7	0.7	1.4444	1	0.0247	0.0211	2497	2678	1748
3.840	1	7.5	0	1.5000	1	0.1709	0.1637	2992	921	1960	3.375	0.3	0.7	0.7	1.4444	0.3	0.4726	0.4737	6460	4474	1427
3.840	1	7.5	0	1.5000	0.3	0.3078	0.3098	4732	826	2205	3.375	0.3	0.7	0.7	1.4444	0.5	0.2496	0.2440	3966	2781	1551
3.840	1	7.5	0	1.5000	0.5	0.2451	0.2422	3950	862	2077	3.375	0.3	0.7	0.7	1.4444	0.7	0.1299	0.1251	3120	2678	1639
3.840	1	7.5	0	1.5000	0.7	0.2065	0.2012	3438	887	2014	3.375	0.3	0.7	0.7	1.5556	1	0.0597	0.0470	2551	2675	1739
3.840	1	7.5	0	1.6250	1	0.1708	0.1642	2953	925	1961	3.375	0.3	0.7	0.7	1.5556	0.3	0.4943	0.4943	6805	4555	1421
3.840	1	7.5	0	1.6250	0.3	0.3081	0.3100	4714	838	2204	3.375	0.3	0.7	0.7	1.5556	0.5	0.2770	0.2666	4196	2852	1544
3.840	1	7.5	0	1.6250	0.5	0.2451	0.2424	3926	868	2076	3.375	0.3	0.7	0.7	1.5556	0.7	0.1615	0.1503	3167	2674	1627
3.840	1	7.5	0	1.6250	0.7	0.2064	0.2016	3407	893	2012	3.375	0.3	0.7	0.7	1.6667	1	0.0830	0.0650	2639	2672	1733
3.840	1	7.5	0	1.7500	1	0.1707	0.1646	2921	929	1963	3.375	0.3	0.7	0.7	1.6667	0.3	0.5091	0.5084	7050	4610	1415
3.840	1	7.5	0	1.7500	0.3	0.3076	0.3096	4680	842	2207	3.375	0.3	0.7	0.7	1.6667	0.5	0.2948	0.2816	4390	2898	1530
3.840	1	7.5	0	1.7500	0.5	0.2451	0.2425	3903	874	2077	3.375	0.3	0.7	0.7	1.6667	0.7	0.1825	0.1671	3299	2672	1620
3.840	1	7.5	0	1.7500	0.7	0.2064	0.2018	3384	898	2011	3.375	0.3	0.7	0.7	1.7778	1	0.0995	0.0780	2715	2670	1727
3.840	1	7.5	0	1.8750	1	0.1706	0.1649	2896	931	1964	3.375	0.3	0.7	0.7	1.7778	0.3	0.5197	0.5185	7224	4649	1411
3.840	1	7.5	0	1.8750	0.3	0.3069	0.3091	4649	844	2211	3.375	0.3	0.7	0.7	1.7778	0.5	0.3076	0.2930	4559	2932	1530
3.840	1	7.5	0	1.8750	0.5	0.2449	0.2425	3879	877	2078	3.375	0.3	0.7	0.7	1.7778	0.7	0.1972	0.1793	3423	2671	1612
3.840	1	7.5	0	1.8750	0.7	0.2063	0.2020	3363	899	2012	3.375	0.3	0.7	0.7	1.8889	1	0.1119	0.0883	2778	2669	1722

ODTh	alfa	Eback	beta	TWOD	Ewall	δy(%)	δx(%)	M(lb-in)	V (lb)	Th (lb)	ODTh	alfa	Eback	beta	TWOD	Ewall	δy(%)	δx(%)	M(lb-in)	V (lb)	Th (lb)
3.840	1	7.5	0	2.0000	1	0.1705	0.1651	2875	932	1964	3.375	0.3	0.7	0.7	1.8889	0.3	0.5277	0.5263	7354	4678	1407
3.840	1	7.5	0	2.0000	0.3	0.3063	0.3085	4620	846	2214	3.375	0.3	0.7	0.7	1.8889	0.5	0.3169	0.3013	4692	2956	1525
3.840	1	7.5	0	2.0000	0.5	0.2454	0.2428	3881	886	2074	3.375	0.3	0.7	0.7	1.8889	0.7	0.2078	0.1882	3520	2672	1596
3.840	1	7.5	0	2.0000	0.7	0.2061	0.2020	3344	902	2013	3.375	0.3	7.5	0.7	1.3333	1	0.1412	0.1410	2256	2214	1198
3.840	1	5	0	1.3750	1	0.1663	0.1527	3394	776	1728	3.375	0.3	7.5	0.7	1.3333	0.3	0.3643	0.3640	4925	3519	1257
3.840	1	5	0	1.3750	0.3	0.3086	0.3114	5291	632	1918	3.375	0.3	7.5	0.7	1.3333	0.5	0.2569	0.2554	3372	2362	1212
3.840	1	5	0	1.3750	0.5	0.2420	0.2368	4394	683	1814	3.375	0.3	7.5	0.7	1.3333	0.7	0.1949	0.1949	2876	2252	1202
3.339	1	5	0	1.3750	0.7	0.2030	0.1935	3866	730	1756	3.375	0.3	7.5	0.7	1.4444	1	0.1536	0.1519	2290	2218	1142
3.339	1	5	0	1.5000	1	0.1667	0.1548	3358	783	1730	3.375	0.3	7.5	0.7	1.4444	0.3	0.3721	0.3709	5010	3566	1228
3.339	1	5	0	1.5000	0.3	0.3083	0.3116	5244	642	1923	3.375	0.3	7.5	0.7	1.4444	0.5	0.2672	0.2643	3461	2404	1169
3.339	1	5	0	1.5000	0.5	0.2422	0.2382	4364	691	1819	3.375	0.3	7.5	0.7	1.4444	0.7	0.2060	0.2046	2910	2251	1154
3.339	1	5	0	1.5000	0.7	0.2033	0.1951	3840	736	1761	3.375	0.3	7.5	0.7	1.5556	1	0.1613	0.1588	2312	2209	1106
3.339	1	5	0	1.6250	1	0.1669	0.1564	3323	788	1732	3.375	0.3	7.5	0.7	1.5556	0.3	0.3760	0.3747	5028	3592	1214
3.339	1	5	0	1.6250	0.3	0.3085	0.3120	5220	653	1923	3.375	0.3	7.5	0.7	1.5556	0.7	0.2148	0.2118	2933	2222	1114
3.339	1	5	0	1.6250	0.5	0.2423	0.2391	4337	697	1823	3.375	0.3	7.5	0.7	1.6667	1	0.1663	0.1635	2325	2214	1094
3.339	1	5	0	1.6250	0.7	0.2034	0.1963	3813	740	1764	3.375	0.3	7.5	0.7	1.6667	0.3	0.3787	0.3771	5058	3612	1202
3.339	1	5	0	1.7500	1	0.1671	0.1576	3288	791	1732	3.375	0.3	7.5	0.7	1.6667	0.5	0.2767	0.2729	3545	2445	1129
3.339	1	5	0	1.7500	0.3	0.3085	0.3123	5201	662	1923	3.375	0.3	7.5	0.7	1.6667	0.7	0.2193	0.2159	2947	2223	1095
3.339	1	5	0	1.7500	0.5	0.2421	0.2395	4305	702	1827	3.375	0.3	7.5	0.7	1.7778	1	0.1703	0.1671	2335	2196	1099
3.339	1	5	0	1.7500	0.7	0.2035	0.1971	3778	745	1767	3.375	0.3	7.5	0.7	1.7778	0.3	0.3809	0.3790	5087	3625	1196
3.339	1	5	0	1.8750	1	0.1671	0.1584	3262	795	1735	3.375	0.3	7.5	0.7	1.7778	0.7	0.2224	0.2187	2957	2225	1081
3.339	1	5	0	1.8750	0.3	0.3080	0.3121	5165	667	1926	3.375	0.3	7.5	0.7	1.8889	1	0.1734	0.1702	2343	2196	1102
3.339	1	5	0	1.8750	0.5	0.2419	0.2398	4272	707	1830	3.375	0.3	7.5	0.7	1.8889	0.5	0.2815	0.2774	3584	2466	1108
3.339	1	5	0	1.8750	0.7	0.2035	0.1977	3750	748	1769	3.375	0.3	7.5	0.7	1.8889	0.7	0.2247	0.2207	2963	2232	1072
3.339	1	5	0	2.0000	1	0.1672	0.1591	3236	797	1735	3.375	0.3	5	0.7	1.3333	1	0.1420	0.1437	3269	3264	1826
3.339	1	5	0	2.0000	0.3	0.3076	0.3119	5135	672	1928	3.375	0.3	5	0.7	1.3333	0.3	0.4494	0.4562	7603	5873	1900
3.339	1	0.7	1	1.3750	1	0.1903	0.1871	2436	1287	2306	3.375	0.3	5	0.7	1.3333	0.5	0.3011	0.3042	5046	3986	1825
3.339	1	0.7	1	1.3750	0.3	0.3396	0.3418	3546	1279	2566	3.375	0.3	5	0.7	1.3333	0.7	0.2183	0.2205	3748	3345	1796
3.339	1	0.7	1	1.3750	0.5	0.2706	0.2690	3009	1278	2427	3.375	0.3	5	0.7	1.4444	1	0.1679	0.1665	3294	3270	1797
3.339	1	0.7	1	1.3750	0.7	0.2290	0.2262	2751	1281	2370	3.375	0.3	5	0.7	1.4444	0.3	0.4675	0.4740	7813	5970	1848
3.339	1	0.7	1	1.5000	1	0.1903	0.1871	2436	1287	2306	3.375	0.3	5	0.7	1.4444	0.5	0.3211	0.3229	5262	4061	1759
3.339	1	0.7	1	1.5000	0.3	0.3396	0.3418	3546	1279	2566	3.375	0.3	5	0.7	1.4444	0.7	0.2413	0.2412	3986	3355	1722
3.339	1	0.7	1	1.5000	0.5	0.2706	0.2690	3009	1278	2427	3.375	0.3	5	0.7	1.5556	1	0.1847	0.1817	3307	3269	1786
3.339	1	0.7	1	1.5000	0.7	0.2290	0.2262	2751	1281	2370	3.375	0.3	5	0.7	1.5556	0.3	0.4781	0.4844	7942	6025	1825
3.339	1	0.7	1	1.6250	1	0.1903	0.1871	2436	1287	2306	3.375	0.3	5	0.7	1.5556	0.5	0.3345	0.3352	5440	4113	1717
3.339	1	0.7	1	1.6250	0.3	0.3396	0.3418	3546	1279	2566	3.375	0.3	5	0.7	1.5556	0.7	0.2555	0.2541	4170	3358	1717
3.339	1	0.7	1	1.6250	0.5	0.2706	0.2690	3009	1278	2427	3.375	0.3	5	0.7	1.6667	1	0.1959	0.1919	3316	3275	1786
3.339	1	0.7	1	1.6250	0.7	0.2290	0.2262	2751	1281	2370	3.375	0.3	5	0.7	1.6667	0.3	0.4870	0.4922	8054	6068	1799
3.339	1	0.7	1	1.7500	1	0.1903	0.1871	2436	1287	2306	3.375	0.3	5	0.7	1.6667	0.5	0.3425	0.3426	5535	4143	1689
3.339	1	0.7	1	1.7500	0.3	0.3396	0.3418	3546	1279	2566	3.375	0.3	5	0.7	1.6667	0.7	0.2654	0.2633	4301	3359	1720
3.339	1	0.7	1	1.7500	0.5	0.2706	0.2690	3009	1278	2427	3.375	0.3	5	0.7	1.7778	1	0.2037	0.1989	3322	3280	1784
3.339	1	0.7	1	1.7500	0.7	0.2290	0.2262	2751	1281	2370	3.375	0.3	5	0.7	1.7778	0.3	0.4929	0.4974	8126	6098	1780
3.339	1	0.7	1	1.8750	1	0.1903	0.1871	2436	1287	2306	3.375	0.3	5	0.7	1.7778	0.5	0.3487	0.3485	5602	4164	1667
3.339	1	0.7	1	1.8750	0.3	0.3396	0.3418	3546	1279	2566	3.375	0.3	5	0.7	1.7778	0.7	0.2722	0.2695	4391	3358	1714
3.339	1	0.7	1	1.8750	0.5	0.2706	0.2690	3009	1278	2427	3.375	0.3	5	0.7	1.8889	1	0.2095	0.2044	3376	3289	1779
3.339	1	0.7	1	1.8750	0.7	0.2290	0.2262	2751	1281	2370	3.375	0.3	5	0.7	1.8889	0.3	0.4967	0.5010	8159	6118	1768
3.339	1	0.7	1	2.0000	1	0.1903	0.1871	2436	1287	2306	3.375	0.3	5	0.7	1.8889	0.5	0.3537	0.3531	5670	4182	1672

ODTh	alfa	Eback	beta	TWOD	Ewall	δy(%)	δx(%)	M(lb-in)	V (lb)	Th (lb)	ODTh	alfa	Eback	beta	TWOD	Ewall	δy(%)	δx(%)	M(lb-in)	V (lb)	Th (lb)
3.339	1	0.7	1	2.0000	0.3	0.3396	0.3418	3546	1279	2566	3.375	0.3	5	0.7	1.8889	0.7	0.2779	0.2748	4470	3350	1716
3.339	1	0.7	1	2.0000	0.5	0.2706	0.2690	3009	1278	2427	3.375	0.5	0.7	0.5	1.3333	1	0.3564	0.3069	6585	4038	2440
3.339	1	0.7	1	2.0000	0.7	0.2290	0.2262	2751	1281	2370	3.375	0.5	0.7	0.5	1.3333	0.3	0.9421	0.9705	12520	8036	2171
3.339	1	7.5	1	1.3750	1	0.1806	0.1766	2240	1223	2196	3.375	0.5	0.7	0.5	1.3333	0.5	0.6367	0.6277	8927	5346	2263
3.339	1	7.5	1	1.3750	0.3	0.3214	0.3217	3388	1205	2440	3.375	0.5	0.7	0.5	1.3333	0.7	0.4810	0.4486	7473	4077	2316
3.339	1	7.5	1	1.3750	0.5	0.2566	0.2536	2832	1210	2306	3.375	0.5	0.7	0.5	1.4444	1	0.3669	0.3215	6293	4030	2425
3.339	1	7.5	1	1.3750	0.7	0.2173	0.2134	2547	1216	2253	3.375	0.5	0.7	0.5	1.4444	0.3	0.9512	0.9814	12570	8054	2165
3.339	1	7.5	1	1.5000	1	0.1806	0.1766	2240	1223	2196	3.375	0.5	0.7	0.5	1.4444	0.5	0.6477	0.6422	8863	5357	2259
3.339	1	7.5	1	1.5000	0.3	0.3214	0.3217	3388	1205	2440	3.375	0.5	0.7	0.5	1.4444	0.7	0.4922	0.4640	7291	4063	2313
3.339	1	7.5	1	1.5000	0.5	0.2566	0.2536	2832	1210	2306	3.375	0.5	0.7	0.5	1.5556	1	0.3735	0.3311	6108	4024	2416
3.339	1	7.5	1	1.5000	0.7	0.2173	0.2134	2547	1216	2253	3.375	0.5	0.7	0.5	1.5556	0.3	0.9568	0.9883	12580	8064	2162
3.339	1	7.5	1	1.6250	1	0.1806	0.1766	2240	1223	2196	3.375	0.5	0.7	0.5	1.5556	0.5	0.6545	0.6515	8829	5363	2259
3.339	1	7.5	1	1.6250	0.3	0.3214	0.3217	3388	1205	2440	3.375	0.5	0.7	0.5	1.5556	0.7	0.4991	0.4738	7183	4053	2310
3.339	1	7.5	1	1.6250	0.5	0.2566	0.2536	2832	1210	2306	3.375	0.5	0.7	0.5	1.6667	1	0.3780	0.3379	5978	4020	2410
3.339	1	7.5	1	1.6250	0.7	0.2173	0.2134	2547	1216	2253	3.375	0.5	0.7	0.5	1.6667	0.3	0.9608	0.9932	12600	8072	2160
3.339	1	7.5	1	1.7500	1	0.1806	0.1766	2240	1223	2196	3.375	0.5	0.7	0.5	1.6667	0.5	0.6591	0.6577	8808	5368	2260
3.339	1	7.5	1	1.7500	0.3	0.3214	0.3217	3388	1205	2440	3.375	0.5	0.7	0.5	1.6667	0.7	0.5037	0.4808	7106	4046	2310
3.339	1	7.5	1	1.7500	0.5	0.2566	0.2536	2832	1210	2306	3.375	0.5	0.7	0.5	1.7778	1	0.3812	0.3430	5885	4016	2407
3.339	1	7.5	1	1.7500	0.7	0.2173	0.2134	2547	1216	2253	3.375	0.5	0.7	0.5	1.7778	0.3	0.9636	0.9968	12600	8077	2158
3.339	1	7.5	1	1.8750	1	0.1806	0.1766	2240	1223	2196	3.375	0.5	0.7	0.5	1.7778	0.5	0.6624	0.6624	8792	5371	2260
3.339	1	7.5	1	1.8750	0.3	0.3214	0.3217	3388	1205	2440	3.375	0.5	0.7	0.5	1.7778	0.7	0.5072	0.4859	7055	4040	2309
3.339	1	7.5	1	1.8750	0.5	0.2566	0.2536	2832	1210	2306	3.375	0.5	0.7	0.5	1.8889	1	0.3837	0.3470	5810	4013	2404
3.339	1	7.5	1	1.8750	0.7	0.2173	0.2134	2547	1216	2253	3.375	0.5	0.7	0.5	1.8889	0.3	0.9656	0.9994	12610	8080	2157
3.339	1	7.5	1	2.0000	1	0.1806	0.1766	2240	1223	2196	3.375	0.5	0.7	0.5	1.8889	0.5	0.6649	0.6659	8780	5374	2260
3.339	1	7.5	1	2.0000	0.3	0.3214	0.3217	3388	1205	2440	3.375	0.5	0.7	0.5	1.8889	0.7	0.5098	0.4899	7019	4035	2308
3.339	1	7.5	1	2.0000	0.5	0.2566	0.2536	2832	1210	2306	3.375	0.5	7.5	0.5	1.3333	1	0.1802	0.1679	2406	2290	1102
3.339	1	7.5	1	2.0000	0.7	0.2173	0.2134	2547	1216	2253	3.375	0.5	7.5	0.5	1.3333	0.3	0.3904	0.3858	5247	3702	1130
3.339	1	5	1	1.3750	1	0.1770	0.1730	2198	1194	2146	3.375	0.5	7.5	0.5	1.3333	0.5	0.2873	0.2796	3774	2518	1046
3.339	1	5	1	1.3750	0.3	0.3145	0.3146	3315	1178	2387	3.375	0.5	7.5	0.5	1.3333	0.7	0.2302	0.2205	3005	2330	1064
3.339	1	5	1	1.3750	0.5	0.2512	0.2482	2790	1182	2257	3.375	0.5	7.5	0.5	1.4444	1	0.1840	0.1728	2401	2281	1107
3.339	1	5	1	1.3750	0.7	0.2129	0.2090	2499	1188	2203	3.375	0.5	7.5	0.5	1.4444	0.3	0.3937	0.3882	5285	3714	1123
3.339	1	5	1	1.5000	1	0.1770	0.1730	2198	1194	2146	3.375	0.5	7.5	0.5	1.4444	0.5	0.2930	0.2842	3872	2535	1060
3.339	1	5	1	1.5000	0.3	0.3145	0.3146	3315	1178	2387	3.375	0.5	7.5	0.5	1.4444	0.7	0.2348	0.2253	3031	2290	1077
3.339	1	5	1	1.5000	0.5	0.2512	0.2482	2790	1182	2257	3.375	0.5	7.5	0.5	1.5556	1	0.1868	0.1761	2404	2241	1115
3.339	1	5	1	1.5000	0.7	0.2129	0.2090	2499	1188	2203	3.375	0.5	7.5	0.5	1.5556	0.3	0.3947	0.3894	5274	3718	1122
3.339	1	5	1	1.6250	1	0.1770	0.1730	2198	1194	2146	3.375	0.5	7.5	0.5	1.5556	0.5	0.2951	0.2862	3881	2539	1054
3.339	1	5	1	1.6250	0.3	0.3145	0.3146	3315	1178	2387	3.375	0.5	7.5	0.5	1.5556	0.7	0.2371	0.2281	3037	2271	1082
3.339	1	5	1	1.6250	0.5	0.2512	0.2482	2790	1182	2257	3.375	0.5	7.5	0.5	1.6667	1	0.1887	0.1791	2405	2232	1113
3.339	1	5	1	1.6250	0.7	0.2129	0.2090	2499	1188	2203	3.375	0.5	7.5	0.5	1.6667	0.5	0.2960	0.2873	3866	2541	1054
3.339	1	5	1	1.7500	1	0.1770	0.1730	2198	1194	2146	3.375	0.5	7.5	0.5	1.6667	0.7	0.2388	0.2296	3045	2260	1082
3.339	1	5	1	1.7500	0.3	0.3145	0.3146	3315	1178	2387	3.375	0.5	7.5	0.5	1.7778	1	0.1901	0.1807	2406	2222	1116
3.339	1	5	1	1.7500	0.5	0.2512	0.2482	2790	1182	2257	3.375	0.5	7.5	0.5	1.7778	0.3	0.3956	0.3908	5243	3721	1122
3.339	1	5	1	1.7500	0.7	0.2129	0.2090	2499	1188	2203	3.375	0.5	7.5	0.5	1.7778	0.5	0.2968	0.2883	3857	2543	1057
3.339	1	5	1	1.8750	1	0.1770	0.1730	2198	1194	2146	3.375	0.5	7.5	0.5	1.7778	0.7	0.2403	0.2309	3063	2248	1089
3.339	1	5	1	1.8750	0.3	0.3145	0.3146	3315	1178	2387	3.375	0.5	7.5	0.5	1.8889	1	0.1910	0.1818	2407	2214	1116
3.339	1	5	1	1.8750	0.5	0.2512	0.2482	2790	1182	2257	3.375	0.5	7.5	0.5	1.8889	0.3	0.3954	0.3905	5248	3723	1123
3.339	1	5	1	1.8750	0.7	0.2129	0.2090	2499	1188	2203	3.375	0.5	7.5	0.5	1.8889	0.5	0.2972	0.2888	3848	2543	1058

ODTh	alfa	Eback	beta	TWOD	Ewall	δy(%)	δx(%)	M(lb-in)	V (lb)	Th (lb)	ODTh	alfa	Eback	beta	TWOD	Ewall	δy(%)	δx(%)	M(lb-in)	V (lb)	Th (lb)
3.339	1	5	1	2.0000	1	0.1770	0.1730	2198	1194	2146	3.375	0.5	7.5	0.5	1.8889	0.7	0.2413	0.2318	3070	2239	1095
3.339	1	5	1	2.0000	0.3	0.3145	0.3146	3315	1178	2387	3.375	0.5	5	0.5	1.3333	1	0.2302	0.2045	3616	2889	1488
3.339	1	5	1	2.0000	0.5	0.2512	0.2482	2790	1182	2257	3.375	0.5	5	0.5	1.3333	0.3	0.5183	0.5127	7018	5068	1443
3.339	1	5	1	2.0000	0.7	0.2129	0.2090	2499	1188	2203	3.375	0.5	5	0.5	1.3333	0.5	0.3783	0.3627	5268	3500	1352
3.339	0	0.7	1	1.3750	1	-0.0820	-0.0699	2792	1527	2220	3.375	0.5	5	0.5	1.3333	0.7	0.3002	0.2796	4344	2929	1420
3.339	0	0.7	1	1.3750	0.3	0.3230	0.3212	4067	1185	2211	3.375	0.5	5	0.5	1.4444	1	0.2383	0.2147	3536	2880	1481
3.339	0	0.7	1	1.3750	0.5	0.1223	0.1262	2697	1291	2214	3.375	0.5	5	0.5	1.4444	0.3	0.5230	0.5183	7020	5082	1440
3.339	0	0.7	1	1.3750	0.7	0.0134	0.0217	2233	1392	2213	3.375	0.5	5	0.5	1.4444	0.5	0.3844	0.3703	5229	3510	1357
3.339	0	0.7	1	1.5000	1	-0.0259	-0.0286	2272	1510	2212	3.375	0.5	5	0.5	1.4444	0.7	0.3072	0.2884	4280	2918	1419
3.339	0	0.7	1	1.5000	0.3	0.3599	0.3527	4396	1174	2209	3.375	0.5	5	0.5	1.5556	1	0.2434	0.2215	3484	2872	1481
3.339	0	0.7	1	1.5000	0.5	0.1699	0.1634	2761	1281	2206	3.375	0.5	5	0.5	1.5556	0.3	0.5266	0.5224	7042	5094	1436
3.339	0	0.7	1	1.5000	0.7	0.0658	0.0611	2312	1380	2209	3.375	0.5	5	0.5	1.5556	0.5	0.3879	0.3750	5197	3515	1356
3.339	0	0.7	1	1.6250	1	0.0084	-0.0025	1928	1498	2207	3.375	0.5	5	0.5	1.5556	0.7	0.3113	0.2940	4233	2914	1418
3.339	0	0.7	1	1.6250	0.3	0.3815	0.3723	4647	1168	2207	3.375	0.5	5	0.5	1.6667	1	0.2469	0.2264	3438	2866	1479
3.339	0	0.7	1	1.6250	0.5	0.1987	0.1868	2885	1273	2201	3.375	0.5	5	0.5	1.6667	0.3	0.5286	0.5246	7055	5102	1433
3.339	0	0.7	1	1.6250	0.7	0.0977	0.0861	2361	1370	2206	3.375	0.5	5	0.5	1.6667	0.5	0.3910	0.3795	5175	3521	1356
3.339	0	0.7	1	1.7500	1	0.0315	0.0154	1913	1489	2205	3.375	0.5	5	0.5	1.6667	0.7	0.3142	0.2978	4202	2910	1420
3.339	0	0.7	1	1.7500	0.3	0.3954	0.3853	4842	1164	2206	3.375	0.5	5	0.5	1.7778	1	0.2493	0.2299	3401	2863	1480
3.339	0	0.7	1	1.7500	0.5	0.2172	0.2026	3007	1268	2198	3.375	0.5	5	0.5	1.7778	0.3	0.5301	0.5263	7075	5109	1431
3.339	0	0.7	1	1.7500	0.7	0.1188	0.1036	2392	1363	2209	3.375	0.5	5	0.5	1.7778	0.5	0.3928	0.3819	5166	3525	1360
3.339	0	0.7	1	1.8750	1	0.0480	0.0288	1938	1482	2204	3.375	0.5	5	0.5	1.7778	0.7	0.3163	0.3008	4172	2904	1420
3.339	0	0.7	1	1.8750	0.3	0.4054	0.3947	4984	1160	2196	3.375	0.5	5	0.5	1.8889	1	0.2511	0.2325	3369	2861	1484
3.339	0	0.7	1	1.8750	0.5	0.2302	0.2138	3106	1262	2196	3.375	0.5	5	0.5	1.8889	0.3	0.5327	0.5285	7113	5121	1424
3.339	0	0.7	1	1.8750	0.7	0.1337	0.1160	2415	1357	2208	3.375	0.5	5	0.5	1.8889	0.5	0.3944	0.3838	5173	3529	1365
3.339	0	0.7	1	2.0000	1	0.0602	0.0389	1967	1476	2204	3.375	0.5	5	0.5	1.8889	0.7	0.3177	0.3029	4150	2902	1419
3.339	0	0.7	1	2.0000	0.3	0.4130	0.4020	5091	1158	2206	3.375	0.7	0.7	0.3	1.3333	1	0.2896	0.2557	6640	2412	1603
3.339	0	0.7	1	2.0000	0.5	0.2396	0.2221	2432	1353	2208	3.375	0.7	0.7	0.3	1.3333	0.3	0.6297	0.6502	10250	5090	1140
3.339	0	0.7	1	2.0000	0.7	0.1448	0.1254	1727	874	1932	3.375	0.7	0.7	0.3	1.3333	0.5	0.4499	0.4434	7679	3387	1246
3.339	0	7.5	1	1.3750	1	0.1133	0.1167	3290	823	2148	3.375	0.7	0.7	0.3	1.3333	0.7	0.3647	0.3412	7447	2528	1419
3.339	0	7.5	1	1.3750	0.3	0.2968	0.3026	2632	843	2022	3.375	0.7	0.7	0.3	1.4444	1	0.2893	0.2578	6531	2416	1593
3.339	0	7.5	1	1.3750	0.5	0.2111	0.2136	2199	837	2004	3.375	0.7	0.7	0.3	1.4444	0.3	0.6305	0.6524	10210	5091	1141
3.339	0	7.5	1	1.3750	0.7	0.1589	0.1627	1768	881	1931	3.375	0.7	0.7	0.3	1.4444	0.5	0.4504	0.4457	7645	3387	1245
3.339	0	7.5	1	1.5000	1	0.1279	0.1296	3404	829	2160	3.375	0.7	0.7	0.3	1.4444	0.7	0.3647	0.3434	7368	2526	1413
3.339	0	7.5	1	1.5000	0.3	0.3050	0.3102	2670	853	2018	3.375	0.7	0.7	0.3	1.5556	1	0.2891	0.2593	6449	2420	1586
3.339	0	7.5	1	1.5000	0.5	0.2235	0.2247	2248	842	2004	3.375	0.7	0.7	0.3	1.5556	0.3	0.6311	0.6540	10180	5093	1143
3.339	0	7.5	1	1.5000	0.7	0.1717	0.1740	1791	888	1943	3.375	0.7	0.7	0.3	1.5556	0.5	0.4508	0.4476	7622	3386	1245
3.339	0	7.5	1	1.6250	1	0.1366	0.1374	3436	839	2159	3.375	0.7	0.7	0.3	1.5556	0.7	0.3641	0.3443	7291	2526	1410
3.339	0	7.5	1	1.6250	0.3	0.3102	0.3148	2688	853	2030	3.375	0.7	0.7	0.3	1.6667	1	0.2891	0.2609	6390	2415	1576
3.339	0	7.5	1	1.6250	0.5	0.2301	0.2312	2285	885	1948	3.375	0.7	0.7	0.3	1.6667	0.3	0.6315	0.6552	10160	5094	1144
3.339	0	7.5	1	1.6250	0.7	0.1827	0.1824	1809	900	1930	3.375	0.7	0.7	0.3	1.6667	0.5	0.4511	0.4488	7602	3386	1245
3.339	0	7.5	1	1.7500	1	0.1428	0.1427	3452	849	2169	3.375	0.7	0.7	0.3	1.6667	0.7	0.3641	0.3455	7239	2525	1407
3.339	0	7.5	1	1.7500	0.3	0.3125	0.3167	2700	861	2034	3.375	0.7	0.7	0.3	1.7778	1	0.2889	0.2618	6339	2417	1571
3.339	0	7.5	1	1.7500	0.5	0.2349	0.2355	2302	891	1953	3.375	0.7	0.7	0.3	1.7778	0.3	0.6318	0.6561	10130	5094	1146
3.339	0	7.5	1	1.7500	0.7	0.1879	0.1870	1821	908	1931	3.375	0.7	0.7	0.3	1.7778	0.5	0.4512	0.4498	7586	3385	1246

ODTh	alfa	Eback	beta	TWOD	Ewall	δy(%)	δx(%)	M(lb-in)	V (lb)	Th (lb)	ODTh	alfa	Eback	beta	TWOD	Ewall	δy(%)	δx(%)	M(lb-in)	V (lb)	Th (lb)
3.339	0	7.5	1	1.8750	1	0.1471	0.1465	2709	875	2036	3.375	0.7	0.7	0.3	1.7778	0.7	0.3640	0.3464	7200	2524	1404
3.339	0	7.5	1	1.8750	0.5	0.2387	0.2389	1831	916	1930	3.375	0.7	0.7	0.3	1.8889	1	0.2888	0.2625	6295	2419	1567
3.339	0	7.5	1	2.0000	1	0.1504	0.1493	2716	880	2042	3.375	0.7	0.7	0.3	1.8889	0.3	0.6320	0.6568	10110	5095	1147
3.339	0	7.5	1	2.0000	0.5	0.2410	0.2409	1411	820	1682	3.375	0.7	0.7	0.3	1.8889	0.5	0.4514	0.4506	7573	3385	1247
3.339	0	5	1	1.3750	1	0.0405	0.0465	3090	676	1824	3.375	0.7	0.7	0.3	1.8889	0.7	0.3640	0.3472	7167	2523	1402
3.339	0	5	1	1.3750	0.3	0.2559	0.2630	2292	702	1761	3.375	0.7	7.5	0.3	1.3333	1	0.2041	0.1932	3087	2147	1073
3.339	0	5	1	1.3750	0.5	0.1557	0.1625	1820	762	1707	3.375	0.7	7.5	0.3	1.3333	0.3	0.4142	0.4148	5281	3827	1111
3.339	0	5	1	1.3750	0.7	0.0972	0.1037	1488	807	1671	3.375	0.7	7.5	0.3	1.3333	0.5	0.3122	0.3059	3986	2604	1022
3.339	0	5	1	1.5000	1	0.0708	0.0730	3307	659	1813	3.375	0.7	7.5	0.3	1.3333	0.7	0.2567	0.2462	3696	2177	1065
3.339	0	5	1	1.5000	0.3	0.2776	0.2820	2380	695	1769	3.375	0.7	7.5	0.3	1.4444	1	0.2038	0.1939	3016	2153	1081
3.339	0	5	1	1.5000	0.5	0.1778	0.1822	1915	750	1713	3.375	0.7	7.5	0.3	1.4444	0.3	0.4150	0.4148	5318	3834	1109
3.339	0	5	1	1.5000	0.7	0.1231	0.1267	1534	792	1666	3.375	0.7	7.5	0.3	1.4444	0.5	0.3115	0.3058	3920	2603	1031
3.339	0	5	1	1.6250	1	0.0894	0.0898	3430	673	1820	3.375	0.7	7.5	0.3	1.4444	0.7	0.2563	0.2464	3615	2182	1074
3.339	0	5	1	1.6250	0.3	0.2895	0.2928	2433	696	1762	3.375	0.7	7.5	0.3	1.5556	1	0.2037	0.1945	2968	2157	1091
3.339	0	5	1	1.6250	0.5	0.1932	0.1956	1972	740	1716	3.375	0.7	7.5	0.3	1.5556	0.3	0.4145	0.4146	5316	3834	1109
3.339	0	5	1	1.6250	0.7	0.1393	0.1412	1565	786	1667	3.375	0.7	7.5	0.3	1.5556	0.5	0.3114	0.3061	3882	2604	1034
3.339	0	5	1	1.7500	1	0.1019	0.1011	3459	683	1818	3.375	0.7	7.5	0.3	1.5556	0.7	0.2559	0.2466	3553	2186	1081
3.339	0	5	1	1.7500	0.3	0.2975	0.2998	2466	698	1766	3.375	0.7	7.5	0.3	1.6667	1	0.2036	0.1950	2931	2160	1098
3.339	0	5	1	1.7500	0.5	0.2029	0.2043	2013	740	1709	3.375	0.7	7.5	0.3	1.6667	0.3	0.4139	0.4143	5305	3832	1111
3.339	0	5	1	1.7500	0.7	0.1510	0.1515	1587	794	1667	3.375	0.7	7.5	0.3	1.6667	0.5	0.3118	0.3060	3897	2607	1047
3.339	0	5	1	1.8750	1	0.1111	0.1095	3490	689	1825	3.375	0.7	7.5	0.3	1.6667	0.7	0.2558	0.2469	3514	2182	1083
3.339	0	5	1	1.8750	0.3	0.3027	0.3051	2489	703	1773	3.375	0.7	7.5	0.3	1.7778	1	0.2034	0.1952	2896	2164	1102
3.339	0	5	1	1.8750	0.5	0.2097	0.2104	2041	749	1710	3.375	0.7	7.5	0.3	1.7778	0.3	0.4133	0.4138	5301	3830	1112
3.339	0	5	1	1.8750	0.7	0.1591	0.1587	1604	803	1665	3.375	0.7	7.5	0.3	1.7778	0.5	0.3117	0.3061	3895	2607	1051
3.339	0	5	1	2.0000	1	0.1181	0.1158	3520	697	1832	3.375	0.7	7.5	0.3	1.7778	0.7	0.2558	0.2471	3482	2180	1085
3.339	0	5	1	2.0000	0.3	0.3067	0.3088	2525	710	1779	3.375	0.7	7.5	0.3	1.8889	1	0.2032	0.1954	2868	2164	1105
3.339	0	5	1	2.0000	0.5	0.2147	0.2148	2063	758	1712	3.375	0.7	7.5	0.3	1.8889	0.3	0.4133	0.4137	5300	3830	1113
3.339	0	5	1	2.0000	0.7	0.1652	0.1641	4906	1529	2286	3.375	0.7	7.5	0.3	1.8889	0.5	0.3113	0.3059	3892	2607	1054
3.339	1	0.7	1	1.3750	1	0.1566	0.0887	6398	1125	2346	3.375	0.7	7.5	0.3	1.8889	0.7	0.2556	0.2469	3456	2182	1091
3.339	1	0.7	1	1.3750	0.3	0.4561	0.4355	5208	1243	2318	3.375	0.7	5	0.3	1.3333	1	0.1979	0.1823	3352	1899	913.9
3.339	1	0.7	1	1.3750	0.5	0.3024	0.2626	4916	1373	2308	3.375	0.7	5	0.3	1.3333	0.3	0.4097	0.4092	5245	3540	959.7
3.339	1	0.7	1	1.3750	0.7	0.2238	0.1711	4579	1509	2281	3.375	0.7	5	0.3	1.3333	0.5	0.3049	0.2964	4358	2387	883.1
3.339	1	0.7	1	1.5000	1	0.1691	0.1062	6430	1122	2329	3.375	0.7	5	0.3	1.3333	0.7	0.2474	0.2358	3856	1957	878.9
3.339	1	0.7	1	1.5000	0.3	0.4667	0.4478	5112	1235	2297	3.375	0.7	5	0.3	1.4444	1	0.1981	0.1843	3294	1900	919.5
3.339	1	0.7	1	1.5000	0.5	0.3143	0.2771	4695	1361	2301	3.375	0.7	5	0.3	1.4444	0.3	0.4093	0.4094	5209	3540	962
3.339	1	0.7	1	1.5000	0.7	0.2363	0.1873	4373	1496	2277	3.375	0.7	5	0.3	1.4444	0.5	0.3046	0.2972	4310	2387	885.7
3.339	1	0.7	1	1.6250	1	0.1768	0.1176	6447	1121	2318	3.375	0.7	5	0.3	1.4444	0.7	0.2476	0.2370	3809	1960	891.1
3.339	1	0.7	1	1.6250	0.3	0.4733	0.4557	5059	1230	2281	3.375	0.7	5	0.3	1.5556	1	0.1982	0.1856	3247	1901	927.3
3.339	1	0.7	1	1.6250	0.5	0.3216	0.2863	4564	1353	2293	3.375	0.7	5	0.3	1.5556	0.3	0.4088	0.4093	5174	3539	964.6
3.339	1	0.7	1	1.6250	0.7	0.2439	0.1977	4227	1487	2275	3.375	0.7	5	0.3	1.5556	0.5	0.3044	0.2978	4270	2387	887.5
3.339	1	0.7	1	1.7500	1	0.1820	0.1255	6455	1120	2312	3.375	0.7	5	0.3	1.5556	0.7	0.2477	0.2380	3769	1959	898.1
3.339	1	0.7	1	1.7500	0.3	0.4778	0.4611	5024	1228	2269	3.375	0.7	5	0.3	1.6667	1	0.1982	0.1865	3203	1904	933
3.339	1	0.7	1	1.7500	0.5	0.3265	0.2926	4477	1347	2288	3.375	0.7	5	0.3	1.6667	0.3	0.4081	0.4089	5144	3537	966.9
3.339	1	0.7	1	1.7500	0.7	0.2490	0.2049	4122	1480	2272	3.375	0.7	5	0.3	1.6667	0.5	0.3042	0.2981	4237	2386	889.2
3.339	1	0.7	1	1.8750	1	0.1858	0.1315	6460	1119	2307	3.375	0.7	5	0.3	1.6667	0.7	0.2477	0.2386	3733	1960	903.5
3.339	1	0.7	1	1.8750	0.3	0.4810	0.4651	5001	1226	2262	3.375	0.7	5	0.3	1.7778	1	0.1981	0.1872	3167	1907	938.7
3.339	1	0.7	1	1.8750	0.5	0.3300	0.2970	4414	1343	2283	3.375	0.7	5	0.3	1.7778	0.3	0.4075	0.4086	5117	3535	968.7

ODTh	alfa	Eback	beta	TWOD	Ewall	δy(%)	δx(%)	M(lb-in)	V (lb)	Th (lb)	ODTh	alfa	Eback	beta	TWOD	Ewall	δy(%)	δx(%)	M(lb-in)	V (lb)	Th (lb)
3.339	1	0.7	1	1.8750	0.7	0.2527	0.2101	4044	1475	2271	3.375	0.7	5	0.3	1.7778	0.5	0.3040	0.2984	4210	2386	890.9
3.339	1	0.7	1	2.0000	1	0.1887	0.1360	6461	1118	2304	3.375	0.7	5	0.3	1.7778	0.7	0.2476	0.2391	3700	1961	908.2
3.339	1	0.7	1	2.0000	0.3	0.4833	0.4679	4985	1225	2256	3.375	0.7	5	0.3	1.8889	1	0.1981	0.1878	3142	1908	943.4
3.339	1	0.7	1	2.0000	0.5	0.3326	0.3004	4368	1340	2280	3.375	0.7	5	0.3	1.8889	0.3	0.4068	0.4081	5091	3533	971.1
3.339	1	0.7	1	2.0000	0.7	0.2554	0.2140	1886	873	2004	3.375	0.7	5	0.3	1.8889	0.5	0.3036	0.2983	4182	2386	893.1
3.339	1	7.5	1	1.3750	1	0.1574	0.1470	3565	842	2163	3.375	0.7	5	0.3	1.8889	0.7	0.2475	0.2395	3670	1962	911.4
3.339	1	7.5	1	1.3750	0.3	0.3301	0.3286	2742	815	2095	3.375	1	0.7	1	1.3333	1	0.1703	0.1642	1590	965.9	1833
3.339	1	7.5	1	1.3750	0.5	0.2441	0.2395	2368	848	2032	3.375	1	0.7	1	1.3333	0.3	0.3250	0.3242	2522	933.2	2123
3.339	1	7.5	1	1.3750	0.7	0.1993	0.1914	1893	884	1981	3.375	1	0.7	1	1.3333	0.5	0.2498	0.2454	2128	933.4	1969
3.339	1	7.5	1	1.5000	1	0.1621	0.1527	3520	849	2170	3.375	1	0.7	1	1.3333	0.7	0.2081	0.2026	1847	948.1	1900
3.339	1	7.5	1	1.5000	0.3	0.3315	0.3307	2751	833	2081	3.375	1	0.7	1	1.4444	1	0.1703	0.1642	1590	965.9	1833
3.339	1	7.5	1	1.5000	0.5	0.2493	0.2451	2377	858	2014	3.375	1	0.7	1	1.4444	0.3	0.1672	0.1571	2128	933.4	1969
3.339	1	7.5	1	1.5000	0.7	0.2039	0.1967	1898	905	1965	3.375	1	0.7	1	1.4444	0.5	0.2498	0.2454	1847	948.1	1900
3.339	1	7.5	1	1.6250	1	0.1653	0.1564	3489	854	2178	3.375	1	0.7	1	1.4444	0.7	0.2081	0.2026	1590	965.9	1833
3.339	1	7.5	1	1.6250	0.3	0.3322	0.3319	2759	868	2053	3.375	1	0.7	1	1.5556	1	0.1703	0.1642	1590	965.9	1833
3.339	1	7.5	1	1.6250	0.5	0.2545	0.2494	2380	870	2011	3.375	1	0.7	1	1.5556	0.3	0.0827	0.0738	2522	933.2	2123
3.339	1	7.5	1	1.6250	0.7	0.2063	0.1996	1901	919	1953	3.375	1	0.7	1	1.5556	0.5	0.0747	0.0654	2127	933.7	1969
3.339	1	7.5	1	1.7500	1	0.1673	0.1590	3469	857	2183	3.375	1	0.7	1	1.6667	1	0.1703	0.1642	1847	948.1	1900
3.339	1	7.5	1	1.7500	0.3	0.3328	0.3329	2761	878	2053	3.375	1	0.7	1	1.6667	0.3	0.3250	0.3242	1590	965.9	1833
3.339	1	7.5	1	1.7500	0.5	0.2559	0.2512	2383	878	2008	3.375	1	0.7	1	1.6667	0.5	0.2498	0.2453	2522	933.2	2123
3.339	1	7.5	1	1.7500	0.7	0.2082	0.2018	1901	920	1960	3.375	1	0.7	1	1.6667	0.7	0.2081	0.2026	2128	933.4	1969
3.339	1	7.5	1	1.8750	1	0.1683	0.1606	3446	861	2189	3.375	1	0.7	1	1.7778	1	0.1703	0.1642	1847	948.1	1900
3.339	1	7.5	1	1.8750	0.3	0.3326	0.3329	2761	881	2056	3.375	1	0.7	1	1.7778	0.3	0.3250	0.3242	1590	965.9	1833
3.339	1	7.5	1	1.8750	0.5	0.2565	0.2520	2385	885	2009	3.375	1	0.7	1	1.7778	0.5	0.2498	0.2454	2522	933.2	2123
3.339	1	7.5	1	1.8750	0.7	0.2096	0.2038	1902	922	1964	3.375	1	0.7	1	1.7778	0.7	0.2081	0.2026	2128	933.4	1969
3.339	1	7.5	1	2.0000	1	0.1691	0.1619	3414	869	2198	3.375	1	0.7	1	1.8889	1	0.1703	0.1642	1847	948.1	1900
3.339	1	7.5	1	2.0000	0.3	0.3312	0.3316	2762	889	2059	3.375	1	0.7	1	1.8889	0.3	0.3250	0.3242	1440	886.4	1716
3.339	1	7.5	1	2.0000	0.5	0.2570	0.2528	2389	906	1991	3.375	1	0.7	1	1.8889	0.5	0.2498	0.2454	2409	877.9	1978
3.339	1	7.5	1	2.0000	0.7	0.2119	0.2057	2259	795	1779	3.375	1	0.7	1	1.8889	0.7	0.2081	0.2026	1893	850.2	1842
3.339	1	5	1	1.3750	1	0.1320	0.1112	3701	635	1882	3.375	1	7.5	1	1.3333	1	0.1607	0.1525	1655	867	1775
3.339	1	5	1	1.3750	0.3	0.3152	0.3111	2909	692	1819	3.375	1	7.5	1	1.3333	0.3	0.3037	0.2991	1440	886.4	1716
3.339	1	5	1	1.3750	0.5	0.2282	0.2173	2537	743	1790	3.375	1	7.5	1	1.3333	0.5	0.2346	0.2277	2409	877.9	1978
3.339	1	5	1	1.3750	0.7	0.1785	0.1632	2185	782	1752	3.375	1	7.5	1	1.3333	0.7	0.1958	0.1881	1893	850.2	1842
3.339	1	5	1	1.5000	1	0.1420	0.1235	3669	633	1885	3.375	1	7.5	1	1.4444	1	0.1607	0.1525	1655	867	1775
3.339	1	5	1	1.5000	0.3	0.3210	0.3189	2904	693	1794	3.375	1	7.5	1	1.4444	0.3	0.3037	0.2991	1440	886.4	1716
3.339	1	5	1	1.5000	0.5	0.2362	0.2261	2470	735	1780	3.375	1	7.5	1	1.4444	0.5	0.2346	0.2277	2409	877.9	1978
3.339	1	5	1	1.5000	0.7	0.1866	0.1730	2124	778	1739	3.375	1	7.5	1	1.4444	0.7	0.1958	0.1881	1893	850.2	1842
3.339	1	5	1	1.6250	1	0.1480	0.1311	3674	646	1883	3.375	1	7.5	1	1.5556	1	0.1607	0.1525	1655	867	1775
3.339	1	5	1	1.6250	0.3	0.3250	0.3235	2884	695	1791	3.375	1	7.5	1	1.5556	0.3	0.3037	0.2991	1440	886.4	1716
3.339	1	5	1	1.6250	0.5	0.2404	0.2311	2426	730	1773	3.375	1	7.5	1	1.5556	0.5	0.2346	0.2277	2409	877.9	1978
3.339	1	5	1	1.6250	0.7	0.1916	0.1794	2065	773	1735	3.375	1	7.5	1	1.5556	0.7	0.1958	0.1881	1893	850.2	1842
3.339	1	5	1	1.7500	1	0.1519	0.1365	3733	663	1864	3.375	1	7.5	1	1.6667	1	0.1607	0.1525	1655	867	1775
3.339	1	5	1	1.7500	0.3	0.3295	0.3273	2867	698	1792	3.375	1	7.5	1	1.6667	0.3	0.3037	0.2991	1440	886.4	1716
3.339	1	5	1	1.7500	0.5	0.2431	0.2345	2395	729	1767	3.375	1	7.5	1	1.6667	0.5	0.2346	0.2277	2409	877.9	1978
3.339	1	5	1	1.7500	0.7	0.1951	0.1838	2025	775	1730	3.375	1	7.5	1	1.6667	0.7	0.1958	0.1881	1893	850.2	1842
3.339	1	5	1	1.8750	1	0.1548	0.1404	3740	677	1860	3.375	1	7.5	1	1.7778	1	0.1607	0.1525	1655	867	1775
3.339	1	5	1	1.8750	0.3	0.3315	0.3293	2848	699	1792	3.375	1	7.5	1	1.7778	0.3	0.3037	0.2991	1440	886.4	1716

ODTh	alfa	Eback	beta	TWOD	Ewall	δy(%)	δx(%)	M(lb-in)	V (lb)	Th (lb)	ODTh	alfa	Eback	beta	TWOD	Ewall	δy(%)	δx(%)	M(lb-in)	V (lb)	Th (lb)
3.339	1	5	1	1.8750	0.5	0.2453	0.2373	2409	736	1749	3.375	1	7.5	1	1.7778	0.5	0.2346	0.2277	2409	877.9	1978
3.339	1	5	1	1.8750	0.7	0.1981	0.1870	1989	783	1730	3.375	1	7.5	1	1.7778	0.7	0.1958	0.1881	1893	850.2	1842
3.339	1	5	1	2.0000	1	0.1567	0.1433	3723	688	1864	3.375	1	7.5	1	1.8889	1	0.1607	0.1525	1655	867	1775
3.339	1	5	1	2.0000	0.3	0.3320	0.3301	2827	710	1793	3.375	1	7.5	1	1.8889	0.3	0.3037	0.2991	1410	852.1	1663
3.339	1	5	1	2.0000	0.5	0.2469	0.2395	2388	746	1748	3.375	1	7.5	1	1.8889	0.5	0.2346	0.2277	2368	852.9	1920
3.339	1	5	1	2.0000	0.7	0.1997	0.1893	5055	1377	2055	3.375	1	7.5	1	1.8889	0.7	0.1958	0.1881	1838	818.6	1788
3.339	1	0.7	0	1.3750	1	0.2553	0.2212	7514	932	2368	3.375	1	5	1	1.3333	1	0.1564	0.1482	1618	833.5	1722
3.339	1	0.7	0	1.3750	0.3	0.5042	0.5213	6215	1052	2265	3.375	1	5	1	1.3333	0.3	0.2950	0.2901	1410	852.1	1663
3.339	1	0.7	0	1.3750	0.5	0.3793	0.3707	5618	1203	2163	3.375	1	5	1	1.3333	0.5	0.2281	0.2211	2368	852.9	1920
3.339	1	0.7	0	1.3750	0.7	0.3146	0.2920	4975	1363	2059	3.375	1	5	1	1.3333	0.7	0.1905	0.1828	1838	818.6	1788
3.339	1	0.7	0	1.5000	1	0.2552	0.2240	7510	930	2365	3.375	1	5	1	1.4444	1	0.1564	0.1482	1618	833.5	1722
3.339	1	0.7	0	1.5000	0.3	0.5055	0.5244	6172	1046	2267	3.375	1	5	1	1.4444	0.3	0.2950	0.2901	1410	852.1	1663
3.339	1	0.7	0	1.5000	0.5	0.3795	0.3732	5550	1193	2167	4.860	1	5	1	1.4444	0.5	0.2281	0.2211	2368	853	1920
3.339	1	0.7	0	1.5000	0.7	0.3144	0.2942	4913	1353	2060	4.860	1	5	1	1.4444	0.7	0.1905	0.1828	1838	819.9	1788
3.339	1	0.7	0	1.6250	1	0.2551	0.2259	7505	928	2363	4.860	1	5	1	1.5556	1	0.1564	0.1482	1618	833.5	1722
3.339	1	0.7	0	1.6250	0.3	0.5065	0.5267	6143	1043	2268	4.860	1	5	1	1.5556	0.3	0.2950	0.2901	1410	852.1	1663
3.339	1	0.7	0	1.6250	0.5	0.3798	0.3751	5499	1185	2171	4.860	1	5	1	1.5556	0.5	0.2282	0.2212	2368	852.9	1920
3.339	1	0.7	0	1.6250	0.7	0.3141	0.2959	4866	1345	2063	4.860	1	5	1	1.5556	0.7	0.1905	0.1828	1838	818.6	1788
3.339	1	0.7	0	1.7500	1	0.2549	0.2273	7497	926	2361	4.860	1	5	1	1.6667	1	0.1564	0.1482	1618	834	1721
3.339	1	0.7	0	1.7500	0.3	0.5071	0.5283	6122	1041	2268	4.860	1	5	1	1.6667	0.3	0.2950	0.2901	1410	852.1	1663
3.339	1	0.7	0	1.7500	0.5	0.3800	0.3766	5460	1178	2174	4.860	1	5	1	1.6667	0.5	0.2281	0.2211	2368	852.9	1920
3.339	1	0.7	0	1.7500	0.7	0.3139	0.2970	4829	1338	2066	4.860	1	5	1	1.6667	0.7	0.1905	0.1828	1838	818.6	1788
3.339	1	0.7	0	1.8750	1	0.2547	0.2284	7487	924	2360	4.860	1	5	1	1.7778	1	0.1564	0.1482	1618	833.5	1722
3.339	1	0.7	0	1.8750	0.3	0.5075	0.5294	6103	1039	2268	4.860	1	5	1	1.7778	0.3	0.2950	0.2901	1410	852.1	1663
3.339	1	0.7	0	1.8750	0.5	0.3801	0.3777	5428	1173	2176	4.860	1	5	1	1.7778	0.5	0.2281	0.2211	2368	852.9	1920
3.339	1	0.7	0	1.8750	0.7	0.3137	0.2979	4797	1333	2068	4.860	1	5	1	1.7778	0.7	0.1905	0.1828	1838	818.6	1788
3.339	1	0.7	0	2.0000	1	0.2546	0.2293	7480	924	2359	4.860	1	5	1	1.8889	1	0.1564	0.1482	1618	833.6	1722
3.339	1	0.7	0	2.0000	0.3	0.5079	0.5304	6088	1038	2269	4.860	1	5	1	1.8889	0.3	0.2950	0.2901	4472	1489	2618
3.339	1	0.7	0	2.0000	0.5	0.3802	0.3785	5402	1169	2178	4.860	1	5	1	1.8889	0.5	0.2281	0.2211	3151	1589	2646
3.339	1	0.7	0	2.0000	0.7	0.3135	0.2986	2548	913	1952	4.860	1	5	1	1.8889	0.7	0.1905	0.1828	3083	1732	2715
3.339	1	7.5	0	1.3750	1	0.1789	0.1685	4063	836	2204	4.860	0.3	0.7	0.7	1.3333	0.3	0.4223	0.4201	7434	1394	2681
3.339	1	7.5	0	1.3750	0.3	0.3352	0.3357	3336	855	2076	4.860	0.3	0.7	0.7	1.3333	1	0.0120	0.0242	4456	1535	2684
3.339	1	7.5	0	1.3750	0.5	0.2610	0.2564	2911	881	2016	4.860	0.3	0.7	0.7	1.3333	0.3	0.4180	0.4260	3853	1636	2707
3.339	1	7.5	0	1.3750	0.7	0.2183	0.2106	2494	920	1955	4.860	0.3	0.7	0.7	1.3333	0.5	0.2201	0.2242	3187	1721	2710
3.339	1	7.5	0	1.5000	1	0.1790	0.1698	3994	838	2211	4.860	0.3	0.7	0.7	1.3333	0.7	0.1109	0.1185	8021	1383	2680
3.339	1	7.5	0	1.5000	0.3	0.3336	0.3346	3282	864	2080	4.860	0.3	0.7	0.7	1.4444	1	0.0571	0.0572	4770	1520	2680
3.339	1	7.5	0	1.5000	0.5	0.2607	0.2567	2855	888	2019	4.860	0.3	0.7	0.7	1.4444	0.3	0.4444	0.4509	3934	1615	2701
3.339	1	7.5	0	1.5000	0.7	0.2180	0.2112	2449	925	1957	4.860	0.3	0.7	0.7	1.4444	0.5	0.2548	0.2522	3250	1710	2707
3.339	1	7.5	0	1.6250	1	0.1789	0.1706	3951	846	2216	4.860	0.3	0.7	0.7	1.4444	0.7	0.1512	0.1499	8392	1375	2678
3.339	1	7.5	0	1.6250	0.3	0.3330	0.3343	3244	870	2082	4.860	0.3	0.7	0.7	1.5556	1	0.0843	0.0780	5116	1503	2682
3.339	1	7.5	0	1.6250	0.5	0.2604	0.2569	2827	897	2018	4.860	0.3	0.7	0.7	1.5556	0.3	0.4609	0.4668	3980	1603	2699
3.339	1	7.5	0	1.6250	0.7	0.2182	0.2120	2415	928	1959	4.860	0.3	0.7	0.7	1.5556	0.5	0.2746	0.2690	3290	1701	2703
3.339	1	7.5	0	1.7500	1	0.1788	0.1712	3957	856	2212	4.860	0.3	0.7	0.7	1.5556	0.7	0.1750	0.1689	8638	1369	2677
3.339	1	7.5	0	1.7500	0.3	0.3339	0.3351	3213	875	2085	4.860	0.3	0.7	0.7	1.6667	1	0.1022	0.0921	5392	1497	2680
3.339	1	7.5	0	1.7500	0.5	0.2601	0.2570	2799	902	2018	4.860	0.3	0.7	0.7	1.6667	0.3	0.4721	0.4776	4010	1593	2698
3.339	1	7.5	0	1.7500	0.7	0.2181	0.2123	2386	931	1961	4.860	0.3	0.7	0.7	1.6667	0.5	0.2876	0.2807	3317	1694	2702
3.339	1	7.5	0	1.8750	1	0.1787	0.1716	3912	863	2215	4.860	0.3	0.7	0.7	1.6667	0.7	0.1905	0.1816	8813	1365	2677

ODTh	alfa	Eback	beta	TWOD	Ewall	δy(%)	δx(%)	M(lb-in)	V (lb)	Th (lb)	ODTh	alfa	Eback	beta	TWOD	Ewall	δy(%)	δx(%)	M(lb-in)	V (lb)	Th (lb)
3.339	1	7.5	0	1.8750	0.3	0.3331	0.3343	3206	883	2082	4.860	0.3	0.7	0.7	1.7778	1	0.1148	0.1024	5598	1490	2679
3.339	1	7.5	0	1.8750	0.5	0.2605	0.2573	2768	904	2020	4.860	0.3	0.7	0.7	1.7778	0.3	0.4801	0.4854	4030	1573	2699
3.339	1	7.5	0	1.8750	0.7	0.2177	0.2123	2362	935	1965	4.860	0.3	0.7	0.7	1.7778	0.5	0.2968	0.2891	3337	1687	2702
3.339	1	7.5	0	2.0000	1	0.1785	0.1718	3886	865	2219	4.860	0.3	0.7	0.7	1.7778	0.7	0.2010	0.1904	8940	1361	2679
3.339	1	7.5	0	2.0000	0.3	0.3324	0.3339	3198	891	2080	4.860	0.3	0.7	0.7	1.8889	1	0.1241	0.1101	5757	1485	2678
3.339	1	7.5	0	2.0000	0.5	0.2609	0.2577	2750	906	2020	4.860	0.3	0.7	0.7	1.8889	0.3	0.4861	0.4913	4174	1575	2698
3.339	1	7.5	0	2.0000	0.7	0.2176	0.2125	2947	787	1719	4.860	0.3	0.7	0.7	1.8889	0.5	0.3038	0.2954	2929	1154	2215
3.339	1	5	0	1.3750	1	0.1748	0.1560	4511	646	1928	4.860	0.3	0.7	0.7	1.8889	0.7	0.2090	0.1975	6217	1201	2402
3.339	1	5	0	1.3750	0.3	0.3350	0.3369	3728	693	1815	4.860	0.3	7.5	0.7	1.3333	1	0.1423	0.1424	4336	1165	2300
3.339	1	5	0	1.3750	0.5	0.2578	0.2500	3298	740	1757	4.860	0.3	7.5	0.7	1.3333	0.3	0.3431	0.3441	3674	1153	2253
3.339	1	5	0	1.3750	0.7	0.2145	0.2011	2893	793	1724	4.860	0.3	7.5	0.7	1.3333	0.5	0.2471	0.2464	2975	1106	2210
3.339	1	5	0	1.5000	1	0.1751	0.1588	4472	653	1930	4.860	0.3	7.5	0.7	1.3333	0.7	0.1922	0.1920	6297	1179	2404
3.339	1	5	0	1.5000	0.3	0.3350	0.3378	3687	701	1821	4.860	0.3	7.5	0.7	1.4444	1	0.1524	0.1513	4481	1124	2289
3.339	1	5	0	1.5000	0.5	0.2582	0.2521	3256	745	1761	4.860	0.3	7.5	0.7	1.4444	0.3	0.3490	0.3496	3716	1112	2253
3.339	1	5	0	1.5000	0.7	0.2149	0.2037	2844	799	1727	4.860	0.3	7.5	0.7	1.4444	0.5	0.2559	0.2539	3004	1102	2213
2.667	1	5	0	1.6250	1	0.1752	0.1608	4431	662	1933	4.860	0.3	7.5	0.7	1.4444	0.7	0.2008	0.1998	6371	1165	2401
2.667	1	5	0	1.6250	0.3	0.3346	0.3380	3652	708	1824	4.860	0.3	7.5	0.7	1.5556	1	0.1585	0.1568	4547	1104	2293
2.667	1	5	0	1.6250	0.5	0.2583	0.2535	3223	751	1764	4.860	0.3	7.5	0.7	1.5556	0.3	0.3527	0.3527	3744	1080	2232
2.667	1	5	0	1.6250	0.7	0.2151	0.2054	2801	804	1730	4.860	0.3	7.5	0.7	1.5556	0.5	0.2606	0.2582	3022	1102	2203
2.667	1	5	0	1.7500	1	0.1754	0.1623	4404	671	1934	4.860	0.3	7.5	0.7	1.5556	0.7	0.2074	0.2052	6397	1155	2402
2.667	1	5	0	1.7500	0.3	0.3345	0.3382	3618	713	1827	4.860	0.3	7.5	0.7	1.6667	1	0.1628	0.1606	4596	1090	2294
2.667	1	5	0	1.7500	0.5	0.2583	0.2543	3187	756	1767	4.860	0.3	7.5	0.7	1.6667	0.3	0.3550	0.3549	3762	1070	2237
2.667	1	5	0	1.7500	0.7	0.2152	0.2066	2768	807	1731	4.860	0.3	7.5	0.7	1.6667	0.5	0.2638	0.2609	3037	1103	2194
2.667	1	5	0	1.8750	1	0.1755	0.1636	4401	683	1931	4.860	0.3	7.5	0.7	1.6667	0.7	0.2112	0.2084	6419	1147	2404
2.667	1	5	0	1.8750	0.3	0.3353	0.3389	3586	717	1831	4.860	0.3	7.5	0.7	1.7778	1	0.1661	0.1635	4613	1080	2294
2.667	1	5	0	1.8750	0.5	0.2580	0.2547	3155	759	1769	4.860	0.3	7.5	0.7	1.7778	0.3	0.3569	0.3564	3775	1074	2236
2.667	1	5	0	1.8750	0.7	0.2152	0.2076	2741	808	1732	4.860	0.3	7.5	0.7	1.7778	0.5	0.2660	0.2630	3047	1101	2195
2.667	1	5	0	2.0000	1	0.1755	0.1647	4382	690	1931	4.860	0.3	7.5	0.7	1.7778	0.7	0.2141	0.2108	6430	1141	2404
2.667	1	5	0	2.0000	0.3	0.3353	0.3393	3555	721	1833	4.860	0.3	7.5	0.7	1.8889	1	0.1685	0.1658	4640	1072	2293
2.667	1	5	0	2.0000	0.5	0.2579	0.2552	3127	762	1770	4.860	0.3	7.5	0.7	1.8889	0.3	0.3580	0.3574	3783	1073	2237
2.667	1	5	0	2.0000	0.7	0.2152	0.2083	1693	1279	2310	4.860	0.3	7.5	0.7	1.8889	0.5	0.2678	0.2647	3482	1465	2621
2.667	1	0.7	1	1.3750	1	0.2011	0.1988	2449	1296	2594	4.860	0.3	7.5	0.7	1.8889	0.7	0.2159	0.2125	7543	1465	2846
2.667	1	0.7	1	1.3750	0.3	0.3682	0.3708	2122	1284	2459	4.860	0.3	5	0.7	1.3333	1	0.1506	0.1534	4996	1443	2745
2.667	1	0.7	1	1.3750	0.5	0.2894	0.2886	1918	1279	2392	4.860	0.3	5	0.7	1.3333	0.3	0.4282	0.4371	4164	1443	2674
2.667	1	0.7	1	1.3750	0.7	0.2432	0.2414	1693	1279	2310	4.860	0.3	5	0.7	1.3333	0.5	0.2953	0.2997	3546	1378	2609
2.667	1	0.7	1	1.5000	1	0.2011	0.1988	2449	1296	2594	4.860	0.3	5	0.7	1.3333	0.7	0.2204	0.2234	7764	1428	2852
2.667	1	0.7	1	1.5000	0.3	0.3682	0.3708	2122	1284	2459	4.860	0.3	5	0.7	1.4444	1	0.1723	0.1723	5292	1382	2742
2.667	1	0.7	1	1.5000	0.5	0.2894	0.2886	1918	1279	2392	4.860	0.3	5	0.7	1.4444	0.3	0.4413	0.4500	4214	1369	2676
2.667	1	0.7	1	1.5000	0.7	0.2432	0.2414	1693	1279	2310	4.860	0.3	5	0.7	1.4444	0.5	0.3116	0.3145	3583	1378	2604
2.667	1	0.7	1	1.6250	1	0.2011	0.1988	2449	1296	2594	4.860	0.3	5	0.7	1.4444	0.7	0.2392	0.2401	7905	1396	2843
2.667	1	0.7	1	1.6250	0.3	0.3682	0.3708	2122	1284	2459	4.860	0.3	5	0.7	1.5556	1	0.1857	0.1843	5456	1347	2750
2.667	1	0.7	1	1.6250	0.5	0.2894	0.2886	1918	1279	2392	4.860	0.3	5	0.7	1.5556	0.3	0.4503	0.4583	4243	1329	2675
2.667	1	0.7	1	1.6250	0.7	0.2432	0.2414	1693	1279	2310	4.860	0.3	5	0.7	1.5556	0.5	0.3212	0.3235	3609	1377	2604
2.667	1	0.7	1	1.7500	1	0.2011	0.1988	2449	1296	2594	4.860	0.3	5	0.7	1.5556	0.7	0.2507	0.2505	7981	1376	2838
2.667	1	0.7	1	1.7500	0.3	0.3682	0.3708	2122	1284	2459	4.860	0.3	5	0.7	1.6667	1	0.1947	0.1924	5554	1323	2752
2.667	1	0.7	1	1.7500	0.5	0.2894	0.2886	1918	1279	2392	4.860	0.3	5	0.7	1.6667	0.3	0.4559	0.4635	4309	1321	2678
2.667	1	0.7	1	1.7500	0.7	0.2432	0.2414	1693	1279	2310	4.860	0.3	5	0.7	1.6667	0.5	0.3281	0.3303	3627	1374	2604

ODTh	alfa	Eback	beta	TWOD	Ewall	δy(%)	δx(%)	M(lb-in)	V (lb)	Th (lb)	ODTh	alfa	Eback	beta	TWOD	Ewall	δy(%)	δx(%)	M(lb-in)	V (lb)	Th (lb)
2.667	1	0.7	1	1.8750	1	0.2011	0.1988	2449	1296	2594	4.860	0.3	5	0.7	1.6667	0.7	0.2582	0.2574	8050	1362	2835
2.667	1	0.7	1	1.8750	0.3	0.3682	0.3708	2122	1284	2459	4.860	0.3	5	0.7	1.7778	1	0.2010	0.1981	5634	1304	2749
2.667	1	0.7	1	1.8750	0.5	0.2894	0.2886	1918	1279	2392	4.860	0.3	5	0.7	1.7778	0.3	0.4601	0.4674	4414	1318	2671
2.667	1	0.7	1	1.8750	0.7	0.2432	0.2414	1693	1279	2310	4.860	0.3	5	0.7	1.7778	0.5	0.3338	0.3360	3640	1371	2607
2.667	1	0.7	1	2.0000	1	0.2011	0.1988	2449	1296	2594	4.860	0.3	5	0.7	1.7778	0.7	0.2642	0.2632	8101	1350	2830
2.667	1	0.7	1	2.0000	0.3	0.3682	0.3708	2122	1284	2459	4.860	0.3	5	0.7	1.8889	1	0.2058	0.2024	5693	1290	2750
2.667	1	0.7	1	2.0000	0.5	0.2894	0.2886	1918	1279	2392	4.860	0.3	5	0.7	1.8889	0.3	0.4635	0.4706	4473	1318	2674
2.667	1	0.7	1	2.0000	0.7	0.2432	0.2414	1556	1210	2200	4.860	0.3	5	0.7	1.8889	0.5	0.3378	0.3398	7517	2405	4045
2.667	1	7.5	1	1.3750	1	0.1909	0.1876	2336	1220	2466	4.860	0.3	5	0.7	1.8889	0.7	0.2682	0.2668	15230	2101	4090
2.667	1	7.5	1	1.3750	0.3	0.3485	0.3493	1987	1214	2332	4.860	0.5	0.7	0.5	1.3333	1	0.3471	0.3177	10820	2222	4067
2.667	1	7.5	1	1.3750	0.5	0.2745	0.2723	1766	1211	2272	4.860	0.5	0.7	0.5	1.3333	0.3	0.8688	0.9069	8804	2288	4087
2.667	1	7.5	1	1.3750	0.7	0.2310	0.2279	1556	1210	2200	4.860	0.5	0.7	0.5	1.3333	0.5	0.6040	0.6116	7315	2393	4040
2.667	1	7.5	1	1.5000	1	0.1909	0.1876	2336	1220	2466	4.860	0.5	0.7	0.5	1.3333	0.7	0.4635	0.4513	15300	2095	4079
2.667	1	7.5	1	1.5000	0.3	0.3485	0.3493	1987	1214	2332	4.860	0.5	0.7	0.5	1.4444	1	0.3556	0.3291	10850	2218	4048
2.667	1	7.5	1	1.5000	0.5	0.2745	0.2723	1766	1211	2272	4.860	0.5	0.7	0.5	1.4444	0.3	0.8758	0.9150	8733	2286	4074
2.667	1	7.5	1	1.5000	0.7	0.2310	0.2279	1556	1210	2200	4.860	0.5	0.7	0.5	1.4444	0.5	0.6119	0.6212	7193	2386	4037
2.667	1	7.5	1	1.6250	1	0.1909	0.1876	2336	1220	2466	4.860	0.5	0.7	0.5	1.4444	0.7	0.4722	0.4628	15330	2092	4073
2.667	1	7.5	1	1.6250	0.3	0.3485	0.3493	1987	1214	2332	4.860	0.5	0.7	0.5	1.5556	1	0.3608	0.3365	10870	2215	4036
2.667	1	7.5	1	1.6250	0.5	0.2745	0.2723	1766	1211	2272	4.860	0.5	0.7	0.5	1.5556	0.3	0.8802	0.9202	8694	2285	4065
2.667	1	7.5	1	1.6250	0.7	0.2310	0.2279	1556	1210	2200	4.860	0.5	0.7	0.5	1.5556	0.5	0.6168	0.6273	7108	2381	4034
2.667	1	7.5	1	1.7500	1	0.1909	0.1876	2336	1220	2466	4.860	0.5	0.7	0.5	1.5556	0.7	0.4776	0.4700	15360	2090	4068
2.667	1	7.5	1	1.7500	0.3	0.3485	0.3493	1987	1214	2332	4.860	0.5	0.7	0.5	1.6667	1	0.3644	0.3418	10880	2213	4028
2.667	1	7.5	1	1.7500	0.5	0.2745	0.2723	1766	1211	2272	4.860	0.5	0.7	0.5	1.6667	0.3	0.8832	0.9239	8670	2283	4058
2.667	1	7.5	1	1.7500	0.7	0.2310	0.2279	1556	1210	2200	4.860	0.5	0.7	0.5	1.6667	0.5	0.6202	0.6315	7047	2377	4032
2.667	1	7.5	1	1.8750	1	0.1909	0.1876	2336	1220	2466	4.860	0.5	0.7	0.5	1.6667	0.7	0.4812	0.4749	15370	2089	4065
2.667	1	7.5	1	1.8750	0.3	0.3485	0.3493	1987	1214	2332	4.860	0.5	0.7	0.5	1.7778	1	0.3670	0.3457	10890	2212	4021
2.667	1	7.5	1	1.8750	0.5	0.2745	0.2723	1766	1211	2272	4.860	0.5	0.7	0.5	1.7778	0.3	0.8855	0.9266	8652	2282	4053
2.667	1	7.5	1	1.8750	0.7	0.2310	0.2279	1556	1210	2200	4.860	0.5	0.7	0.5	1.7778	0.5	0.6227	0.6346	7001	2375	4030
2.667	1	7.5	1	2.0000	1	0.1909	0.1876	2336	1220	2466	4.860	0.5	0.7	0.5	1.7778	0.7	0.4838	0.4785	15380	2088	4063
2.667	1	7.5	1	2.0000	0.3	0.3485	0.3493	1987	1214	2332	4.860	0.5	0.7	0.5	1.8889	1	0.3690	0.3488	10900	2212	4017
2.667	1	7.5	1	2.0000	0.5	0.2745	0.2723	1766	1211	2272	4.860	0.5	0.7	0.5	1.8889	0.3	0.8871	0.9286	8636	2281	4049
2.667	1	7.5	1	2.0000	0.7	0.2310	0.2279	1529	1182	2150	4.860	0.5	0.7	0.5	1.8889	0.5	0.6245	0.6370	3121	1109	2284
2.667	1	5	1	1.3750	1	0.1871	0.1839	2301	1193	2414	4.860	0.5	0.7	0.5	1.8889	0.7	0.4857	0.4813	6562	1090	2444
2.667	1	5	1	1.3750	0.3	0.3413	0.3420	1953	1187	2282	4.860	0.5	7.5	0.5	1.3333	1	0.1745	0.1653	4801	1029	2366
2.667	1	5	1	1.3750	0.5	0.2689	0.2667	1734	1184	2221	4.860	0.5	7.5	0.5	1.3333	0.3	0.3639	0.3618	3853	1065	2325
2.667	1	5	1	1.3750	0.7	0.2263	0.2233	1529	1182	2150	4.860	0.5	7.5	0.5	1.3333	0.5	0.2723	0.2672	3128	1113	2268
2.667	1	5	1	1.5000	1	0.1871	0.1839	2301	1193	2414	4.860	0.5	7.5	0.5	1.3333	0.7	0.2211	0.2139	6577	1087	2434
2.667	1	5	1	1.5000	0.3	0.3413	0.3420	1953	1187	2282	4.860	0.5	7.5	0.5	1.4444	1	0.1780	0.1695	4933	1050	2314
2.667	1	5	1	1.5000	0.5	0.2689	0.2667	1734	1184	2221	4.860	0.5	7.5	0.5	1.4444	0.3	0.3657	0.3636	3897	1073	2292
2.667	1	5	1	1.5000	0.7	0.2263	0.2233	1529	1182	2150	4.860	0.5	7.5	0.5	1.4444	0.5	0.2770	0.2707	3132	1114	2242
2.667	1	5	1	1.6250	1	0.1871	0.1839	2301	1193	2414	4.860	0.5	7.5	0.5	1.4444	0.7	0.2242	0.2172	6598	1085	2423
2.667	1	5	1	1.6250	0.3	0.3413	0.3420	1953	1187	2282	4.860	0.5	7.5	0.5	1.5556	1	0.1801	0.1722	4933	1051	2307
2.667	1	5	1	1.6250	0.5	0.2689	0.2667	1734	1184	2221	4.860	0.5	7.5	0.5	1.5556	0.3	0.3668	0.3645	3928	1079	2270
2.667	1	5	1	1.6250	0.7	0.2263	0.2233	1529	1182	2150	4.860	0.5	7.5	0.5	1.5556	0.5	0.2784	0.2722	3133	1112	2237
2.667	1	5	1	1.7500	1	0.1871	0.1839	2301	1193	2414	4.860	0.5	7.5	0.5	1.5556	0.7	0.2264	0.2193	6590	1085	2422
2.667	1	5	1	1.7500	0.3	0.3413	0.3420	1953	1187	2282	4.860	0.5	7.5	0.5	1.6667	1	0.1815	0.1739	4922	1053	2306
2.667	1	5	1	1.7500	0.5	0.2689	0.2667	1734	1184	2221	4.860	0.5	7.5	0.5	1.6667	0.3	0.3672	0.3650	3949	1084	2257

ODTh	alfa	Eback	beta	TWOD	Ewall	δy(%)	δx(%)	M(lb-in)	V (lb)	Th (lb)
2.667	1	5	1	1.7500	0.7	0.2263	0.2233	1529	1182	2150
2.667	1	5	1	1.8750	1	0.1871	0.1839	2301	1193	2414
2.667	1	5	1	1.8750	0.3	0.3413	0.3420	1953	1187	2282
2.667	1	5	1	1.8750	0.5	0.2689	0.2667	1734	1184	2221
2.667	1	5	1	1.8750	0.7	0.2263	0.2233	1529	1182	2150
2.667	1	5	1	2.0000	1	0.1871	0.1839	2301	1193	2414
2.667	1	5	1	2.0000	0.3	0.3413	0.3420	1953	1187	2282
2.667	1	5	1	2.0000	0.5	0.2689	0.2667	1734	1184	2221
2.667	1	5	1	2.0000	0.7	0.2263	0.2233	3436	1516	2209
2.667	0	0.7	1	1.3750	1	-0.1850	-0.1769	3196	1208	2185
2.667	0	0.7	1	1.3750	0.3	0.2975	0.2956	2455	1299	2169
2.667	0	0.7	1	1.3750	0.5	0.0516	0.0539	2261	1389	2191
2.667	0	0.7	1	1.3750	0.7	-0.0750	-0.0695	2954	1503	2186
2.667	0	0.7	1	1.5000	1	-0.1033	-0.1180	3329	1204	2180
2.667	0	0.7	1	1.5000	0.3	0.3589	0.3448	2450	1296	2162
2.667	0	0.7	1	1.5000	0.5	0.1233	0.1085	2205	1380	2175
2.667	0	0.7	1	1.5000	0.7	0.0014	-0.0132	2631	1491	2174
2.667	0	0.7	1	1.6250	1	-0.0536	-0.0807	3455	1199	2175
2.667	0	0.7	1	1.6250	0.3	0.3950	0.3746	2448	1284	2164
2.667	0	0.7	1	1.6250	0.5	0.1661	0.1423	2183	1373	2168
2.667	0	0.7	1	1.6250	0.7	0.0477	0.0219	2394	1482	2167
2.667	0	0.7	1	1.7500	1	-0.0203	-0.0549	3563	1195	2174
2.667	0	0.7	1	1.7500	0.3	0.4183	0.3945	2481	1280	2160
2.667	0	0.7	1	1.7500	0.5	0.1950	0.1658	2173	1368	2163
2.667	0	0.7	1	1.7500	0.7	0.0788	0.0460	2216	1476	2164
2.667	0	0.7	1	1.8750	1	0.0038	-0.0359	3657	1193	2172
2.667	0	0.7	1	1.8750	0.3	0.4347	0.4091	2517	1279	2156
2.667	0	0.7	1	1.8750	0.5	0.2158	0.1829	2164	1363	2159
2.667	0	0.7	1	1.8750	0.7	0.1013	0.0639	2078	1471	2162
2.667	0	0.7	1	2.0000	1	0.0217	-0.0216	3736	1190	2172
2.667	0	0.7	1	2.0000	0.3	0.4469	0.4204	2551	1277	2155
2.667	0	0.7	1	2.0000	0.5	0.2313	0.1962	2167	1359	2159
2.667	0	0.7	1	2.0000	0.7	0.1181	0.0780	1132	847	1909
2.667	0	7.5	1	1.3750	1	0.1003	0.1040	2210	807	2135
2.667	0	7.5	1	1.3750	0.3	0.3120	0.3179	1777	815	2113
2.667	0	7.5	1	1.3750	0.5	0.2013	0.2097	1447	812	2014
2.667	0	7.5	1	1.3750	0.7	0.1498	0.1562	1158	843	1927
2.667	0	7.5	1	1.5000	1	0.1202	0.1221	2269	829	2155
2.667	0	7.5	1	1.5000	0.3	0.3236	0.3295	1824	835	2004
2.667	0	7.5	1	1.5000	0.5	0.2274	0.2292	1484	806	2021

Right table:

ODTh	alfa	Eback	beta	TWOD	Ewall	δy(%)	δx(%)	M(lb-in)	V (lb)	Th (lb)
4.860	0.5	7.5	0.5	1.6667	0.5	0.2792	0.2731	3136	1115	2226
4.860	0.5	7.5	0.5	1.6667	0.7	0.2279	0.2206	6591	1084	2419
4.860	0.5	7.5	0.5	1.7778	1	0.1825	0.1751	4911	1054	2307
4.860	0.5	7.5	0.5	1.7778	0.3	0.3675	0.3652	3956	1088	2252
4.860	0.5	7.5	0.5	1.7778	0.5	0.2796	0.2737	3137	1115	2220
4.860	0.5	7.5	0.5	1.7778	0.7	0.2288	0.2215	6605	1085	2421
4.860	0.5	7.5	0.5	1.8889	1	0.1832	0.1758	4905	1055	2306
4.860	0.5	7.5	0.5	1.8889	0.3	0.3680	0.3656	3951	1088	2250
4.860	0.5	7.5	0.5	1.8889	0.5	0.2800	0.2741	4421	1479	2901
4.860	0.5	7.5	0.5	1.8889	0.7	0.2294	0.2222	8749	1388	3103
4.860	0.5	5	0.5	1.3333	1	0.2250	0.2071	6585	1349	2990
4.860	0.5	5	0.5	1.3333	0.3	0.4858	0.4853	5404	1407	2931
4.860	0.5	5	0.5	1.3333	0.5	0.3607	0.3515	4392	1474	2887
4.860	0.5	5	0.5	1.3333	0.7	0.2894	0.2755	8765	1386	3101
4.860	0.5	5	0.5	1.4444	1	0.2316	0.2150	6580	1349	2983
4.860	0.5	5	0.5	1.4444	0.3	0.4894	0.4894	5379	1411	2923
4.860	0.5	5	0.5	1.4444	0.5	0.3660	0.3580	4367	1472	2876
4.860	0.5	5	0.5	1.4444	0.7	0.2951	0.2824	8758	1386	3101
4.860	0.5	5	0.5	1.5556	1	0.2358	0.2202	6562	1348	2981
4.860	0.5	5	0.5	1.5556	0.3	0.4912	0.4917	5367	1410	2916
4.860	0.5	5	0.5	1.5556	0.5	0.3688	0.3615	4348	1475	2868
4.860	0.5	5	0.5	1.5556	0.7	0.2985	0.2865	8760	1385	3099
4.860	0.5	5	0.5	1.6667	1	0.2385	0.2238	6551	1349	2982
4.860	0.5	5	0.5	1.6667	0.3	0.4924	0.4932	5349	1409	2913
4.860	0.5	5	0.5	1.6667	0.5	0.3705	0.3638	4325	1474	2865
4.860	0.5	5	0.5	1.6667	0.7	0.3007	0.2895	8788	1381	3085
4.860	0.5	5	0.5	1.7778	1	0.2404	0.2263	6543	1350	2979
4.860	0.5	5	0.5	1.7778	0.3	0.4942	0.4949	5333	1407	2909
4.860	0.5	5	0.5	1.7778	0.5	0.3717	0.3653	4306	1473	2860
4.860	0.5	5	0.5	1.7778	0.7	0.3024	0.2919	8820	1377	3073
4.860	0.5	5	0.5	1.8889	1	0.2418	0.2283	6535	1350	2978
4.860	0.5	5	0.5	1.8889	0.3	0.4957	0.4963	5320	1407	2907
4.860	0.5	5	0.5	1.8889	0.5	0.3727	0.3668	7054	1534	2397
4.860	0.5	5	0.5	1.8889	0.7	0.3039	0.2939	11220	1088	2601
4.860	0.7	0.7	0.3	1.3333	1	0.2742	0.2524	9055	1210	2494
4.860	0.7	0.7	0.3	1.3333	0.3	0.5743	0.5984	7957	1360	2450
4.860	0.7	0.7	0.3	1.3333	0.5	0.4206	0.4202	6993	1525	2401
4.860	0.7	0.7	0.3	1.3333	0.7	0.3423	0.3297	11220	1087	2598
4.860	0.7	0.7	0.3	1.4444	1	0.2740	0.2536	9035	1208	2494
4.860	0.7	0.7	0.3	1.4444	0.3	0.5750	0.6000	7919	1355	2451

ODTh	alfa	Eback	beta	TWOD	Ewall	δy(%)	δx(%)	M(lb-in)	V (lb)	Th (lb)	ODTh	alfa	Eback	beta	TWOD	Ewall	δy(%)	δx(%)	M(lb-in)	V (lb)	Th (lb)
2.667	0	7.5	1	1.5000	0.7	0.1682	0.1723	1175	842	1931	4.860	0.7	0.7	0.3	1.4444	0.5	0.4210	0.4217	6947	1519	2404
2.667	0	7.5	1	1.6250	1	0.1324	0.1333	2336	833	2164	4.860	0.7	0.7	0.3	1.4444	0.7	0.3424	0.3310	11210	1087	2596
2.667	0	7.5	1	1.6250	0.3	0.3331	0.3384	1844	855	2001	4.860	0.7	0.7	0.3	1.5556	1	0.2739	0.2544	9022	1208	2494
2.667	0	7.5	1	1.6250	0.5	0.2381	0.2381	1509	820	1992	4.860	0.7	0.7	0.3	1.5556	0.3	0.5754	0.6011	7886	1351	2454
2.667	0	7.5	1	1.6250	0.7	0.1799	0.1822	1186	846	1927	4.860	0.7	0.7	0.3	1.5556	0.5	0.4213	0.4228	6909	1513	2406
2.667	0	7.5	1	1.7500	1	0.1408	0.1409	2309	837	2184	4.860	0.7	0.7	0.3	1.5556	0.7	0.3423	0.3319	11200	1089	2594
2.667	0	7.5	1	1.7500	0.3	0.3343	0.3397	1527	836	1971	4.860	0.7	0.7	0.3	1.6667	1	0.2737	0.2551	9009	1209	2494
2.667	0	7.5	1	1.7500	0.7	0.1889	0.1895	1194	854	1917	4.860	0.7	0.7	0.3	1.6667	0.3	0.5759	0.6022	7860	1348	2456
2.667	0	7.5	1	1.8750	1	0.1468	0.1461	2363	858	2173	4.860	0.7	0.7	0.3	1.6667	0.5	0.4215	0.4236	6875	1509	2409
2.667	0	7.5	1	1.8750	0.3	0.3398	0.3438	1861	853	2033	4.860	0.7	0.7	0.3	1.6667	0.7	0.3423	0.3326	11190	1090	2593
2.667	0	7.5	1	1.8750	0.5	0.2468	0.2470	1542	870	1920	4.860	0.7	0.7	0.3	1.7778	1	0.2736	0.2556	8998	1209	2494
2.667	0	7.5	1	1.8750	0.7	0.1976	0.1956	1201	873	1906	4.860	0.7	0.7	0.3	1.7778	0.3	0.5762	0.6029	7830	1348	2461
2.667	0	7.5	1	2.0000	1	0.1519	0.1503	2369	867	2186	4.860	0.7	0.7	0.3	1.7778	0.5	0.4216	0.4243	6844	1508	2416
2.667	0	7.5	1	2.0000	0.3	0.3398	0.3435	1870	853	2031	4.860	0.7	0.7	0.3	1.7778	0.7	0.3420	0.3327	11180	1091	2592
2.667	0	7.5	1	2.0000	0.5	0.2527	0.2531	1549	874	1935	4.860	0.7	0.7	0.3	1.8889	1	0.2733	0.2556	8991	1209	2494
2.667	0	7.5	1	2.0000	0.7	0.2008	0.1986	1275	848	1658	4.860	0.7	0.7	0.3	1.8889	0.3	0.5764	0.6034	7812	1346	2462
2.667	0	5	1	1.3750	1	0.0054	0.0077	2041	742	1844	4.860	0.7	0.7	0.3	1.8889	0.5	0.4218	0.4249	3721	1081	2172
2.667	0	5	1	1.3750	0.3	0.2495	0.2607	1485	771	1751	4.860	0.7	0.7	0.3	1.8889	0.7	0.3420	0.3333	6654	1072	2372
2.667	0	5	1	1.3750	0.5	0.1339	0.1424	1175	802	1695	4.860	0.7	7.5	0.3	1.3333	1	0.1940	0.1854	4943	1024	2271
2.667	0	5	1	1.3750	0.7	0.0652	0.0716	1117	787	1649	4.860	0.7	7.5	0.3	1.3333	0.3	0.3836	0.3849	4285	1053	2217
2.667	0	5	1	1.5000	1	0.0444	0.0433	2149	712	1854	4.860	0.7	7.5	0.3	1.3333	0.5	0.2920	0.2879	3667	1094	2176
2.667	0	5	1	1.5000	0.3	0.2770	0.2864	1576	728	1766	4.860	0.7	7.5	0.3	1.3333	0.7	0.2405	0.2336	6639	1074	2376
2.667	0	5	1	1.5000	0.5	0.1644	0.1708	1248	746	1697	4.860	0.7	7.5	0.3	1.4444	1	0.1939	0.1860	4932	1029	2274
2.667	0	5	1	1.5000	0.7	0.1027	0.1060	1001	781	1647	4.860	0.7	7.5	0.3	1.4444	0.3	0.3828	0.3845	4224	1062	2224
2.667	0	5	1	1.6250	1	0.0699	0.0669	2228	698	1858	4.860	0.7	7.5	0.3	1.4444	0.5	0.2916	0.2878	3622	1100	2179
2.667	0	5	1	1.6250	0.3	0.2932	0.3008	1628	702	1763	4.860	0.7	7.5	0.3	1.4444	0.7	0.2401	0.2337	6644	1074	2375
2.667	0	5	1	1.6250	0.5	0.1859	0.1904	1290	729	1701	4.860	0.7	7.5	0.3	1.5556	1	0.1938	0.1864	4919	1029	2276
2.667	0	5	1	1.6250	0.7	0.1256	0.1272	1022	771	1641	4.860	0.7	7.5	0.3	1.5556	0.3	0.3827	0.3843	4183	1064	2224
2.667	0	5	1	1.7500	1	0.0877	0.0837	2370	683	1845	4.860	0.7	7.5	0.3	1.5556	0.5	0.2912	0.2876	3585	1103	2180
2.667	0	5	1	1.7500	0.3	0.3091	0.3138	1661	686	1760	4.860	0.7	7.5	0.3	1.5556	0.7	0.2399	0.2339	6636	1075	2378
2.667	0	5	1	1.7500	0.5	0.2008	0.2038	1318	721	1703	4.860	0.7	7.5	0.3	1.6667	1	0.1936	0.1865	4923	1036	2276
2.667	0	5	1	1.7500	0.7	0.1415	0.1420	1036	765	1636	4.860	0.7	7.5	0.3	1.6667	0.3	0.3823	0.3840	4144	1062	2224
2.667	0	5	1	1.8750	1	0.1004	0.0957	2399	679	1819	4.860	0.7	7.5	0.3	1.6667	0.5	0.2911	0.2875	3560	1106	2181
2.667	0	5	1	1.8750	0.3	0.3206	0.3226	1683	685	1764	4.860	0.7	7.5	0.3	1.6667	0.7	0.2396	0.2340	6633	1076	2380
2.667	0	5	1	1.8750	0.5	0.2107	0.2127	1339	721	1699	4.860	0.7	7.5	0.3	1.7778	1	0.1935	0.1867	4928	1040	2274
2.667	0	5	1	1.8750	0.7	0.1532	0.1527	1047	762	1638	4.860	0.7	7.5	0.3	1.7778	0.3	0.3819	0.3836	4116	1065	2226
2.667	0	5	1	2.0000	1	0.1097	0.1047	2442	688	1822	4.860	0.7	7.5	0.3	1.7778	0.5	0.2912	0.2875	3533	1103	2180
2.667	0	5	1	2.0000	0.3	0.3275	0.3289	1699	686	1763	4.860	0.7	7.5	0.3	1.7778	0.7	0.2394	0.2340	6631	1078	2382
2.667	0	5	1	2.0000	0.5	0.2189	0.2201	1355	725	1697	4.860	0.7	7.5	0.3	1.8889	1	0.1935	0.1869	4927	1042	2277
2.667	0	5	1	2.0000	0.7	0.1618	0.1604	4972	1531	2300	4.860	0.7	7.5	0.3	1.8889	0.3	0.3815	0.3833	4100	1069	2226
2.667	1	0.7	1	1.3750	1	0.1448	0.0216	5204	1137	2370	4.860	0.7	7.5	0.3	1.8889	0.5	0.2908	0.2872	4090	921.1	1910
2.667	1	0.7	1	1.3750	0.3	0.4930	0.4440	4737	1260	2329	4.860	0.7	7.5	0.3	1.8889	0.7	0.2394	0.2339	6419	927.6	2043
2.667	1	0.7	1	1.3750	0.5	0.3109	0.2313	4732	1379	2313	4.860	0.7	5	0.3	1.3333	1	0.1892	0.1773	5316	860.3	1968
2.667	1	0.7	1	1.3750	0.7	0.2194	0.1194	4481	1513	2260	4.860	0.7	5	0.3	1.3333	0.3	0.3790	0.3806	4705	883	1944
2.667	1	0.7	1	1.5000	1	0.1636	0.0498	5097	1143	2339	4.860	0.7	5	0.3	1.3333	0.5	0.2868	0.2809	4037	928	1912
2.667	1	0.7	1	1.5000	0.3	0.5113	0.4667	4476	1252	2296	4.860	0.7	5	0.3	1.3333	0.7	0.2350	0.2255	6399	930.1	2049
2.667	1	0.7	1	1.5000	0.5	0.3292	0.2556	4368	1369	2274	4.860	0.7	5	0.3	1.4444	1	0.1893	0.1784	5271	862.7	1973

ODTh	alfa	Eback	beta	TWOD	Ewall	δy(%)	δx(%)	M(lb-in)	V (lb)	Th (lb)	ODTh	alfa	Eback	beta	TWOD	Ewall	δy(%)	δx(%)	M(lb-in)	V (lb)	Th (lb)
2.667	1	0.7	1	1.5000	0.7	0.2388	0.1463	4178	1500	2252	4.860	0.7	5	0.3	1.4444	0.3	0.3783	0.3803	4653	889.9	1949
2.667	1	0.7	1	1.6250	1	0.1749	0.0678	5048	1147	2323	4.860	0.7	5	0.3	1.4444	0.5	0.2865	0.2812	3984	931.2	1915
2.667	1	0.7	1	1.6250	0.3	0.5226	0.4810	4318	1249	2274	4.860	0.7	5	0.3	1.4444	0.7	0.2349	0.2263	6385	932.7	2055
2.667	1	0.7	1	1.6250	0.5	0.3404	0.2712	4146	1363	2251	4.860	0.7	5	0.3	1.5556	1	0.1892	0.1791	5233	864.3	1976
2.667	1	0.7	1	1.6250	0.7	0.2504	0.1633	3965	1491	2246	4.860	0.7	5	0.3	1.5556	0.3	0.3777	0.3800	4613	895.1	1952
2.667	1	0.7	1	1.7500	1	0.1825	0.0809	4212	1245	2260	4.860	0.7	5	0.3	1.5556	0.5	0.2863	0.2816	3942	934.8	1918
2.667	1	0.7	1	1.7500	0.5	0.3479	0.2820	3992	1359	2244	4.860	0.7	5	0.3	1.5556	0.7	0.2348	0.2269	6370	935	2061
2.667	1	0.7	1	1.7500	0.7	0.2581	0.1751	3811	1484	2240	4.860	0.7	5	0.3	1.6667	1	0.1891	0.1796	5203	867	1980
2.667	1	0.7	1	1.8750	1	0.1880	0.0904	4978	1144	2308	4.860	0.7	5	0.3	1.6667	0.3	0.3771	0.3797	4575	899.7	1954
2.667	1	0.7	1	1.8750	0.3	0.5340	0.4966	4137	1245	2249	4.860	0.7	5	0.3	1.6667	0.5	0.2861	0.2817	3907	938.3	1921
2.667	1	0.7	1	1.8750	0.5	0.3534	0.2901	3877	1355	2238	4.860	0.7	5	0.3	1.6667	0.7	0.2347	0.2273	6356	937.5	2066
2.667	1	0.7	1	1.8750	0.7	0.2636	0.1839	3696	1479	2236	4.860	0.7	5	0.3	1.7778	1	0.1889	0.1800	5169	871.4	1984
2.667	1	0.7	1	2.0000	1	0.1922	0.0979	4959	1146	2303	4.860	0.7	5	0.3	1.7778	0.3	0.3764	0.3792	4540	903.3	1957
2.667	1	0.7	1	2.0000	0.3	0.5379	0.5019	4078	1246	2240	4.860	0.7	5	0.3	1.7778	0.5	0.2858	0.2817	3877	941.7	1923
2.667	1	0.7	1	2.0000	0.5	0.3576	0.2964	3790	1352	2234	4.860	0.7	5	0.3	1.7778	0.7	0.2345	0.2276	6345	939.2	2070
2.667	1	0.7	1	2.0000	0.7	0.2677	0.1906	1342	861	1994	4.860	0.7	5	0.3	1.8889	1	0.1888	0.1803	5138	875	1987
2.667	1	7.5	1	1.3750	1	0.1603	0.1427	2415	807	2195	4.860	0.7	5	0.3	1.8889	0.3	0.3758	0.3787	4512	904.8	1958
2.667	1	7.5	1	1.3750	0.3	0.3535	0.3503	1893	790	2119											
2.667	1	7.5	1	1.3750	0.5	0.2544	0.2466	1584	811	2078											
2.667	1	7.5	1	1.3750	0.7	0.2046	0.1932	1237	849	2014											
2.667	1	7.5	1	1.5000	1	0.1656	0.1514	2456	845	2173											
2.667	1	7.5	1	1.5000	0.3	0.3621	0.3581	1900	806	2093											
2.667	1	7.5	1	1.5000	0.5	0.2613	0.2539	1591	821	2052											
2.667	1	7.5	1	1.5000	0.7	0.2111	0.2008	1240	852	1985											
2.667	1	7.5	1	1.6250	1	0.1700	0.1572	2405	852	2185											
2.667	1	7.5	1	1.6250	0.3	0.3626	0.3597	1905	823	2086											
2.667	1	7.5	1	1.6250	0.5	0.2652	0.2582	1598	836	2008											

Biographical Information

Margarita Takou has earned her undergraduate and graduate degree in Civil Engineering from the National Technical University of Athens (NTUA) in Athens, Greece. She completed her Doctor of Philosophy degree in Civil Engineering, in the structures and applied mechanics area at the University of Texas at Arlington (UTA) in 2016.

During her doctoral degree, Ms. Takou worked as a teaching assistant for different courses, among them Finite Element Analysis and Masonry Design.

Ms. Takou was a recipient of Gerontelis Foundation Scholarships in 2013. She also received a competitive graduate fellowship for a 4-year period from University of Texas at Arlington.

Topics from this research were presented at conference meetings and workshop, including Transportation Research Board Annual meeting, Texas Water, and American Water Work Association conference.

Ms. Takou's dissertation title, Numerical and Experimental Investigation of Buried Large Diameter Steel Pipes with Controlled Low Strength Material, was supervised by Dr. Ali Abolmaali.